TENTH SYMPOSIUM (INTERNATIONAL)

ON

COMBUSTION

At The University of Cambridge

Cambridge, England

August 17–21, 1964

ABSTRACTS OF PAPERS

UNPUBLISHED PRELIMINARY DATA

THE COMBUSTION INSTITUTE

UNION TRUST BUILDING

PITTSBURGH, PENNSYLVANIA 15219

TENTH SYMPOSIUM (INTERNATIONAL)

ON

COMBUSTION

At The University of Cambridge

Cambridge, England

August 17-21, 1964

ABSTRACTS OF PAPERS

THE COMBUSTION INSTITUTE

UNION TRUST BUILDING

PITTSBURGH, PENNSYLVANIA 15219

The Combustion Institute gratefully acknowledges the support accorded the Tenth Symposium (International) on Combustion by the U. S. Army Ballistic Research Laboratories, under Contract No. DA-31-124-ARO-D-197, the National Aeronautics and Space Administration under Grant NsG-506, the National Science Foundation, under Grant GN-260, the National Academy of Sciences, National Research Council Committee on Fire Research, the British Section of The Combustion Institute, and numerous private industrial firms which will be listed in the symposium program and publication.

THE COMBUSTION INSTITUTE

Officers

President ..... Bernard Lewis

Vice President ..... Hoyt C. Hottel

Treasurer ..... Stewart Way

Assistant Treasurer ..... Bernard M. Sturgis

Secretary ..... Glenn C. Williams

Executive Office

Union Trust Building, Pittsburgh, Pennsylvania 15219
Mrs. Helen G. Barnes, Executive Secretary

Board of Directors

Dr. William G. Agnew	General Motors Research Laboratories
Dr. David Altman	United Technology Center
Dr. William H. Avery	The Johns Hopkins University
Mr. William J. Bennet	The Marquardt Corporation
Dr. J. S. Clarke	Joseph Lucas Limited
Dr. Louis Deffet	Centre des Recherches pour L'Industrie des Produits Explosifs
Dr. Newman A. Hall	Commission on Engineering Education
Dr. Amos G. Horney	Air Force Office of Scientific Research
Professor Hoyt C. Hottel	Massachusetts Institute of Technology
Professor Wilhelm Jost	University of Göttingen
Dr. Bernard Lewis	Combustion and Explosives Research, Inc.
Dr. J. P. Longwell	Esso Research and Engineering Company
Mr. J. B. Macauley	USA Department of Defense
Mr. A. J. Nerad	General Electric Company
Dr. Walter T. Olson	Lewis Research Center, NASA
Dr. Bruce H. Sage	California Institute of Technology
Dr. Bernard M. Sturgis	E. I. du Pont de Nemours & Company, Inc.
Dr. Stewart Way	Westinghouse Research Laboratories
Professor Glenn C. Williams	Massachusetts Institute of Technology

Western States Section

Dr. Robert S. Levine, Chairman	Rocketdyne
Dr. Ernest S. Starkman, Vice Chairman	University of California
Dr. M. Wesley Rigg, Treasurer, (deceased)	Office of Naval Research
Mr. Gilbert S. Bahn, Secretary	The Marquardt Corporation

The Combustion Institute Committee

United States

Dr. David Altman, Chairman	United Technology Center
Dr. Richard D. Geckler	Aerojet-General Corporation
Dr. Amos G. Horney	Office of Scientific Research, USAF

Dr. J. P. Longwell	Esso Research and Engineering Company
Dr. Walter T. Olson	Lewis Research Center, NASA
Professor Glenn C. Williams	Massachusetts Institute of Technology
Great Britain	
Mr. S. L. Bragg, Chairman	Rolls-Royce Ltd., Derby
Dr. J. S. Clarke, O.B.E., Treasurer	Joseph Lucas Limited, Birmingham
Professor F. H. Garner	University of Birmingham
Dr. J. W. Linnett, F.R.S.	Queen's College, Oxford
Dr. W. G. Parker, Secretary	College of Advanced Technology, Birmingham
Dr. T. M. Sugden	Thornton Research Centre
Australia	
Dr. D. R. Warren	Aeronautical Research Laboratories, Melbourne
Belgium	
Dr. Louis Deffet	Centre de Recherches pour l'Industrie des Produits Explosifs, Brussels
Canada	
Professor A. L. Thompson	McGill University, Montreal
France	
Professor Paul Laffitte	Faculté des Sciences de l'Université de Paris
Germany	
Professor Wilhelm Jost	Chemisches Institut der Universität, Göttingen
Hungary	
Professor Zoltan G. Szabó	University of Szeged
India	
Dr. M. S. Thacker	Council of Scientific and Industrial Research New Delhi
Israel	
Dr. Avraham Hermoni	Ministry of Defence, Tel-Aviv
Italy	
Professor Carlo Padovani	Politecnico di Milano
Japan	
Professor Tsutomu Hikita	University of Tokyo
Netherlands	
Professor E. F. M. van der Held	Central Techn. Inst. T.N.O., Delft
Spain	
Dr. Gregorio Millán	Instituto Nacional de Tecnica Aeronáutica, Madrid
Sweden	
Dr. Allan Wetterholm	Nitroglycerin AB, Gyttorp

Switzerland Professor K. Clusius	Physikalisch-Chemisches Institut der Universität, Zürich
Turkey Professor Hikmet Binark	Teknik Universitesi, Istanbul

1964 SYMPOSIUM SUBCOMMITTEES

Dr. J. S. Clarke, Honorary President — Joseph Lucas, Ltd.

Papers Subcommittee

Dr. Raymond Friedman, Chairman	Atlantic Research Corporation
Dr. W. G. Agnew	General Motors Research Laboratories
Dr. P. G. Ashmore	University of Cambridge
Dr. W. H. Avery	APL, The Johns Hopkins University
Dr. R. R. Baldwin	The University of Hull
Dr. M. Barrère	O.N.E.R.A.
Professor S. Bauer	Cornell University
Mr. W. J. Bennet	The Marquardt Corporation
Professor S. W. Benson	University of Southern California
Dr. W. G. Berl	APL, The Johns Hopkins University
Dr. A. L. Berlad	General Dynamics/Astronautics
Dr. M. S. Biondi	University of Pittsburgh
Professor M. Boudart	University of California
Professor F. P. Bowden	University of Cambridge
Mr. S. L. Bragg	Rolls-Royce Ltd.
Dr. S. R. Brinkley, Jr.	Combustion and Explosives Research, Inc.
Dr. H. P. Broida	University of California, Santa Barbara
Dr. J. H. Burgoyne	Imperial College of Science and Technology
Dr. H. F. Calcote	AeroChem Research Laboratories, Inc.
Professor A. B. Cambel	Northwestern University
Dr. H. M. Cassel	75 E. Wayne Ave., Silver Spring, Md. 20901
Dr. A. E. Clarke	Lucas Gas Turbine Equipment Ltd.
Professor F. S. Dainton	The University of Leeds
Dr. G. Dixon-Lewis	The Houldsworth School of Applied Science
Dr. R. E. Duff	University of California
Dr. G. L. Dugger	APL, The Johns Hopkins University
Professor H. W. Emmons	Harvard University
Dr. R. H. Essenhigh	The Pennsylvania State University
Dr. Marjorie W. Evans	Stanford Research Institute
Dr. C. P. Fenimore	General Electric Company
Professor J. B. Fenn	Princeton University
Dr. W. L. Fite	General Atomic
Dr. S. N. Foner	APL, The Johns Hopkins University
Dr. J. L. Franklin	Rice University
Dr. R. M. Fristrom	APL, The Johns Hopkins University
Dr. D. Garvin	National Bureau of Standards
Professor A. G. Gaydon	Imperial College of Science and Technology
Dr. M. Gerstein	Dynamic Science Corporation
Dr. M. Gilbert (deceased)	United Technology Center
Professor I. Glassman	Princeton University
Dr. A. S. Gordon	U. S. Naval Ordnance Test Station
Professor P. Gray	The University of Leeds
Mr. John H. Grover	Atlantic Research Corporation
Dr. R. J. Heaston	Army Research Office, Arlington
Mr. B. Karlovitz	Combustion and Explosives Research, Inc.
Dr. W. E. Kaskan	Valley Forge Space Technology Center
Dr. F. Kaufman	Ballistic Research Laboratories
Professor T. Kinbara	Sophia University, Tokyo
Professor G. B. Kistiakowsky	Harvard University
Dr. P. H. Kydd	General Electric Research Laboratory

Professor P. Laffitte	University of Paris
Dr. R. S. Levine	Rocketdyne
Dr. Joseph B. Levy	Atlantic Research Corporation
Dr. Bernard Lewis (ex officio)	Combustion and Explosives Research, Inc.
Professor P. A. Libby	Polytechnic Institute of Brooklyn
Professor J. W. Linnett	Oxford University
Dr. J. P. Longwell	Esso Research and Engineering Company
Dr. Andrej Maček	Atlantic Research Corporation
Dr. G. H. Markstein	Cornell Aeronautical Laboratory, Inc.
Dr. J. F. Masi	Air Force Office of Scientific Research
Dr. F. T. McClure	APL, The Johns Hopkins University
Professor P. S. Myers	The University of Wisconsin
Dr. W. Nachbar	Stanford University
Professor J. A. Nicholls	The University of Michigan
Dr. P. L. Nichols, Jr.	Aerojet-General Corporation
Dr. W. T. Olson	Lewis Research Center, NASA
Professor A. K. Oppenheim	University of California
Professor Howard B. Palmer	The Pennsylvania State University
Professor W. G. Parker	College of Advanced Technology
Professor S. S. Penner	University of California, La Jolla
Dr. A. V. Phelps	Westinghouse Electric Corporation
Professor G. Porter	The University of Sheffield
Dr. A. E. Potter	Lewis Research Center, NASA
Mr. E. W. Price	U.S. Naval Ordnance Test Station
Dr. R. Roberts	Office of Naval Research
Dr. A. F. Robertson	National Bureau of Standards
Mr. K. E. Rumbel	Atlantic Research Corporation
Professor N. W. Ryan	University of Utah
Dr. G. L. Schott	University of California
Dr. John E. Scott, Jr.	University of Virginia
Dr. Arch Scurlock	Atlantic Research Corporation
Professor D. G. Shepherd	Cornell University
Professor E. S. Starkman	University of California
Dr. T. M. Sugden	Thornton Research Centre
Professor M. Summerfield	Princeton University
Dr. P. H. Thomas	Department of Scientific and Industrial Research, Fire Research Station
Dr. R. J. Thompson, Jr.	Rocketdyne
Professor M. W. Thring	The University of Sheffield
Dr. B. A. Thrush	University of Cambridge
Professor A. R. Ubbelohde	Imperial College of Science and Technology
Dr. Robert W. Van Dolah	U.S. Bureau of Mines
Professor A. Van Tiggelen	Université de Louvain
Dr. G. von Elbe	Atlantic Research Corporation
Dr. H. Gg. Wagner	University of Göttingen
Professor A. D. Walsh	University of St. Andrews
Dr. S. Way	Westinghouse Research Laboratories
Dr. P. P. Wegener	Yale University
Dr. F. J. Weinberg	Imperial College of Science and Technology
Dr. A. A. Westenberg	APL, The Johns Hopkins University
Dr. D. D. White	General Electric Research Laboratory
Professor F. A. Williams	Harvard University
Professor G. C. Williams	Massachusetts Institute of Technology
Dr. H. Wise	Stanford Research Institute
Dr. H. G. Wolfhard	Institute for Defense Analyses
Professor M. J. Zucrow	Purdue University
Professor E. E. Zukoski	California Institute of Technology

Awards Subcommittee

Mr. A. J. Nerad, Chairman	General Electric Company
Dr. W. G. Berl	APL, The Johns Hopkins University
Dr. N. A. Hall	Commission on Engineering Education
Dr. A. G. Horney	Office of Scientific Research, USAF
Dr. B. Lewis (ex officio)	Combustion and Explosives Research, Inc.
Dr. R. N. Pease, (deceased)	Princeton University
Dr. E. H. Seymour	Reaction Motors Division, Thiokol
Dr. G. C. Williams	Massachusetts Institute of Technology

Finance Subcommittee

Dr. W. E. Kuhn, Chairman	Texaco Inc.
Mr. A. H. Batchelder	California Research Corporation
Dr. M. Ference, Jr.	Ford Motor Company
Dr. R. D. Geckler	Aerojet-General Corporation
Dr. J. McAfee	Gulf Research & Development Company
Lt. Gen. D. Putt	United Aircraft Corporation
Mr. R. K. Scales	Ethyl Corporation

Nominations Subcommittee for Directors

Dr. W. T. Olson, Chairman	Lewis Research Center, NASA
Mr. J. B. Macauley	Office of the Secretary of Defense
Dr. G. C. Williams	Massachusetts Institute of Technology

Nominations Subcommittee for Officers

Dr. G. C. Williams, Chairman	Massachusetts Institute of Technology
Dr. N. A. Hall	Commission on Engineering Education
Dr. A. G. Horney	Air Force Office of Scientific Research
Mr. A. J. Nerad	General Electric Research Laboratory
Dr. B. M. Sturgis	E. I. du Pont de Nemours & Company

Publications Subcommittee

Dr. W. G. Berl, Chairman	Applied Physics Laboratory, The Johns Hopkins University
Mrs. H. G. Barnes	The Combustion Institute
Mr. S. L. Bragg	Rolls-Royce Ltd.
Dr. H. W. Emmons	Harvard University
Dr. R. Friedman	Atlantic Research Corporation
Dr. F. Kaufman	Ballistic Research Laboratories
Mr. M. Klatzkin	Mono of Maryland
Dr. B. Lewis	Combustion and Explosives Research, Inc.
Dr. A. K. Oppenheim	University of California
Dr. W. G. Parker	College of Advanced Technology
Dr. T. M. Sugden	"Shell" Research Ltd.
Dr. F. J. Weinberg	Imperial College of Science and Technology

Cambridge University Subcommittee

Dr. T. M. Sugden, Chairman
Dr. B. A. Thrush, Vice Chairman
Dr. P. J. Padley, Secretary
Dr. T. Boddington
Dr. J. A. Green
Dr. D. Harrison
Dr. P. F. Knewstubb
Mr. F. D. Robinson

Ladies Subcommittee

Mrs. R. G. W. Norrish, Chairman
Mrs. T. M. Sugden, Vice Chairman
Mrs. B. A. Thrush, Secretary
Mrs. P. F. Knewstubb
Mrs. E. A. Moelwyn-Hughes
Mrs. J. H. Purnell

CONTENTS

LIST OF AUTHORS

Name	Affiliation and Location	Page
BECKER, H. A.	Department of Chemical Engineering, Queen's University, Kingston, Ontario, Canada	117
BEER, J. M.	Department of Fuel Technology, Pennsylvania State University, University Park, Pennsylvania 16802	93
BEHRENS, H.	I. S. L. Institut Franco-Allemand de Recherches de Saint-Louis (Haut-Rhin), France	172
BELLES, F. E.	Lewis Research Center, NASA, Cleveland Ohio 44135	45
BERL, W. G.	Applied Physics Laboratory, The Johns Hopkins University, Silver Spring, Maryland	13
BILLIG, F. S.	Applied Physics Laboratory, The Johns Hopkins University, Silver Spring, Maryland	97
BIONDI, M. A.	Department of Physics, University of Pittsburgh, Pittsburgh, Pennsylvania 15213	38
BLACKMORE, D. R.	Department of Chemistry, University of Manchester, Manchester 1, England	49
BLACKSHEAR, P. L., Jr.	Mechanical Engineering Department, University of Minnesota, Minneapolis, Minnesota 55455	138
BLUNDELL, R. V.	Associated Ethyl Company, Ltd., Bletchley, England	30
BONNE, U.	Institut für Physikalische Chemie, Universität Göttingen, Bürgerstr 50, Göttingen, Germany	33
BONNER, B. H.	The Donnan Laboratories, The University of Liverpool, Liverpool 7, England	22
BORGERS, A. J.	Physical Laboratory, State University, Utrecht, The Netherlands	128
BOUDART, M.	Department of Chemical Engineering, University of California, Berkeley, California 94720	76
BOWEN, J. R.	Department of Chemical Engineering, University of California, Berkeley, California 94720	76
BOYLE, V. M.	Ballistic Research Laboratories, Aberdeen Proving Ground, Maryland 21005	67
BOYNTON, F. P.	Space Science Laboratories, General Dynamics/ Astronautics, San Diego, California 92112	156
BRADLEY, J. N.	Department of Inorganic and Physical Chemistry, The University of Liverpool, Liverpool, England	20

Name	Affiliation and Location	Page
DAVIES, R. M.	Gas Council, Midlands Research Station, Wharf Lane, Solihull, Warwickshire, England	136
DEMBROW, D.	Applied Physics Laboratory, The Johns Hopkins University, Silver Spring, Maryland	13
DIMICK, R. C.	Department of Mechanical and Industrial Engineering, University of Illinois, Urbana, Illinois	132
DIXON-LEWIS, G.	The University, Leeds 2, England	32
DREMIN, A. N.	Institute of Chemical Physics, USSR Academy of Sciences, Vorobyevskoye chaussee, 2-6, Moscow V-334, USSR	64
EBERSTEIN, I. J.	Guggenheim Laboratories for the Aerospace Propulsion Sciences, Princeton University, Princeton, New Jersey	61
EDMONDSON, H.	Department of Fuel Science, Houldsworth School of Applied Science, The University, Leeds 2, England	126
EMMONS, H. W.	Harvard University, Cambridge 38, Massachusetts	82
EVANS, B. E.	Department of Chemical Physics, Stanford Research Institute, Menlo Park, California	128
FALK, F.	Applied Physics Laboratory, The Johns Hopkins University, Silver Spring, Maryland	13
FENIMORE, C. P.	Research Laboratory, General Electric Company, Schenectady, New York	32
FERRISO, C. C.	Space Science Laboratory, General Dynamics/ Astronautics, San Diego, California 92112	156
FEUGIER, A.	Laboratoire de Chimie Inorganique, l'Université Catholique de Louvain, Louvain, Belgium	41
FISH, A.	Department of Chemical Engineering, Imperial College, London S. W. 7, England	27
FONTIJN, A.	AeroChem Research Laboratories, Princeton, New Jersey	36
FOSS, W. I.	Research Laboratory, General Electric Company, Schenectady, New York	14
FOSTER, P. J.	Department of Fuel Technology and Chemical Engineering, University of Sheffield, Sheffield 1, England	173
FRANCIS, W. E.	Gas Council, Midlands Research Station, Solihull, Warwickshire, England	94

Name	Affiliation and Location	Page
HAJAL, I.	L'Université de Paris, 1, rue Victor-Cousin, Paris V, France	11
HALL, A. R.	Rocket Propulsion Establishment, Ministry of Aviation, Westcott, Nr. Aylesbury, Bucks., England	145
HALPERIN, B.	Lawrence Radiation Laboratory, University of California, Livermore, California	74
HARRISON, A. J.	Research Laboratories, Lucas Gas Turbine Equipment Ltd., Burnley, England	97
HART, R. W.	Applied Physics Laboratory, The Johns Hopkins University, Silver Spring, Maryland	89
HAY, J.	Department of Chemistry, University of Edinburgh, Edinburgh 9, Scotland	55
HAYES, B.	Los Alamos Scientific Laboratory, University of California, Los Alamos, New Mexico	71
HESELDEN, A. J. M.	Fire Research Station, Boreham Wood, Herts., England	84
HINCK, E. C.	Thiokol Chemical Corporation, Reaction Motors Division, Denville, New Jersey	1
HOARE, D. E.	Chemistry Department, Queen's College, Dundee, Scotland	30
HOGAN, J. M.	AeroChem Research Laboratories Inc., Princeton, New Jersey	36
HOMANN, K. H.	Institut für Physikalische Chemie, Universität Göttingen, Göttingen, Germany	33
HOTTEL, H. C.	Department of Chemical Engineering, Massachusetts Institute of Technology, Cambridge, Massachusetts 02139	14, 85, 117
HOWE, N. M., Jr.	George C. Marshall Space Flight Center, NASA, Huntsville, Alabama	96
JACKSON, D.	Chemistry Department, The University, Hull, England	28
JACKSON, E. G.	Joint Research Committee of the Gas Council, Houldsworth School of Applied Science, The University, Leeds 2, England	95
JAFFE, J. H.	Department of Physics, The Weizmann Institute, Rehovoth, Israel	161

Name	Affiliation and Location	Page
SUTTON, M. M.	Gas Research Department, The Houldsworth School of Applied Science, The University, Leeds 2, England	32
TAKENO, T.	Aeronautical Research Institute, University of Tokyo, Tokyo, Japan	104
TAO, L. N.	IIT Research Institute, Technology Center, Chicago 16, Illinois	82
TARIFA, C. S.	Instituto Nacional de Tecnica Aeronáutica, Madrid, Spain	86
THOMAS, P. H.	Department of Scientific & Industrial Research, Fire Research Station, Boreham Wood, Herts., England	84
THRING, M. W.	Department of Fuel Technology, University of Sheffield, Sheffield 1, England	93
THRUSH, B. A.	Department of Physical Chemistry, University of Cambridge, Cambridge, England	26
THYNNE, J. C. J.	Department of Physical Chemistry, The University, Leeds 2, Yorkshire, England	28
TINNEY, E. R.	R. L. Albrook Hydraulic Laboratory, Washington State University, Pullman, Washington	140
TIPPER, C. F. H.	The Donnan Laboratories, The University of Liverpool, Liverpool 7, England	20, 22
TOONG, T. Y.	Department of Mechanical Engineering, Massachusetts Institute of Technology, Cambridge, Massachusetts 02139	102
TOPPS, J. E. C.	National Gas Turbine Establishment, Ministry of Aviation, Pyestock, Farnborough, Hants., England	115
TRAVERS, B. E. L.	Rocket Propulsion Establishment, Ministry of Aviation, Westcott, Nr. Aylesbury, Bucks., England	130
TROFIMOV, V. S.	Institute of Chemical Physics, Academy of Sciences, Moscow V-334, USSR	64
TSUCHIYA, S.	Aeronautical Research Institute, University of Tokyo, Komaba, Meguro-ku, Tokyo, Japan	165
TSUJI, H.	Aeronautical Research Institute, University of Tokyo, Komaba, Meguro-ku, Tokyo, Japan	104
TURCOTTE, D. L.	Graduate School of Aerospace Engineering, Cornell University, Ithaca, New York 14850	130
TURNER, J. M. C.	Department of Chemistry, University of Edinburgh, Edinburgh, Scotland	55

Name	Affiliation and Location	Page
WILLIAMS, G. C.	Department of Chemical Engineering, Massachusetts Institute of Technology, Cambridge, Massachusetts 02139	14, 85, 117
WILLIAMS, H.	Rocket Propulsion Establishment, Ministry of Aviation, Westcott, Nr. Aylesbury, Bucks., England	130
WILSON, W. E., Jr.	Applied Physics Laboratory, The Johns Hopkins University, Silver Spring, Maryland	5
WINTERFELD, G.	Deutsche Versuchsanstalt für Luft-un Raumfahrt, Institut für Luftstrahlantriebe, (RHLD) Germany	119
WOHL, K. (deceased)	Department of Chemical Engineering, University of Delaware, Newark, Delaware	175
WOLFHARD, H. G.	Research and Engineering Support Division, Institute for Defense Analyses, Washington, D. C. 20009	1
WOOLDRIDGE, C. E.	United Technology Center, Division of United Aircraft Corporation, Sunnyvale, California	113
WORTBERG, G.	Insititut für Mechanik, Technische Hochschule Aachen, 51 Aachen, Germany	129
WRAY, K. L.	Avco-Everett Research Laboratory, Everett 49, Massachusetts	35
WRIGHT, F. J.	Central Basic Research Laboratory, Esso Research and Engineering Company, Linden, New Jersey	25
YUMOTO, T.	Fire Research Institute of Japan, 700 Shinkawa, Mitaka, Tokyo, Japan	143
YUSHCHENKOVA, N. I.	Academy of Sciences, Institute of Chemical Physics, Moscow V-334, USSR	134
ZEEGERS, P. J. Th.	Physical Laboratory, State University, Utrecht, The Netherlands	2

FLAME CHEMISTRY

1. THE NATURE OF OH RADIATION IN LOW-PRESSURE FLAMES

E. C. Hinck, T. F. Seamans and M. Vanpée

Thiokol Chemical Corporation

and

H. G. Wolfhard

Institute for Defense Analyses

This paper will advance evidence to show that the major portion of the radiation from OH molecules in low-pressure flames is due to chemiluminescence. This emission is chemiluminescent to the extent that O and H atoms are present in greater than equilibrium amounts in both the reaction zones and post reaction zones of low-pressure flames.

A brief documented review of the spectroscopic evidence of pre-dissociation and pre-association of OH is followed by a presentation of new experimental evidence pertaining to O and H association in low-pressure flames and the peculiar vibrational intensity distributions resulting from this process.

Chemiluminescent radiation is the subject of much controversial discussion. This controversy is due mainly to the scarcity of facts and the difficulty of such experimental methods as may provide undisputed facts. The chemiluminescence in the reaction zone of hydrocarbon flames is an exception insofar as the $CH + O_2 \longrightarrow CO + OH^*$ mechanism is generally accepted and well documented. The pre-dissociation and pre-association of OH, however, have been more of a scientific curiosity. The work on low-pressure flames has shown that non-equilibrium conditions leading to non-thermal radiation are not only found in reaction zones, but also in gases subject to quite rapid cooling. The decay of the concentrations of O, H and OH atoms in rapidly cooling gases is delayed for kinetic reasons, as three-body collisions are scarce, especially at low pressure, through the recombination reactions:

$$H + H + M \longrightarrow H_2 + M$$

$$O + O + M \longrightarrow O_2 + M$$

$$H + OH + M \longrightarrow H_2O + M$$

O, H and OH will, however, tend to be in equilibrium with each other through the following bimolecular reactions which are fast and reversible due to the small activation energies required.

$$O + H_2 \rightleftharpoons OH + H$$

$$H + O_2 \rightleftharpoons OH + O$$

$$OH + H_2 \rightleftharpoons H_2O + H$$

The net result of the recombination and dissociation reactions is an excess of H, O and OH above equilibrium and a deficiency in the molecular species H_2O, O_2 and H_2. These

excess radical concentrations result in the bimolecular association:

a) $O + H \longrightarrow OH\ (^2\Sigma^-) \longrightarrow OH\ (^2\Sigma^+)\sqrt{\ } = 2,3 \longrightarrow OH\ (^2\pi) + h\nu$

predominant at low pressure and the termolecular recombination

b) $O + H + M \longrightarrow OH\ (^2\Sigma^+)\sqrt{\ } = 0,1 + M \longrightarrow OH\ (^2\pi) + M + h\nu$

predominant at higher pressures.

A 10 cm burner was used in the experimental portion of the investigation to pressures of 3.3 mm Hg. The reaction zone was perfectly flat and spectral scans along the flame centerline were performed using extremely small fields of view (1.1 mm wide in the flowline direction) of a Perkin-Elmer Monochromator 12 C Special. The system was calibrated and values of absolute spectral radiance are presented versus distance above the burner for the OH bands of interest. Great care was taken to eliminate scattered light within the optical system. The burner was provided with a shroud flow of air (or nitrogen) and contained in an altitude chamber which in turn was connected to a vacuum pump system having a capacity of 650 cfm at 1 mm Hg. Flames of oxygen with ammonia, hydrogen and ethylene were burned at pressures below 25 mm Hg. In addition to the ultraviolet emission measurements, temperature profiles were obtained using line reversal methods which allowed calculation of blackbody radiation which was then compared to the measured absolute radiation to show the extent of the OH chemiluminescence.

The distribution of OH band radiance ratios in the reaction and post reaction zones are compared to the equilibrium ratios at 3000°K and deviations from equilibrium (of an order of magnitude in some cases) are indicated. In all cases the (0, 0) OH emission is greater than that of a blackbody at the corresponding temperature indicating pronounced non-thermal radiation. Temperature measurements have shown that the ethylene and ammonia-oxygen flames attain their adiabatic flame temperatures and do so close to the burner, whereas hydrogen-oxygen flames attain only 70% of their adiabatic flame temperatures and do so approximately 10 cm above the burner. This is explained by the slowness of the recombination reactions mentioned above which account for over 50% of the total combustion enthalpy (57.8 Kcal) of the $H_2 + 1/2\ O_2$ flame reaction and therefore delay the rise to maximum temperature until well into the region of cooling.

2. CHEMILUMINESCENCE OF OH-RADICALS AND K-ATOMS BY RADICAL RECOMBINATION IN FLAMES

P. J. Th. Zeegers

State University Utrecht

In the reaction zone of a premixed hydrocarbon-air flame, radicals like CH, C_2, H, OH and O, are formed in excess as products of the combustion chain reactions. Among these radicals the CH and C_2 radicals disappear rapidly above the reaction zone if sufficient oxygen is available for combustion. The other radicals mentioned may persist for some time after leaving the reaction zone, since they recombine to stable molecules by ternary reactions only, which are relatively slow. Consequently, the burned flame gas mixture in the region adjacent to the reaction zone is found not

to be in chemical equilibrium, but it will approach gradually to equilibrium with increasing distance from the reaction zone. Since in usual flames the partial pressures of the radicals are but small anywhere, these deviations from over-all flame equilibrium are mostly of second order. However, a study of their behavior might still be of interest as these radicals may have some peculiar effects upon the rate of excitation of metals and hydroxyl-radicals (chemiluminescence), upon the rate of ionization of alkali metals (chemi-ionization), upon the emission of continuous flame background and upon the adiabatic flame temperature as well.

The use of premixed, homogeneous C_2H_2-air flames with a relatively fast upward moving gas flow enabled us to study the decay of excess radicals with time by measuring the H- and OH-radical concentrations as function of height above the reaction zone.

The decay of H- and OH-radicals is based upon the recombination reactions: 1/

$$OH \text{ (or H)} + H + M \longrightarrow H_2O \text{ (or } H_2) + M \qquad (1)$$

$$CO + O + M \longrightarrow CO_2 + M \qquad (2)$$

$$O + O + M \longrightarrow O_2 + M \qquad (3)$$

in which M stands for a third particle
and the partially equilibriated reactions:

$$H + H_2O \rightleftarrows H_2 + OH \qquad (4)$$

$$O + H_2 \rightleftarrows OH + H \qquad (5)$$

$$H + O_2 \rightleftarrows OH + O \qquad (6)$$

$$CO + OH \rightleftarrows CO_2 + H \qquad (7)$$

We should not make the same simplifications in our C_2H_2 - air flame as these were made by Sugden and coworkers working with $H_2/N_2/O_2$ flames, where reactions (2) and (7) play no part at all. 2/

The variation of H- and OH-radical concentrations with height as predicted by theory could be shown to agree to the experimental results only if we take into account:

1. The occurrence of the recombination reactions (2) and (3) and the partial CO/CO_2 equilibrium, given by (7).

2. The fact that the H_2-, O_2- and CO-concentrations are not necessarily large compared with the radical concentrations, so their values are affected by recombination reactions.

3. The circumstance that the values of the excess radical concentrations do not exceed the equilibrium values to such a large extent that we are allowed to neglect the reverse dissociation reactions (1) - (3).

4. The effect on the gas composition and equilibrium constants associated with

the initial rise and fall of the temperature downstream of the flame.

Chemiluminescence may occur when the third particle M in the recombination reactions (1) - (3) is an OH-radical or a K-atom. K-atoms may be introduced into the flame by spraying the corresponding salt solution.

We were able to relate the height-dependence of the chemiluminescence of OH-radicals at 3064 Å and of K-atoms at 4034 Å to the variation with height of H- and OH-radicals on the basis of the proposed excitation reactions. Since the deviations from equilibrium radical concentrations are not excessively large, it was essential to take into account also the reverse reactions (1) - (3) leading to deactivation of excited OH-radicals and K-atoms. From the results obtained it was possible to derive an over-all rate constant for the chemiluminescence reactions proposed.

A special absorption technique was developed for measuring the ground-state OH concentration as function of height. A graphical method was used for discriminating between suprathermal chemiluminescence excitation, to be investigated, from the thermal excitation, which was of comparable order of magnitude.

References

1. Alkemade, C. Th. J., and Zeegers, P. J. Th.; to be published.

2. Bulewicz, E. M., James, C. G., and Sugden, T. M., Proc. Roy. Soc. A235, 89 (1956)

3. THE REACTION OF ALKALI ATOMS IN LEAN FLAMES

W. E. Kaskan

General Electric Space Sciences Laboratory

The chemistry of alkali metals in flame gases has been the subject of study for a number of years. Most recently, Sugden and his collaborators have seeded $H_2/O_2/N_2$ flames with all of the alkalies and have concluded that, in the flames they studied, the principal compound formed was the hydroxide, and that of these LiOH and NaOH were respectively the most and the least stable.

An examination of this work shows that, for the most part, the flames used were rich and temperatures exceeded 2000°K. These facts, coupled with the observation that it was difficult to make reversal temperature measurements on relatively cool lean flames (due presumably to alkali atoms removed by compound formation), suggested that a study of alkali metals in lean flames would be profitable.

Such a study has been made of Na- and K-seeded lean $H_2/O_2/N_2$ flames burning at 1 atmosphere on cooled porous metal burners, in the temperature range 1370-1700°K. Alkali metal atom concentrations were determined absolutely by observation of the absorption in the resonance lines as a function of distance and, therefore, as a function of time from the burner. OH concentrations were measured in a similar manner.

Na and K behaved similarly. The atom concentrations were at a

maximum in or near the flame zone, and decayed downstream to less than 1% of the original concentration in some cases. The kinetics of the decay, however, were not as expected. Sugden and his collaborators have adduced evidence to the effect that alkali atoms, A, are involved in the equilibrated reaction

$$A + H_2O \gtrless AOH + H. \qquad (1)$$

Since both in their flames and the ones employed here H atoms are at a maximum near the flame zone and decay downstream, and H_2O is effectively a constant, the occurrence of this reaction would cause a decay of A with time. In lean flames (H) has been shown to be proportional to $(OH)^3$, so that, if equation 1 is balanced, the ratio A/AOH should be proportional to $(OH)^3$ in any one flame. By making the assumption that all alkali not present as atoms was present as hydroxide, the A/AOH ratio was computed and compared with the cube of the experimentally determined OH. It was found that this expected behavior was not observed, and that A/OH was more nearly proportional to $(OH)^2$. Although this behavior could perhaps be explained by assuming that alkali also existed in the form AO, this interpretation is not entirely satisfactory.

On the other hand, the data are capable of an entirely different interpretation. It was shown that the initial parts of the decays were first order in both A and O_2, and that the derived rate constants obtained by assuming the reaction

$$A + O_2 \ (+M?) \longrightarrow AO_2 \ (+M) \qquad (2)$$

were independent of temperature, but somewhat dependent on (H_2O). This suggests that the disappearance of A is controlled by reaction 2 with the (possibly intermediate) product AO_2 and not AO + O, because of the lack of temperature dependence. The 3-body rate constants assuming M = H_2O are reasonable. Reaction 2 also seems reasonable by analogy to the reaction in which HO_2 is formed, based on the chemical similarity of H and A.

4. STRUCTURE, KINETICS AND MECHANISM OF A METHANE-OXYGEN FLAME INHIBITED WITH METHYL-BROMIDE*

Wm. E. Wilson, Jr.

The Johns Hopkins University

Most studies of flame inhibition have involved measuring the effect of additives on flame speed. Such work has led to the suggestion of a mechanism whereby the inhibitor removes active radicals such as H, OH, and O; substituting less active species such as CH_3 and Br. However, there has been no direct evidence for the actual mechanism or the amount by which radical concentration is lowered.

Recent work by Fristrom and Westenberg at The Johns Hopkins University Applied Physics Laboratory and Fenimore and Jones at the General Electric Research Labo-

* This work was supported by the U. S. Army Engineering Research and Development Laboratory (Ft. Belvoir) through contract NOw-62-06-4-c with the Bureau of Naval Weapons.

ratory have shown how temperature and composition profiles of low pressure flames may be used to obtain information on kinetics and mechanism of flame reactions. It was felt that further understanding of flame inhibition would come from intensive studies of a few selected inhibitors. This paper reports a study of a low pressure, methane-oxygen flame inhibited by CH_3Br. Profiles of temperature and concentration of all major species were measured. The net rates and some radical concentrations were calculated. Important results are: evidence for decrease in radical concentration, evidence for the mechanism by which radicals are removed, and a preliminary rate constant for the reaction $CH_3Br + OH \longrightarrow CH_2Br + H_2O$.

The flame was stablized at 1/20 atm. pressure on a flat, porous, ceramic plate; the entire system was made of glass and ceramic to avoid corrosion problems. A continuous sample was withdrawn through a small quartz probe with a 75μ orifice, quenched by rapid decompression to 100μ Hg and carried through a flow system to a mass spectrometer. Temperature was measured by .001" diameter, coated thermocouples.

The temperature and composition profiles were analyzed according to previously described methods to give net rates of appearance and disappearance. 1/ The temperature, composition, and rate profiles are given in the paper.

Since the rate constant, k, of the reaction $CO + OH \longrightarrow CO_2 + H$ is known, and the CO concentration, $[CO]$, and the net rate of appearance of CO_2, K_{CO_2} have been measured, the OH concentration may be calculated (neglecting the reverse rate) from

$$[OH] = K_{CO_2}/k[CO]$$

The OH concentration of the CH_3Br inhibited flame and a cooler uninhibited flame is shown in Fig. 1.

HBr is formed very early in the flame, but by the time the luminous zone is reached the HBr concentration has fallen below the minimum observable, 10^{-4} mole fraction. Presumably HBr would continue to be formed as long as CH_3Br is present, but as the luminous zone is approached it would be so rapidly removed via $HBr + OH \longrightarrow H_2O + Br$ that the steady state concentration would be too low to measure. The reaction $H + CH_3Br \longrightarrow HBr + CH_3$ accounts for the formation of HBr. This would be the fastest reaction of H in the cooler part of the flame. Thus the H atom is replaced by CH_3 which, although a reactive species, does not diffuse as rapidly and cannot contribute to chain branching, as in $H + O_2 \longrightarrow OH + O$.

It is shown that the reaction with H can account for only a fraction of the main CH_3Br disappearance. After all possibilities are considered it is concluded that the main reaction is probably $CH_3Br + OH \longrightarrow CH_2Br + H_2O$. The subsequent reactions which CH_2Br may undergo are discussed.

The comparison in Fig. 1 indicates some decrease in OH concentration in the early part of the flame, as the OH concentration of the inhibited flame is almost the same as for the cooler uninhibited flame. However, the main reduction occurs later as shown by the dip in the OH concentration curve for the inhibited flame. This decrease in OH concentration to $\frac{1}{4}$ its peak value, which occurs in the luminous zone after the CH_3Br has disappeared, must be due to reaction with HBr or other inhibiting species formed in the flame. It is not clear whether the inhibiting species regenerates itself in a chain reaction such as $HBr + OH \longrightarrow H_2O + Br$, $Br + CH_4 \longrightarrow HBr + CH_3$, etc. so that each Br atom deactivates many active species, or if a deactivation of one active radical by each Br atom is sufficient to account for the decrease in OH concentration. Some evidence is given for Br attack on CH_4. Calculated H concentrations are also given in the paper.

The calculated OH concentrations may be combined with the measured concentrations and net rates to give rate constants for some reactions. A preliminary rate constant of 2 X 10^{13} sec/molecule/cm^3 is calculated for the reaction $CH_3Br + OH \longrightarrow CH_2Br + H_2O$ in the 1800-2000°K temperature range.

Reference

1. Westenberg, A. A. and Fristrom, R. M.: J. Phys. Chem. 65, 591 (1961)

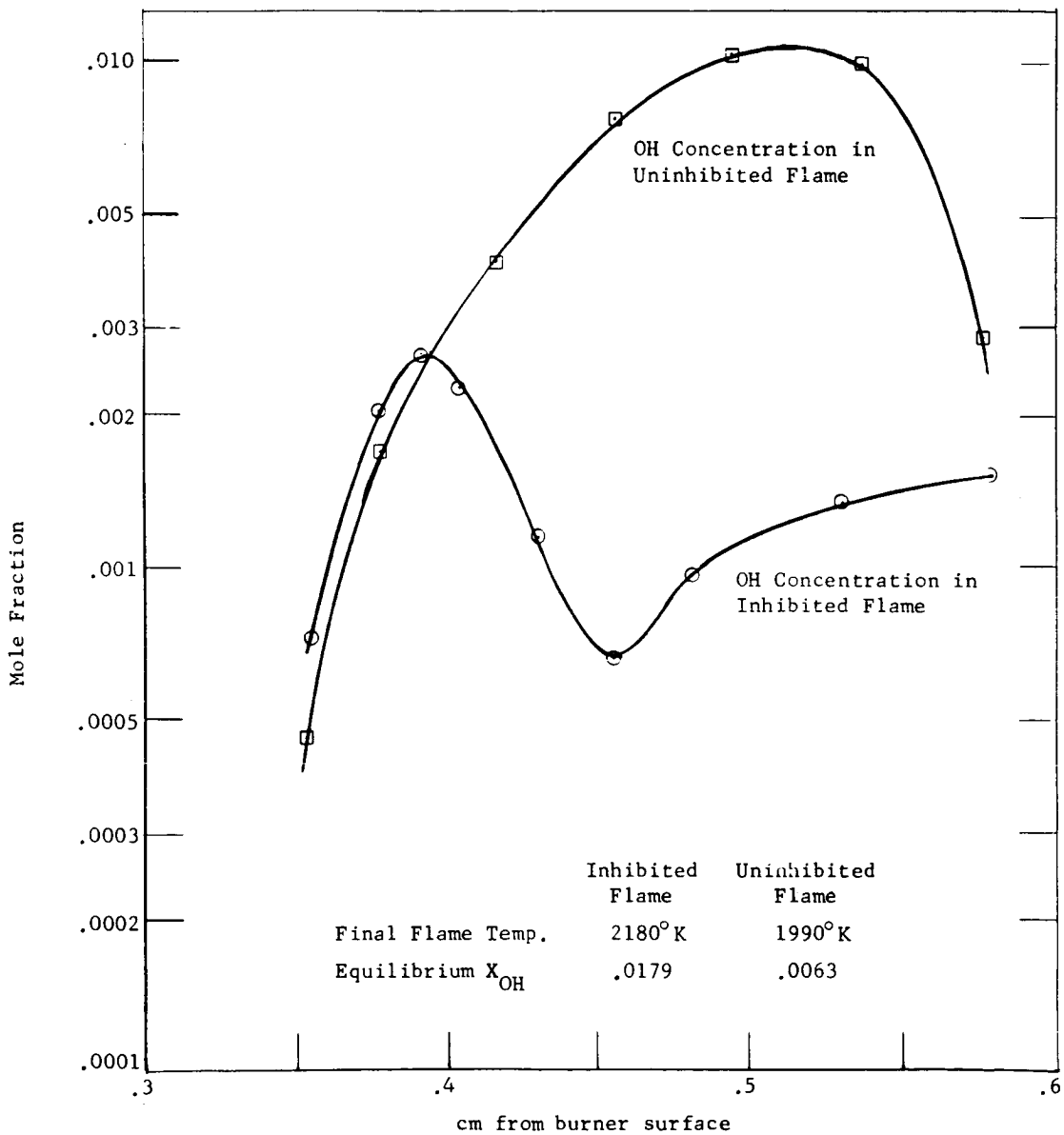

Fig. 1. OH Concentration in Inhibited and Uninhibited Flames Calculated from $[OH] = K_{CO_2}/k[CO]$ for Inhibited Flame and $[OH] = -K_{CH_4}/k[CH_4]$ for Uninhibited Flame.

5. HYDROGEN ATOM CONCENTRATIONS IN HYDROGEN/ OXYGEN/NITROGEN FLAMES

K. N. Bascombe

Explosives Research and Development Establishment, England

Flat flames of premixed hydrogen/oxygen/nitrogen have been stabilized on a low pressure burner operating between 30 and 100 mm Hg. The flames, all fuel-rich and containing unburned up to 80% nitrogen, were sufficiently thick (1 - 2 cm) to permit reasonably detailed investigations of the reaction zone processes. Final flame temperatures, measured by silica-coated platinum/platinum - 10% rhodium thermocouples, were in the limited range, 1000° to 1130°K; these temperatures were, in some cases, 100° below the calculated values, the difference being accounted for mainly by heat loss to the flame-stabilizing matrix. Completely free, near-limit flames were not sufficiently stable for study.

The hydrogen atom concentrations in the burned gases of these flames were measured by the method of Fenimore and Jones [1], which involves the addition of deuterium oxide to the flame. The formation of HD by the reaction.

$$H + D_2O \longrightarrow HD + OD$$

is then followed downstream from the reaction zone by probe sampling and mass-spectrometric analysis. This method is particularly applicable to low-pressure flames as ternary recombination of H atoms (and other free radicals) is relatively much less rapid than at atmospheric pressure, at which all measurements previously reported have been made.

The experimental H atom concentrations were found to be in excess of the theoretical by a factor of about 10^6, decreasing in general with temperature rise. At any given burned gas temperature it was found that this excess decreased with pressure increase; no simple relationship was clearly established, although near the ignition limit $[H]$ may be independent of pressure. In accord with this was the observation that the burned gas temperature of a given mixture increased with pressure rise; for nearly free flames this rise agreed well with the experimental $[H]$ values, taking into account the specific heat of the flame gases.

The results are discussed in terms of a simplified flame mechanism. The rate-determining step is considered to be the disappearance of O_2 by the competing processes:

$$H + O_2 \xrightarrow{k_1} OH + O \qquad (1)$$

$$H + O_2 + M \xrightarrow{k_2} HO_2 + M \qquad (2)$$

(where M is a third body or "chaperon") to be followed in the flame by

$$OH + H_2 \longrightarrow H_2O + H$$

$$O + H_2 \longrightarrow OH + H$$

$$HO_2 \longrightarrow \text{products}$$

This leads to two alternative reaction paths, as follows:

$$(H +) O_2 + 3H_2 \longrightarrow 2H_2O + 2H (+H) \qquad (3)$$

$$H + M + O_2 + \text{reactants} \longrightarrow \text{products} + nH \qquad (4)$$

On this theory the observed burned gas H atom concentration for any given flame gives a measure of the relative extent by which the reaction proceeds by the two paths, summed over the whole reaction zone. If this extent can be estimated, a value may be obtained for n, and information thus obtained on the steps involved in path (4) above.

This has been done by measurement of the oxygen concentration (by probe sampling) and temperature profiles through the reaction zone. On the assumption that O_2 disappears only through reactions (1) and (2), data from the literature for k_1 and k_2 have been used to obtain an H atom concentration profile through the reaction zone. The concentration so measured was found to tend downstream towards the burned gas value, determined by the D_2O addition method; a slight maximum in [H] was found.

The progress of reactions (1) and (2) through the reaction zone was assessed by graphical integration, and the sum of both reactions over the whole zone agreed well with the oxygen input to the flame. The results led to a value of -2 for n, i.e., net removal of 2 H atoms per O_2 consumed by reaction (2). Consideration of various possibilities for the removal of HO_2 in the flame has not so far led to any firm conclusions on this point. The interpretation which presents the least difficulties is perhaps the formation of hydrogen peroxide by

$$H + HO_2 + M \longrightarrow H_2O_2 + M \qquad (5)$$

to be followed for example by

$$H + H_2O_2 \longrightarrow H_2O + OH \qquad (6)$$

In order to make reaction (5) sufficiently fast, however, it is necessary to assume an improbably long lifetime for the collision complex H_2O_2*.

Reference

1. Fenimore, C. P. and Jones, G. W.: J. Phys. Chem., 62, 693 (1958).

6. OBSERVATIONS ON THE KINETICS OF HYDROGEN-CHLORINE FLAMES

R. Corbeels and K. Scheller

USAF Aerospace Research Laboratories

The relatively simple reaction scheme of hydrogen-chlorine mixtures has prompted flame studies [1, 2] of this system to extract chemical kinetic information. Indeed, Boudart [3] has pointed out that the work of Rozlovskiy [1] and Slootmaekers and Van Tiggelen [2] suggest a new chain branching kinetic step for the production

of chlorine atoms in flames not found in the classical Nernst scheme. To obtain further information regarding the mechanisms of reaction in hydrogen-chlorine flames, an investigation was undertaken of the effect of additives, particularly chlorides of the Group IV elements on such flames. The results are reported in this paper.

Since very wide disagreement was noted in the literature for the burning velocities of H_2-Cl_2 flames, it was necessary as a first step to measure burning velocities of H_2-Cl_2 mixtures diluted with varying quantities of nitrogen. It was found that the very great difference in mobility between hydrogen and chlorine produced strong diffusional effects in the flames, sharply limiting their range of stability. Burning velocities were measured by a Schlieren cone technique for stoichiometric to rich (140% of stoichiometric hydrogen) and nitrogen dilutions ranging from 20 to 50%. A maximum burning velocity of 235 cms/sec was obtained for 120% of stoichiometric hydrogen at the lowest nitrogen dilution. Manifestations of instability, such as open-tipped and cellular flames, usually found at the lean limits of hydrogen-containing combustible mixtures were observed to occur at stoichiometric and slightly rich mixture ratios in this system. These various phenomena are illustrated and discussed. Measurements were made of flame temperatures by comparing independently determined values of spatial and burning velocities. The results are shown to be in good agreement with theoretical adiabatic flame temperatures.

The burning velocities measured in the present investigation differ widely from those reported in the literature. Reasons for this discrepancy are discussed and the implications of these new results upon the kinetics deduced from flame speed data are presented. In particular, doubt is thrown on the necessity for assuming a new chain branching step to explain the kinetics of the H_2-Cl_2 flame.

Small quantities of CCl_4 were found to exert a surprisingly strong promotional effect on H_2-Cl_2 flames. Addition of as little as 0.1% of CCl_4 produced a 50% increase of burning velocity in the composition of maximum burning velocity (120% stoichiometric). Kinetic schemes to explain this effect are suggested and analyzed. In an attempt to elucidate further and test these reaction mechanisms, studies were made with other Group IV chlorides. Their effect was observed to be much smaller than that of CCl_4 suggesting that the promotion was fairly peculiar to the carbon-chlorine bond. Product gases of the CCl_4 mixtures were analyzed by vapor phase chromatographic methods and a series of burning velocity experiments were conducted with partially chlorinated methane additives in additional efforts to explain the promotional effects of CCl_4 on H_2-Cl_2 flames.

References

1. Rozlovskiy, A. I.: Z. Fiz. Khim., 30, 2489, 2713 (1956).

2. Slootmaekers, P. J. and Van Tiggelen, A.: Bull. Soc. Chim. Belg., 67, 135 (1958).

3. Boudart, M.: Eighth Symposium (International) on Combustion, p. 43. The Williams & Wilkins Co., 1962.

7. THE DECOMPOSITION FLAME OF HYDROGEN AZIDE

P. Laffitte, I. Hajal, J. Combourieu

The University of Paris

Experiments have shown that gaseous HN_3 contained in tubes at pressures higher than 5 mm Hg detonates easily if ignited by a spark. The distance traveled before a stable wave sets in is short (about 50 cm at 10 mm Hg and negligible at 100 mm Hg). Despite this pronounced tendency to detonate, stationary flames of HN_3 or of its mixtures with nitrogen have been stabilized on burners.

HN_3 (or mixtures with N_2) is stored in the gaseous state in a large vessel. Storage of liquid HN_3 is avoided because it is highly explosive. The vessel is connected through a valve and an orifice flowmeter to the burner which is housed in a low pressure chamber cooled by flowing nitrogen and continuously evacuated through a valve by a rotary pump. By adjusting the various valves the flow of burning mixture and the pressure may be maintained at given constant values for a few minutes. Simultaneous snapshots are taken of the flame cone, manometers and flowmeter.

Stability limits

Critical flows at flashback have been determined on different burners for HN_3 and several HN_3/N_2 flames at 50 mm Hg. Stability regions between flashback and blowoff for 30% HN_3 + 70% N_2 flames have also been plotted. The influence of pressure on flashback critical boundary velocity gradients in correlation with the theoretical equations deduced from a thermal concept of flame propagation [1, 2] leads to an over-all reaction order ν close to 2 for HN_3 decomposition at high temperatures.

The quenching diameter (d)

As mentionned in the literature [3], the tip of the stability region of a flame on a burner represents the quenching conditions. These quenching conditions have been determined for several HN_3/N_2 mixtures. From the effect of pressure on d and the theoretical equations given by Potter and Berlad [4] over-all reaction orders close to 2 have been deduced for mixtures containing 50, 70, 85 and 100% HN_3, and close to 1.5 for 30% HN_3 + 70% N_2.

Burning velocity

The total area method (ratio of the volumetric flow rate of unburned gas to the inner area of the luminous zone) has been applied to flames on burners of diameters ϕ between 2 and 3 times the quenching diameter d. Under such conditions, the result is relatively unaffected by the choice of the burner. From the relations based on the Peclet number, given by Cullen [5], it may be seen that the error on the result is less than 10% for ϕ = 2 d and 1% for ϕ = 3 d. On such burners, high flame cones with constant Reynolds numbers greater than 1000 (which is the condition of reliability given by Wolfhard [3]) can be obtained.

The burning velocity at 50 mm Hg and 296°K varies between 180 cm/s and 960 cm/s when the gas composition is varied from 30% HN_3 + 70% N_2 to 100% HN_3. There is little change with pressure except in the neighborhood of the flammability limit. On the basis of a thermal concept of flame propagation, this leads to a reaction order close to 2.

Comparison of HN_3 and DN_3 flames

The purpose of this comparison is to establish whether hydrogen atoms play an important part in the propagation process. Theories of deflagration based on diffusion of active centers would predict in this case a variation of the burning velocity of at least 18%. The actual variation is about 10% for pure HN_3 and negligible for 30% HN_3 + 70% N_2. The quenching diameters and flashback critical boundary velocity gradients are little affected. It therefore seems that H radicals are not essentially responsible for the fast propagation of the flame.

Discussion of the overall reaction order (ν) of the decomposition

From what has been said above it appears that ν is close to 2 in most cases (mixtures containing 50% to 100% HN_3) while it varies between 2 and 1.5 for 30% HN_3 + 70% N_2. On the other hand the decomposition of HN_3 at much lower temperatures [6, 7] is of the first order. Therefore either of the following assumptions may be advanced:

1. The chemical reaction follows different mechanisms, according to the pressure and temperature in the media;

2. The decomposition is unimolecular, the second order appearing at high temperatures and low pressures when the activation rate of the molecules by impact becomes insufficient to maintain a stationary concentration of active molecules.

Activation energy

Several equations are given in the literature for the burning velocity, quenching distance, and for the product or ratio of these two characteristics. By using some of these equations together with experimental data, calculated temperatures, and transport properties of the mixtures undergoing chemical change, an approximate value is derived for the activation energy. It is not far from the values obtained at lower temperatures. [6, 7]

References

1. Lewis, B. and von Elbe, G.: Combustion, Flames and Explosions of Gases. Academic Press, 1951.

2. Wohl, K.: Fourth Symposium (International) on Combustion, p. 68. The Williams & Wilkins Co., 1953.

3. Wolfhard, H. G.: AGARD Symposium 1381, AGARD 55.

4. Potter, A. E. and Berlad, A. L.: Sixth Symposium (International) on Combustion, p. 27. Reinhold Publishing Corp. 1957.

5. Cullen, R. E.: Transactions of the A.S.M.E., p. 43 (1953).

6. Meyer and Schumacher, Z. Physik. Chem. 170A, 33 (1934).

7. Gray, P. and Waddington, T. C.: Nature 179, 576 (1957).

8. COMBUSTION CHARACTERISTICS OF MONOPROPYLPENTABORANE FLAMES*

W. G. Berl, P. Breisacher, D. Dembrow, F. Falk, T. O'Donovan
J. Rice and V. Sigillito

The Johns Hopkins University

An account will be given of several complementary experiments on the combustion of fuel-lean monopropylpentaborane-air mixtures and of related alkylated boronhydrides: viz, determination of burning velocities; measurement of heat release rates in the Longwell-Weiss "homogeneous reactor"; analysis of composition in turbulent flames; and determination of composition and temperature profiles in the reaction zone of a flat flame at reduced pressure.

Details of experimental procedures, when they differ from conventional procedures, will be given.

The principal conclusions from these interrelated studies are as follows:

1. On the basis of temperature and composition profiles within the reaction zone of flat flames it can be shown that for sufficiently fuel-lean mixtures the combustion reaction proceeds only approximately 50 per cent toward equilibrium. The boron portion of the molecule is rapidly and completely oxidized (presumably to HBO_2). Most of the propyl sidechain carbon appears in the form of a complex mixture of hydrocarbons, aldehydes, alcohols, etc. A pathway will be presented suggesting the mechanism by which the divergent reactions proceed simultaneously. It is believed that the chain reactions responsible for the rapid boron oxidation are also involved in the decomposition and partial oxidation of the hydrocarbon sidechain. The normal, heat-releasing oxidation of the hydrocarbon either does not take place at all (i.e., if the temperature rise in the boron flame zone is too low) or occurs in a separate zone sufficiently uncoupled from the boron oxidation as not to affect its rate appreciably.

2. Burning velocity measurements of monopropylpentaborane-air and of pentaborane/ethylene-air are compared and are found to be identical if the B/C/H/O atomic ratios are matched. It is concluded that the flame-speed-determining reactions are identical, whether or not the hydrocarbon moiety is initially part of the fuel molecule structure. The strongly depressant effect of hydrocarbons on burning velocity of boron hydrides is also independent of the fuel structure.

3. Heat release measurements in the "homogeneous reactor" tend to substantiate the effects noted in (2), namely that the hydrocarbon sidechain has an inhibiting effect on the rate of boron oxidation, regardless of whether or not a boron-carbon bond exists in the initial fuel molecule.

4. Composition profile determinations in turbulent flames reinforce the general view that the hydrocarbon oxidation reactions leading to the thermodynamically stable reaction products are only loosely coupled to the rapid oxidation of the boron-containing portion of the fuel molecule.

The above analysis will be extended to hydrocarbon derivatives of decaborane, with essentially similar conclusions.

---

* This work supported by the Bureau of Naval Weapons, Department of the Navy under contract NOw62-0604-c and Aeronautical Laboratory, USAF, MIPR (33-615) 58-52.

This study is an extension of work previously presented (Seventh Symposium on Combustion) on "Flame Front Structures of Lean Diborane-Air and Diborane-Hydrocarbon-Air Mixtures".

9. COMBUSTION OF FUEL-LEAN MIXTURES IN ADIABATIC, WELL-STIRRED REACTORS

P. H. Kydd and W. I. Foss

General Electric Research Laboratory

The use of a well-insulated, well-stirred reaction volume as a combustor allows one to investigate a hitherto-unused combustion regime beyond the lean flammability limit. The combustion of H_2, CO, CH_4, C_2H_4, C_3H_8, and mixtures of these has been studied in this regime at pressures up to 2 atm in three quite different reactors.

The reaction responsible for releasing most of the heat of combustion has a large apparent activation energy in all cases and is very fast. The activation energies and relative rates for different fuels agree with those determined in flames at higher temperatures. The rate of heat release with hydrogen does not depend on the partial pressure of oxygen when the latter is present in large excess, and is proportional to the total pressure. Mixtures of hydrogen with other fuels exhibit lower rates of combustion than does hydrogen alone.

A qualitative explanation of the results in terms of the currently accepted mechanism of hydrogen combustion is presented.

10. KINETIC STUDIES IN STIRRED REACTORS:

Combustion of Carbon Monoxide and Propane

H. C. Hottel, G. C. Williams, N. M. Nerheim*, and G. R. Schneider**

Massachusetts Institute of Technology

The burning rates of carbon monoxide and of propane premixed with oxygen, nitrogen and water vapor were measured. Carbon monoxide was burned in a one-inch diameter spherical reactor over a 14-fold range of equivalence ratio from 0.14 to 1.9, a 7-fold range of oxygen-nitrogen ratio, a 10^5- fold range of water vapor concentration, and a 6-fold range of absolute pressure, with a resultant temperature range of 1280° to 1680°K. Lean mixtures of propane were burned in a three-inch diameter reactor over a range of equivalence ratio of 0.51 to 0.95, a 6-fold range of pressure, a 3-fold range of water vapor concentration and a range of temperature of 1400° to 1900°K.

---

* California Institute of Technology

** Rocketdyne Div., North American Aviation

Burning rates were determined from measured flow rates and analysis of reactor products removed through water-cooled sampling tubes. The experimental burning rates were correlated with operating parameters by simplified over-all rate expressions.

The resulting expression for the rate of combustion of carbon monoxide is

$$\dot{N}_{CO_2} = 12 \times 10^{10}\, e^{-16,000/RT} f_{O_2}^{0.3} f_{CO} f_{H_2O}^{0.5} \left(\frac{P}{RT}\right)^{1.8}$$

where $\dot{N}_{CO_2}$ is the reaction rate in g moles/(sec) (ml), f_1 is the mole fraction of constituent i in the reactor. In this, f_{O_2} lies between 0.06 and 0.12; for a wider range of mole fraction of unreacted oxygen a simple power function did not fit the data, which were better correlated by replacing f_{O_2} by $17.5\, f_{O_2}/(1+25 f_{O_2})$.

A plausible kinetic mechanism leads to an over-all rate formulation in accord in form with the above rate expression. One mechanism suggested calls for a burning rate limited by the reaction

$$CO + OH \longrightarrow CO_2 + H \qquad (1)$$

The OH and H involved in this step multiply by chain branching in accordance with the following three processes, assumed to be in equilibrium, and chains are

$$OH + H_2 \longrightarrow H_2O + H \qquad (2)$$

$$H + O_2 \longrightarrow OH + O \qquad (3)$$

$$O + H_2 \longrightarrow OH + H \qquad (4)$$

terminated by three-body collisions, R + R + M stable products, where R is any of the above radicals. The values of the rate constants required to fit this theory to experimental data at a single mean temperature were consistent with literature values.

In the burning of propane the only unburned species found in the gas samples were carbon monoxide and, in much smaller concentration, hydrogen. The above rate expression for CO, with the constant changed from 12 to 8.7, was found to fit the propane data fairly well, although a somewhat better fit is achieved by the relation

$$\dot{N}_{CO_2} = 2.9 \times 10^{10} e^{-15,000/RT} f_{O_2}^{0.35} f_{CO} f_{H_2O}^{0.4} \left(\frac{P}{RT}\right)^{1.75} \text{g moles/sec ml}$$

A possible mechanism is suggested similar to that given for CO above, but involving the additional very fast reaction of propane to CO, H_2 and H_2O at the expense of some of the free radicals appearing in steps 1-4.

11. COMPOSITION PROFILES OF THE DIETHYL ETHER-AIR TWO-STAGE REACTION STABILIZED IN A FLAT-FLAME BURNER

W. G. Agnew and J. T. Agnew

General Motors Research Laboratories

The self-ignition process, by which initially slow low-temperature reactions develop into rapid high-temperature aerodynamic flames, is one aspect of hydrocarbon combustion which is of particular interest in the field of internal combustion engines, wherein the largest part of hydrocarbon fuels is consumed. In an effort to better understand this process, the two-stage diethyl ether-air low temperature oxidation process has been stabilized in a flat-flame burner, and attempts have been made to delineate the chemical reaction mechanism by tracing concentrations of the intermediate products with the use of combined gas chromatographic and mass spectrometric techniques.

Experimental Methods

All of the experimental data presented were obtained with a rich ether-air mixture having an equivalence ratio of 3.9. With such a mixture, two cool flames, characterized by excited formaldehyde emission, are spatially stabilized in the flat-flame burner at distances of 0.25 and 0.7 inches from the burner exit. Samples of the reacting mixture were obtained at ten positions from the burner exit to a distance of 0.9 inch beyond the burner exit. Sampling was by means of a fine quartz probe with nominal tip dimensions of 0.6 mm o.d. and 0.13 mm i.d. Lines from the probe to and including the 25 cc. sampling volume of the gas chromatograph were heated and evacuated to 0.5 atm. The mixture flowed continuously through the sampling system until the sampling valve was switched to the position which allowed the helium carrier gas to sweep the portion trapped in the sample volume into the chromatographic column for analysis. The effluent from the chromatographic column passed through a heated line to the ionization chamber of a Bendix TOF mass spectrometer, which was used for identification of the analyzed compounds.

Results

In addition to ether, nitrogen, and oxygen, quantitative data for twenty-seven intermediate and/or final products have been determined as a function of position in the reaction zone. The concentrations of the various products range from 20 volume per cent to less than 50 parts per million. The total mole fraction, obtained by summing up the experimentally determined mole fractions of the various species at the ten sampling positions, deviated only ± 3.5 per cent from unity, indicating that no major intermediate products went undetected. Mass balances for the C and H atoms deviated by about $\pm 8\%$, whereas the O atom balance indicated a maximum deficiency of about 11% at the leading edge of the second-stage flame. Behind the first cool flame approximately 30 per cent of the original ether and oxygen were converted to products, and the following species accounted for 96 per cent of the products:

Major Reaction Products After First-Stage Flame	Concentration Moles/100 Moles (N_2 + Ar)
Water	5.95
Acetaldehyde	4.82
Carbon Monoxide	2.46
Hydrogen	1.92
Methyl Alcohol	1.30

Ethylene	1.23
Acetic Acid	.81
2-Methyl-1, 3-Dioxacyclopentane	.50
Carbon Dioxide	.46
Formaldehyde	.27
	19.72

In the second cool flame approximately 75 per cent of the original ether and oxygen were converted, and only six species accounted for 91 per cent of the products:

Major Reaction Products in Second-Stage Flame	Concentration Moles/100 Moles (N_2 + Ar)
Carbon Monoxide	14.63
Hydrogen	13.10
Water	12.78
Ethylene	6.73
Methane	4.95
Acetaldehyde	4.20
	56.39

Behind the second-stage flame, the original reactants are completely consumed, and five species account for 94 per cent of the products:

Major Reaction Products Behind Second-Stage Flame	Concentration Moles/100 Moles (N_2 + Ar)
Carbon Monoxide	27.48
Water	21.65
Hydrogen	19.40
Methane	11.77
Ethylene	7.98
	88.28

The outstanding gross features of the composition profile data are:

(1) The early appearance and subsequent disappearance of acetaldehyde, formaldehyde, and the ring compound 2-methyl-1, 3-dioxacyclopentane.

(2) Low concentrations of carbon dioxide throughout the flame zone, albeit in increasing amounts.

(3) A steady increase in the concentrations of carbon monoxide, hydrogen, and water; carbon monoxide being the major product at the 0.9 inch position.

(4) Appearance of methane rather late in the reaction with subsequent steady increase to significant amounts at the 0.9 inch position.

(5) Early appearance of ethylene with subsequent steady increase to the 0.8 inch position, and then a slight decrease at the 0.9 inch position.

(6) Formation and subsequent degradation of other oxygenated compounds between stages.

(7) Appearance of highly unsaturated hydrocarbons in the late stages of the reaction.

Comparison of calculated equilibrium compositions with those experimentally obtained provides clear evidence for lack of chemical equilibrium in the products behind the second cool flame.

Thermochemical calculations from the measured composition profiles indicate that the reactions are neither appreciably endothermic nor exothermic in the first 0.5 inch, but the product enthalpy increases primarily as a result of heat transfer into the mixture. Just before the second-stage flame a strong endothermic reaction sets in, which draws its heat from an equally strong exothermic reaction in and immediately behind the second-stage flame. This interlocked thermochemical process appears to be the modus operandi of the stabilized two-stage flame.

Reaction Mechanisms

For discussion purposes the reaction zone is divided into three regimes. In the first regime, from the burner port up to and including the appearance of the first cool flame, the initial reactions of the ether molecule are of primary interest. In the rich mixture involved it is reasonable to expect that degradation of ether occurs both by thermal decomposition and by hydrogen abstraction. Hydrogen abstraction is considered to be primarily by hydroxyl radicals, but also in part by other oxygenated radicals, and by hydrogen atoms. Thus, the principal reactions in the first regime are (reaction numbers correspond to those used in the complete paper):

Decomposition,

$$C_2H_5OC_2H_5 \longrightarrow C_2H_5O\dot{C}H_2 + \dot{C}H_3 \qquad (1)$$

Hydrogen Abstraction by $\cdot OH$,

$$C_2H_5OC_2H_5 + \cdot OH \longrightarrow C_2H_5OC_2\dot{H}_4 + H_2O \qquad (9)$$

Hydrogen Abstraction by Oxygenated Radicals, e.g.,

$$C_2H_5OC_2H_5 + CH_3COO\cdot \longrightarrow C_2H_5OC_2\dot{H}_4 + CH_3COOH \qquad (18)$$

Hydrogen Abstraction by $H^{\cdot}$,

$$C_2H_5OC_2H_5 + H\cdot \longrightarrow C_2H_5OC_2\dot{H}_4 + H_2 \qquad (32)$$

In addition to the foregoing initiating reactions, the following secondary reactions are proposed to explain the observed products:

$$C_2H_5O\ \dot{C}H_2 \longrightarrow CH_3CHO + \dot{C}H_3 \qquad (3)$$

$$C_2H_5OC_2\dot{H}_4 \longrightarrow C_2H_5O\cdot + C_2H_4 \qquad (19)$$

$$C_2H_5OC_2\dot{H}_4 \longrightarrow C_2\dot{H}_5 + CH_3CHO \qquad (21)$$

$$C_2H_5OC_2\dot{H}_4 + O_2 \longrightarrow C_2H_5OCH(CH_3)\,OO\cdot \qquad (10)$$

$$C_2H_5OCH(CH_3)OO\cdot \longrightarrow \overline{CH_2OCH(CH_3)O\dot{C}H_2} + \cdot OH \qquad (11)$$

$$C_2H_5OCH(CH_3)OO\cdot \longrightarrow CH_3\dot{C}OOH + C_2H_5O\cdot \qquad (12)$$

$$C_2H_5O\cdot \longrightarrow CH_3CHO + H\cdot \qquad (34)$$

$$CH_3CHO + O_2 \longrightarrow CH_3C(O)OOH \longrightarrow \begin{cases} CH_3COO\cdot + \cdot OH \\ CH_3COOH + \cdot O \end{cases} \qquad (13), (14), (16)$$

$$CH_3CHO + {}^{\cdot}OH \longrightarrow CH_3CO^{\cdot} + H_2O \qquad (36)$$

$$CH_3CO^{\cdot} \longrightarrow CH_3^{\cdot} + CO \qquad (37)$$

$$CH_3O^{\cdot} + {}^{\cdot}OH \longrightarrow HCHO^{*} + H_2O \qquad (31)$$

$$CH_3^{\cdot} + O_2 \begin{cases} \longrightarrow (x)HCHO^{*} + (1 - x)\,HCHO + {}^{\cdot}OH & (5) \\ \longrightarrow CH_3OO^{\cdot} \longrightarrow HCHO + {}^{\cdot}OH & (6), (7) \\ \qquad\qquad\quad \longrightarrow CO + H_2 & (8) \end{cases}$$

In the second regime, between the two cool flames, the concentrations of ethylene, hydrogen, and carbon monoxide continue to increase by the same mechanisms as in the first regime. However, new features of the second regime are the appearance and rapid increase in the concentration of methane, the attainment of peak concentrations of the oxygenated intermediates, and the appearance of acetylene late in the regime.

Additional production of methane and carbon monoxide is believed to occur by a Rice-Herzfeld decomposition of acetaldehyde, while methane is also probably formed in a sub-chain mechanism involving ethylene, hydrogen, and methyl radicals:

$$CH_3^{\cdot} + H_2 \longrightarrow CH_4 + H^{\cdot} \qquad (47)$$

$$C_2H_4 + H^{\cdot} \longrightarrow C_2H_5^{\cdot} \qquad (41)$$

$$C_2H_5^{\cdot} + H_2 \longrightarrow CH_4 + CH_3^{\cdot} \qquad (48)$$

The $HCO^{\cdot}$ radical produced in the decomposition of acetaldehyde may react with hydrogen atoms to give excited formaldehyde:

$$HCO^{\cdot} + H^{\cdot} \longrightarrow HCHO^{*} \qquad (52)$$

with consequent luminous emission. This reaction is supported by an earlier observation by the authors that with slightly leaner mixtures, emission from the second-stage flame is that of HCO^{*} rather than $HCHO^{*}$.

Acetylene production is considered to be due to the decomposition of ethylene:

$$C_2H_4 \longrightarrow C_2H_2 + H_2 \qquad (49)$$

Principal features of the third regime are further major increases in the concentrations of methane, carbon monoxide, water, acetylene, and hydrogen, and slight increases in the concentrations of hydrogen and ethylene. These changes are brought about primarily by increases with temperature in the rates of reactions mentioned earlier. No additional elementary reactions are involved in the third reaction regime.

The fact that these products are not in temperature equilibrium indicates that certain of the elementary reactions are rate-limiting. Additional research with other mixture ratios and other fuels should lead to further confirmation of the reaction mechanisms. Ultimately, a kinetic study made with the aid of high-speed computer techniques might validate the proposed reaction mechanism and at the same time provide estimates of rate constants for some of the presently ill-defined elementary reactions.

12. A MASS SPECTROSCOPIC STUDY OF STABILIZED "LOW TEMPERATURE" FLAMES OF ALDEHYDES

J. N. Bradley, G. A. Jones, G. Skirrow and C. F. H. Tipper

The University of Liverpool

Williams, Johnson and Carhart [1] have shown that cool flames and two-stage ignitions in hydrocarbon/oxygen mixtures can be stabilized in a flow system with a vertical tube reactor. The aim of the present work was to study the temperature and composition profiles of such stabilized "low temperature" flames with a view to determining the processes responsible for the various types of ignition.

The apparatus was similar to that of Williams et al [1]. The reactor was a cylindrical purex tube [40 cms long and 4 cm diameter] fitting closely into a second glass tube wound with heating tape [the windings being about 1 cm apart]. This was enclosed by a light tight metal box with a window in one side for viewing and photographing the flames. The whole could be moved vertically. A stream of nitrogen carried fuel from thermostated flasks to a T-piece where oxygen and argon were added. The mixture passed into the bottom of the reactor and through a bed of glass beads to ensure complete mixing. Temperatures were measured with a very fine platinum/platinum-rhodium thermocouple encased in a very thin quartz sheath. Composition profiles were determined mainly by means of an A. E. I. M. S. 10 mass spectrometer [mass range 2-100]. This was mounted on a framework so that it was directly above the reactor and was evacuated by a high speed mercury diffusion pump and an oil pump. Sampling was by a fine vertical quartz probe attached to the mass spectrometer so that the gas mixture passed directly into the ionization chamber. The internal diameter of the probe tip was such that the change in pressure inside the mass spectrometer when the pressure outside the tip varied from 10^{-3} mm to one atmosphere was $1 - 3 \times 10^{-7}$ mm.

Acetaldehyde and propionaldehyde were used as fuels. By means of an envelope round the probe attached to a separate gas handling system the mass spectra of individual reactants, of probable products and of mixtures were obtained [with an electron energy of 15 eV]. Tests showed that no appreciable fractionation of mixtures occurred in the probe. By correcting the mass spectra of the reaction mixture for background, using the calibration spectra and relating all peak heights to that for mass 40 [argon] [thus allowing for variation in flow speed through the probe as the temperature varied] it was possible to determine the relative concentrations of molecular species present.

The reactor, at a suitable temperature, was first "flushed out" with the aldehyde-nitrogen mixture and then oxygen and argon were added. As the concentration of oxygen was increased a cool flame formed as a flat disc [$\sim$ 2 mm thick and very pale blue]. On increasing the proportion of oxygen slowly a second stage flame in the form of a brighter blue parabola [tip toward the cool flame] appeared; this moved towards the cool flame becoming flatter and brighter and a third flame [yellow in color and a thin cone in shape] formed just above it. By careful control of conditions it was possible to cause the one, two or three flames to remain "stationary" for as long as 30 minutes. Under these circumstances temperature or composition profiles were determined by moving the reactor with respect to the thermocouple or probe tip, taking measurements at suitable points.

The linear flow rate through the reactor was about 5-10 cms sec^{-1} so that the whole oxidation process took only a few seconds. With acetaldehyde and a tube temperature of 200°C stable flames were observed with ratios of aldehyde:oxygen:inert gas of between 4:1:13 and 2:1:9 [cool flame only], of about 1:1:5 [two flames] and about 2:3:9 [three flames]. With just a cool flame no change from initial conditions was detected until about half a second before the luminous zone when the temperature started to rise and reactants to be consumed. Through the luminous zone the temperature rose to about 425°C, the concentrations of aldehyde and oxygen fell to about half [or less with oxygen] of their originial values and carbon monoxide, carbon dioxide, formaldehyde, methanol and methane were produced. On decreasing the relative amount of oxygen in the mixture entering the reactor, the yield of methane and methanol rose relative to formaldehyde. About half a second after the luminous zone the temperature began to decrease gradually and little further oxidation occurred. With the two stage ignition, between the flames [the temperature was 470-490°C] the concentrations of aldehyde and oxygen decreased and that of methane increased while the amounts of other components did not alter appreciably. However just before the second flame the concentration of methanol fell and that of formaldehyde rose quite markedly, though both fell sharply nearly to zero in this flame [temperature ~ 690°C] as did the aldehyde and oxygen while the amounts of carbon monoxide, carbon dioxide and methane rose sharply and some acetylene and hydrogen were formed. As the initial proportion of oxygen was increased and the second flame became brighter, the yield of methane and acetylene in this flame rose as did its temperature, but in the yellow flame [temperature 800°C only a little above that of the blue flame 770°C] the amount of methane decreased whereas that of acetylene was considerable and some "soot" appeared to be produced. On adding a small proportion of methane to the initial gas mixture the yellow flame became much brighter and the concentration of acetylene and the soot formation rose markedly.

With propionaldehyde as the fuel the reactor temperature had to be raised to about 270°C to obtain a cool flame and then the two and three stage flames appeared on increasing the initial proportion of oxygen only slightly. Some acetaldehyde and ethanol as well as methane, carbon monoxide, carbon dioxide and methanol were formed in the cool flame but the main organic product was formaldehyde.

The main products of the cool flame of acetaldehyde can be accounted for by the decomposition of acetyl radicals to give methyl radicals and carbon monoxide followed by the reaction of the methyl radicals with oxygen to give formaldehyde and methanol or with aldehyde to give methane. Just before the second stage flame some methanol probably oxidized giving more formaldehyde, the reaction of which with oxygen gave enhanced branching, producing the blue flame. This is in line with the ease of formation of two stage flames with propionaldehyde where the cool flame gave a relatively high yield of formaldehyde. Probably oxygen catalyzed pyrolysis of the methane gave acetylene and hydrogen and the yellow flame was the decomposition flame of the acetylene.

Reference

1. Williams, K. G., Johnson, J. E. and Carhart, H. W.: Seventh Symposium on Combustion, p. 392, Butterworths, 1959.

13. THE COOL FLAME COMBUSTION OF HYDROCARBONS

B. H. Bonner and C. F. H. Tipper

The University of Liverpool

The cool-flame combustion of organic fuels has been the subject of a number of investigations, but the elementary chemical reactions occurring in the low-temperature ignition region, and in particular those responsible for cool-flame formation, are still by no means clear. 1/ With a view to obtaining more information on such reactions the oxidation of two typical hydrocarbons, cyclohexane and n-heptane, has been studied between 200° and 350°C and total pressures of 20 to 200 mm using either an uncoated vessel [the surface being acid treated] or one coated with boric oxide, potassium chloride, sodium hydroxide or lead oxide. Some work has also been done with propane as fuel.

A conventional static system was used with a cylindrical pyrex reaction vessel [volume, 150 ml]. The progress of an oxidation was followed by measuring the pressure or temperature change in the vessel with a Bourdon gauge or differential thermocouple arrangement respectively. The products were also investigated by means of paper and gas-liquid chromatography, particular attention being paid to the peroxides and aldehydes formed. It was also possible to observe the cool-flames through a window in the furnace.

The pressure-temperature limits of cool-flame production were determined for 1:1 hydrocarbon/O_2 mixtures and also some mixture composition limits at single temperatures. A cool flame was indicated by a pressure and temperature "kick" after an induction period (τ) and observation showed that they spread out from the center of the vessel.

Uncoated Vessel

The lowest temperature for cool-flame formation was about 230°C with n-heptane, 250°C with cyclohexane and 290-300°C with propane. At these lower limits and the same total pressure the intensity of the flame decreased and τ increased on changing from C_7H_{16} to C_8H_{12} to C_3H_8. The lowest total pressure for cool-flame combustion of n-heptane and cyclohexane at the lower limit temperatures occurred with about 35-40% hydrocarbon in the mixture. Outside the limits there was an extensive zone of slow oxidation. Packing the vessel shifted the cool-flame peninsulas to higher temperatures and pressures. The flame speeds were estimated to be 5-10 cm sec^{-1}.

The main peroxidic products before a cool flame below 300°C were dihydroperoxyheptane with C_7H_{16}, cyclohexylhydroperoxide with C_6H_{12} and hydrogen peroxide with C_3H_8. With the first two fuels the amount of hydroperoxide increased to a maximum ($\sim 10^{-6}$ mole) during the induction period, but fell almost to zero after the passage of the cool-flame, being replaced by H_2O_2. Small amounts of aldehydes (together with other products, e.g., ketones, olefins) were formed during τ but the yield was greatly increased by the passage of the flame.

Addition of acetaldehyde initially only decreased τ for a cyclohexane/O_2 mixture appreciably if the amount added was at least 100 times greater than the total concentration of aldehyde present in the mixture just before the cool-flame. However, preforming small quantities of $C_6H_{11}OOH$ in the vessel [by reaction of a 90%

hydrocarbon/10% O_2 mixture] could reduce τ to almost zero.

Coated Vessels

A boric oxide surface raised the lower cool-flame limit with cyclohexane by about 20°C and τ was reduced by hydration of the surface, but otherwise the results were the same as with an uncoated vessel. A fresh sodium hydroxide surface had a very marked inhibiting effect on cool-flame formation with both n-heptane and cyclohexane but this effect decreased with aging, the reproducible lower limit for the former being approximately the same as and for the latter being only about 12°C higher than with an uncoated vessel.

With a potassium chloride coating the lower cool-flame limit of cyclohexane was raised by about 40°C and the slow reaction region disappeared completely. Observation showed that the speed of the cool-flames was much less ($\sim$1-2 cm sec^{-1}). No products could be detected in the induction period until just before the cool-flame but then they were much the same as with the uncoated vessel. If the vessel was only half-coated with KCl the limit was somewhat lower than with the fully-coated vessel but otherwise the results were unchanged.

Coating with PbO raised the lower limit with n-heptane by about 25°C and with cyclohexane by about 60°C, the cool-flames propagating "slowly." The products with C_7H_{16} were much the same, but with C_6H_{12} the main peroxide present was H_2O_2.

The results indicate strongly that, at any rate with saturated hydrocarbons as fuels, the ease of formation of cool-flames is related to the ease of build up of hydroperoxides, in particular dihydroperoxides, in the mixture at the beginning of the oxidation under particular conditions. Presumably homogeneous decomposition of the hydroperoxides leads to much more rapid branching of the free radical chains than the oxidation of aldehydes. The general chain mechanism given can thus be suggested:

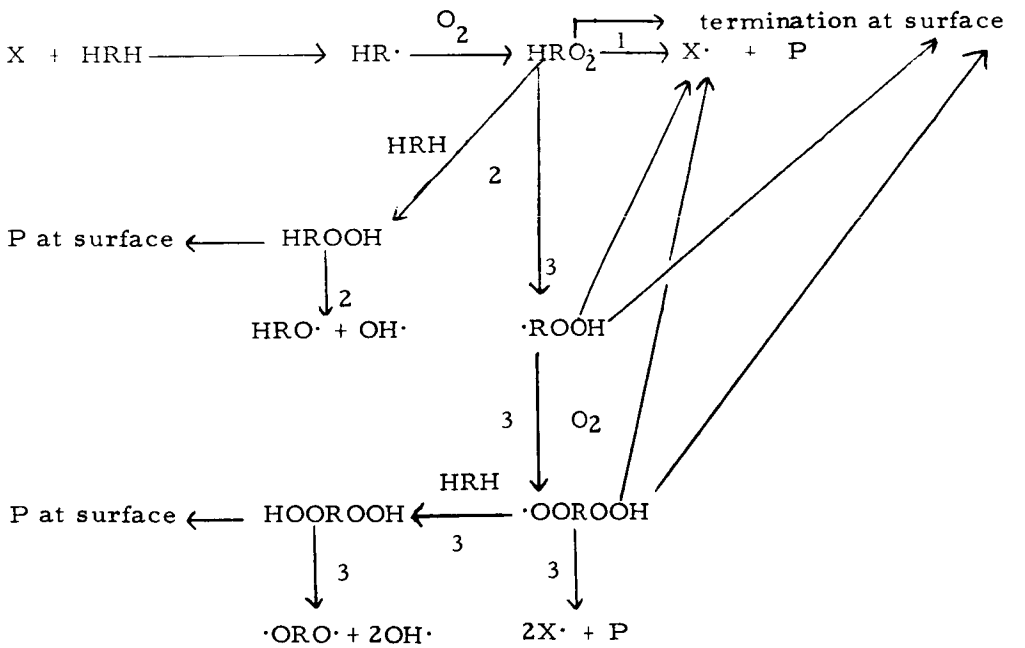

HRH represents the hydrocarbon, X· a radical which is not peroxy, (e.g., OH·, alkoxy) and P non peroxidic products (e.g., aldehydes, ketones, olefins, cyclic ethers). Examples of such types of elementary reactions have been given previously. 1/

Route 1 leads to relatively slow branching, e.g., propane, route 2 to much more rapid branching, e.g., cyclohexane with an uncoated vessel, and route 3 to relatively very rapid branching, e.g., n-heptane. The inhibition of cool-flame production by KCl and PbO is probably due to the increase in the rates of destruction of the various peroxy radicals and hydroperoxides at the surface.

Reference

1. Minkoff, G. J. and Tipper, C. F. H.: Chemistry of Combustion Reactions. Butterworths, 1962.

DISCUSSION

ON

ELEMENTARY COMBUSTION REACTIONS

14. REVIEW PAPER

P. G. Ashmore

Manchester College of Science and Technology, England

(No Abstract)

15. THE REACTION OF OXYGEN ATOMS WITH NEOPENTANE AND OTHER ALKANES--MECHANISM AND RATES

Franklin J. Wright

Esso Research and Engineering Company

The reaction of oxygen atoms with neopentane and other alkanes has been studied in the gas phase at 30°C. Oxygen atoms, $O(^3P)$, were produced in the absence of molecular oxygen and other potentially active species by the titration technique developed by Kaufman which is based on the reaction $N + NO \longrightarrow N_2 + O$.

Apart from CO, CO_2 and water, the principal products of the reaction of oxygen atoms with neopentane are acetone and 1,1 dimethylcyclopropane together with smaller amounts of pivaldehyde and neopentyl alcohol. The effect of pressure and hydrocarbon concentration on these products has been investigated.

The results of the present work support the displacement mechanism previously advanced to explain the behavior of the iso-butane-oxygen atom system. It had been concluded from that study that neither abstraction of a single hydrogen by the oxygen atoms nor insertion of the oxygen atoms into a C-H bond played an important role and that the reaction products are formed in a more direct fashion by the simultaneous replacement by an oxygen atom of two groups on the parent hydrocarbon with the attendant formation of a carbonyl group. This hypothesis will account for the detailed behavior of both the neopentane and iso-butane systems; it encompasses many of the observations made on other alkanes, in particular the product distributions, and it offers an explanation for the observed reaction rates.

The formation of 1,1 dimethylcyclopropane appears to result from a one step abstraction whereby the oxygen atom simultaneously removes two hydrogens from the parent hydrocarbon rather than a two step process involving a neopentyl radical.

The over-all rates of the reaction of oxygen atoms with n-butane, iso-butane and neopentane as well as the rates of several primary reactions have been calculated from the observed variations of the yields of reaction products with initial hydrocarbon concentrations. The values of the over-all rates for n-butane, iso-butane and neopentane were found to be 1.1×10^{-14}, 0.6×10^{-14} and 0.3×10^{-14} cc $mole^{-1}$ sec^{-1}, respectively at 30°C.

16. THE KINETICS OF HYDROGEN ATOM RECOMBINATION

B. A. Thrush and F. S. Larkin

The University of Cambridge

The homogeneous recombination of hydrogen atoms has been studied in a fast flow system at temperatures between 200° and 350°K, using a calorimetric probe technique. Data for argon as third body agree with shock-tube studies of the dissociation reaction in the presence of argon, the over-all temperature dependence of the recombination reaction being close to T^{-1}. Experiments in which water was added to the discharge products show that water is not particularly effective as a third body in contrast to its behavior in the $H + O_2$ reaction.

17. PROPAGATION OF THE HYDROGEN-HALOGEN CHAIN

J. R. Airey, J. C. Polanyi and D. R. Snelling

University of Toronto

In these experiments partially dissociated deuterium gas passed into the center of a 1-foot diameter glass sphere, internally coated with a reflecting layer of gold. The sphere constituted an integrating sphere for infrared emission; part of the emission finds its way, after multiple reflection, through an exit slot covered by a sapphire window. Under one set of conditions a mixture of chlorine and hydrogen entered the vessel through a second tube concentric with the deuterium inlet. The following chain of reactions takes place:

$$D + X_2 \xrightarrow{1} DX^\dagger + X$$

$$X + H_2 \xrightarrow{2} HX + H$$

$$H + X_2 \xrightarrow{3} HX^\dagger + X$$

$$X + H_2 \xrightarrow{2} \text{etc.}$$

$$H + X \xrightarrow{+W} HX$$

$$X + X \xrightarrow{+W} X_2$$

$$H + H \xrightarrow{+W} H_2$$

The most probable third body, W, in the chain termination step at these pressures (ca. 4.10^{-2} mm Hg) is the metal wall. The total pressure is too low for appreciable $HX^\dagger$ (vibrationally excited HX) to be formed in the gas phase recombination, H + X + M. It follows that any vibrationally excited HX (evidenced by infrared emission) must be formed in a chain propagating step. Reaction 2 is normally thermoneutral. Nonetheless it could give rise to appreciable $HCl^\dagger$ if Cl were translationally hot.

Studies of the energy distribution among products of the reactions $H + Cl_2 \longrightarrow HCl + Cl$, $H + Br_2 \longrightarrow HBr + Br$ and (in a preliminary fashion) $D + Cl_2 \xrightarrow{1} DCl + Cl$, have shown in every case that the most probable reaction path channels the heat of reaction preferentially into relative translation of the products and into rotation of the new molecule. The energy available for distribution among the products of reaction 1 is Q + E (heat of reaction + activation energy) = 49 kcal/mole. This is almost an order-of-magnitude greater than the activation energy of reaction 2 ($E_2 \approx 5.5$ kcal/mole).

The question at issue is whether reaction 2 is predominantly $\underline{X} + H_2$, where $\underline{X}$ represents a translationally-hot atom. To put this to the test experiments were performed in which (a) the ratio of $[Cl_2] : [H_2]$ was altered (Cl_2 is a good deactivator for $\underline{Cl}$, whereas H_2 is a poor one), and (b) argon was added. It was found that (a) was without effect on the chain length, and (b) increased the chain length (presumably by decreasing the importance of the chain termination at the wall).

We conclude that reaction 2 involves predominantly thermalized X atoms.

Even if we accept the argument that $\underline{X}$ is formed in reaction 1, it does not follow from the observations reported here that the collision efficiency of the reaction $X + H_2$ is insensitive to the presence of translational energy in the attacking atom. The reaction $\underline{X} + H_2 \xrightarrow{2} HX + H$ would only become important as a chain carrier if it could compete favorably with translational-translational transfer, which requires only about 7 collisions.

From the failure to observe hot-atom effects in this system, we may only conclude that any enhancement in the rate of reaction 2 is insufficient to bring it into the region of collision efficiency $\geqslant 0.14$.

18. QUANTITATIVE ASPECTS OF FREE RADICAL REACTIONS IN COMBUSTION

C. F. Cullis, A. Fish and J. F. Gibson

Imperial College

Methods are described whereby quantitative information can be obtained regarding the kinetic parameters of certain of the elementary reactions involved in combustion if similar data on other constituent steps are available. Thus, by a complete stationary state analysis of a theoretical model and comparison of its predictions with the results of over-all kinetic experiments, the validity of the model may be tested. Insertion of the kinetic parameters which can be obtained by direct measurement then enables similar data to be obtained for other elementary reactions which are not readily accessible to direct study.

This paper shows in particular how such general methods can be applied to the spontaneous ignition of n-heptane + oxygen + inert gas mixtures at temperatures from 440-650°C. In this temperature region, an "olefin" mechanism describes the ignition limit, predicting closely the experimental variations of the limiting pressure for ignition with reactant and inert gas concentrations, with temperature and with the size and shape of the reaction vessel. It is thus shown, for example, how a value of the activation energy for the reaction:

$$HO_2^{\cdot} + C_7H_{16} \longrightarrow H_2O_2 + C_7H_{15}^{\cdot}$$

can be obtained using the known value of the activation energy for the decomposition of hydrogen peroxide. The relative efficiencies of oxygen and nitrogen as the "second body" in the homolytic breakdown of hydrogen peroxide have also been estimated and the results are able to account quantitatively for the marked promoting effect of inert gases on the ignition of n-heptane.

19. THE USE OF THE HYDROGEN-OXYGEN REACTION IN THE EVALUATION OF VELOCITY CONSTANTS

R. R. Baldwin, D. Jackson, R. W. Walker and S. J. Webster

The University of Hull

Studies of the H_2/O_2 reaction have given information on some of the reactions of the radicals H, O, OH and HO_2 with hydrocarbons, CO and H_2O_2 in the region of 500°C. The inhibiting action of hydrocarbons on the second limit has given Arrhenius parameters for H + RH in the case of ethane, propane, n- and i-butane. More restricted information on the reaction of O and OH with these hydrocarbons is also obtained. Studies of the yields of CO_2 and H_2O in slowly reacting $H_2/CO/O_2$ mixtures enable the ratios $k_{OH + CO}/k_{OH + H_2}$ and $k_{HO_2 + CO}/k_{HO_2 + H_2}$ to be evaluated. Studies of the decomposition of H_2O_2 sensitized by H_2 give the relative rates of OH + H_2 and OH + H_2O_2, as well as the ratio of the rates of H + H_2O_2 = H_2O + OH and H + H_2O_2 = H_2 + HO_2. Study of the reduction of this sensitizing effect by traces of added O_2 enables the ratio of the rates H + H_2O_2 = H_2 + HO_2 and H + O_2 + M = HO_2 + M to be determined.

20. ARRHENIUS PARAMETERS FOR ELEMENTARY COMBUSTION REACTIONS: H-ATOM ABSTRACTION FROM N-H BONDS

Peter Gray

University of Leeds

and

J. C. J. Thynne

University of Edinburgh

Results are presented of studies on the kinetics of hydrogen-atom abstraction by methyl radicals from substrates containing nitrogen-hydrogen bonds, viz, ammonia, trideuteroammonia, hydrazine, unsymmetrical dimethylhydrazine, methylamine trideuteromethylamine and methylamine-d_2. The new results are summarized as follows:

Values of Arrhenius Parameters for Hydrogen Abstraction Reactions

Reactions	$Log_{10}(A/cm^3 mole^{-1} sec^{-1})$	$(E/kcal.mole^{-1})$
$CH_3 + ND_3 \longrightarrow CH_3D$	11.00	10.95
$CH_3 + NH_3 \longrightarrow CH_4$	10.84	9.8
$CH_3 + N_2H_4 \longrightarrow CH_4$	11.00	5.0
$CH_3 + (CH_3)_2NNH_2 \longrightarrow CH_4$	11.34	5.8
$CH_3 + CH_3ND_2 \longrightarrow CH_3D$	9.61	7.0
$CH_3 + CH_3ND_2 \longrightarrow CH_4$	11.15	9.0
$CH_3 + CD_3NH_2 \longrightarrow CH_3D$	10.90	10.1
$CH_3 + CD_3NH_2 \longrightarrow CH_4$	9.77	6.0
$CH_3 + CH_3NH_2 \longrightarrow CH_4 (+ \cdot CH_2NH_2)$	11.0	8.7
$CH_3 + CH_3NH_2 \longrightarrow CH_4 (+ CH_3\dot{N}H)$	9.55	5.7
$CH_3 + CH_3N = N CH_3 \longrightarrow CH_4$	10.94	7.81

The implications of these results may be summarized as follows;

(1) Primary isotope effects, i.e., the relative reactivities of H and D are in accord with expectations based on zero-point energy differences for a single X-H bond-stretching frequency; (2) secondary isotope effects are insignificant; (3) hydrazine is attacked much more readily than ammonia (300-fold ratio of reactivities at 150°C) and this is a consequence of a lowered activation energy, both A-factors being near to "normal"; (4) when methylamine is attacked, both N and C sites are reactive; at 150°C, three out of every five H atoms come from the amine group and two from the methyl group; (5) dimethyl hydrazine is more reactive than methylamine, though the reactivity of different sites is not yet established.

Attention is paid in discussion to the interpretation of these results in terms of (a) H-N bond dissociation energies, especially in hydrazine and (b) the isoelectronic pairs CH_4 and C_2H_6; NH_3 and N_2H_4; H_2O and H_2O_2.

21. RATES OF RADICAL REACTIONS IN METHANE OXIDATION

R. V. Blundell*, W. G. A. Cook**, D. E. Hoare and G. S. Milne

Queen's College, Scotland

A variety of methane and oxygen mixtures were oxidized in acid, washed Pyrex and silica vessels mostly at temperatures between 500° and 550°C. The resultant mixtures were analyzed after varying reaction times for the reactants and the chief products (except water) i. e., carbon monoxide, carbon dioxide and formaldehyde.

Assuming that methane was chiefly oxidized as a result of reaction with hydroxyl radicals and that formaldehyde and carbon monoxide reacted either with hydroxyl radicals or hydroperoxy radicals (all of which reactions are exothermic) comparative rates of reaction were obtained. This method of comparison depends on less assumptions than the "steady state" treatment used by Semenov.

The results were shown to be in agreement with a value of 2. 1 for the relative rates of reaction of hydroxyl radicals with methane and carbon monoxide at 525°C and suggest a higher value at temperatures of 650° and 750°C. A value of 33 $\pm$ 3 was obtained for the relative rates of reaction of hydroxyl radicals with formaldehyde and methane at 550°C. Hydroperoxy radicals were shown to react 340 $\pm$ 80 times faster with formaldehyde than with carbon monoxide at 525°C. Direct reaction of formaldehyde with oxygen was shown to be slow compared with the other reactions considered except in the early stages when some direct (presumably heterogeneous) formation of carbon dioxide was observed.

---

*Associated Ethyl Co., Ltd.

**Imperial Chemical Industries

22. REACTIONS OF METHYL AND METHOXYL RADICALS WITH NITROGEN DIOXIDE AND NITRIC OXIDE

L. Phillips and R. Shaw

Explosives Research and Development Establishment, England

The reactions of methyl and methoxyl radicals with nitrogen dioxide have been studied at 50° and 90°C using the acetaldehyde/NO_2 system as radical source. Rate constants for the addition (1) $CH_3\cdot + NO_2 \longrightarrow CH_3NO_2$ and the disproportion (2) $CH_3\cdot + NO_2 \longrightarrow CH_3O\cdot + NO$ have been measured relative to that for the nitric oxide/methyl reaction (6) $CH_3 + NO \longrightarrow CH_3NO$. Taking $k_6 = 1 \times 10^{12}$ mole^{-1} cm^3 sec^{-1}, $k_1 = 1.7 \times 10^{12}$ and $k_2 = 3.3 \times 10^{12}$ mole^{-1} cm^3 sec^{-1} at 90°C; E_1 and E_2 are approximately zero. At pressures of acetaldehyde or neopentane greater than 100 mm Hg., both reactions (1) and (2) are second-order at 90°C. The relative rate constants for addition reactions (3) $CH_3O\cdot + NO \longrightarrow CH_3ONO$ and (4) $CH_3O\cdot + NO_2 \longrightarrow CH_3ONO_2$

are given by $k_3/k_4 = 1.8$. Methyl nitrite is produced at least mainly by reaction (3); direct addition of nitrogen dioxide to methyl to form methyl nitrite, if it occurs, is insignificant. The reaction $CH_3NO + NO_2 \longrightarrow CH_3NO_2 + NO_2$ was shown to be important under the experimental conditions used.

23. THE EFFECT OF SULFUR DIOXIDE ON THE SECOND PRESSURE LIMIT OF EXPLOSIONS OF HYDROGEN-OXYGEN MIXTURES

P. Webster and A. D. Walsh

Queen's College, Scotland

It is shown that SO_2 inhibits the hydrogen-oxygen reaction at the second pressure limit of explosion at 511°C. For additions of SO_2 up to ca. 3 mm Hg, the inhibition (apart from the effect of SO_2 as a third body in the reaction $H + O_2 + M = HO_2 + M$ .... (4)) is due to the removal of H atoms by the reaction $H + SO_2 + M' = HSO_2 + M'$ .... (8). The rate constant of (8) is determined to be 2.0 ± 0.3 times that of reaction (4) when $M = M' = H_2$ and so to be ca. 4×10^{-32} cm^6 $molecule^{-2}$ sec^{-1} at 511°C. For additions of SO_2 greater than ca. 3 mm Hg, it appears that an additional inhibiting reaction becomes appreciable. This further reaction is probably the removal of O atoms by the reaction $O + SO_2 + M'' = SO_3 + M''$ .....(10). If so, the rate constant of (10) when $M'' = H_2$ is probably not less than 10^{-32} cm^6 $molecule^{-2}$ sec^{-1} at 511° C, with the implication that reaction (10) produces a triplet, excited, state of SO_3.

24. H AND O ATOM PROFILES MEASURED BY ESR IN C_2-HYDROCARBON-O_2 FLAMES

A. A. Westenberg and R. M. Fristrom

The Johns Hopkins University

The feasibility of measuring labile atom profiles in flames by probe sampling combined with quantitiative ESR spectroscopy is demonstrated for the first time. The technique relies on using O_2 as a reference calibrating gas, the validity of this procedure having been proven elsewhere. In this case the O_2 was present as a diluent in the flame gases. The great potentialities of this technique for flame kinetic studies are shown by preliminary examples of absolute mole fraction profiles of H and O atoms measured in 0.1 atm flat flames of C_2H_6-O_2, C_2H_4-O_2, and C_2H_2-O_2. These are the same flames whose major stable species concentration profiles were previously reported at the Seventh Symposium, and data obtained subsequently on their temperature and velocity profiles are also given. The major species profiles were corrected for diffusion and converted to net reaction rate profiles in the usual way. Profiles of OH concentration were computed from the measured CO_2 formation rates using a rate con-

stant for CO + OH $\longrightarrow$ CO_2 + H fitted to a variety of reported data. The striking fact about the data is that the OH and fuel disappearance rate profiles definitely precede the appearance of any measurable H or O in each flame, thus pointing strongly to the exclusive reaction of the fuel with OH rather than with H or O. Since the O_2 loss rate coincides with that of the fuel, it seems likely that the O_2 reacts with the hydrocarbon fragment left after OH attack, with reaction via H + O_2 $\longrightarrow$ OH + O occurring only later in the flame. The consequences of these observations are discussed. Rate constants estimated from the data are (cm^3 $mole^{-1}$ sec^{-1}): 5 x 10^{12} for C_2H_6 + OH in the range 1300-1550°K, 1 x 10^{13} for C_2H_4 + OH in the range 1250-1400°K and 5 x 10^{15} exp (-13000/RT) for H_2CO + OH.

25. RADICAL RECOMBINATION AND HEAT EVOLUTION IN H_2-O_2 FLAMES

C. P. Fenimore and G. W. Jones

General Electric Research Laboratory

Fuel-lean H_2-O_2-Ar-N_2O flames were probed; their rates of heat evolution, $\dot{h}$, deduced from the temperature traverses; and their concentrations of H atoms deduced on the assumption that $-d[N_2O]/dt$ = (known rate constant) x $[H][N_2O]$. The $\dot{h}$ were corrected for the contribution from nitrous oxide combustion, the corrections averaging 40 per cent, and fitted to

$$\dot{h} \text{ - correction} = kQ\,[H]\,[O_2]\,[H_2O]\ ,$$

where k is the rate constant for $H+O_2 + H_2O \longrightarrow HO_2+H_2O$, and Q = heat evolved per mole of HO_2 formed. The reasonable k obtained in this way, $1x10^{17}$ cm^6 $mole^{-2}$ sec^{-1}, shows that the heat of H_2-O_2 combustion is probably evolved at the rate of formation of HO_2. The dependence of $[H]$ on pressure and mass flow is also consistent with a recombination of radicals via HO_2.

In fuel rich flames, the rate of heat evolution may be controlled by HO_2 formation far enough upstream where $[O_2]$ is considerable and the temperature is relatively low. Later in the reaction zone of rich flames, HO_2 is a less important species.

26. SOME REACTIONS OF HYDROGEN ATOMS AND SIMPLE RADICALS AT HIGH TEMPERATURES

G. Dixon-Lewis, M. M. Sutton and A. Williams

University of Leeds

Investigations of the structure of flames supported by a hydrogen-nitrogen-oxygen and a hydrogen-nitrogen-nitrous oxide mixture on an Egerton-Powling type flat flame burner have been used to derive information on the elementary reactions involved. At

atmospheric pressure the flames have final temperatures of 1072°K and 1573°K, respectively. Temperature and composition profiles are obtained by probing, and both concentration diffusion and thermal diffusion are considered in the subsequent analysis. Hydrogen atoms are estimated by added D_2, D_2O or chemiluminescence. Further results were obtained by adding traces of nitrous oxide and carbon dioxide respectively to the oxygen supported flame.

Rate constants were found as follows (l. mole.$^{-1}$ sec.$^{-1}$)

$H + O_2 = OH + O$	$k = 1.6 \times 10^7$ at 915°K.
$H + D_2O = OD + HD$	$k = 3.6 \times 10^6$ at 1072°K.
$H + N_2O = OH + N_2$	$k = 3.1 \times 10^7$ at 900°K.
	$= 2.9 \times 10^8$ at 1357°K.
$H + CO_2 = OH + CO$	$k = 5.2 \times 10^5$ at 1072°K.
$OH + H_2 = H + H_2O$	$k = 1.5 \times 10^9$ at 915°K.

Apparent second order rate constants for the recombination reactions of H + H and H + OH in the burned gas of the particular flames are also given, and third order rate constants derived over a limited composition range.

27. CARBON FORMATION IN PREMIXED FLAMES

U. Bonne, K. H. Homann and H. Gg. Wagner

University of Göttingen

The formation of carbon was studied in premixed flat flames at reduced pressure for mixtures of the following fuels with oxygen: C_2H_2, C_2H_4, C_3H_8, C_6H_6, C_2H_5OH, (CS_2 and $CS_2 + H_2$).

Mass spectrometic analysis of the flames by an arrangement which was sensitive to stable products as well as to radicals gave the concentration profile of the products in the reaction zone before and during formation of carbon particles. By electron micrographs of particles collected with the same "molecular beam" technique, the particle size distribution function, growth and concentration were determined. Optical analysis gave OH-concentration emission profiles, the concentration, average size and number of particles, and the temperature.

The experimental data obtained for various mixture compositions show that the polyacetylenes formed in the reaction zone play a decisive role in the formation and growth of the soot particles. The concentration of the polyacetylenes goes through a maximum early in the reaction zone and reaches constant fuel value in the burned gas. With increasing fuel content their final concentration increases. The carbon particles become detectable ($\sim$40 Å) a short distance behind the oxidation zone. In the region where the polyacetylene concentrations decrease the size of the particles increases by

agglomeration of small particles and by addition of high polyacetylenes and polyacetylene radicals; the number density of carbon particles goes down. Finally a state is reached where the radicals are consumed and where the particle diameter, particle number and the total amount of carbon formed become constant, although the concentration of acetylene and of polyacetylenes is comparatively high.

28. THE OXIDATION REACTIONS OF ACETYLENE AND METHANE

G. P. Glass, G. B. Kistiakowsky, J. V. Michael, and H. Niki

Harvard University

The high temperature oxidation reactions of acetylene and methane have been studied in shock waves using two techniques. A time-of-flight mass spectrometer has been used to determine the concentration of reactants, intermediates and products at 50 microsec. intervals throughout the reaction. In another apparatus the chemiluminescent radiation emitted by CH and C_2 and the ionization accompanying the oxidation have been monitored.

The oxidation of acetylene proceeds by fast chain branching reactions. Most of the observations presented in this paper are well explained by the chain branching mechanism:

1) $H + O_2 \longrightarrow OH + O$

2) $O + C_2H_2 \longrightarrow OH + C_2H$

3) $OH + C_2H_2 \longrightarrow C_2H + H_2O$

4) $C_2H + O_2 \longrightarrow 2CO + H$

5) $C_2H + O_2 \longrightarrow CO_2 + CH$

6) $C_2H + C_2H_2 \longrightarrow C_4H_2 + H$

7) $CH + O_2 \longrightarrow CO + OH.$

Reaction (1) is the slowest reaction and thus controls the rate of chain branching.

The oxidation is accompanied by chemi-ionization. The $C_3H_3^+$ ion is observed in abundance early in the reaction and we believe that under our conditions this species is the first ion to be formed. A cyclic structure, having stability derived from delocalization of its π electron system, is proposed for this ion. The mechanism of chemiluminescence is also discussed.

The oxidation of methane is characterized by an induction period which is followed by fast chain branching reactions. The duration of the induction period is controlled by the rate of production of oxygen atoms. A mechanism involving a straight chain reaction to produce an intermediate which itself takes part in chain branching reactions is suggested.

29. KINETICS OF O_2 DISSOCIATION AND RECOMBINATION *

Kurt L. Wray

AVCO-Everett Research Laboratory

Shock tube investigations of relaxation processes in O_2 and O_2-Ar mixtures have been carried out for several years at our laboratory. Here we briefly review the techniques utilized, the results obtained and give more detailed comparisons with other work. Three experimental programs have been carried out employing the uv absorption technique to measure the O_2 concentration.

The first experiment dealt with the dissociation rate of O_2 by Ar catalysts from 5000° to 18,000°K. It was found that there exists an incubation time (of the order of a vibrational relaxation time) before the O_2 dissociates. When this data was used in conjunction with the subsequently obtained recombination data, a $T^{-1/2}$ pre-exponential factor was clearly indicated for the rate constant expression which is

$$k_d = 4.2\ (\pm 14\%) \times 10^{-8} T^{-1/2} \exp(-D/RT) \text{cm}^6/\text{particle}^2\text{-sec}.$$

The second experiment measured the recombination rate of O-atoms by Ar catalysts between 1500° and 3000°K. The excess O-atoms were produced by shocking dilute O_3-Ar mixtures. At 2000°K the measured recombination coefficient k_r is about $0.7 \times 10^{-34} \text{cm}^6/\text{particle}^2\text{-sec}$. This study, with the previously mentioned dissociation work, showed that $K_{eq} = k_d/k_r$.

The third investigation involved the details of the shock front structure in O_2 from Mach 4-21. Between Mach 4 and 10 translational and rotational processes occurred simultaneously within the shock front. Between Mach 10 and 14 vibrational relaxation moved up to and finally was swallowed by the "shock front." Around Mach 16 the dissociation process started within the "shock front."

The shock tube k_d results for Ar catalyst, when extrapolated to 300°K, compare well with recombination studies. But, the high catalytic efficiencies for O and O_2 found around 5000°K ($Ar:O_2:O \approx 1:18:50$) are not apparent at 300°K. For O_2, the extrapolated high temperature work is about 40 times that measured at 300°K while that for O-atoms is 100-800 times that reputed to be measured at 300°K, depending on how the extrapolation is made. Although there is some doubt as to whether the catalytic efficiency of the O-atom has been correctly measured at 300°K, estimates of its value by reinterpretation of other work in the literature still fails to close this gap to better than a factor of 10. It is suggested that for the chemically active catalyst O and O_2 the temperature dependence changes markedly between 300°K and approximately 3000°K.

---

*This work was supported by Advanced Research Projects Agency, monitored by the Army Missile Command, United States Army, under Contract DA-19-020-AMC-0210 (part of Project DEFENDER).

30. REVIEW PAPER

T. M. Sugden

"Shell" Research Ltd., England

(No Abstract)

31. CHEMI-IONIZATION AND CHEMILUMINESCENCE IN THE REACTION OF ATOMIC OXYGEN WITH C_2H_2, C_2D_2 AND C_2H_4

A. Fontijn, W. J. Miller and J. M. Hogan

AeroChem Research Laboratories, Inc.

Chemi-ions are produced in oxygen atom-hydrocarbon molecule reactions; this phenomenon has been studied in two experimental facilities. In a room temperature, Wood-Bonhoeffer flow system study of the acetylene reaction, maximum ion concentration and CH* emission decrease approximately proportionately upon CO_2 addition; in the ethylene reaction, light emission decreases but ion concentration increases. Ion concentration in the C_2H_4 reaction is two orders of magnitude lower than in the C_2H_2 reaction, and CH 4310 A emission is three orders of magnitude lower.

Addition of free radical scavengers, NO and O_2, demonstrates that the chemi-ions and light emitters have free radical precursors. Addition of NO gives rise to CN violet system emission, and O_2 enhances OH emission; the absolute intensity of these emissions decreases with large scavenger concentrations.

Individual ions are identified by a mass spectrometer in an atomic diffusion flame system; CHO^+ is a dominant ion in these reactions. Upon CO_2 addition in the ethylene reaction, $C_3H_5^+$ decreases whereas the maximum concentration of other ions increases. Pressure increase also decreases $C_3H_5^+$ preferentially. In the acetylene reaction there were no preferential decreases.

The results are commensurate with the following chemi-ionization reactions

$$CH + O \longrightarrow CHO^+ + e^- \qquad (1a)$$

$$CH^* + O \longrightarrow CHO^+ + e^- \qquad (1b)$$

$$CH^* + \begin{pmatrix} C_2H_2 \\ \text{or} \\ C_2H_4 \end{pmatrix} \longrightarrow \begin{pmatrix} C_3H_3^+ \\ \text{or} \\ C_3H_5^+ \end{pmatrix} \qquad \begin{pmatrix} a \\ 2 \\ b \end{pmatrix}$$

Reaction (1a) is thought to dominate in the ethylene reaction and (1b) or (2a) in the acetylene reaction.

32. ION-MOLECULE REACTIONS IN METHANE-OXYGEN AND ACETYLENE-OXYGEN SYSTEMS*

J. L. Franklin** and M. S. B. Munson

Humble Oil & Refining Company

Studies of ion-molecule reactions in methane-oxygen and acetylene-oxygen mixtures show comparatively few and relatively slow reactions between the hydrocarbons and oxygen. In methane-oxygen mixtures the principal cross-product ions are $CH_3O_2^+$, CH_2O^+, CHO^+, and CH_3O^+, the first two being formed from O_2^+ and the last two from CH_4^+. In addition, CH_4^+ reacts with O_2 to form CH_3^+. In acetylene-oxygen mixtures $C_2H_2O^+$, CHO^+, and C_2HO^+ are the only cross product ions formed in significant amounts. The first two are formed from O_2^+, and the latter probably comes principally from C_2H^+. CH_2^+ and $C_3H_3^+$ are enhanced by oxygen, but the reactions are not well established.

---

*Supported in part by Project SQUID under Contract Nonr-3623 (S-18).

**Rice University

33. ELECTRON ATTACHMENT AND DETACHMENT IN PURE O_2 AND IN O_2-CO_2 AND O_2-H_2O MIXTURES*

A. V. Phelps and J. L. Pack

Westinghouse Research Laboratories

Electron attachment and detachment processes of possible interest in combustion problems are radiative attachment and photodetachment, dissociative attachment and associative detachment, and three-body attachment and collisional detachment. These processes are reviewed briefly and typical rate coefficients are given. Measurements have been made of the rates of electron attachment and detachment in pure O_2 and in O_2-CO_2 and O_2-H_2O mixtures. Extrapolation of these results to thermal energies at temperatures from 400° to 570°K yields equilibrium constants for the electrons and negative ions. Ion identification is based on the density dependence of the equilibrium constants.

At low gas densities ($\sim 10^{18}$ molecules/cc) the attachment and detachment coefficients are obtained by analysis of the time variation of the current of electrons and ions resulting from the injection of a pulse of photoelectrons into a gas filled region with a uniform electric field. At higher gas densities ($\sim 10^{19}$ molecules/cc) the ratio of the attachment and detachment coefficients and the equilibrium constant are obtained from the drift velocity of the pulse of electrons and ions in the uniform electric field. Auxiliary experiments are required to obtain such quantities as the electron drift velocity in the various gases.

---

*This work was supported in part by the Air Force Weapons Laboratory.

The attachment and detachment coefficients and the equilibrium constants obtained for pure O_2 are consistent with the assumption that the process being studied is $e + 2O_2 \rightleftharpoons O_2^- + O_2$ and that the electron affinity of the O_2^- molecule is 0.44 eV. Attempts to observe a more stable form of this ion have been unsuccessful and lead to the conclusion that the de-excitation rate coefficient for this ion by N_2 is less than 10^{-18} cm^3/sec.

The rate coefficient and equilibrium constant data for the O_2-CO_2 mixtures are consistent with the reaction $e + O_2 + CO_2 \rightleftharpoons CO_4^-$ with an electron affinity of 1.2 eV but with a very high degree of freedom of internal motion. It has not been possible to determine whether the process proceeds via the formation of an O_2^- ion or whether a highly excited CO_4^- ion is formed and then collisionally stabilized. The extremely large cross sections for electron energy loss in CO_3 made the O_2-CO_2 mixture studies particularly useful for determining such quantities as the thermal mobility and attachment coefficient in essentially pure oxygen.

Preliminary results in O_2-H_2O mixtures show that the rate of negative ion formation by thermal electrons in pure H_2O is negligibly small, that the three-body attachment coefficient for negative ion formation due to collisions between electrons, oxygen molecules and water molecules is about five times that for electrons and two oxygen molecules, and that O_2^- ions are converted into more stable ions at a rather slow rate compared to that observed in O_2-CO_2 mixtures.

34. RECOMBINATION OF MOLECULAR POSITIVE IONS WITH ELECTRONS*

M. A. Biondi, T. R. Connor and C. S. Weller

University of Pittsburgh

and

W. H. Kasner

Westinghouse Research Laboratories

Results of studies of the recombination of electrons with molecular positive ions are presented. Theoretical arguments indicate that the dissociative process--in which a molecular ion captures an electron without change of energy, forming an unstable excited molecule which then dissociates -- provides a highly efficient recombination mechanism. The nature of the process responsible for the large recombination rates observed in laboratory afterglow studies is investigated using combined microwave, optical spectrometric and interferometric, and mass spectrographic techniques. Dissociative recombination is shown to be the process operative in the laboratory studies, since it is found that (a) molecular positive ions must be present to observe a large recombination rate, (b) when diatomic ions are present, excited atoms are

*The research described in this report has been supported, in part, by the Office of Naval Research, the Defense Atomic Support Agency, and the U. S. Army Research Office (Durham).

formed in the recombination process, and (c) these excited atoms have kinetic energy of dissociation substantially in excess of thermal energy.

Under conditions where the electrons, ions, and gas are all at the ambient temperature, T = 300°K, the two-body recombination coefficients for mass-identified Ne_2^+, N_2^+, O_2^+ and NO^+ ions are all somewhat in excess of 10^{-7} cm^3/sec. The more complex polyatomic ion N_4^+ exhibits a rather larger ($\sim 10^{-6}$ cm^3/sec) recombination coefficient. The dissociative recombination rates may exhibit a variety of temperature dependence, depending on the details of the potential curves describing the molecular states involved in the process, and the little available experimental evidence indicates substantially different variations with electron temperature for different ions.

It is concluded that diatomic ions involved in combustion processes may exhibit recombination coefficients of the order of 10^{-7} cm^3/sec at 300°K, and the coefficients may decrease with increasing temperature. More complex polyatomic ions may exhibit larger recombination coefficients, but the evidence concerning their behavior is meager.

35. SOME OBSERVATIONS ON THE IONIZATION OF ALKALI AND ALKALINE EARTH ELEMENTS IN HYDROGEN FLAMES

K. Schofield* and T. M. Sugden**

University of Cambridge

We have examined the intensity of atomic resonance radiation from controlled traces of sodium and potassium in premixed hydrogen-oxygen-nitrogen flames of known temperature at atmospheric pressure under conditions where a substantial fraction (sometimes nearly all) of the alkali metal would be ionized at equilibrium. Sodium generally gives much less than the expected equilibrium ionization, and it is concluded that the ionization is a slow process. For potassium, it is possible to follow the progress of ionization. The results suggest a bimolecular rate constant for the recombination process

$$K^+ + e^- + (M) \longrightarrow K + (M)$$

of 3.3×10^{-9} cm^3 $molecule^{-1}$ sec^{-1}, M being an average flame gas constituent at atmospheric pressure.

Addition of alkaline earth results in the production of ions such as Sr^+ and $SrOH^+$, observed by mass spectrometry, much more readily than alkali ions are produced from the corresponding elements. A mechanism of the type

$$SrO + H \longrightarrow SrOH^+ + e^-$$

$$Sr + OH \longrightarrow SrOH^+ + e^-$$

$$SrOH + H \longrightarrow Sr^+ + H_2O$$

---

*Present Address: University of California

**Present Address: "Shell" Research Ltd.

is discussed, and found adequately to fit the facts. The heat of formation of $SrOH^+$ is discussed. Interference effects between the ionization of sodium and that of strontium lead to the conclusion that the former is catalyzed towards equilibrium by the reaction

$$Na + SrOH^+ \longrightarrow Na^+ + SrOH$$

while the latter, which has reached a quasi-equilibrium steady-state, is reduced because of the common ion effect of the electrons produced from sodium.

36. NEGATIVE AND SECONDARY ION FORMATION IN LOW PRESSURE FLAMES

H. F. Calcote, S. C. Kurzius and W. J. Miller

AeroChem Research Laboratories, Inc.

Mass spectrometry and Langmuir probes have been used in a study of negative and secondary positive ion formation in low pressure flames. Individual positive and negative ion profiles have been examined as a function of pressure and flame composition. The effects of various additives (including N_2, CO_2, CH_3OH, CH_2O and CH_3CHO) have also been studied in these flames, as well as in a low pressure atomic diffusion flame.

Two mechanisms for secondary positive ion formation have been set forth: The first consists of a series of charge exchange reactions involving the primary ion (e.g., CHO^+) and stable neutral combustion intermediates:

$$CHO^+ + CH_2O \longrightarrow CH_2OH^+ + CO$$

$$CHO^+ + CH_3OH \longrightarrow CH_3OH_2^+ + CO$$

$$CHO^+ + CH_3CHO \longrightarrow CH_3CHOH^+ + CO$$

$$CHO^+ + C_2H_2O \longrightarrow C_2H_3O^+ + CO$$

The plausibility of these reactions has been demonstrated by addition of CH_2O, CH_3OH, and CH_3CHO to atomic diffusion flames. The second mechanism is one in which a primary ion undergoes a chain of oxidative degradation reactions which include the observed ions as intermediates.

Addition of N_2 and CO_2 to combustion flames, together with the observed effects of varying flame stoichiometry, has led to the conclusion that, in addition to CHO^+, an important primary ion is $C_3H_3^+$. The process responsible for the formation of $C_3H_3^+$ is probably

$$CH^* + C_2H_2 \longrightarrow C_3H_3^+ + e$$

Langmuir probe studies of a C_3H_8 - air flame at 40 Torr have confirmed the importance of diffusional loss mechanisms in low-pressure flames and have led to the

conclusion that the recombination coefficient, α, is temperature-independent. The measured values for the recombination coefficient and ambipolar diffusion coefficient are: $\alpha = 2.4 \times 10^{-7}$ cm^3/sec; $D_a = 60$ cm^2/sec (referred to 1 Torr, 298°K). Taken together with values in the literature we conclude that: $\alpha = 2.4 \pm 0.4 \times 10^{-7}$ cc/sec independent of temperature and pressure.

Mass spectrometric negative ion profiles indicate the presence of significant quantities of negative ions in flames at 1 to 3 Torr. Dissociative attachment processes are the most probable formation route, and C_2^- is apparently the first negative ion formed via:

$$e + C_2H_2O^* \longrightarrow C_2^- + H_2O$$

37. IDENTIFICATION OF NEGATIVE FLAME IONS

A. Feugier and A. Van Tiggelen

University of Louvain

(No Abstract)

REACTION KINETICS

38. SHOCK TUBE STUDY OF THE HYDROGEN-OXYGEN REACTION

T. Asaba, W. C. Gardiner, Jr., and R. F. Stubbeman*

The University of Texas

Several studies of the hydrogen-oxygen reaction at high temperatures have been reported in recent years. They have confirmed that the dominant reactions of the induction period are:

Chain initiation: $H_2 + O_2 = 2\ OH$ (or H, O) (0)

Chain branching: $H + O_2 = O + OH$ (1)

$O + H_2 = H + OH$ (2)

$OH + H_2 = H + H_2O$. (3)

The over-all result of the branching chain reaction is rapid growth of chain carrier concentrations with little release of heat. Subsequent, slower termolecular reactions lead to final chemical equilibrium and the release of heat.

A solution of the rate equations for these reactions was obtained under conditions appropriate for comparison with experimental data. In an early paper, Schott and Kinsey employed steady-state approximations and assumed constant hydrogen and oxygen concentrations in order to derive an expression for the rate of growth of hydroxyl radical concentration. This led to a relation between oxygen concentration, induction time and temperature which could be compared with their experimental results. A different approach taken was numerical integration of the rate equations under the constraint of constant shock flow. Since reaction (1) is 17 kcal endothermic, whereas reactions (2) and (3) are about thermoneutral or exothermic (ΔE_2 = 3 kcal, ΔE_3 = -16 kcal), it was natural to assume that reaction (1) was rate controlling. Recent experimental work, however, has shown that the rate coefficients of reactions (1) and (2) are actually about equal in the temperature range of interest. This means that the analysis given by Schott and Kinsey is applicable only when the ratio of hydrogen to oxygen is very large.

We have solved the system of rate equations for reactions (0-3) without resorting to any steady-state approximation or assumptions about the values of the rate coefficients. The analytic solution contains constants which are readily computed for any given temperatures, compositions, and rate coefficients. It incorporates assumptions of constant temperature and reactant concentration, and ignores the fact that the experiments are actually performed in flowing gas. In order to determine whether any perceptible errors are introduced thereby, a reaction profile was computed with the input data for which Schott, using a program written by R. E. Duff, has given a numerical integration. There is no difference between the two solutions until well after the observed end of the induction period.

---

* Esso Research and Engineering Company

Experimental

The data presented in this paper are induction periods in hydrogen-oxygen-argon mixtures, initial pressure 5-15 torr, heated to reaction temperature (1400-2400°K) in incident shock waves. The induction period is experimentally defined as the time between shock heating and first observable increase in hydroxyl radical concentration.

Our apparatus is of conventional design. Temperatures are determined by shock velocity measurement using a series of resistance gauges and a rastersweep oscilloscope. Hydroxyl radical is observed by absorption of 3067 A radiation from a microwave discharge in argon containing a trace of Bi vapor. This wavelength corresponds to the (0-0) R_2 10 rotational line of the $^2\Sigma - {}^2\pi$ system of OH. A monochromator was used to isolate the 3067 line.

Results

For comparison of experimentally measured induction times with theoretical predictions a graph of log $[O_2]\cdot t_i$ versus inverse temperature was constructed. Such a plot will be seen to have no theoretical significance except in the limit of very rich mixtures, but it does serve very well for comparison purposes. Figure 1 shows the results. Rate coefficient expressions used to compute the lines were:

$$k_0 = 10^{11} \exp(-70,000/RT)$$

$$k_1 = 10^{12} \exp(-16,900/RT)$$

$$k_2 = 10^{10} \exp(-7,700/RT)$$

$$k_3 = 10^{10.8} \exp(-5,900/RT).$$

The lines correspond to 1:3, 1:1 and 3:1 mixtures of hydrogen and oxygen. Induction times for OH absorption: Solid triangles are $H_2:O_2$ = .17:1; Open triangles are $H_2:O_2$ = .29:1; Circles are $H_2:O_2$ = 1:1; Open rectangles are $H_2:O_2$ = 2:1; Solid rectangles are $H_2:O_2$ = 3:1.

The degree to which the concentrations of hydrogen and oxygen influence the induction times, or the degree to which reactions (1) and (2) determine the rate of the induction period reactions, is of fundamental interest. This was investigated by the following procedure. The branching rate can be written formally as $d(\log x)/dt = k[O_2]^m[H_2]^n$. Integrated from shock heating to the observed end of the induction period, assumed to be some constant chain center concentration, this yields $k[O_2]^m[H_2]^n \cdot t_i$ = constant or in logarithmic form log constant = log k + m log $[O_2]$ + n log $|H_2|$ + log t_i. For one concentration held constant, the slope of log $1/t_i$ versus log [ ] for the other concentration gives m or n. Under the conditions of our experiments the constant concentration was about 1%, which was thus used for this calculation also. For constant oxygen concentration, n varies from .8 for very lean mixtures to .6 for 1:1 mixtures. For constant hydrogen concentration, m varies from .62 for very rich mixtures to .5 for 1:1 mixtures. For most of the experimental mixtures used, n and m will be close to the 1:1 values.

Discussion

Our results clearly show that induction times in the hydrogen-oxygen reaction in shock waves depend on the concentrations of both hydrogen and oxygen. They indicate also that the degree of dependence on hydrogen concentration can be predicted in reasonable agreement with experiment using rate constants for the elementary reactions involved that are in accord with previous results.

It is significant that for reasonable values for the appearance concentration and rate constants, the assumed induction scheme allows the calculation of induction periods which reproduce both the temperature and concentration dependence of the reaction. Upon examination of the sensitivity of the solution to variation of the rate coefficient parameters it was found that for a given appearance value, the slope, position and curvature of the plotted log $[O_2] \cdot t_i$ values depend strongly on the assumed set of rate coefficient parameters. There was little or no dependence upon k_3, since it is larger than the other rate coefficients. Too high a value for k_0 causes the linearly increasing portion of the OH concentration history to continue to higher concentrations and has the end effect of curving the plotted induction period downwards at high temperatures. The activation energy of k_1 affects the slope while that of k_2 affects only the position of the line. This is a consequence of the fact that the activation energy of k_1 is considerably larger than the activation energy of k_2. The apparent activation energy determined from the plot is about 18 kcal.

The effect of vibrational equilibration of oxygen was investigated under conditions where the oxygen vibrational relaxation times were comparable to the induction times. A small but clear effect was observed. It was necessary to replace the hydrogen with deuterium and to use krypton in place of argon, in order to obtain sufficient lengthening of the vibrational relaxation times. The size of the effect of slow vibrational relaxation in these mixtures shows that no effect will be observed in usual mixtures containing hydrogen and argon.

39. ON THE MECHANISM AND EXPLOSION LIMITS OF HYDROGEN AND OXYGEN CHAIN SELF-IGNITION IN SHOCK WAVES.

V. V. Voevodsky and R. I. Soloukhin

Novosibirsk University

The self-ignition induction lags of 1:1 hydrogen oxygen mixtures behind reflected shock waves were measured at pressures of 0.5-3.5 atm in the temperature range of 750-1650°K. The explosion limits of self-ignition were established. A qualitative change in the development of explosion (according to schlieren photographs and pressure records) is observed upon crossing the so-called "second limit" of chain explosion extrapolated to high pressures. This change may be explained by the transition from the region of highly branched chains (at higher temperatures) into the region of long straight chains with rare branchings which are propagated by the HO_2 radicals.

The quantitative evaluation of induction lags based on the chain scheme of reaction is in good agreement with the experimental data up to the second explosion limit. In the region between the second and third explosion limits, measured induction lags were less than those theoretically calculated. This effect is explained by the influence of reactions of oxygen molecules vibrationally excited in shock waves.

The induction period data and the agreement of the explosion limits in experiment and theory show that the hydrogen branched chain oxidation scheme is applicable at high temperatures and pressures.

40. EFFECTS OF CONCENTRATION AND OF VIBRATIONAL RELAXATION ON THE INDUCTION PERIOD OF THE H_2-O_2 REACTION

F. E. Belles and M. R. Lauver

NASA, Lewis Research Center

If a gaseous mixture containing hydrogen and oxygen is suddenly heated to a temperature greater than about 1000°K, for example by means of a shock wave, its ignition is preceded by a short induction period. During this period chain-branching occurs, and since the induction period comes before the heat-releasing part of the reaction, the chain-branching process takes place under conditions of essentially constant temperature and pressure. Moreover, the induction period is so short--a few to a few hundred microseconds--that wall effects cannot make themselves felt.

Thus, measurements of the induction period permit the chain-branching process to be studied in a relatively uncomplicated environment. This fact was first recognized by Schott and Kinsey [1], who made an extensive set of measurements covering a wide range of temperatures and $[H_2] / [O_2]$ ratios from 0.25 to 5.

Only four reactions are needed to describe the buildup of free radicals during the induction period. First, there must be an initiation reaction involving molecular species. In the lower range of temperatures (1000-2000°K) this has been assumed to be the following:

$$H_2 + O_2 \longrightarrow 2OH \qquad \text{(i)}$$

After a short initiation period, the following reactions branch the chain:

$$OH + H_2 \longrightarrow H_2O + H \qquad \text{(1)}$$

$$H + O_2 \longrightarrow OH + O \qquad \text{(11)}$$

$$O + H_2 \longrightarrow OH + H \qquad \text{(111)}$$

Rate constants are available for all these reactions [2,3].

Schott and Kinsey found that their data were well correlated by plotting the parameter $(t_i[O_2])$ against reciprocal temperature. They took the induction period t_i, which of course must always be defined rather arbitrarily, as the time at which $[OH]$ reached the limit of detectability in their experiments, about 10^{-6} mole/liter. They noted that the above correlation is the one to be expected if chain-branching is controlled by the rate of the slow step, reaction (11).

However, Schott and Kinsey observed a trend in their data such that $(t_i[O_2])$ increased with increasing mole fraction of oxygen, at constant temperature. This is not anticipated on the basis of the simplified kinetic model in which the controlling rate is that of reaction (11). They tentatively ascribed this trend to slow vibrational relaxation of O_2, which might tend to reduce k_2 below its thermal-equilibrium value.

In order to investigate more fully this important possibility, it is first necessary to account for concentration effects that are neglected in the simplified kinetic model. This was done by integrating the whole set of equations (i - 111) without any simplifying assumptions. The problem can be solved either by means of the approximate analytic solution of Brokaw [4] or by machine calculation [5]; the two methods give almost identical results.

These calcualtions show that ($t_i[O_2]$) should in fact increase as the ratio $[H_2] / [O_2]$ decreases, and that in addition there is some dependence upon $[O_2]$. Values of ($t_i [O_2]$), calculated using rate constants close to those reported in the literature [2,3], for reactions (1 - 111), encompass Schott and Kinsey's measurements. Further comparison is made with new data obtained in a shock tube by methods already described [5], utilizing light emitted by electronically excited OH. These new data are for 5% and 20% hydrogen in air. Calculations show that induction times for the leaner mixture should be about twice as great as those for the richer one, and the measurements confirm this prediction. The most important comparison is with the new data of White and Moore [6], which cover an extreme range of $[H_2] / [O_2]$ ratios. The calculations satisfactorily reproduce the observed fact that ($t_i [O_2]$) increases nearly a hundred-fold as $[H_2] / [O_2]$ is decreased from 24 to 0.0075, at a given temperature.

Thus, simple calculations can interpret the observed effects of temperature, pressure, and concentration on induction time. It is not necessary to invoke any influence due to slow vibrational relaxation. Consequently, it is of interest to see whether calculations can confirm that vibrational effects should indeed be small or absent.

Of the molecular participants in the branching reactions, either the hydrogen or the oxygen might remain vibrationally cold during all or part of the induction period. White and Millikan [7] have reported the rate of relaxation of O_2 by H_2 and their data, together with other in the literature, is sufficient to estimate [8] the relaxation time t_v for O_2 in any mixture containing O_2, H_2, N_2, and Ar.

In order to compute an upper limit for the possible effect of slow relaxation it was assumed that the temperature at which reaction (11) proceeds is equal to the vibrational temperature of O_2, which can be written as:

$$T_{v,\,O_2} = T - (T - 300) \exp\ (-t/t_v) \qquad (1)$$

where T is the over-all temperature of the induction zone. The rate constant k_2 then becomes a function of time:

$$k_2\,(t) = A_2 \exp\ (-\frac{E_2}{R T_{v,O_2}}) \qquad (2)$$

Induction times were calculated by machine integration, using the time-dependent k_2, and the results compared with induction times calculated by means of the simple time-independent rate constants. Remarkably, the extreme assumption embodied in Eq. (2), that all the activation energy for reaction (11) must come from vibrations of the O_2 molecule, has only a small effect on the induction time. For example, the times calculated at 1800°K for the mixtures studied by Schott and Kinsey [1] are only increased about 10 per cent by the relaxation effect.

Similar calculations, with time-dependent k_1 or k_3, cannot be carried out because vibrational relaxation times for H_2 in the presence of O_2 are not known. However, White and Moore [6] have found that the relaxation is rapid, so by analogy with the results calculated for O_2, the effects (if they exist) should again be small.

References

1. Schott, G. L. and Kinsey, J. L.: J. Chem. Phys. 29, 1177 (1958).
2. Duff, R. E.: J. Chem. Phys. 28, 1193 (1958).
3. Kaufman, F. and DelGreco, F. P.: Ninth Symposium (International) on Combustion, p 659, Academic Press, 1963.
4. Brokaw, R. S.: Tenth Symposium (International) on Combustion, (this volume).
5. Belles, F. E. and Lauver, M. R.: J. Chem. Phys. 40, 415 (1964).
6. White, D. R. and Moore, G. E.: Tenth Symposium (International) on Combustion, (this volume).
7. White, D. R. and Millikan, R. C.: J. Chem. Phys. 39, 2107 (1963).
8. Millikan, R. C. and White, D. R.: J. Chem. Phys. 39, 3209 (1963).

41. ANALYTIC SOLUTIONS TO THE IGNITION KINETICS OF THE HYDROGEN-OXYGEN REACTION

Richard S. Brokaw

NASA, Lewis Research Center

Solutions to the ignition kinetics have been obtained assuming negligible depletion of reactants during the induction period for the following scheme of reactions:

$$OH + H_2 \xrightarrow{k_1} H_2O + H \qquad \text{I}$$

$$H + O_2 \xrightarrow{k_2} OH + O \qquad \text{II}$$

$$O + H_2 \xrightarrow{k_3} OH + H \qquad \text{III}$$

$$H + O_2 + M \xrightarrow{k_6} HO_2 + M \qquad \text{VI}$$

$$HO_2 + H_2 \xrightarrow{k_{11}} H_2O_2 + H \qquad \text{XI}$$

These five reactions, together with terms describing the destruction of chain carriers after diffusion to the walls, suffice to explain qualitatively the ignition behavior of the hydrogen-oxygen system, including the existence of the first, second, and third explosion limits.

The radical concentrations as a function of time are given, to a very good approximation by

$$c_i = A_i e^{\lambda t} \qquad i = OH,\ H,\ O,\ HO_2 \qquad (1)$$

where λ is the positive root of the quartic equation

$$\lambda^4 + \left[(k_1 + k_3 + k_{11})c_{H_2} + (k_2 + k_6 c_M)c_{O_2}\right]\lambda^3$$

$$+ \left[k_1 k_3 c_{H_2}^2 + (k_1 + k_3)k_6 c_{H_2} c_{O_2} c_M + (k_1 c_{H_2} + k_2 c_{O_2} + k_3 c_{H_2})k_{11} c_{H_2}\right]\lambda^2$$

$$+ k_1 k_3 c_{H_2}^2\left[(k_6 c_M - 2k_2)c_{O_2} + k_{11} c_{H_2}\right]\lambda - 2k_1 k_2 k_3 k_{11} c_{H_2}^3 c_{O_2} = 0 \qquad (2)$$

Similar analytic solutions have been obtained by Kondratiev [1] for reactions I-III and VI.

The following approximate expressions for the positive root of Eq. (2) have been developed:

$$\lambda \cong \frac{2k_2k_{11}c_{H_2}}{k_6c_M - 2k_2} \qquad k_6c_M > 2k_2 \tag{3}$$

$$\lambda \cong \left[\frac{2k_1k_2k_3k_{11}c_{H_2}^2c_{O_2}}{k_1k_3c_{H_2} + (k_1 + k_3)k_6c_{O_2}c_M}\right]^{1/2} \qquad k_6c_M = 2k_2 \tag{4}$$

$$\lambda \cong \left(\frac{k_1k_3(2k_2 - k_6c_M)c_{H_2}^2c_{O_2}\left\{\left[1 + \frac{4k_3(2k_2 - k_6c_M)c_{H_2}c_{O_2}}{(k_3c_{H_2} + k_6c_{O_2}c_M)^2}\right]^{1/2} - 1\right\}}{2k_2c_{O_2}\frac{k_3c_{H_2} - k_6c_{O_2}c_M}{k_3c_{H_2} + k_6c_{O_2}c_M} + (k_1c_{H_2} + k_2c_{O_2})\left\{\left[1 + \frac{4k_3(2k_2 - k_6c_M)c_{H_2}c_{O_2}}{(k_3c_{H_2} + k_6c_{O_2}c_M)^2}\right]^{1/2} + 1\right\}}\right)^{1/2} \qquad 2k_2 > k_6c_M \tag{5}$$

The ignition delay τ is then given by

$$\tau = \frac{1}{\lambda}\ln\left(\frac{C}{P}\right) \tag{6}$$

where C is a constant involving the rate of initiation (the initial source of radicals) and the criterion of ignition (a critical radical concentration or heat release rate).

The condition $k_6c_M > 2k_2$ corresponds to a low temperature-high pressure region of long ignition delays (above the third explosion limit). Here delays of one to several seconds are observed in the range 560-600°C. Equations (3) and (6) are found to describe the ignition behavior in this regime, including the variation of ignition delay with pressure [2] and composition [2,3] (H_2, O_2, and H_2O vapor).

The condition $2k_2 > k_6c_M$ corresponds to a high temperature-low pressure region of short delays (measured in milliseconds or microseconds). Equations (5) and (6) are found to reproduce delays computed by numerical integration of the rate equations [4,5] within a few per cent, and account reasonably well for the observed effect of hydrogen concentration [6]. Belles and Lauver [7] show that eqs. (5) and (6) account for shock tube ignition delays over a very wide range of hydrogen-oxygen mixture ratio.

Finally, ignition delays for the Von Neumann spike condition in Chapman-Jouguet detonations in the neighborhood of the lean limit of detonability in air have been calculated. (Here eq. (4) is used to bridge the gap between the long- and short-delay regions.) These delays decrease by two orders of magnitude as the hydrogen mole fraction increases from 0.135 to 0.145. This is very close to the experimental limit [8] (hydrogen mole fraction 0.14 to 0.15) and thus supports the notion that the condition $2k_2 > k_6c_M$ must be satisfied for a stable detonation.

References

1. Kondratiev, V. N.: Kinetics of Chemical Gas Reactions, AEC-tr-4493, February 1962, pp 678-680. (English Translation of a Text published by the Academy of Sciences USSR, Moscow, 1958.)

2. Coward, H. F. (work of H. B. Dixon): J. Chem. Soc. 1934, 1382.

3. Anagnostou, E., Brokaw, R. S., and Butler, J. N.: Effect of Concentration on Ignition Delays for Various Fuel-Oxygen-Nitrogen Mixtures at Elevated Temperatures. NACA TN 3887, 1956.

4. Momtchiloff, I. N., Taback, E. D., and Buswell, R. F.: Ninth Symposium (International) on Combustion, p. 220, Academic Press, 1963.

5. Belles, F. E., and Lauver, M. R.: J. Chem. Phys. 40, 415 (1964).

6. Fouré, C.: Rech. Aeron. No. 42, 33 (1954).

7. Belles, F. E., and Lauver, M. R.: Tenth Symposium (International) on Combustion, (this volume).

8. Gordon, W. E., Mooradian, A. J., and Harper, S. A.: Seventh Symposium (International) on Combustion, p. 752, Butterworths, 1959.

42. THE INHIBITION OF THE SECOND LIMIT OF THE HYDROGEN-OXYGEN REACTION BY HYDROGEN BROMIDE AND HYDROGEN CHLORIDE

D. R. Blackmore, G. O'Donnell* and R. F. Simmons

University of Manchester

The effect of hydrogen bromide and hydrogen chloride on the second limit of the hydrogen-oxygen reaction has been studied over a wide range of mixture composition and vessel diameter using barium bromide- and barium chloride-coated vessels, respectively. Hydrogen bromide has been found to be a very efficient inhibitor, and in contrast the same quantity of hydrogen chloride has only a small effect on the explosion limit; hydrogen bromide is approximately 400 times more effective as an inhibitor than hydrogen chloride. The mechanism of the inhibition is discussed, and with hydrogen bromide it is concluded that the primary termination reaction is a removal of hydrogen atoms by the hydrogen bromide:

$$H + HBr \longrightarrow H_2 + Br \qquad (14)$$

The majority of the the bromine atoms produced in reaction (14), however, react to give chain propagation by reaction with hydrogen, and only a small fraction react to give chain termination. It is concluded that chain termination arises by the quadratic process:

$$Br + HO_2 \longrightarrow HBr + O_2 \qquad (18)$$

*Esso Research Ltd., England

It is shown that the corresponding inhibition mechanism cannot be operative in the case of inhibition by hydrogen chloride, and the relative efficiency of the two inhibitors is discussed in terms of the rate of reaction of halogen atoms with hydrogen.

It is very striking that whereas bromine compounds are very effective in inhibiting flame propagation, chlorine compounds are relatively ineffective [1]. It is generally accepted that bromine compounds readily react with chain centers which are important for the propagation of the flame to give chain termination. On the other hand, it is not known whether the inhibitor preferentially reacts with one type of chain center or whether it reacts with any chain center which might be present in the system. In an attempt to obtain further evidence on this point, the influence of hydrogen bromide and hydrogen chloride on the second explosion limit of the hydrogen-oxygen has been studied. Hydrogen and oxygen atoms and hydroxyl radicals are the important chain centers in the chain branching mechanism of this reaction, and it will be seen that an examination of the kinetic characteristics of the inhibition shows there is preferential reaction of hydrogen bromide with hydrogen atoms.

Reference

1. Coward, H. F. and Jones, G. W.: Limits of flammability of gases and vapors. U. S. Bur. Mines Bull. No. 503, 155 pp., 1952.

43. REACTIONS OF THE HNO MOLECULE

M. A. A. Clyne

University of Cambridge

The HNO molecule in hydrogen-rich H_2 + O_2 flames containing nitric oxide has been detected by means of its characteristic red and infrared emission spectrum (Bulewicz and Sugden 1960). The HNO molecule is likewise a reaction intermediate in the hydrogen + oxygen thermal chain reaction sensitized by nitric oxide and studied in static systems. However, most kinetic investigations of the HNO molecule have been made either,

(i) in the Hg-photosensitized reaction of NO with H_2 using product analysis, or

(ii) in the flash photolysis of NO + NH_3 mixtures or nitromethane with the use of kinetic absorption spectroscopy to follow HNO concentrations (Dalby 1958), or

(iii) in discharge-flow experiments with H + NO and using chemiluminescence methods to follow [H].

Studies of the last type (iii) have been made in the present work. In discharge-flow experiments at total pressures of about 2 mm Hg, and with [H]/[NO] near unity, reaction (1) forms HNO which is predominantly removed by reaction (2),

$$H + NO + M \longrightarrow HNO + M \qquad (1)$$

$$H + HNO \longrightarrow H_2 + NO \qquad (2)$$

and assuming

$$d[HNO]/dt = 0,$$

$$[HNO] = \frac{k_1[NO][M]}{k_2}$$

In the high pressure studies (i) where [H] is very small, reactions (3)-(5) are predominant for HNO removal, since these reactions are favored over reaction (2) by high [M] and [NO]/[H]:-

$$HNO + HNO = N_2O + H_2O \quad (3)$$

$$HNO + NO = N_2O + OH \quad (4)$$

$$HNO + 2NO = N_2 + HNO_3 \text{ etc.} \quad (5).$$

A new type of high pressure discharge-flow system was therefore developed, in order to study HNO reactions under conditions where reactions (2) and (3)-(5) compete. In this system, the reaction H + NO + H_2 could be studied at total pressures up to 73 mm Hg. Hydrogen atom concentrations, which were determined by measurements of the intensity of the HNO emission spectrum, were 0.15 mm Hg in a total pressure of H_2 of 73 mm Hg.

Highly purified nitric oxide was introduced to the H atom flow, and the products of reaction were trapped and analyzed. Less than 1% of nitric oxide was consumed in the reaction of 0.5 mm nitric oxide with atomic hydrogen, and the only detectable reaction product was nitrous oxide. Higher oxides of nitrogen were absent. The nitrous oxide yield $[N_2O]_o/[NO]_o$ was found to decrease linearly with log $[NO]_o$, where $[NO]_o$ is the initial concentration of nitric oxide. A typical value for $[N_2O]_o/[NO]_o$ was 1×10^{-3}. The results are consistent with a mechanism including reactions (1), (2) and (3) or (4), with (2) predominant for HNO removal. Our data give $k_3 > 3\times10^7$ or $k_4 > 6\times10^7$ cm^{3}mole^{-1}s^{-1}, while Dalby's work shows that $k_4 < 1\times10^7$ cm^{3}mole^{-1}s^{-1}. While reaction (2) is the most rapid process removing HNO in our experiments, it is concluded, therefore, that reaction (3) is predominant over reaction (4), with $k_2 > 3\times10^{10}$ cm^{3}mole^{-1}s^{-1} and $k_3 > 3\times10^7$ cm^{3}mole^{-1}s^{-1} at 300°K.

44. DETERMINATION OF THE RATE CONSTANT FOR THERMAL CRACKING OF METHANE BY ADIABATIC COMPRESSION AND EXPANSION

V. N. Kondratiev

USSR Academy of Sciences

The method of adiabatic compression and expansion worked out by Ryabinin [1] more than ten years ago has not found due application in measuring rate constants of elementary chemical reactions at high temperatures and pressures. The possibility of such an application was shown only recently by Markevich et al. [2] for the thermal cracking of methane. It was ascertained that due to specific temperature variations in the course of compression and expansion, calculation may be made considerably less tedious.

The experimental data obtained in this work permit fairly accurate determination of the rate constant for unimolecular decomposition of methane molecules. The following conditions may be considered as most favorable.

1. With a system containing a low percentage of the reacting gas considerably diluted with some inert gas, for example argon, the reaction-induced variations in temperature may be neglected and the reaction considered as strictly adiabatic.

2. Since under adiabatic compression the reaction becomes measurable only at temperatures and pressures higher than certain limiting T* and p* values which differ only slightly from T_{max} and p_{max}, $\gamma = \frac{C_p}{C_V}$ may be considered as constant throughout the ranges of T_{max} - T* and p_{max} - p*.

3. Hydrogen and ethane were shown to be the main reaction products of the initial reaction (i.e., at low compression) [2b]. Consequently, under these conditions the reaction will follow a simple mechanism

$$CH_4 \longrightarrow CH_3 + H$$

$$H + CH_4 = CH_3 + H_2$$

$$2CH_3 \longrightarrow C_2H_6$$

Under the assumption of a stationary H atom concentration, the rate of hydrogen formation will be

$$\frac{d(H_2)}{dt} = A_1(CH_4)e^{-E/RT}$$

where A_1 is the frequency factor in the rate constant for the reaction $CH_4 = CH_3 + H$. The data obtained by Markevich et al., [2b], as well as the majority of other published data, seem to be in favor of a unimolecular mechanism for this reaction (under the experimental conditions used).

4. Due to the high activation energy E, the reaction proceeds at a temperature close to T_{max}. This assumption is similar to that taken as a basis for the theory of thermal flame propagation by Zeldovich and Frank-Kamenetzkii [3], namely, that combustion proceeds at a temperature differing only slightly from the maximum combustion temperature.

Introducing the value $\psi = \frac{(H_2)}{(CH_4)}$ and making use of the first three conditions, we obtain, after certain transformations, on the basis of the assumed reaction mechanism and from the equation for piston motion,

$$d(\psi\alpha) = -x_o \frac{A_1 e^{-E/RT} dT}{T \sqrt{\frac{2(\gamma - 1)}{m} \frac{p_o V_o}{T_o} (T_{max} - T)}}$$

where x_o is the length of the reactor channel, m is the piston mass, and p_o, V_o, T_o are the initial pressure, volume and temperature.

Integration, making allowance for the fourth of the above conditions, gives

$$\psi^*\alpha^* = x_o \frac{A_1 e^{-E/RT_{max}}}{\sqrt{\frac{E(\gamma - 1)}{2\pi m} \frac{p_o V_o}{RT_o}}} \chi^*$$

where ψ^* is the final value of the $(H_2)/(CH_4)$ ratio, α^* is the degree of compression at T = T* and

$$\chi^* = \frac{2}{\sqrt{\pi}} \int_0^{\xi^*} e^{-\xi^2} d\xi , \qquad \xi^* = \sqrt{\frac{E}{RT_{max}} \left(1 - \frac{T^*}{T_{max}}\right)} .$$

It will be seen from the last expression that by plotting $\lg \frac{\psi^* \sqrt{\gamma - 1}}{\chi^*}$ versus $\frac{1}{T_{max}}$ we obtain a straight line, and that the E and A_1 values may be derived from its parameters. A straight line of this kind plotted from the data of 2b/ would yield the following rate constant for unimolecular decomposition of methane molecules

$$k_1 = 1 \times 10^{15} e^{-103000/RT} sec^{-1}.$$

Of all the rate constants for the decomposition of methane molecules, the most accurate seems to be that determined by Skipper and Ruherwein 4/

$$k_1 = 10^{14.71} e^{-101000/RT} sec^{-1}$$

which, in fact, coincides with ours.

Let us add that, according to Nikitin, at temperatures considerably lower than the characteristic temperature for the slowest vibrations of the CH_4 molecule (1860°K), the rate constant for bimolecular decomposition of methane $CH_4 + Ar = CH_3 + H + Ar$ is $k_2 = 10^{21} e^{-E/RT}$ $cm^3 mole^{-1} sec^{-1}$, with an accuracy to within a power of ten. From general considerations based on the theory of unimolecular reactions, a reaction will be first order when the rate of activation, i.e., the rate of a bimolecular step, is considerably higher than that of an active molecule decomposition. The pertinent condition of unimolecularity is expressed by the inequality

$$A_2(Ar) \gg A_1$$

where A_2 is the frequency factor in the rate constant of a bimolecular reaction. The validity of this inequality will be apparent if we assume that $A_1 = 10^{15}$ sec^{-1}, $A_2 = 10^{21}$ $cm^3 mole^{-1} sec^{-1}$ (see above) and $(Ar) = (Ar)_0 \alpha = 2.5 \times 10^{19} \times 20 : 6 \times 10^{23} = 10^{-3}$ mole cm^3. This may be considered as evidence that the thermal dissociation of methane under experimental conditions 2b/ obeys a strictly unimolecular law.

For the determination of rate constants of elementary chemical reactions, the method of adiabatic compression and expansion seems no less accurate than the shock tube method.

References

1. Yu. N. Ryabinin: Zhur. Exp. Teor. Fiz. 23, 461 (1952).

2. a. A. M. Markevich, V. V. Azatyan, N. A. Sokolova: Kinetika i Kataliz 3, 431 (1962); b. I. E. Volokhonovich, A. M. Markevich, I. F. Masterovoy, V. V. Azatyan, Dokl. Akad. Nauk SSSR 146, 387 (1962).

3. Ya. B. Zeldovich, D. A. Frank-Kamenetzkii: Zhur. Fiz. Khim 12, 100 (1938).

4. G. B. Skinner, R. A. Ruherwein: J. Phys. Chem. 63, 1736 (1959).

45. ANALYTICAL INVESTIGATIONS OF STABLE PRODUCTS DURING REACTION OF ADIABATICALLY COMPRESSED HYDROCARBON/AIR SYSTEMS

A. Martinengo, J. Melczer and E. Schlimme

University of Göttingen

In continuation of the investigations of W. Jost and co-workers [1,2] concerning the oxidation of adiabatically compressed hydrocarbon-air systems (temperature region about 700°K), stable reaction products have been determined analytically as a function of the reaction time (10^{-3} - 10^{-2} sec) and compared with simultaneously observed pressure records.

The experimental procedure was as follows: At a given time interval after the end of compression, the reacting mixture was expanded adiabatically (by destroying a diaphragm) into a sampling vessel of about 2 liter filled with N_2 or He under low pressure (100-200 mm Hg depending on conditions). The temperature decrease caused by expansion ($\sim$ 200°K/msec at the beginning of expansion) within the reacting mixture has been proved to be sufficient to stop reaction. The mixture in the sampling vessel was then analyzed by means of different methods (infrared spectroscopy, gas chromatography, conventional chemical methods), and was regarded as representative for the composition of the reacting mixture at the beginning of the expansion. Since reaction under conditions of adiabatic compression is sufficiently reproducible, this procedure allows one to determine some stable products at any time on the reaction path.

The dependence of concentration on time of some characteristic intermediate products (carbonyl compounds, n-paraffins, olefins, CO, etc.) during reaction is dependent on initial conditions of temperature, pressure and fuel concentration. In the case of a "two-stage ignition" ("lean" mixture), during the first "stage" (reaction time $\sim$ 10 msec) the main products are carbonyl compounds, which disappear at the onset of "explosion" (marked pressure increase). The detected C_1 - C_8 aldehydes were observed to have the same concentration-time dependence, though formaldehyde and acetaldehyde have been detected in greater amounts than the higher compounds. The acetone concentration during the late reaction phase of iso-paraffin oxidation is more than twice that found in the same experiments carried out with n-paraffins. If one adds di-tertiary butylperoxide to the initial mixture, acetone appears at the beginning of reaction (decomposition of the peroxide), is then consumed, and reappears as a reaction product together with the aldehydes. If the O_2 content of the mixture is decreased, the rates of formation of acetone, aldehydes and olefins decrease together with a simultaneous increase of over-all reaction time. At O_2 concentrations below 8 volume per cent no "ignition" is indicated by the pressure record. In this case large amounts of the mentioned products have been detected in the "end gas."

Though pressure records do not indicate a "pre-reaction stage" in rich mixtures ("single stage ignition"), nearly the same processes as in lean mixtures ("two stage ignition") have been observed, but with much shorter reaction times. At the moment of maximum aldehyde concentration, the gas temperature is the same in both cases.

Although CO appears in the final phase of reaction as the principal reaction product, a comparable addition of CO (about 0.1 volume per cent) to the initial mixture does not increase markedly the over-all reaction velocity. While traces of CO

are consumed in the very early reaction phase, the formation of CO in the final phase is practically independent of the amount of CO initially added. Addition of acetaldehyde indicates a similar picture: the rate of formation and the absolute amount of acetic aldehyde produced during reaction are not affected by the amount of acetaldehyde already present.

References

1. Jost, W.: Third Symposium on Combustion, Flame and Explosion Phenomena, p. 424, The Williams & Wilkins Co., 1949.

2. Jost, W.: Ninth Symposium (International) on Combustion, p. 1013, Academic Press, 1963.

46. HOMOGENEOUS AND HETEROGENEOUS PROCESSES IN THE GAS PHASE OXIDATION OF ISOBUTANE AND ISOBUTENE

James Hay, John H. Knox and James M. C. Turner

University of Edinburgh

According to most theories of the slow gas phase oxidation of hydrocarbons, the major product producing reactions are homogeneous and it is supposed that the main effect of surface is on kinetically important reactions which produce relatively little final product. According to one theory of hydrocarbon oxidation all primary products arise from the homogeneous unimolecular decomposition of peroxy radicals or from reactions of radicals produced from such decompositions. If this is so the distribution of the products formed directly from the peroxy radicals should be unaffected by reactant pressures (in particular, oxygen pressure) and should change gradually with temperature provided that conditions are chosen to avoid secondary oxidation.

By analyzing the reaction products from the oxidation of isobutane and isobutene between 250° and 350°C when the extent of oxidation is sufficiently small that secondary oxidation is negligible we have found that, while the percentage yields of the major products (about 80% isobutene from isobutane, and about 75% acetone + formaldehyde from isobutene) are little affected, reactant pressure and temperature have such profound effects on the distribution of the minor products that the simple hypothesis outlined above is untenable. Furthermore, investigations of the effect of change of surface have revealed that the initial distribution of minor products is highly sensitive to the nature of the reaction vessel wall: the surfaces investigated were clean Pyrex; HF washed Pyrex; KCl, B_2O_3 and NaOH coated Pyrex; and silver plated Pyrex.

It is concluded that contrary to general belief a considerable part, if not the whole, of the minor products arises in heterogeneous processes which by consequence play a very important part in the reactions between 250° and 350°C. However, general considerations demand that the heterogeneous processes are not independent but are consequent on primary homogeneous processes involving free radicals.

It is proposed that three primary homogeneous reactions occur in the early stage of the oxidation of isobutane and three in the oxidation of isobutene:

Isobutane

$$C_4H_{10} + X \text{ - } C_4H_9 + HX$$

$$C_4H_9 + O_2 = C_4H_8 + HO_2$$

$$C_4H_9 + O_2 = C_4H_9OO$$

Isobutene

$$C_4H_8 + HO_2 = Me_2CO + CH_2OH$$

$$C_4H_8 + HO_2 = Me_2COH + CH_2O$$

$$C_4H_8 + HO_2 = C_4H_8OOH$$

and that these homogeneous reactions are followed by the heterogeneous decompositions of the peroxy radicals into complex surface sensitive mixtures of products.

$$C_4H_8OO + \text{wall} = \text{complex mixture A}$$

$$C_4H_8OOH + \text{wall} = \text{complex mixture B}$$

With isobutene there will necessarily be secondary homogeneous processes producing formaldehyde or CO by oxidation of CH_2OH and acetone by oxidation of Me_2COH.

This mechanism explains why the ratio of major to minor products is little affected by composition, total pressure, temperature or surface while the distribution of minor products is highly sensitive to these parameters.

47. DETERMINATION OF THE DECOMPOSITION KINETICS OF HYDRAZINE USING A SINGLE-PULSE SHOCK TUBE*

E. T. McHale, B. E. Knox, and H. B. Palmer

The Pennsylvania State University

A single-pulse shock tube has been used to study the kinetics of thermal decomposition of hydrazine over the temperature range, 950° to 1160°K, and over the pressure range from 2.8 to 5.4 atmospheres. Argon-hydrazine mixtures were used in which the argon:hydrazine ratio was varied between about 50:1 and 120:1. Residence times in the shock ranged between 1.3 and 3.5 milliseconds.

Analyses of the shocked and quenched gas near the end plate were performed using a mass spectrometer in conjunction with a discharge and a cold trap. In this way it was possible to obtain accurate analyses of all species present, including hydrazine. From the analyses the stoichiometry of the decomposition was determined

* Work partially supported by Project Squid under contract to the Office of Naval Research, Department of the Navy, Contract No. Nonr 1858(25)NR-098-038; and by the Army Research Office - Durham. Reproduction in full or in part is permitted for any use of the United States Government.

to be given accurately by $2N_2H_4 \longrightarrow 2NH_3 + H_2 + N_2$, over the full range of experimental conditions, a result that has not been demonstrated with any precision in previous shock tube work on the reaction.

The decomposition is probably first-order in $[N_2H_4]$ and independent of total concentration. An unambiguous determination of order cannot be gleaned from the data; i.e., the possibility of 3/2-order in $[N_2H_4]$ cannot be excluded at present. The first-order rate constants for sixteen runs using freshly prepared, very pure and dry hydrazine yield the Arrhenius expression:

$$k = 1.1 \times 10^{13} \exp(-55 \text{ kcal/RT}) \text{ sec}^{-1}. \qquad \text{(a)}$$

However, an effect of hydrazine history is found. Hydrazine that has aged in storage under N_2 for several weeks after purification decomposes considerably faster at the lower temperatures and yields (23 runs):

$$k = 1.1 \times 10^{9} \exp(-34.3 \text{ kcal/RT}) \text{ sec}^{-1}. \qquad \text{(b)}$$

We have not yet discovered the reason for the effect of aging. The results for the aged hydrazine agree with the rate constants reported by Moberly [1]. The effect is not due to water.

The present experiments are in the same temperature region as the flow reactor experiments of Szwarc [2], but are at much higher pressure. The pressures are of the same order as those in the shock tube work of Michel and Wagner [3], but the temperatures are lower. Finally the shock tube study by Diesen [4] was in roughly the same low pressure range as that of Szwarc, but covered much higher temperatures. These four studies are thus complementary and should permit some clarification of the main features of the decomposition. A detailed comparison can be carried out if one presumes (with support from experiment and also from Gilbert's analysis [5] of the work of Szwarc) that the primary step,

$$(1) \quad N_2H_4 \longrightarrow 2NH_2$$

is in the low-pressure unimolecular regime in the studies of Szwarc and of Diesen and is in the high-pressure regime in the other two studies. The comparison leads to the conclusions that:

(a) the rate constant from Szwarc's work does not imply $D_{(H_2N\text{-}HN_2)} = 60$ kcal, but rather a figure closer to 65 kcal and an empirical activation energy of about 55 kcal around 1000°K.

(b) Application of unimolecular reaction theory to Szwarc's data leads to the conclusion that about 6 effective oscillators participate in step 1.

(c) The data of Diesen and those of Szwarc are difficult to reconcile. If Szwarc's data are accepted, Diesen's rate constants appear to be too low at all temperatures, the discrepancy being much worse at high temperatures than at low.

(d) Our high-pressure results for fresh N_2H_4 can be accounted for by a simple non-chain reaction sequence consisting of step 1 followed by

$$(2)\quad NH_2 + N_2H_4 \longrightarrow NH_3 + N_2H_3$$

$$(3)\quad NH_2 + N_2H_3 \longrightarrow NH_3 + N_2 + H_2.$$

The validity of this mechanism hangs entirely on the stability of N_2H_3. If N_2H_3 decomposes rapidly to $N_2H + H_2$ (decomposition to $N_2H_2 + H$ is very endothermic and cannot be rapid), then a chain reaction must result. The simpler scheme leads to

$$-d[N_2H_4]/dt = 2k_1[N_2H_4] .$$

Values of k_1 (now a high-pressure unimolecular rate constant) computed from the data can be compared with the low-pressure results using order-of-magnitude arguments involving unimolecular rate theory. They appear to be compatible with the 6 oscillators mentioned in (b).

(e) The results of Wagner and Michel above about 1250°K, where they express the most confidence in their data, are reasonably compatible with our results at lower temperatures on the basis of the simple non-chain mechanism. It appears that at their highest temperature--i. e., above about 1400°K--NH_2 does not attain a steady state and the rate constant falls from $2k_1$ to k_1 at the highest temperatures.

(f) The best Arrhenius expression for k_1 at high pressure is given by $k_1 \doteq 10^{15} \exp(-65 \text{ kcal/RT}) \text{ sec}^{-1}$, using the revised figure for $D(H_2N\text{-}NH_2)$. The high pre-exponental factor is in accord with theoretical expectations.

References

1. Moberly, W. H.: J. Phys. Chem. 66, 366 (1962).

2. Szwarc, M.: Proc. Roy. Soc. (London) A198, 267 (1949).

3. Michel, K. W., and Wagner, H. Gg.: private communication (see also Jost, W., Technical Summary Rept. No. 3, Contract No. AF61 (514) - 1142, Göttingen, W. Germany, Feb., 1962).

4. Diesen, R. W.: J. Chem. Phys. 39, 2121 (1963).

5. Gilbert, M.: Combustion and Flame 2, 149 (1958).

48. THE PYROLYSIS AND OXIDATION OF HYDRAZINE BEHIND SHOCK WAVES

K. W. Michel and H. Gg. Wagner

University of Göttingen

The thermal decomposition of hydrazine highly diluted with Ar or He (0.03 - 0.5 per cent N_2H_4) has been investigated spectrophotometrically behind incident and reflected shock waves with Mach numbers of $2 < M < 3.5$ in the temperature range 1100°K to 1600°K. At the same time, extinction coefficients have been established up to temperatures of about 1500°K for some points of the ultraviolet band of hydrazine. In addition, the kinetic behavior and ultraviolet extinction coefficients of ammonia, which appears as a decomposition product of hydrazine, were measured under a variety of shock conditions up to temperatures of about 2900°K.

Two shock tubes were used for this purpose. One was square with internal dimensions of 3.2 cm on a side and a 2.50 m long low-pressure section; the other was round with an internal diameter of 10 cm and a 4.20 m low-pressure section. Kinetic and spectroscopic results obtained behind reflected shocks in the large and the small tube were identical, within the accuracy of these measurements.

In order to determine the over-all conversion of hydrazine to ammonia, nitrogen and hydrogen, a method was used involving spectrophotometric recording of hydrazine behind incident shock waves and of ammonia behind reflected shock waves in a single experiment. As the reflected shock travels through the wake of the incident shock after the decomposition of hydrazine, it raises the density and the temperature to $T > 2000$°K. At these temperatures the extinction coefficient of one decomposition product, NH_3, is high enough to produce an absorption signal at 2300 Å, which can easily be evaluated. Since the extinction coefficients of NH_3 had been determined in independent experiments, the amount of NH_3 formed in the decomposition of N_2H_4 could be derived. NH_3 appearing behind the reflected shock could be identified unequivocally on the basis of its kinetic behavior at temperatures above 2100°K. Using this method it was established that the parameter ν in the over-all equation for the thermal decomposition of hydrazine

$$N_2H_4 \longrightarrow NH_3 + (2 - 3/2\,\nu)H_2 + (1 - 1/2\,\nu)N_2$$

varies from $\nu = 1$ at lower temperatures (1100-1200°K) to $\nu = 0.5$ (1500-1600°K). The stoichiometry in the high temperature range had to be determined from the remaining absorption after all hydrazine had decomposed in reflected shock studies. At temperatures higher than 1500°K, the extinction coefficient of NH_3 has risen to such a value, that this procedure becomes applicable. NH_3 decomposes too slowly at $T < 2000$°K for chemical equilibrium to be established within the available reaction time. At temperatures higher than 2000°K, when N_2H_4 decomposes within less than one μ sec, no ammonia could be detected as a reaction product, within the accuracy of this determination (10 per cent). On the other hand, if the reaction was not complete (T = 1100-1250°K) in the volume element under observation when the reflected shock arrived, the quantity of ammonia measured in the reflected wave corresponded to not more than the hydrazine quantity decomposed behind the incident wave with $\nu = 0.8$ - 1.0. Hence, two different decomposition mechanisms seem to apply for low and high temperatures. The stoichiometry of the decomposition at low temperatures is in substantial agreement with results in decomposition flames.

The absorption traces of hydrazine show an induction period prior to the decline. This and the pronounced dependence of half-lives upon the molar partial density of hydrazine (which varied between 3 and 30 · 10^{-8} mole/cm^3) is in accord with the interpretation in terms of a chain mechanism. The temperature dependence of half-lives in the range from 1100°K to 1300°K is reflected by the expression

$$\log \tau_{1/2} = -12.67 + 43.2\ \text{kcal}/2.3 \cdot RT$$

where $\tau_{1/2}$ is in sec, at a molar partial density of N_2H_4 of $\rho_5 \simeq 24 \cdot 10^{-8}$ mole/cm^3, and $\log \tau_{1/2} = -12.50 + 43.2\text{kcal}/2.3 \cdot RT$ ($\tau_{1/2}$ in sec), with $\rho_5 \approx 7 \cdot 10^{-8}$ mole/cm^3.

As one approaches higher temperatures (T > 1300°K) and lower partial densities of N_2H_4, the induction period disappears, the rate law for the decomposition becomes first order and the rate constant becomes independent of the partial density of N_2H_4 A slight pressure dependence, however, could be detected as the total density ρ_T (Ar) was varied between $2.5 \cdot 10^{-5}$ and $7.5 \cdot 10^{-5}$ mole/cm^3. The first-order rate constants follow the rate laws

$$\log k \approx 12.8 - \frac{52\ \text{kcal/mole}}{2.3\ RT}\ ,\ k \text{ in } [\text{sec}]^{-1} \text{ at } \rho_T = 7.5 \cdot 10^{-5}\ \text{mole/cm}^3$$

and

$$\log k \approx 12.0 - \frac{48\ \text{kcal/mole}}{2.3\ RT}\ ,\ k \text{ in } [\text{sec}]^{-1} \text{ at } \rho_T = 2.5 \cdot 10^{-5}\ \text{mole/cm}^3.$$

This indicates that the unimolecular decomposition of hydrazine was measured close to the high-pressure limit in the temperature range between 1300° and 1600°K.

In fast reactions, as investigated here, the transient concentration of radicals is so high, that it is possible to detect them photometrically. In the pyrolysis of N_2H_4 the significance of NH radicals was investigated on the basis of their light absorption at 3360 Å. At temperatures below 1400°K no absorption due to NH was recorded even with as high molar partial densities of N_2H_4 as $50 \cdot 10^{-8}$ mole/cm^3. Hence, NH does not seem to be of any importance in the chain decomposition. At temperatures above 1400°K, however, NH appeared in increasing amounts with an induction period, which became shorter with increasing temperature. NH disappeared again in these experiments according to a first-order rate law. Its formation is attributed to secondary reactions following unimolecular dissociation.

Addition of oxygen to a hydrazine-argon mixture (0.3 per cent N_2H_4, molar partial density $20 \cdot 10^{-8}$ mole/cm^3 N_2H_4) causes noticeable acceleration of the decomposition only when it is added in appreciable amounts ($[O_2] / [N_2H_4] > 2$). The absorption traces with a tenfold excess of O_2 with respect to N_2H_4 reveal a decomposition mechanism different from that of the thermal decomposition of N_2H_4. At higher temperatures, however, the effect of O_2 becomes less pronounced and disappears completely at T > 1350°K. The apparent energy of activation for a mixture consisting of 0.28 per cent N_2H_4 and 2.8 per cent O_2 is as low E ≈ 30 kcal/mole.

In investigating the kinetic behavior of the decomposition product NH_3, the unimolecular character of its pyrolysis has been clearly established by varying the molar partial density of NH_3 by a factor of 100 and the total gas density by a factor of 10. The first-order rate constant is proportional to the total gas density throughout the measured temperature range (2100-2900°K), this indicating that the decomposition

occurs in the limiting low-pressure region. The second-order rate constant, with Ar as a collision partner, is

$$k = 10^{15.6} \cdot \exp\left(-\frac{79.5 \text{ kcal/mole}}{RT}\right) \left[\text{cm}^3/\text{mole}\cdot\text{sec}\right].$$

Simultaneously with the decomposition of NH_3, large quantities of NH radicals are detected, the kinetic significance of which is discussed.

49. THE GAS PHASE DECOMPOSITION OF HYDRAZINE AND ITS METHYL DERIVATIVES

I. J. Eberstein and I. Glassman

Princeton University

The gas phase decomposition kinetics of hydrazine, hydrazine-water mixtures, unsymmetrical dimethylhydrazine (UDMH) and monomethylhydrazine (MMH) were studied in a new type adiabatic flow reactor described previously. [1] The importance of these studies is that all compounds were investigated under the same conditions of temperature, pressure, experimental configuration, etc., so that an explicit evaluation of these comparative rates can be made.

The major efforts were with hydrazine, UDMH, and MMH, which in their liquid phase are used extensively as monopropellants and bipropellant fuels. In the gas phase, the over-all reaction order in all cases was found to be very close to unity; however, there was some indication that the reaction order for UDMH might be slightly less.

For hydrazine the rate constant could be best represented by the expression

$$k = 10^{10.33} \exp\left[\frac{-36,170}{RT}\right] \text{ sec}^{-1}$$

The observed reaction rates agree with the results of shock tube studies by Jost. [2] This comparison also shows the useful range of this type flow reactor to be in a rate regime just below normally thought for a shock tube. The high temperature flow reactor data just overlap the low temperature regime of Jost's shock tube results. The activation energy obtained agrees well with that deduced from laminar flame studies by Gray and Lee. [3]

In addition to the rate measurements, chemical samples were taken with water-cooled probes near the end of the reaction zones. The observed stoichiometry was in good agreement with the reaction products reported by Murray and Hall. [4]

The effect of large amounts of water (25%-50%) on hydrazine decomposition was studied. It was found that the rate of decomposition of hydrazine-water mixtures was slower than that of the anhydrous material by approximately a factor of 10, and was independent of the amount of water added. It was also found that slightly wet hydrazine behaved kinetically like the hydrazine-water mixtures, and that the decomposition of

wet hydrazine, and of hydrazine-water mixtures was independent of the surface-to-volume ratio of the reactor. The amount of water in the wet hydrazine is only slightly greater than in the anhydrous material, which contains 0.5% water. Thus it seems that water inhibits the gaseous decomposition of hydrazine by very effectively suppressing some reaction step.

The first order rate constant for UDMH was found to be:

$$k = 10^{9.29} \exp\left[\frac{-28,800}{RT}\right] \text{ sec}^{-1}$$

The activation energy agrees with that found by other investigators. [5,6] Furthermore, the decomposition of UDMH was found to be independent of surface-to-volume ratio, in agreement with the observation of Cordes. [5]

The surface area to volume ratio in the reaction is varied by changing the size of the flow tubes; 2, 3 and 4 inch ducts were used. The over-all rate constant for MMH decomposition was found to be

$$k = 10^{13.4} \exp\left[\frac{-47,000}{RT}\right] \text{ sec}^{-1}$$

The rates in the 4 inch duct were slightly lower.

A comparison of the reaction rates of the three monopropellants shows that, in the temperature regime of this study, i.e., 800-1000°K., UDMH decomposition is fastest, hydrazine decomposition is slowest, and the monomethylhydrazine decomposition rate is intermediate. It is somewhat surprising that the reaction rate of hydrazine, which is known for its poor stability, should be the slowest.

It is not unlikely, however, that the rate of homogeneous gas phase decomposition of hydrazine is indeed relatively slow, and that hydrazine explosions are surface initiated. Such a conclusion is confirmed by the strong effect which most surface materials have on the decomposition of hydrazine vapor.

Reaction mechanisms for the thermal gas phase decomposition of hydrazine, and its methyl derivatives, were postulated and studied numerically.

In studying mechanisms for hydrazine decomposition, the rate constants for the initiation reaction found by Szwarc-Gilbert, [6,7] and propagation and termination reactions suggested by Gilbert [8] and Adams and Stocks [9] were used. The mechanism in this study differed from those postulated by previous investigators, in that it included a set of branching reactions

$$N_2H_3 \longrightarrow NH + NH_2$$

$$N_2H_4 + NH \longrightarrow N_2H_3 + NH_2$$

The branching reactions were included for two reasons. The NH radical has been observed in flames, [10] and without branching, the over-all activation energy computed for the reaction from the mechanism was too high, and the over-all reaction rate was too low.

The logarithm of the computed rate constant was plotted against 1/T. The resulting curve was found to agree with experimental data obtained in this study and in shock tube studies by Jost. [2] Also, the stoichiometry calculated from the mechanism agreed with that measured experimentally.

Thus, the postulated mechanism accurately predicts the experimental observations on gaseous hydrazine decomposition. However, it does not explain the effect of

small amounts of water on the hydrazine decomposition rate. To explain this effect, Ramsay's [11] postulate that the N_2H_3 radical is formed in an excited state, $N_2H_3^*$ which can either branch to give NH + NH_2, i.e.,

$$N_2H_3^* \longrightarrow NH + NH_2$$

or be deactivated to a relatively stable form of N_2H_3, i. e.,

$$N_2H_3^* + X \longrightarrow N_2H_3 + X$$

proved to be quite useful. Namely, the inhibitive effect of water now appears to vibrationally relax the N_2H_3 radical, thus preventing it from branching. Water is generally excellent for promoting vibrational relaxation, and also, has vibrational frequencies close to those of hydrazine, suggesting the possibility of resonance transfer of vibrational energy.

Mechanisms for decomposition of the two methyl derivatives of hydrazine are more complex than for hydrazine, and therefore cannot be established with much reliability from the available data. However, such mechanisms have been postulated, and the rate constants calculated from these mechanisms do agree with experimentally observed values.

References

1. Crocco, L., Glassman, I., and Smith, I. E.: J. Chem. Phys. 31, 506-510 (1959)

2. Jost, W.: Investigations of Gaseous Detonations and Shock Wave Experiments with Hydrazine. Aeronautical Research Laboratories Report ARL 62-330, April 1962.

3. Gray, P. and Lee, J. C., with Leach and Taylor: Sixth Symposium (International) on Combustion, p. 255, Reinhold Publishing Corp., 1957.

4. Murray, R. C. and Hall, A. R.: Flame Speeds in Hydrazine Vapor and in Mixtures of Hydrazine and Ammonia with Oxygen. Transactions of the Faraday Society, 47, 743-751 (1951).

5. Cordes, H. F.: J. Phys. Chem. 65, 1473-1477 (1961)

6. Gray, P. and Spencer, M.: Combustion and Flame, 6, 337-345 (1962)

7. Gilbert, M.: An Approximate Treatment of Hydrazine Decomposition in a Laminar, non-Isothermal Flow. Jet Propulsion Laboratory Progress Report 20-336. Pasadena, California, July 1957.

8. Gilbert, M.: The Hydrazine Flame. JPL Prog. Rep. 20-318. Pasadena, 1957.

9. Adams, G. K. and Stocks, G. W.: Fourth Symposium (International) on Combustion, p. 239, The Williams & Wilkins Co., 1953.

10. Hall, A. R. and Wolfhard, H. G.: Hydrazine Decomposition Flames at Subatmospheric Pressures. Trans. Faraday Soc. 52, 1520-1525 (1956).

11. Ramsay, D. A.: J. Phys. Chem. 57, 415 (1953).

DETONATION

50. DETONATION LIMITS IN COMPOSITE EXPLOSIVES

William E. Gordon

Combustion and Explosives Research, Inc.

Characteristic differences in the effect of density distinguish composite explosives (based on ammonium nitrate or ammonium perchlorate as oxidizer with an organic fuel) from molecular explosives like TNT or pure ammonium perchlorate. The behavior suggests that the reaction slows down when density is increased in composite explosives, while in molecular explosives it speeds up. Cook [1] ascribes the effect to diffusion as the rate controlling mechanism. This paper describes a model for diffusion-controlled reaction based on the "hole" concept in liquids, in which the activation energy for diffusion is equated simply to pV. The marked effect of density therefore results from the strong dependence of pressure on density (p varying about as the density cubed) and the appearance of this factor in an exponential term. On this basis the following approximate expression is derived for dependence of detonation velocity D on explosive density ρ_o

$$\frac{D}{D_\infty^*} = \left(\frac{\rho_o}{\rho_o^*}\right)^m \left[1 - \frac{\ell}{d} \exp b \left(\frac{\rho_o}{\rho_o^*}\right)^{2m+1}\right]$$

where d is charge diameter, ℓ and b are constants related to various explosive parameters, m is the exponent of order unity in the expression for ideal velocity D as a function of density, and the asterisk refers to a reference state. From this expression one derives that the critical diameter d_c for these materials is an exponential function of density of the type

$$\log_e (d_c/\ell) = b (\rho_o/\rho_o^*)^{2m+1} .$$

Experimental evidence to support this behavior is given; and the implications of these results for the problem of determining critical diameter in composite solid propellants are discussed.

Reference

1. Cook, M. A.: The Science of High Explosives, p. 141, Reinhold Publishing Corp., 1958.

51. ON THE NATURE OF THE CRITICAL DIAMETER

A. N. Dremin and V. S. Trofimov

USSR Academy of Sciences

It has been established by many investigators concerned with the detonation of liquid explosives that the shock front of a detonation wave is not smooth. As in gas detonations, oblique shocks due to instability of the ignition plane travel over the detonation wave front. The ignition plane instability is a function of the temperature dependence of the reaction.

In traveling over the shock front of a detonation wave, the oblique waves collide and initiate a reaction. The induction period of the latter at the points of collision is considerably shorter than that observed beyond the shock front.

Consequently, initiating centers will not form when the conditions for inter-collisions and collisions with reactor walls are unfavorable. When detonation passes from the tube into the air, the oblique waves at the edge find nothing to collide with. Thus no active centers will form at the shock periphery at the point of detonation exit. As a result, there will be no formation of new oblique shocks at the periphery of the detonation near the exit, and this, in turn, will lead to the disappearance of neighboring initiating centers. This may be seen from smear-camera records obtained for the detonation of transparent explosives, as observed from the butt end.

It was shown experimentally that detonation will proceed at the same rate if reaction-quenching waves do not penetrate as far as the axis of the charge. When they reach the latter, detonation stops. It will be apparent from this that the reaction-quenching waves may penetrate to a distance equal to one-half the critical diameter.

Let us consider what governs the penetration of reaction-quenching waves. After destruction of the oblique shocks, there remains a smooth shock wave at the detonation periphery; it is compressed by detonation products, as by a piston. The main shock compresses the explosive and initiates a reaction after a certain induction period τ which depends upon the temperature and pressure behind the wave. A rarefied wave comes from the charge edge at a rate C, thus the reaction has to occur at a place unattained by this wave, after a time τ. The reaction will then proceed into the charge as a detonation over the shock-compressed substance. It overtakes the reaction-quenching wave at a distance d_{cr} and stops the destruction of oblique waves.

An equation for the critical diameter of detonation of a liquid explosive may be obtained on the basis of the above considerations

$$d_{cr} = 2\, V\tau\, U \left(\frac{1}{D - U} + \frac{1}{U - C}\right) \qquad (1)$$

Here V is the velocity of oblique shocks traveling over the detonation front, U is the velocity of the explosive compressed by the shock relative to the boundary of the quenching wave, D is the rate of detonation propagation over the compressed substance.

It follows from the above equation that, besides depending on kinetic parameters of the explosives, d_{cr} is a function of the mechanical properties of the explosive and its detonation products. It is also quite conceivable that a more active substance would have a higher d_{cr}, due to its mechanical properties.

Equation (1) was used to calculate d_{cr} for nitromethane (NM) at 1° to 20°C and for melted trotyl (TNT) at 82° to 83°C. The value obtained for NM was $d_{cr} = 14.3$ mm, as compared to the experimental 18 mm; for TNT the calculated value was 62, and the experimental was 68 mm.

52. WHITHAM'S SHOCK-WAVE APPROXIMATION APPLIED TO THE INITIATION OF DETONATION IN SOLID EXPLOSIVES

D. C. Pack and F. J. Warner

The Royal College of Science and Technology, Glasgow

In this paper, we consider the initiation or fading of detonation in a solid explosive under conditions of plane, cylindrically symmetric, or spherically symmetric flow. The full set of six partial differential and algebraic equations [Brode, Physics of Fluids, 2 (1959)] is amenable to treatment only on a digital computer, but by applying Whitham's shock-wave approximation [Whitham, J. Fluid Mech., 4 (1958)] we are able to simplify the problem so as to obtain one ordinary differential equation of first order whose solution approximates to the solution of the full set of partial differential equations.

It is argued that the approximation is valid in the early phase of initiation, and for laws of burning where the energy of combustion is released very close to the shock front. If we assume an Abel equation of state, and a pressure-dependent law of burning, then the resultant ordinary differential equation turns out to be of Bernoullian type, and is integrable in terms of elementary functions.

If the law of burning is taken to be

$$Q\frac{\partial f}{\partial t} = kp^{m}(1 - f)^{2/3}$$

where Q, k and m are constants, we obtain the differential equation

$$\frac{dp}{dr} = A\,p^{m-\frac{1}{2}} - \frac{Bp}{r} \quad ,$$

for the pressure p at a distance r from the origin, where A and B are functions of the parameters of the problem. A depends on k, the ratio of specific heats, (assumed constant), the initial density, and the covolume in the Abel equation, while B depends on the number of spatial dimensions, the ratio of specific heats, the initial density, and the covolume. The rate of burning constant k depends on the value of m [Warner, 9th Symp. Combustion].

The isoclines and trajectories of this differential equation are considered, and are seen to fall into three classes. If $m < 3/2$, then the pressure p inceases monotonically for sufficiently large r, no matter what initial conditions are chosen. If $3/2 < m < 3/2 + \frac{1}{B}$, the pressure has a vertical asymptote for some finite value of r, again irrespective of the initial conditions. If, however, $m > 3/2 + \frac{1}{B}$, the pattern depends on the initial conditions chosen. For high values of the initial pressure at a given radius, the trajectory has a vertical asymptote for a finite value of the radius as in the previous case, but for low values of the initial pressure at the same radius, the trajectory always suffers a decrease in pressure, and the pressure tends to zero as the radius tends to infinity. It is argued that the latter behavior represents a fading detonation wave, while all cases where the pressure goes to infinity represent a detonation going to completion. A steady-state Chapman–Jouguet detonation is not achieved because we have neglected the effect of rarefactions traveling forward into the shock front. This is not significant since we are interested only in the initiation phase and are not concerned with the steady-state solution. The boundary between trajectories which fade and trajectories which go to complete combustion is itself a trajectory of

the system, and is thus a critical trajectory. This gives a strong condition on the fading of detonation, since the neglect of rarefactions in the analysis implies that solutions which fade in the approximated problem will certainly fade in the solution of the full set of differential equations, while solutions which just give complete combustion in the approximated problem may fade in the full solution.

It thus seems that, for real explosives in spherically symmetric space, we must have the exponent of pressure in the burning law m greater than $3/2 + \frac{1}{B}$, which under our standard conditions is 1.747. After putting some numerical values into the algebraic results, we estimate that m = 2 would seem to be an appropriate choice on comparison with experimental evidence. The analysis is valid for all values of the ratio of specific heats, but has only been carried out in detail for the Abel equation of state.

53. PRESSURE MEASUREMENTS DURING SHOCK INITIATION OF COMPOSITION-B

V. M. Boyle, R. L. Jameson and F. E. Allison

Ballistic Research Laboratories

When a sufficiently strong shock wave is produced in an explosive material, the wave rapidly develops into a self-sustaining detonation wave. Results of experimental work at the Los Alamos Scientific Laboratory, [1,2] together with careful theoretical calculations performed at the same laboratory, [3,4] have shown that the production of local "hot spots" by the passage of the shock wave is the dominant mechanism responsible for the initiation of a detonation wave in inhomogeneous explosives. The chemical reaction at the hot spots supplies energy to the shock wave causing it to accelerate until steady-state detonation has been established. Experimental studies of the chemically supported shock wave have been largely restricted to measurements of its propagation velocity. [5] Because there are only two conservation equations and four hydrodynamic variables (shock velocity, particle velocity behind the shock, pressure, and density), measurements of the wave velocity provide only a partial description of the shock.

By considering the boundary conditions existing when a shock wave propagates from an inert barrier into an explosive specimen, Liddiard [6] has shown that a linear relation exists between initial values of the shock and particle velocities for pressures up to 72 kilobars in Composition B-3 (60RDX/40TNT) and 137 kilobars in TNT. From an extrapolation of the linear relation, Liddiard estimates the von Neumann spike pressure to be 382 kilobars for Composition B-3. Duff and Houston [7,8] have obtained a measure of the Chapman-Jouguet pressure and an estimate of the von Neumann spike pressure from a careful study of shock propagation through inert materials placed in contact with the explosive ahead of the detonation wave. They relate the shock pressure in the inert material to the pressure in the detonation wave by making the acoustic approximation for the reflected wave.

The measurements to be discussed in this paper were made on the shock front in the explosive as it builds up to a steady-state detonation. A continuous record of the wave, as it accelerates in the explosive, was obtained by using a rotating mirror camera to observe the emergence of the wave from the front surface of an explosive wedge similar to that used at NOL and Los Alamos. To obtain information, other than the wave velocity in the explosive, the front surface of the wedge was covered with a

suitable transparent material (Plexiglas) having known Hugoniot properties. The two-dimensional character of the wave configuration was considered when relating the pressure in the inert media to the pressure of the incident wave in the explosive.

A series of observations were made using Composition-B wedges covered with a thin layer of Plexiglas. The Composition-B differed from that used by Liddiard in that one to two per cent wax had been added to the 60RDX/40TNT mixture. The average shock velocity in the Plexiglas was determined at several points along the surface of the wedge for three different thicknesses of Plexiglas. To determine the shock velocity at the explosive-Plexiglas boundary, the measurements were extrapolated to zero thickness. Values of the pressure and particle velocity in the explosive were calculated from the measured shock velocities in the explosive and the extrapolated velocities in the Plexiglas. The shock velocity in the Composition-B was found to be a linear function of particle velocity up to a pressure of 173 kilobars. At low pressures the data are in general agreement with Liddiard's values for the unreacted explosive; however, a least-squares fit to the data gives a slightly lower slope than that obtained by Liddiard. Consequently an extrapolation of the linear region beyond 173 kilobars indicates a slightly higher von Neumann spike pressure. Above 173 kilobars the data deviate from a straight line indicating a maximum pressure somewhat higher than the Chapman-Jouguet pressure but less than the von Neumann spike pressure. The deviation of the data from a linear relation is believed to result from the fact that appreciable chemical reaction has occurred during the time required for the experimental observations.

References

1. Campbell, A. W., Davis, W. C., and Travis, J. R.: Phys. Fluids 4, 498 (1961).

2. Campbell, A. W., Davis, W. C., Ramsay, J. B., and Travis, J. R.: Phys. Fluids 4, 511 (1961).

3. Evans, M. W., Harlow, F. H., and Meixner, B. D.: Phys. Fluids 5, 651 (1962).

4. Mader, C. L.: Phys. Fluids 6, 375 (1963).

5. Jacobs, S. J., Liddiard, Jr., T. P., and Drimmer, B. E.: Ninth Symposium (International) on Combustion, p. 517, Academic Press, 1963.

6. Liddiard, Jr., T. P.: International Conference on Sensitivity and Hazards of Explosives.

7. Duff, Russell E., and Houston, Edwin: Second ONR Symposium on Detonation (1955).

8. Duff, Russell E., and Houston, Edwin: J. Chem. Phys. 23, 1268 (1955).

54. MEASUREMENTS OF THE DETONATION FRONT STRUCTURE IN CONDENSED PHASE EXPLOSIVES*

B. G. Craig

University of California, Los Alamos Scientific Laboratory

The hydrodynamic theory of one-dimensional, steady-state detonation has been developed by von Neumann [1], by Döring [2], and by Zeldovitch [3], and in a more advanced form by Kirkwood and Wood. [4, 5] For condensed phase (liquid and solid) explosives with reasonable values of the viscosity and the reaction rate the reaction zone structure has a simple form. The leading front of the wave is a shock wave in the unreacted explosive which heats it and causes it to react thermally after an induction period. As reaction proceeds the pressure falls until the reaction is complete and then remains constant. The region between the shock front and the point of complete reaction is called the reaction zone. The pressure decrease, as reaction proceeds and energy is released, seems contrary to common sense at first, but it comes about because the speed of the detonation wave is controlled by the shock velocity in the unreacted material. The flow behind the shock adjusts so that the whole structure moves together. As the reaction releases energy the pressure corresponding to the fixed wave speed decreases, principally because the material is at a higher temperature.

Experimentally we can never achieve a detonation that is truly either one dimensional or steady state, and the exact analysis of an actual experiment is too complicated for present methods. Therefore, we must use approximations and extrapolations to try to guess what an exact treatment of a real experiment would show. Most students of detonations have guessed that in large charges the detonation structure is very similar to the idealized one-dimensional, steady-state structure, led by a shock wave and followed by a pressure decrease, and that in smaller charges the divergence of the flow would make some quantitative differences but that qualitatively the structure would remain the same. In this paper some experimental results are presented which show that this guess is too simple. The sharp shock wave and the following pressure decrease apparently are present and are believed to correspond to the reaction zone; but, they are followed by a further rapid decrease in pressure which is not predicted by any extrapolation of the one-dimensional theory. This new follower of the reaction zone, which we have called the decay zone, depends very strongly on the geometry of the charge.

Recently published studies of gas detonations have shown that a somewhat similar phenomenon exists in gases, and that turbulent flow following the reaction is responsible for it. There is now no convincing evidence to show that there is or is not turbulence in the flow following reaction in condensed-phase explosives.

The experiments which produced the results to be given here were measurements of the free-surface velocity of plates of various thicknessess driven by the explosive. The plate velocities are related to the pressure in the explosive at a distance back in the explosive approximately proportional to the plate thickness, as discussed by Duff and Houston. [6] The velocities were measured using a smear camera technique described by Davis and Craig. [7] The experimental conditions and the quality of explosive, plates, boosters, etc., were very carefully controlled.

---

*Work done under the auspicies of the U. S. Atomic Energy Commission.

In the liquid explosive nitromethane the zone of chemical reaction cannot be observed by plate velocity technique, but its presence can be inferred from other experiments. The decay zone begins at a pressure of about 141 kbar, nearly independent of the charge size. The slope of the pressure fall is also nearly independent of charge size, but the extent of the zone is very strongly dependent on charge diameter and length, and also on the details of the boostering explosive and the confinement of the charge. In a short charge of large diameter, initiated with a plane-wave generator, the decay-zone length approaches zero and is not observed. In a long cylindrical charge initiated with a plane wave, the decay zone increases in length as the detonation runs. For example, in a 37 mm diameter charge after a run of 16 diameters, the decay zone is about 0.8 mm long and the pressure falls about 27 kbar in the zone.

In high-density, pressed TNT charges the chemical reaction zone can be observed with the plate velocity technique, and the decay zone behavior is very similar to that found in nitromethane. However, a new feature is observed. The pressure at the head of the decay wave is not constant but increases with charge size, and is influenced by the diameter, length, boostering, confinement, etc. This effect has undoubtedly led to large errors in measuring the detonation pressure, For example, the decay wave head pressure, which we believe to be what is often called C-J pressure, for very large charges is about 225 kbar. Measured in a 50 mm diameter charge after a run of 15 diameters, the pressure at the head of the decay zone is about 200 kbar.

Several other explosives, including PETN, Composition B, and various plastic-bonded HMX explosives have been studied and have shown the same kinds of behavior. The large change in pressure at the head of the decay zone seems to be present in those explosives which show a large change in detonation velocity with diameter.

References

1. von Neumann, J.: O.S.R.D. Report No. 549 (1942).

2. Döring, W.: Ann. Physik 43, 421 (1943).

3. Zeldovitch, Y. B.: J. Exptl. Theoret. Phys. (U.S.S.R.) 10, 542 (1940).

4. Kirkwood, J. G., and Wood, W. W.: J. Chem. Phys. 22, 1915 (1954).

5. Wood, W. W., and Kirkwood, J. G.: J. Chem. Phys. 25, 1276 (1956).

6. Duff, R. E., and Houston, E.: Second ONR Symposium on Detonation, p. 225 (1955).

7. Davis, W. C., and Craig, B. G.: Rev. Sci. Instr. 32, 579, (1961).

55. ELECTRICAL MEASUREMENTS IN REACTION ZONES OF HIGH EXPLOSIVES*

Bernard Hayes

University of California, Los Alamos Scientific Laboratory

Nanosecond and subnanosecond time resolution experiments on the electrical conducting properties of detonating high explosives have been carried out utilizing a dynamic conductivity cell. The purpose of such studies is threefold: (1) to obtain the electrical conductivity profile behind the detonation front due to the detonation products; (2) to determine the conduction mechanism which determines the type and amount of charge carriers; and (3) to ascertain the feasibility of measuring reaction zone thickness in solid and liquid explosives.

To accomplish these objectives the reaction zone is considered to be a stratified region in which the release of charge carriers closely parallels reaction zone events. If indeed the conductivity of the reaction products is due to the activation of these products then the conductivity profile may be meaningfully interpreted as corresponding to processes going on behind the detonation front. Obtaining the conductivity profile was the reason for developing the dynamic conductivity cell; dynamic in the sense that instantaneous measurements are possible coupled with high sensitivity in order to discern small variations in the conductivity from one stratum to another.

The conductivity cell consists of a small hemispherical probe mounted coaxially in a cylindrical metal case. The tube serves as the container for the explosive as well as the common return for electrical currents. The probe is initially maintained at a potential of a few volts supplied by a transmission line of known impedance $\underline{Z}$. A separate sampling transmission line of impedance $\underline{R}$ is also connected to the probe. When the detonation wave contacts the probe a current begins to flow and the probe voltage changes to accomodate the conductance between the probe and the container wall. As the detonation wave sweeps over the probe more and more surface area of the probe is exposed; the total conductance increases and the probe voltage decreases. The changes in voltage are recorded at the end of the terminated sampling transmission line, and it can be shown that the total conductance at the probe is obtained from the expression

$$g(t) = \int_0^t \frac{d\,g(t)}{dt}\,dt = (1/Z + 1/R)(V/f(t) - 1)$$

where $\underline{V}$ is the initial voltage at the probe before the detonation front arrives, and f(t) is the electric waveform at the probe as a function of time after the detonation contacts the probe. In general f(t) is a monotonically decreasing function somewhat exponential in shape. The cable impedance $\underline{Z}$ serves also to establish the optimum impedance level for each type of explosive as well as supplying the necessary electric current.

With proper design the conductivity cell frequency response can be extended well into the gigacycle region of the electromagnetic spectrum which implies excellent fidelity and reproducibility. This too is the reason the transmission lines are used instead of lumped circuit elements; only high quality transmission lines are capable of the necessary

---

*Work done under the auspices of the U. S. Atomic Energy Commission.

wideband performance. In addition, the recording oscilloscope is of the traveling wave cathode ray tube variety so that every effort is made to obtain only the effects of the detonation wave and to reduce to a minimum any adverse effects of the measuring circuitry.

Having obtained the conductance as a function of time, the conductivity of the explosion products as a function of time behind the detonation front can be calculated when the geometric function for the conductivity cell is known. For the hemisphere used in these experiments the geometric function is

$$S = a \cos^{-1} (1 - Dt/a)$$

where S is an arc length and is a measure of the area of the probe exposed to the detonation products. The radius of the probe is a and D is the detonation velocity. The average conductance becomes

$$g(t) = 4S(t)\sigma(t)$$

and, when the detonation products are assumed to be layered so that each layer is an average over a small time, the conductivity of the n th layer may be written

$$\sigma_n = \frac{g_n(t)/4 - \sum_{i=1}^{n-1} \sigma_i (S_{n+1-i} - S_{n-i})}{S_1}$$

where S_1 is the arc length associated with a Δt; in other words, the minimum resolution in time. For ease in data handling and evaluation the preceding expression was coded for machine operation. Using a conical point instead of a sphere the above expression may be written in closed form as follows

$$\sigma(t) = \frac{V(1/Z+1/R)}{4D\sqrt{1+1/b^2}} \left[f^{-1} - e^{-t} \int_0^t f^{-1} e^t dt \right]$$

where b is the slope of the probe point and e is the base of the natural logarithm. The other symbols are as previously defined.

It should be noted that while quite excellent results have been obtained, implicit in the results are the facts that no corrections have been made to account for any motion of the probe (primarily because for the particular geometry it is not yet clear how to make a correction and in all cases thus far any correction would be quite small); also, the resultant shock wave at the probe is neglected. One reason for neglecting these effects is that they tend to self-cancel one another. The latter effect would be to produce a sheath around the exposed probe tending to make it look larger while the former tends to reduce the probe size. The probes themselves have been made as small as possible consistent with the requirement that the detonation wave should not overtake the hemisphere during an observation period. The usual probes are from 3 to 15 mils in radius.

The results thus far have been quite impressive, particularly since after a few technique shots very worthwhile and interesting results have begun to emerge. To date three different kinds of explosives have been investigated, namely, nitromethane, Composition B, and liquid TNT; liquids primarily because they are homogeneous and do not require any special preparation. The one solid was investigated to compare the present technique with previous results obtained by quite a different method.

Nitromethane was the first explosive critically examined because it was known on a theoretical basis at least that if a reaction zone did exist it would be extremely small and not detectable by other methods. Fortunate also was the fact that its average conductivity was not so large that special cables were required as was the case for the other explosives. The average conductivity of nitromethane is around 150 mhos per meter; a value which is roughly twenty times the conductivity of sea water and more than twice the strongest available electrolyte. In addition, a pronounced conductivity peak occurs at about $1\frac{1}{2}$ to 2 nanoseconds after the detonation front. The repeatability was quite good; both the conductivity scatter and time history scatter varying by only a few per cent for the four shots of this type fired so far.

Composition B was tried next. In this case both the conductivity profile and the value of the conductivity were quite different from those for nitromethane. For one thing, the conductivity peak was nearly an order of magnitude higher but did not occur until nearly 100 nanoseconds after the arrival of the detonation front. In addition a pronounced inflection occurred at about 7.5 nanoseconds.

The third explosive to be investigated thus far has characteristics quite similar to Composition B, namely, liquid TNT; similar in that a conductivity peak occurs preceded by an inflection region reminiscent of a reaction zone. However, the conductivity peak is again an order of magnitude greater than the corresponding peak for Composition B. Or to put it another way, the peak conductivity of liquid TNT is only one order of magnitude below the conductivity of solid carbon at about the same temperature. This is quite an important realization, because now a very probable conduction mechanism is apparent. The vast conductivity changes among the explosives investigated thus far cannot be explained on the basis of simple kinetic theory because their pressures and temperatures are not vastly different. On the other hand, when you consider that the calculated fractional carbon density for detonating liquid TNT is about 26%, it is quite reasonable to expect that the electrical conduction properties should be quite good.

To carry this theme one step further, the curve of the calculated free carbon content in grams per cubic centimeter vs the log of the peak conductivity for the three explosives thus far measured is a straight line plot. Thus, since the binding energy of carbon is not too great, the phenomenon of charge conduction can be attributed to the loosely bound or valence electrons available from the carbon and the bulk conductivity is then governed primarily by the fractional carbon density. Of course, there will also be some conduction from thermal and bond breaking processes and it remains to be investigated if indeed carbon-free explosives have conductivities dictated on the basis of kinetic theory.

Two of the three goals set down in the first paragraph have been achieved. Conductivity profiles are readily generated and the mechanism of charge conduction can be explained. The third, ascertaining if reaction zones can be discerned, is not entirely clear, yet. In the case of nitromethane, where incidentally the fraction carbon density is only about 12%, there is evidence to suppose that the peak in the conductivity profile does indeed correspond to the true nature of a reaction zone. It might also be supposed that the high conductivity of the carbon rich explosives masks the reaction zones in the other explosives tested and that by proper choice of the wide variety of low carbon explosives available a pattern will emerge which supports the present thinking. In any event the lines for research on the problem are quite clear and work is continuing to investigate the many facets opened by this new research tool.

56. THE EQUATION OF STATE OF PBX 9404 AND LX04-01

Mark L. Wilkins, Bailey Squier and Bertram Halperin

University of California, Livermore

Experimentally it is difficult to achieve a one dimensional detonation wave that has traversed any reasonable distance because edge effects enter. Therefore, much of the experimental work on detonations is in two dimensional geometry. However, care must be taken when applying the Chapman-Jouguet theory of detonation waves. In attempts to use this theory with experiments that range from quasi one dimensional to possible two dimensional steady state considerable difficulty can be encountered.

To assure a strictly one dimensional geometry, experiments were done using spheres. From these experiments the Chapman-Jouguet pressure and equation of state of PBX 9404 were derived. The experimental data was used in conjunction with finite difference calculations of the hydrodynamic equations to obtain some previously inaccessible data on high explosives.

One of the difficulties in determining the C-J pressure for high explosives is to make the measurement away from the influence of the initiator, but before two dimensional effects have entered the experiments. A 12 inch diameter sphere of PBX 9404 was considered large enough to permit experiments to be done away from the effects of the initiator. The sphere was detonated at the center by a 1/2 inch diameter spherical detonator. On the surface of the sphere were placed spherical segments of aluminum and magnesium in thicknesses of 1/16, 2/16, 3/16 and 4/16 of an inch. The initial front surface velocities of the metals were measured by pins. Because of the symmetry there was ample space to repeat each of the eight velocity measurements four times. Eight pins were used for each velocity determination. Other laboratories have extrapolated the front surface velocities to remove the influence of the rarefactions behind the shock wave in the metals. The difficulties associated with the velocity extrapolation were avoided by using a computer hydrodynamic code. The method used was to assume an equation of state for the high explosive and iterate with the code until a pressure at the C-J point resulted in a calculated front surface distance-time curve that matched the experimental pin data. For the thin metal used here only a small portion of the high explosive profile is being sampled and hence the early motion of the metal is sensitive to the C-J point. The 1/16 and 2/16 inch thicknesses could not be used because they showed the effect of the von Neumann spike. Actually only one thickness of metal is required for this experiment, the other thicknesses provide independent checks on the pressure determination.

The impedance of the two metals was such that the pressure of the shock wave in the aluminum was above the HE C-J pressure while the pressure associated with the magnesium was below the C-J pressure. The transmitted shock in the aluminum has a sharp pressure gradient that results in a tension wave reflected from the front surface and causes a deceleration of the front surface. Because the transmitted pressure wave in the magnesium has dropped below the C-J pressure it does not have a sharp gradient associated with it and there is no tension present over the range of the experiment. In the iteration method described above, a C-J pressure of 390 kb was deduced from the magnesium data. The aluminum gave the same result when the calculations were allowed to develop 30 kb tensions. Tensions of the order of 30 kb in aluminum have been measured independently by four different laboratories. The experiment was repeated in a 3/4 scale geometry with the same results. The equation of state form used for the C-J pressure determination was obtained from general physical considerations and was determined from a second series of experiments.

Experimental data for pressure, volume points removed from the C-J point have been difficult to obtain. W. Deal located points on the pressure particle curve on the C-J isentrope below the C-J point and the reflected shock Hugoniot above the C-J point by measuring the initial free surface velocity of a layer of inert material placed at the front surface of a slab of high explosive.

Deal's work depends on a knowledge of the equation of state of the inert material. For metals used to obtain data near the C-J point the equations of state are known with precision. Gases were used to give information at low pressures. However, for the important intermediate pressure range there are no materials available. The method selected at LRL for studying the equation of state was to permit the HE to expand across a void before striking an aluminum layer in an outward burning spherical geometry. The outside surface of the aluminum was then observed continuously using streaking cameras. The initial acceleration in these experiments came from pressures lower than the C-J pressure by factors of 2 to 5. The accelerations at late times came from pressures 10 to 100 times lower than the C-J pressure and had a significant effect on the radius vs time path.

The data were interpreted by assuming a form for an equation of state and solving the hydrodynamic equations of motion on a high speed computer to predict the radius vs time curve. Comparisons of experimental and calculated curves were used to suggest a form for the equation of state and later to evaluate some of the parameters of the equation. It should be noted that in these experiments shock heating of the gas is much more important. Hence, attention must be given, in developing an equation of state, to the energy dependence of the C-J isentrope. The hydrodynamic calculations reproduce a Chapman-Jouguet detonation from the center of a sphere. When the detonation front reaches the outside radius of the high explosive the gas expands into the void. When the gas reaches the aluminum, a shock is transmitted into the aluminum shell and a shock is reflected back into the high explosive gas. The early motion of the aluminum shell is thus governed by the shocked high explosive gas. The shock reflected into the high explosive is quickly dissipated and the main acceleration of the shell is from the high explosive gas on the C-J adiabat. By varying the void size the shell can be made to be accelerated by gas representative of different parts of the adiabat. The attempt has been made here to use the early part of the shell acceleration to determine the dependence of the gas to shock heating as well as the major part of the plate acceleration to investigate the Chapman-Jouguet adiabat.

The motion of an aluminum (6061-T6) 12 inch inside diameter hemisphere was observed by two streaking cameras that looked near the top of the hemisphere where the motion was one dimensional during the time of the measurements. A full sphere of HE was used to accelerate the hemisphere. A framing camera was used to monitor the aluminum shell which was found to be intact for displacements up to 10 cm before it finally became unstable. Since the area of the aluminum shell increases as the shell expands the response of the shell motion to the pressure increases.

The equation of state traced out by this method showed that on a Log P vs Log V plot the adiabat became initially steeper for expansion below the C-J point and then leveled off beginning with expansions of two in relative volume. A possible explanation is that endothermic reactions are taking place. The equation of state developed could also be interpreted in terms of repulsive forces being responsible for the inferred dip in the C-J adiabat.

57. STEADY DETONATIONS IN GASEOUS OZONE*

R. W. Getzinger, J. Ray Bowen, A. K. Oppenheim and M. Boudart

University of California, Berkeley

Decomposing ozone contains only three components, O, O_2 and O_3, reacting in a well-studied sequence of elementary steps:

$$O_3 + M \rightleftharpoons O_2 + O + M \qquad (1)$$

$$O + O_3 \longrightarrow O_2 + O_2 \qquad (2)$$

$$O + O + M \longrightarrow O_2 + M \qquad (3)$$

Because of this simplicity, ozone lends itself to studies of deflagration, detonation and of transition from deflagration to detonation. In this first communication on ozone, stable detonation velocities are reported. The work was done at various pressures and compositions and in tubes of three different diameters.

The measurements were made for the following reason. Oxygen molecules produced by reaction (2) with up to 17 vibrational quanta may not have the time to relax during their passage through the reaction wave. [1] If this is the case, part of the enthalpy of reaction would be frozen in and the detonation velocity D would be smaller than that computed on the basis of thermodynamic equilibrium among reaction products.

Ozone was produced by passing purified electrolytic oxygen through a Welsbach T-23 ozonator and purified by fractional distillation in a liquid oxygen cold trap. Gaseous compositions of any desired strength up to 97% ozone in oxygen were obtained in a leak-tight stainless-steel storage tank by appropriate dilution with oxygen through a special mixing valve. Gaseous argon was also added to the tank in this manner when desired.

Stable velocity measurements were made in 30-foot-long Pyrex tubes of 1/4", 1/2", and 1" i.d. for compositions of 70% ozone and above, and initial pressures of 80-200 mm Hg, whenever possible. Four carefully collimated photomultipliers spaced at intervals of 0.500 meters and located some 25 feet from the point of spark or glow coil ignition sent signals at the passing of the detonation wave through gain amplifiers to thyratrons and hence to an oscilloscope. Here the pulses were superimposed upon a raster sweep with 1 μsec time marks for photographing. With the intervals and traverse times accurately known it was possible to obtain an over-all velocity of detonation for a given condition if satisfactory agreement was obtained between the three sub-velocities. Reproducibility of measurements was found to be excellent.

Compositions were determined by the change in pressure during combustion of a small sample of the mixture in question. Checks of this type were made either before or after each detonation, or both. Pressure was carefully determined with a cathetometer or eyeglass from a mercury manometer protected with sulfuric acid. The Pyrex tubes were covered with electrician's tape for protection and to keep external light from reaching the photomultipliers. Leak rates in the tubes were kept at a minimum. For the runs where conditions overlapped with those of Harper and Gordon, [2] excellent agreement (within 2%) was obtained between detonation velocities as measured here and as reported by the previous investigators.

---

*This research was supported by the National Aeronautics and Space Administration under Grant No. NSG-10-59 and by Project SQUID under contract NONR 3623(S-11). One of us (R. W. Getzinger) expresses his thanks to the National Science Foundation for a fellowship.

A program for calculation of the classical detonation parameters as a function of initial pressure and composition was written for use on an IBM 7090 computer. With this program it was possible to determine theoretical detonation velocities for ozone-oxygen and ozone-oxygen-argon mixtures for any initial conditions of interest. A slight modification also permitted an estimation of the effect on the velocity of a loss of some of the heat of reaction caused by incomplete vibrational relaxation.

The measured stable detonation velocities were utilized to obtain plots of velocity versus inverse diameter whenever identical overlapping conditions could be obtained in the three tubes. Extrapolation to infinite diameter yielded the value of detonation velocity for comparison with theory.

The results of this work can be summarized as follows:

1. The extrapolated velocity values are lower than the corresponding theoretical velocities, but only by about $1\frac{1}{2}\%$ in the cases considered. The effect of tube diameter can clearly be seen in all measured velocities.

2. Substitution of argon for oxygen in some of the mixtures produced no change in the measured detonation velocity, in agreement with theoretical expectation.

3. If oxygen molecules were able to relax down to the first excited vibrational level by resonant exchange but were frozen to this last level by too slow a collisional deactivation, [1] a velocity deficit of 5 to 6% should have been observed.

Therefore, it is possible to conclude from the data that if equilibration fails to take place, the effect is of minor importance. Since the effect would be of major importance if vibrational relaxation took place at the slow rate actually measured in shock tubes, our result supports the idea that in the presence of significant amounts of oxygen atoms in the reaction wave, the rate of vibrational relaxation is greatly enhanced. Furthermore, since the conditions for observing a lack of equilibration are particularly acute for ozone, our failure to observe this effect gives some support to the speculation that equilibration in reacting systems in general proceeds rapidly enough so that there may be no need to worry about "non-equilibrium" chemical kinetics or energy chains in the detailed analysis of fast reactions.

References

1. Boudart, M.: Eighth Symposium (International) on Combustion, p. 43, The Williams & Wilkins Co., 1962.

2. Harper, S. A. and Gordon, W. E.: Adv. in Chem. Series 21, 28, Am. Chem. Soc. (1959)

58. STRUCTURE OF GASEOUS DETONATION: IV. INDUCTION ZONE STUDIES*

Donald R. White and George E. Moore

General Electric Research Laboratory

The density structure of the zones of vibrational relaxation and chemical reaction behind shock waves in hydrogen-oxygen and carbon monoxide-oxygen mixtures has been studied interferometrically in an 8.25 cm-square shock tube. For highly detonable mixtures, where a plane shock front and a laminar reaction zone do not stably exist, [1] a converging-diverging section was used to produce a laminar detonation [2] amenable to quantitative interferometric analysis. In such interferometric records, one can discern the density increase due to vibrational relaxation immediately behind the thin shock front and, following a density maximum, the subsequent decrease in density due to exothermic reaction.

The vibrational relaxation time for O_2 in O_2-H_2 mixtures has been determined previously, [3] and can now be calculated for any given mixture. It is shown that this time is short relative to the induction time for all mixture ratios for shocks weaker than $M_s = 6$. Since both induction time and relaxation time are associated with bimolecular processes, this conclusion applies to all initial pressures.

The "von Neumann spike" is seen to be a nearly-constant-density plateau (the induction zone) in H_2-O_2 detonation. The maximum density attained agrees with Hugoniot calculations assuming thermal equilibrium of the internal degrees of freedom but excluding chemical reaction. [4] Measurements of the initially abrupt decrease in density which marks the end of the induction zone suggest that this is probably due in part to the approach to an exothermic "partial equilibrium state" [5] via bimolecular reactions.

The induction time between the shock and the onset of observably exothermic reaction is plotted against $1/T$ using both $[O_2]\,t_i$ and $([O_2][H_2])^{1/2}t_i$ and the latter is seen to provide a better correlation for widely different mixture ratios. The experimental induction times are given within 50% by

$$\log_{10}\left([O_2][H_2]\right)^{1/2}t_i = 3.1 \times 10^3/T - 9.8$$

for $0.0075 \leq [H_2]/[O_2] < 24$, $1200 < T < 2000^{\circ}K$, with concentrations in moles/liter and t_i in seconds. No inert diluents were used in these experiments. The temperature T is calculated from the shock velocity assuming vibrational equilibrium but no reaction.

The early part of the reaction zone in CO-O_2 detonation is seen to differ qualitatively from H_2-O_2 detonation in that the vibrational relaxation is relatively slow and a gradual density decrease replaces the constant density plateau and rather abrupt subsequent decrease in density found in the H_2-O_2 system. The maximum density is again found to correspond to that calculated assuming vibrational relaxation of both reactants prior to the beginning of the reaction.

A single relaxation time is observed for the CO-O_2 mixtures, longer than that expected for the O_2 in the given mixture and shorter than predicted for the CO, using

---

*This research has been supported by the Aerospace Research Laboratories of the United States Air Force.

available correlations of vibrational relaxation times in simple systems. 6/ Attainment of vibrational equilibrium must therefore involve not only translation-to-vibration energy conversion, but also exchange of vibrational energy between the reactants.

The turbulent appearance of the reaction zone behind a free-running detonation is believed to be due to several closely related factors, the presence of transversely propagating (spin) shocks, the contact surfaces or shear layers originating from their intersections with the main shock front, and the gradients resulting from the consequent curvature of the main front. These observations on laminar reaction zones should apply directly to the structure of a free-running detonation, assuming only that the separation of these transverse shocks is large compared to the induction zone thickness.

References

1. White, D. R.: Phys. of Fluids 4, 465 (1961)

2. White, D. R., and Cary, K. C.: Phys. of Fluids 6, 749 (1963)

3. White, D. R., and Millikan, R. C.: J. Chem. Phys. 39, 2107 (1963)

4. White, D. R.: Phys. of Fluids 6, 1011 (1963)

5. Schott, G. L.: J. Chem. Phys. 32, 710 (1960)

6. Millikan, R. C., and White, D. R.: J. Chem. Phys., 39, 3209 (1963)

59. DYNAMICS OF THE GENERATION OF PRESSURE WAVES BY ACCELERATING FLAMES

P. A. Urtiew, A. J. Laderman and A. K. Oppenheim

University of California, Berkeley

The theory of initial flame acceleration in an explosive gas contained in a constant cross-section tube, developed previously for a hemispherically shaped flame, has been extended to include flames of spheroidal shapes. An expression for the flame world-line has been developed which depends only on a single parameter that accounts for the effects of the thermodynamic properties of the mixture and the geometry of the flame front. Its value is determined graphically on the basis of experimental data. This leads to an unambiguous technique for the evaluation of the relative flame propagation speed and for the calculation of the pressure wave generated by the flame.

60. TWO DIMENSIONAL UNCONFINED GASEOUS DETONATION WAVES

J. H. Lee, B. H. K. Lee and I. Shanfield

McGill University, Montreal

The distribution of the fluid properties behind a steadily expanding cylindrical detonation wave is determined by solving the basic equations for the unsteady expansion of the combustion products. An unconfined cylindrical Chapman-Jouguet detonation wave is found to be non-existent at small radius, and must propagate as a strong detonation ($D < u_1 + c_1$). Measurements of the detonation pressure at different radii show that a cylindrical detonation wave is initially overdriven and decays rapidly to a Chapman-Jouguet wave. True transition from cylindrical deflagration to detonation under unconfined conditions is not possible. Pseudo-transition, due to the interaction of the reflected precompression waves off the cylindrical wall with the flame, occurs when a significant amount of normal burning has been completed. Direct initiation of a cylindrical detonation wave requires the instantaneous release of a large quantity of ignition energy. Spinning and pulsating cylindrical detonation waves are not observed near the limits of detonability.

61. THE INFLUENCE OF A COMPRESSIBLE BOUNDARY ON THE PROPAGATION OF GASEOUS DETONATIONS

E. K. Dabora, J. A. Nicholls, R. B. Morrison

The University of Michigan

The influence of a compressible medium adjacent to a gaseous explosive on the behavior of detonation waves in the latter medium is investigated both theoretically and experimentally. In particular, the influence on the propagation velocity and the conditions under which the detonation wave quenches are assessed.

The theoretical analysis shows that a detonation wave in a gaseous explosive bounded by an inert gaseous medium propagates at a lower velocity than it would have if the explosive were inside a tube with a solid wall. The model adopted for the analysis is that the detonation wave is a shock followed by a Chapman-Jouguet plane at a distance equivalent to the reaction length. Within the reaction region a stream tube starting at the detonation front suffers an area increase at the C-J plane. This area increment is based on the over-all deflection angle of the interface which can be evaluated after initially assuming the detonation to be a discontinuity. The velocity decrement is found to be dependent primarily on the ratio of the initial densities of the explosive and the inert gases, the reaction length of the explosive, and the extent of the explosive (channel width) normal to the interface. Extension of some criteria available in the literature for the prediction of composition limits shows that there is a limit to the velocity decrement beyond which the detonation is expected to quench, and therefore deteriorate into a shock.

The experimental setup consists of a tube of rectangular cross section , . 36 in. deep by . 5 in. wide, through which the explosive gas flows at a very low velocity (about 4 ft/sec). At the test section which terminates the tube and in which the channel width can be varied, the explosive flows beside the inert boundary gas but is separated from it by a thin film (250-500 Å thick). The purpose of the latter is to minimize any diffusion effects. The detonation wave is started in the tube and when it reaches the test section it can be observed with its attendant phenomena by either spark schlieren or streak schlieren photography.

The results of extensive tests on hydrogen-oxygen mixtures at NTP bounded by nitrogen are described. For all mixture ratios tested the limiting channel width below which the detonation wave quenches are obtained. On the basis of these, further experiments reveal that a velocity decrement beyond 8-10% leads to quenching. The quenching curve indicates agreement with the explosion limit criterion used by Belles for the prediction of composition limits.

For the stoichiometric hydrogen-oxygen mixture the variation of the velocity with channel width is obtained showing agreement with the theoretical analysis. Further, it is found that the reaction length of this mixture is about 0.14 in. which is in agreement with the value found in the literature by other techniques.

Some results on stoichiometric CH_4-O_2 bounded by different gases are also included. They show general agreement with the theoretical analysis and reveal a reaction length of about 0. 32 in. for this mixture.

Streak photographs of the detonation wave near the quenching limit show at times some periodic fluctuations suggestive of spinning detonations usually observed near composition limits. It appears that a proper choice of channel width and boundary gas can be used to induce "spin" at will. The experimental technique may therefore be useful for the study of this phenomenon.

The main advantage of the experimental technique, however, is that it could be used as a means of evaluating reaction lengths and determining quenching conditions. The latter could very well be useful in elucidating the reaction mechanism of the particular mixture being investigated.

DISCUSSION

ON

AERODYNAMICS IN COMBUSTION

FREE BURNING FIRES

(Co-sponsored by the Committee on Fire Research
U. S. National Academy of Sciences-National Research Council)

62. FUNDAMENTAL PROBLEMS OF THE FREE BURNING FIRE

H. W. Emmons

Harvard University

The growth of knowledge about the free burning fire is observed to be of the slow evolutionary type of cut and try as man has had to attack the unwanted fire through the centuries. Since such fires are the result of intimate interaction of Geometry, Chemistry, Thermodynamics, Fluid Mechanics and Heat Transfer, each at an advanced level, it has not been possible prior to the present century -- almost the present decade -- to use accumulated scientific know-how -- there simply was too small an accumulation. This condition is changing and changing rapidly. In this paper some of the problems of the free burning fire are described, an indication of the present state of understanding is given and some suggestions are made for those avenues of approach that appear hopeful of successful attack in the near future.

Specifically, fire spread over building materials, through buildings and through forests, is described in sufficient detail to indicate where we are today, where we should be going and what it might get us if we went. The innumerable detail problems which must be individually solved and combined to produce solutions to the larger problems are little more than hinted at in the discussion. But it is clear that many man years of research, worth many millions of dollars, will be required to solve these problems, but with the cost of fire to society of many billions of dollars every year the indicated research is more than urgent.

63. THE FIRE PLUME ABOVE A LARGE FREE BURNING FIRE

H. J. Nielsen and L. N. Tao

Illinois Institute of Technology

Earlier analyses of the plume of buoyant gas produced by fires have been limited to the case where no heat is produced in the plume by combustion processes and the temperature is moderate. In a large fire where many structures are burning simultaneously, an environment is produced consisting of hot gases and radiant energy. In this environment wood and other combustible contents of structures undergo a pyrolysis process in which they give up gaseous products some of which are combustible. These gases flow upward and burn in the plume as sufficient oxygen is entrained from the surrounding air.

An analysis of the plume formed under these conditions including the effects of varying gas composition, combustion and radiation losses is possible by methods which are, in principle, the same as those used in previous plume studies. The boundary layer approximations are first applied to the general form of the conservation equations for a reacting gas. The resulting partial differential equations are integrated across the plume and the turbulent transport terms are removed by applying the boundary conditions that gradients of velocity, temperature and concentration approach zero at infinity. In this latter step a set of ordinary differential equations is obtained for the total upward flow of mass, various species, momentum and energy in the plume. Heat produced in the plume by combustion is considered in the energy equation by

including the heat of formation in the definition of enthalpy. Energy lost by radiation is accounted for by assuming the plume to radiate as a black body.

To relate the equations describing the upward flow of mass, species, momentum and energy to the radius of the plume and the state of the gases inside, it is necessary to assume some form for the radial distribution of velocity, concentration and temperature of the gases. In this analysis it is assumed that the distributions are top hat.

Several substances are involved in the combustion process taking place in the plume and a number of chemical reactions take part in the combustion of each substance. It does not seem feasible to treat the combustion process as it actually occurs because of its complexity. To facilitate this analysis the combustion process is idealized to one single over-all reaction.

The number of species to be considered is thus limited to only four, gaseous fuel, product, oxygen and nitrogen. By assuming that the rate at which combustion proceeds is controlled by the entrainment of oxygen into the plume, the species conservation equation is readily integrated for each species.

The differential equations for the mass, momentum and energy are made a complete set by introducing appropriate specific heat relationships to associate the enthalpy and composition of the gas with its temperature and by the relations required to associate temperature and composition with density.

The resulting set of equations was numerically integrated. Size of burning area and rate of pyrolysis of fuels on the ground were assumed and used as starting conditions for the integration. Typical results for conditions in the plume were obtained for various starting conditions. These results show the variation of plume radius, velocity, temperature and gas composition with altitude.

64. ON MODELING FIRE PLUMES

B. R. Morton

Manchester University, U. K.

Theoretical treatments for turbulent diffusion flames and for the strongly heated regions of fire plumes in a still environment may be based on those developed for weakly buoyant plumes, but appropriate modifications must be made to allow for the high temperatures and the large variations in density involved. This paper gives a discussion of some of the modifications that are needed, and deals separately with the effects of large variations in density on the plume dynamics and with aspects of heat transfer by radiation.

The entrainment into strongly buoyant plumes depends on the local ratio ρ/ρ_o of mean plume to ambient densities as well as on the mean plume velocity u, and dimensional arguments can do no more than define a local entrainment function $(\rho/\rho_o)^n E_o$ where n is undetermined and E_o is the well-established entrainment constant for weakly buoyant plumes. The value $n = \frac{1}{2}$ is suggested by the dependence of lateral diffusion on the Reynolds stresses, and the form

$$E = (\rho/\rho_o)^{\frac{1}{2}} E_o$$

is adopted here; comparable assumptions have been made previously.

Equations for the conservation of mean mass flux, mean momentum flux and mean heat flux along the turbulent diffusion column of the plume are obtained making full allowance for the dynamical effects of large variations in density. Provided that the level of intensity of the plume turbulence is not too high, these equations can be reduced approximately to a form directly related to the set of equations used previously in the study of weakly buoyant forced plumes. These sets of equations are related by the transformation.

$$\rho^{\frac{1}{2}} a = \rho_o^{\frac{1}{2}} b ,$$

where a and b are local length scales (essentially plume radii) for the strongly buoyant and weakly buoyant plumes, respectively. Hence the behavior of strongly buoyant plumes can be described in terms of existing solutions for weakly buoyant plumes, and in general it can be seen that strong plumes spread less rapidly than weak ones at first, although they are soon reduced to weakly buoyant behavior unless the large temperature differences are maintained, as by combustion.

Fire plumes are often rich in smoke and soot from imperfect combustion, and in such cases when the mean free path for radiation is small in relation to the plume diameter the opaque radiation approximation may be adopted. In this case the heat transfer by radiation can be divided into a vertical flux along the column of a diffusive character, and the outwards radiation from the edges of the plume through transparent air to the distant environment. It is shown that in many practical cases the vertical flux by radiation is small in relation to vertical convection and to edge radiation, and may be neglected for small values of the parameter $8\pi E_o^2 / 3kb_s$, where k is the absorption coefficient within the plume and b_s is the source radius. Indeed, when flow velocities are high, even the cooling effect of radiation from the plume edges may be small relative to cooling by turbulent entrainment of cold ambient air. A solution of this type is presented.

The purpose of this paper is to discuss questions involved in the formulation of fire plume theories, and therefore few solutions are given in detail and no attempt is made to link the dynamical effects with those due to radiation. However, a wider range of solutions will be available for reference and discussion at the Symposium.

65. BUOYANT DIFFUSION FLAMES: SOME MEASUREMENTS OF AIR ENTRAINMENT, HEAT TRANSFER AND FLAME MERGING

P. H. Thomas, R. Baldwin and A. J. M. Heselden

Fire Research Station, England

Thistledown has been used as a tracer to measure the flow of air towards ethyl alcohol and wood fires 91 cm in diameter and a smaller town gas fire. The total quantity of air below the mean flame height is approximately one order times the stoichiometric requirements, a substantial part of the air flowing upwards around the flame. The total flow also exceeds that estimated from entrainment theory and measurements of flame tip velocity. The mean concentration of oxygen on the flame axis and the heat transfer back towards the fuel surface have also been measured. The convection transfer at 1-2 cm above the fuel surface was found to be about 1/5 of

the total heat transfer at the center increasing to about $\frac{1}{2}$ at the edge. The measured mean axial temperature rise at the mean flame height was about 300-350°C for wood and alcohol and 500°C for town gas. The average period of the eddies outside the flame and the corresponding length were about 0.7 sec and 15 cm respectively. No variation was found with height above the base.

Elementary considerations of entrainment and the motion of flames have been applied to the merging of the flames from two nearby rectilinear fuel beds and there is reasonable agreement between theory and experiment.

66. THE MODELING OF FIRESPREAD THROUGH A FUEL BED

H. C. Hottel, G. C. Williams and F. R. Steward*

Massachusetts Institute of Technology

Data are presented on the effects of artificial irradiation and of humidity on the propagation of a line fire through beds of torn newsprint and computer-card punchings. Intensities of irradiation simulating the flame radiation, which is substantially absent in small model fires, produced up to 200% increases in the velocity of firefront propagation.

Four mathematical models were set up, primarily for the purpose of indicating how to allow, with some rigor, for surface heat losses during the irradiation process. Model I postulated the existence of a thin slab losing heat from its top face at a rate proportional to its temperature excess over the surroundings. Flame convection as a part of the propagating process was formulated in terms of eddy diffusivity and mixing scale. A quantity identified as a heat retention efficiency was formulated for each mechanism of heat transfer to the bed being heated.

Model II substituted a rate of surface heat loss proportional to the 1.6 power of the temperature difference, bed surface to air. A heat retention efficiency was formulated for a slab receiving heat from a line source.

Models III and IV were based on the assumption that surface temperature, rather than ignition energy per unit bed area, was significant, and the fuel bed was a semi-infinite solid. These models led to integral equations, approximate solutions of which indicated the magnitude of temperature rise expected compared to that of a no-loss slab. The surface loss in Model III was linear in temperature, in Model IV nonlinear.

None of the models predicted the experimentally observed decreasing effect of additional increments of artificial irradiation on the propagation velocity. Explanations were suggested.

---

*University of New Brunswick, Fredericton, New Brunswick, Canada.

67. INFLUENCE OF MOISTURE AND WIND UPON THE CHARACTERISTICS OF FREE BURNING FIRES

H. E. Anderson and R. C. Rothermel

United States Forest Service

A study of free burning fires in mat-type beds of two light forest fuels (needles of ponderosa and western white pine) showed measurable effects of certain environmental conditions on the characteristics of fire. Measurements of these characteristics of nearly 200 fires burned under controlled humidity, air velocity, and fuel moisture, provided data for developing equations that enable prediction of rate of fire spread in individual fuel types when moisture content and air velocity are varied. As fuel moisture content increases, rate of spread decreases linearly with no wind. Increasing wind causes rate of spread to increase exponentially or by a power function. The importance and usefulness of a unit combustion area measurement are demonstrated; such measurements make it possible to characterize all fires by use of unit combustion rate and rate of spread. A general equation that predicts rate of spread in any wood fuel may be developed by incorporating fuel particle size and fuel bed compactness with fuel moisture content and air velocity.

68. ON THE FLIGHT PATHS AND LIFETIMES OF BURNING PARTICLES OF WOOD

C. Sánchez Tarifa, P. Pérez del Notario and F. García Moreno

Instituto Nacional de Tecnica Aeroespacial, Madrid

Results of a research program on the burning properties, flight paths and lifetimes of burning particles of wood are given in the paper. This study is related to fire spread produced by firebrands, which is the dominating propagation mechanism in major forest fires.

The laws of variation of the aerodynamic drag and weight of firebrands as function of both time and relative wind speed are experimentally obtained in a wind tunnel. From these data the flight paths and corresponding lifetimes of the firebrands are calculated for given horizontal wind conditions and for a certain model of the convection column above a fire.

The conclusion was drawn that it is an excellent approximation to assume that the firebrands always fly at their final or terminal velocity of fall. This assumption reduces considerably the experimental work as well as the theoretical studies.

The results obtained permit the evaluation of the dangerous areas of possible fire propagation. Comparative results of the potential danger of firebrands with regard to size, shape, kind of wood, moisture content and wind conditions are shown.

A preliminary study of the general laws governing combustion of wood with forced convection is also included.

69. A MODEL STUDY OF WIND EFFECTS ON FREE BURNING FIRES

Abbott A. Putnam

The effects of cross winds up to 13 fps on various arrays of buoyancy-controlled, turbulent-diffusion flames of natural gas were studied.

In previously reported work [1,2], the single sources which made up the arrays were found to follow the relation

$$L^* = 29\, Q_o^{2/5} / g^{1/5}$$

when acting alone, where L^* is the flame height measured from a photograph, and Q_o is the volumetric rate of fuel flow. Heights of flames in arrays and lines of the sources with no wind exposure were then related to the single-source flame height.

In studies with a wind the following were investigated: a single source, six sources in a hexagonal pattern, a series of sources in a single line, and some arrangements of sources in double and triple lines. At each wind velocity and fuel-flow rate for each array, a measurement was made of the height of the blown flame, L_{sv}, and of the horizontal extension of the flame, L_{sh}. Also measured at each condition, with the wind source turned off, was the height of the unblown flame $\bar{L}^*$. The data were then related primarily to this unblown-flame height, rather than to the measured flow rate of the fuel.

For the single source and for two different spacings of six sources in a hexagonal pattern, $L_{sv}/\bar{L}^*$ and $L_{sh}/\bar{L}^*$ were found to correlate the data as a function of $V^2/g\bar{L}^*$. At high values of $V^2/g\bar{L}^*$,

$$L_{sv}/\bar{L}^* \sim (V^2/g\bar{L}^*)^{-1/4},$$

and

$$L_{sh}/\bar{L}^* \sim (V^2/g\bar{L}^*)^{1/6}.$$

For sufficient sources in single, double, or triple lines, it was found that

$$L_{sh}/L_{sv} \sim V/(g\bar{L}^*)^{1/2}.$$

The ratio of blown- to unblown-flame height decreased from unity as $V^2/g\bar{L}^*$ increased; at high values of $V^2/g\bar{L}^*$, this ratio of heights approached the relation

$$L_{sv}/\bar{L}^* \sim (V^2/g\bar{L}^*)^{-1/2}.$$

A theory predicting the blown-flame dimensions in terms of the unblown-flame height was developed on the basis that: (1) the deviations of density from ambient are small, (2) the flame can be treated as a hot plume with all chemical energy released at the plume base, and (3) the amount of air aspirated by the buoyant flame is proportional to the weighted vector sum of the velocities of the plume and of the cross wind. For each of the four theoretical curves (corresponding to the four approximate relations above), good agreement was found between the shape of the theoretical curve and the corresponding experimental data. In addition, for each theoretical curve the arbitrary constant required to fit the curve to the corresponding set of data was found to have a reasonable value.

The data of Thomas, Pickard, and Wraight [3] on blown wood crib fires was then examined. At lower values of the correlating function equivalent to $V^2/g\bar{L}^*$, the results were similar to those obtained for the natural gas flames. At the higher wind velocities, however, the flame appeared to assume a constant shape (but not size), and dimensionless flame height temporarily stayed about the same with increasing values of $V^2/g\bar{L}^*$ before resuming its downward trend. This result was interpreted as indicating that the blowing velocity was relatively so high in this region that there was no effect of buoyancy, either directly or indirectly; the flame was acting merely as if a line source of fuel from a wall were being supplied to burn in a highly turbulent stream.

As a result of this study, it was concluded that further investigation was justified on the change in configuration of the blown fires at high velocities. A need was found for experimentally determined conversion relations to use in correlating data on one fuel with that of another fuel. More, and more accurate, data were felt to be required on the effects of finite source area or source width in blown-flame properties.

References

1. Putnam, A. A., and Speich, C. F.: Ninth Symposium (International) on Combustion, p. 867, Academic Press, 1963.

2. Putnam, A. A.: Combustion and Flame, 7, 306, (1963).

3. Thomas, P. H., Pickard, R. W., and Wraight, H. G. H.: "On the Size and Orientation of Buoyant Diffusion Flames and the Effect of Wind," Department of Scientific and Industrial Research and Fire Offices' Committee, Joint Fire Research Organization, Fire Research Note 516, January, 1963.

DISCUSSION

ON

AERODYNAMICS IN COMBUSTION

ROCKET COMBUSTION INSTABILITY

70. THEORY OF ACOUSTIC INSTABILITY IN SOLID PROPELLANT ROCKET COMBUSTION

R. W. Hart and F. T. McClure

The Johns Hopkins University

The purpose of this paper is to review the problem of unstable combustion in solid propellant rockets, with special emphasis on the status of theory and, where possible, the comparison between theory and experiment. The manifestation of the problem in terms of the appearance of periodic pressure waves, and the consequences which ensue when these reach sufficient amplitude are first outlined. A rocket motor is then viewed as an acoustic cavity. The possible sources and sinks of acoustic energy are enumerated, and the gain-loss balance is discussed with respect to self-excited oscillation, and also with respect to influences of outside perturbations on a stable cavity which has a high Q. The quantitative approach to the representation of the various gain-loss mechanisms in the domain of linear stability theory is then reviewed. Particular emphasis is put on the modifications to ordinary acoustic stability theory which are required because of the existence of a mean flow field. The contributions to linear instability of the response of the burning propellant both to the pressure and velocity components of the acoustic field are then discussed. Attention is then turned to the fundamental theory of the interaction of the burning surface with a pressure oscillation. The linear (small perturbation) theory of the acoustic response of this region is reviewed in terms of the analytic models and postulates that have been made and their theoretical results. Some qualitative comparison with experiment is made.

The remaining part of the paper is then devoted to nonlinear effects. The theory of nonlinear instability in such systems is first reviewed to the extent that it exists. Then, the consequences of oscillation of finite amplitude arising from nonlinear effects are discussed. Under this heading, amplitude limitation in unstable cavities, wave distortion, and changes in the mean properties of the system are considered. In the last category, changes in the mean burning rate due to nonlinear pressure response and due to the erosion associated with the velocity component of the acoustic field are noted. The induction of vortex flow by acoustic streaming, as described by Swithenbank and Sotter and by Flandro, is discussed, with particular reference to its consequences in producing increased erosion, decreased nozzle flow, and angular torques. Brief mention is also made of the effects of the amplitude oscillations on combustion efficiency and the composition of the product gases.

71. EXPERIMENTAL SOLID ROCKET COMBUSTION INSTABILITY

E. W. Price

U. S. Naval Ordnance Test Station

Experience with oscillatory combustion of solid rocket propellants is classified into three categories referred to as high, intermediate, and low frequency instability.

In the frequency range 1,000 cps and up, instability is usually encountered in transverse modes of the rocket motor; results from interaction between acoustic pressure and the combustion process; is suppressed by metal fuel ingredients in the propellant

(particularly aluminum), at least in part through acoustic damping by the metal oxide droplets in the gas. In the frequency range 100-1,000 cps, instability is usually encountered in axial modes of the rocket motor; is often initiated by large disturbances under linearly stable conditions; results from interaction between both acoustic velocity and acoustic pressure with the combustion process; is not suppressed by metal fuel ingredients, but instead may be aggravated by the metal combustion. In the frequency range 1-100 cps, instability may occur in either acoustic or nonacoustic modes. Experience to date, at low frequency, pertains only to cases of interaction of acoustic pressure with combustion, but velocity-coupled contributions seem likely in rockets with dimensions large enough for axial acoustic modes in this frequency range. Low frequency instability is more prevalent at low pressures, and is often confined to a narrow frequency range.

The pattern of instability behavior has emerged as a consequence of extended experience with rocket motors and intensive investigations with burners designed specially for the purpose. The laboratory burners can be designed to control the type of acoustic behavior and the environmental conditions, permitting less equivocal interpretation of test results. The small propellant requirements in the laboratory burners have permitted greatly increased testing, including studies of propellant variables. While the gross aspects of instability behavior have fallen into a fairly orderly pattern, the inner microscopic behavior of the combustion zone under transient conditions is established only on a speculative basis, leaving the combustion scientist's job incomplete.

72. EXPERIMENTAL STATUS OF HIGH FREQUENCY LIQUID ROCKET COMBUSTION INSTABILITY

R. S. Levine

Rocketdyne

A necessary criterion for any self-sustained vibrating system, including unstable rocket combustion, is that enough energy must be supplied to the system at the proper frequency and phase relationship to overcome that lost by damping. However, there is no one unique sustaining combustion process, and there are several kinds of damping, and several different kinds of vibration. When one adds to this picture the fact that two or more kinds of vibration can coexist, the subject becomes complex.

There are several kinds of combustion instability. When the chamber pressure changes slowly enough so that wave motion in the chamber is not a factor, the resultant instability, usually driven by fluctuations in the propellant flow rate and sustained by a "combustion time delay," is called "chugging". At higher frequencies, one can have longitudinal wave motion in the chamber (also sustained by flow fluctuation or by "time delay"), and then cylindrical wave motion.

The most important cylindrical modes are the first transverse and first radial. They have a very nonlinear characteristic - may exist only at very low amplitude unless "triggered" to a critical amplitude - whereupon the amplitude grows enormously and the thrust chamber may experience heavy thermal and mechanical damage.

The stable combustion field in a liquid rocket consists of liquid streams impinging and forming liquid fans, these breaking into ligaments and blobs and finally into a dense cloud of droplets. All of this liquid burns on its surface at a rate controlled

by its surface area and turbulent heat and mass transfer. Some 70%-90% of the product gas is formed by droplet combustion but this plays little part in the instability. The other 30%-10% of the gas is formed from fans, ligaments, and blobs near the injector, and these burn slowly, probably because their specific area is small and because of the low-gas-phase concentration of oxidizer species around fuel fans and fuel species around oxidizer fans.

When high-frequency instability occurs the most dramatic change takes place in this poorly atomized and mixed region as is shown in high speed motion pictures. The high transverse gas velocity shatters the liquid, and particle displacement causes gas-liquid mixing, both resulting in intense gas generation. At low amplitudes these effects damp as well as drive, but at high amplitude the net effect occurs at the proper phase relationship to sustain the high-frequency instability. Other processes may also be important, especially the fact that the feed system must respond to the local chamber pressure changes caused by the instability.

Until recently, the most effective way to avoid destructive high-frequency instability was the empirical selection of injector styles that had a relatively high triggering threshold, and then avoiding triggering by careful control of engine starting and operating procedures. More recently, it has become possible to arrive at empirical stabilization systems, described below, such that the instability initiated by a trigger will die out, and stable combustion will be resumed promptly. This characteristic has been termed "Dynamic Stability".

High speed movies and pressure-time traces are presented, showing in a two-dimensional combustion apparatus processes similar to those occurring in full size chambers. These data include:

1. Stable and unstable combustion with alcohol-liquid oxygen. A backlight-filter arrangement provides for silhouetting the liquid droplets and observing their behavior.

2. Stable and unstable combustion with liquid oxygen-jet fuel. The processes are probably similar to the above, but are difficult to observe because of optically dense hot soot in the combustion gas.

3. A combination of variable-amplitude, transverse high-frequency instability with a feed-system chug. The pressure records are difficult to interpret without photographic support.

4. High-pressure, dense, liquid oxygen-RP combustion showing heavy damping of the pressure waves, except in the injection region where the amplitude is high.

5. Stable and unstable combustion with liquid oxygen-hydrogen. When the hydrogen is injected as a high-velocity gas, the system is generally stable. With liquid hydrogen injection the characteristics are similar to liquid oxygen-jet fuel.

6. Stable and unstable combustion with nitrogen tetroxide-unsymmetrical dimethylhydrazine. These "storable" propellants exhibit a sustaining mechanism like liquid oxygen-jet fuel, but their "sensitive region" is more widespread, and their hypergolicity gives rise to kinds of "triggers" not present with nonhypergolic propellants.

The processes observed in the movies are discussed briefly relative to the various sustaining processes that have been advanced for this kind of instability. These include: loss of ignition, chemical preparation time or time delay; detonation waves; pressure- or temperature-sensitive chemical kinetics; the "exploding" of droplets burning at pressures above their critical pressure; and the shattering and mixing of the streams, fans, and drops by the gas "particle" motion.

Methods of control of high-frequency instability for practical engines include the use of baffles that interfere with the unwanted gas motion, "pre-mix" schemes that rapidly disintegrate the unmixed and poorly atomized portion of the spray, and other designs that may combine these processes with effective damping of the wave motion. The application of the baffle principle to the H-1 (Saturn) engine injector is illustrated.

73. THEORETICAL STUDIES ON LIQUID PROPELLANT ROCKET INSTABILITY

L. Crocco

Princeton University

(No Abstract)

DISCUSSION

ON

AERODYNAMICS IN COMBUSTION

LOW-SPEED AND HIGH-SPEED COMBUSTION PROCESSES

74. THE EFFECT OF THE RESIDENCE TIME DISTRIBUTION ON THE PERFORMANCE AND EFFICIENCY OF COMBUSTORS

J. M. Beér* and K. B. Lee**

The International Flame Research Foundation, IJmuiden, Holland

The fraction of unburned fuel as a function of residence time in a combustor was computed for two extreme cases: the perfectly stirred and the plug flow type combustors. It is shown that an "ideal" residence time distribution can be obtained by the combination of the two types of combustors in such a way that the perfectly stirred part is followed by the plug flow combustor in series. This combination of the two combustor types enables the highest volumetric rates of combustion to be obtained for a given combustion efficiency.

Experiments were carried out both with a 1/10 scale water model of the IJmuiden furnace and also in the IJmuiden tunnel furnace. A salt solution was introduced as a tracer into the "burner fluid" of the water model and the residence time distribution was determined by measuring the decay of the salt concentration with time in the exit stream after cutting off the tracer flow. The form of the residence time distribution curves indicated that the combustor volume can be assumed to consist of two parts, a well stirred and a plug flow type volume fraction in series. By introducing the "burner fluid" in the form of a swirling jet and by varying the degree of swirl, it was possible to vary the ratio of the mean residence time in the perfectly stirred section to that in the whole combustor ($\bar{t}_s/\bar{t}$) over a wide range. Residence time distributions were also determined in the IJmuiden furnace while burning pulverized anthracite. The tracer in this case was argon and principally the same technique was used as in the water model experiments. The comparison of the residence time distributions in the cold model and in the furnace showed good agreement when the value of the dimensionless group $G\phi/G_x.r$ was maintained the same for both model and prototype. ($G\phi$ is the axial flux of the angular momentum of the swirling burner fluid, G_x is the axial flux of the linear momentum and r is the burner radius.) Good agreement was found also between the experimental values of the unburned fraction of the fuel at the boundary of the two types of zones and those predicted from theory.

---

* Present address: The Pennsylvania State University
**Present address: Cabot Corporation, Cheshire, England

75. THE APPLICATION OF PRESSURE-JET BURNERS TO MARINE BOILERS

A. M. Brown and M. W. Thring

University of Sheffield, England

Pressure-jet burners are now required to operate with combustion intensities of over 2 x 10^5 Btu/ft^{3}hr. and with practically no excess air. It is shown experimentally that changes in oil spray characteristics and operating rate alter the mixing and the progress of combustion, so that, as the spray angle increases, the disposition of the unburned fuel moves away from the center until it is concentrated in an annulus outside the highest velocity part of the jet. It has been shown to be possible to model flames of this type successfully on either a velocity similarity or a residence time similarity

basis. It is demonstrated that the application of burners to boilers must be taken into account for satisfactory operation. This is discussed under the following headings. (1) Unwanted combustion oscillations occurring are shown to be of a "non-acoustic" type, which is a function of the mixing characteristics of the flame. They do not occur if the resistance across the burner is increased above a certain point and are usually restricted to the fuel rich region except at very low powers. (2) The mutual interaction between burners has been shown by single model studies to affect the velocity decay and recirculation. It is shown that these jets can be correlated for widely spaced jets with single jet data assuming each jet operates in its own effective cylinder. For close spacings ($R \leqslant \frac{1}{2}$) the entrainment was considerably less than the equivalent single jet. (3) The positioning of the burner is shown to affect the heat transfer to the boiler tubes as well; a side firing arrangement instead of end firing is shown to give considerable improvement. The work suggests that drastic redesign of burners and "honeycomb" combustion chambers could give considerable improvements.

76. STUDIES OF INDUSTRIAL HIGH INTENSITY GAS COMBUSTORS

W. E. Francis

Gas Council, Midlands Research Station, England

This paper describes theoretical and experimental studies of high intensity gas combustors, providing information from which practical combustors have been designed and applied in industrial furnaces and heating equipment. The combustors consist of combinations of an injector, in which low pressure air injects fuel gas, followed by a refractory lined combustion chamber in which the air/gas mixture is burned, and the burned gases, at or near flame temperature, are accelerated through a refractory exit nozzle. The studies included investigations of the fluid dynamics of injection, the burner pressure loss characteristics, flame stability, completeness of combustion and combustion intensity.

In designing a combustor of this type, the objective is to make the best possible use of the air supply pressure to obtain the highest exit velocity of the burned gases, or alternatively the highest air/gas mixture velocity at the mixture nozzle (if a burner of wide stability range is required, i.e., high turndown). This necessitates minimizing the pressure losses in the whole burner, from fuel gas inlet to combustion exit. The pressure losses in the system may be characterized by defining a dimensionless pressure efficiency, i.e., the ratio of the dynamic pressure of combustion gases in the exit nozzle to the dynamic pressure of air in the injector air nozzle. Examples of the calculation of pressure efficiency have been given for both incompressible and compressible conditions.

Experimental determinations of flashback rates have been carried out over a wide range of burner size, and the results in the laminar flow range have correlated with the concept of a critical boundary velocity gradient. In the turbulent region no such correlation has been found.

Compositions of combustion products at the burner exit have been determined experimentally and compared with the calculated equilibrium values to find the combustion chamber length required for complete combustion.

77. OSCILLATORY COMBUSTION IN TUNNEL BURNERS

J. K. Kilham, E. G. Jackson and T. J. B. Smith*

The University of Leeds

The factors leading to resonant combustion in tunnel burners have been investigated and the results have indicated the importance of the upstream mixture feed length. It has been established that the combination of the flame and the tunnel tends to generate organ pipe oscillations at a frequency which depends, among other parameters, on the tunnel length. These oscillations are propagated upstream into the unburned mixture and, in the presence of some type of acoustic termination, there is the possibility of standing waves being set up in the mixture feed system. The standing waves cause pulsations in the mixture flow, giving rise to a fluctuating component of heat release and if they are in phase with the natural tunnel oscillations, resonance will occur accompanied by "screaming" combustion.

In industrial air blast burners there is no precise upstream acoustic termination but the venturi injector or air nozzle has been found to act as a rather indefinite "open" end. In general, however, practical burners showed a marked similarity to the idealized experimental type. The tunnel length and mixture feed arrangement exert a considerable effect on the degree of resonance and a method has been suggested for the suitable matching of these two components in order to avoid oscillations. Recommendations have also been made for the positioning of bends in the mixture manifold.

---

*Present address: University of California, Los Angeles 24.

78. A CONTRIBUTION TO THE STUDY OF LOW FREQUENCY OSCILLATIONS IN FUEL OIL BOILERS

F. Mauss, E. Perthuis and B. Salé

Institut Français du Pétrole

This paper deals with the low frequency type of oscillations in fuel-oil burners. The authors present a simplified theory which is then used to discuss experimental results concerning the nature of the oscillating system and the conditions of its sustained oscillations. Experiments were performed on a standard domestic boiler fitted with a variable length stack. It is shown that there is no break of continuity between acoustical and non-acoustical types of oscillations. Nevertheless the authors' experiments indicate that the measured frequencies are of the same order of magnitude as the acoustical frequencies. These frequencies tend to a limit as the length of the stack is increased. In practical systems an important dispersion of the frequency occurs; this, and the fact that the values of frequency are very low, make it difficult to use tuned damping systems. Increasing the pressure head of the fan and improving the stabilization of the flame seem to be the most advantageous means of reducing the oscillation tendency of boilers. An important damping is provided by the stack and it is easier to avoid oscillations for greater lengths of the stack.

79. PROGRESS AND PROBLEMS IN GAS TURBINE COMBUSTION

Arthur H. Lefebvre

College of Aeronautics, Cranfield, England

In recent years the accumulation of reliable experimental data confirming the previously derived relationships between combustion chamber dimensions, specific pressure loss and the operating conditions of pressure, temperature and velocity, has led to the formulation of design rules and to a much clearer appreciation of the most promising lines of research.

At the present time it is difficult to envisage areas in which fundamental research can make an effective contribution to combustion chamber development, at least in the foreseeable future, but there is ample scope for applied research on ignition, fuel injection methods, fluid dynamic and heat transfer processes, and modeling techniques. Although research on these topics is unlikely to produce significant reductions in chamber size and pressure loss, it should lead to worthwhile improvements in terms of reduced size and weight of ignition equipment, elimination of exhaust smoke, longer flametube life, and to an outlet temperature profile that is less senstive to variations in engine operating conditions.

80. A TENTATIVE MODEL FOR RATES OF COMBUSTION IN CONFINED, TURBULENT FLAMES

N. M. Howe, Jr.* and C. W. Shipman

Worcester Polytechnic Institute

A model of the burning zone of confined, turbulent flames has been tested against measured reaction rates of oxygen in such flames. The burning zone is characterized as parcels of unburned gas dispersed through burned gas, et contra, with burning at the periphery of the parcels in a flame like the laminar combustion wave. The distribution function of the parcels is chosen so that the combustion and composition characteristics of the burning zone are matched to the data when the parcels are assumed to be spherical. It is assumed that the size distribution of the parcels is governed by splitting of the parcels (due to shear in the flow) and by burning.

Most of the available data are adequately described by assuming that parcel splitting is dominant in determining size distribution. By comparison of the model with the data, the splitting probability is found to be proportional to the mean velocity gradient.

The model offers the possibility of describing reaction rate variations in flows of negligible shear and of explaining the phenomenon of flame quenching in highly turbulent flow.

---

*Present Address: Princeton, Massachusetts

81. COMBUSTION PROCESSES IN A SPHERICAL COMBUSTOR

A. E. Clarke, J. Odgers, F. W. Stringer and A. J. Harrison

Lucas Gas Turbine Equipment Ltd., England

The object of the work described was to obtain a better understanding of the combustion processes in a spherical combustor, with the specific aim of determining the maximum loading for the propane/oxygen system.

Details are given of a series of experiments in which various fuel (hydrocarbons and hydrogen) /oxygen/nitrogen mixtures were burned in different sizes of spherical combustor over ranges of equivalence ratio, pressure, injector pressure loss and external heat loss. The reduction in injector pressure loss from 50% to 5% at $\underline{\emptyset} = 1.0$ and from 40% to 1% at $\underline{\emptyset} = 0.6$ had little effect on the stability performance.

The reaction pressure exponent of propane/oxygen/nitrogen mixtures was found to be 2 and it was shown that nitrogen could be regarded as equivalent to an external heat loss. The blow-out data obtained were correlated by means of a semi-empirical reaction equation based upon a mass balance which assumed that fuel was the only unburned product.

The experimental blow-out data were also correlated against burning velocity at 300°K inlet temperature -- this correlation being described by the equation

$$\left\{N/VP^2\right\}_{max.} = 0.1\ Su^{1.75}.$$

Attempts were then made to predict the peak loading for a propane/oxygen mixture using (a) the derived semi-empirical equation and (b) extrapolation of the buring velocity correlation and general practical data. The former gave a value of some 7,100 g. mol. / (sec.)(l.)(atm.^{2}) and the latter some 2, 900 g. mol. /(sec.)(l.)(atm.^{2}). Attempts to explain this discrepancy have so far failed unless it is assumed that reaction order and/ or activation energy varies with composition.

82. SUPERSONIC COMBUSTION OF STORABLE LIQUID FUELS IN MACH 3.0 TO 5.0 AIR STREAMS

Frederick S. Billig

The Johns Hopkins University

Supersonic combustion of reactive aluminum alkyl fuels has been experimentally demonstrated in two-dimensional ducted combustors and adjacent to a flat plate. Fuel was injected from the combustor walls through multiple orifices and ignited spontaneously. Stable supersonic heat release was maintained as evidenced by schlieren and direct motion pictures of the flow field and deduced from static and pitot pressure measurements in the combustion zone. The results from the ducted combustor tests were correlated with simple theoretical models thus enabling a reasonable determination of combustion efficiency.

A theoretical model of constant pressure heat release on a flat plate in supersonic flow is postulated. Normal force coefficients and specific impulse values are tabulated for a variety of flight Mach numbers and altitudes. Additional refinements in this theoretical model were required to adequately describe the experimental results. In a test simulating Mach 5 flight at 66,000 feet altitude a side force specific impluse of 1350 seconds was measured at equivalence ratio of one. Combustion was only partially completed 12 inches downstream of fuel injection. Based on the theoretical model an additional 12 inches of combustor length and 36 inches of expansion length would be required to obtain the estimated theoretical impulse of 5760 sec.

The interaction of a vaporizing liquid droplet with a supersonic stream is considered. Additional refinements were made in the existing theories on droplet trajectory to include the influences of a separated zone and the normal component of velocity of the external stream. Calculations of the trajectory and evaporation of the estimated mean droplet size based on the modified technique were in general agreement with the observed flame zone and deduced combustion efficiency.

83. A SIMPLE MODEL FOR HEAT ADDITION TO SUPERSONIC STREAMS

M. M. Gibson

Northern Research and Engineering Corporation International, London

The paper describes a simple analysis of a flame spreading from the center of a two-dimensional constant-area duct containing a shock-free supersonic stream of pre-mixed combustible gases. With the aid of some simplifying assumptions, the flame width is expressed as a function of the mass fraction burned. The flame length is established by formulating an "entrainment law" based on the growth rate of a turbulent wake. A maximum possible stagnation temperature ratio for complete combustion is found. Flame lengths are calculated for initial free-stream Mach numbers of 2, 3, 5 and 7. When the combustion is complete these are found to be of order 50 to 100 duct widths.

COMBUSTION AND FLOW

84. STABILITY OF LAMINAR JET FLAMES

Itsuro Kimura

University of Tokyo

It has been often noticed that a self-excited flame oscillation of low frequency can appear when laminar fuel jets burn in open air. In the paper presented at the Ninth Symposium by the author, some experimental results on this phenomenon were reported. [1] It was established that the oscillation has no connection with the size of the combustion chamber and the length of the fuel pipe.

The present paper presents the results of the study of this phenomenon based on the hypothesis that the oscillation of the flame is caused by the instability of the laminar jet flow. The discussions on the stability are based on the instability theory in inviscid gases, which is justified by the fact that the stability characteristics of free boundary layers become insensitive to viscous effects, when the Reynolds number is fairly large.

Instability theory for axially symmetrical parallel flows

Instability theory for two-dimensional parallel flows is developed fully, and in the inviscid case simple criteria for the instability are given. [2, 3] By analogy to the two-dimensional case, the criteria for the instability of axially symmetrical parallel flows are derived, in the case of axially symmetrical disturbance.

The analysis is based on the following assumptions:

1. The gas is inviscid (non-viscous and non-conductive);
2. The Mach number is small although the Froude number is large enough;
3. The gas behaves like a perfect gas;

The velocity perturbations are assumed to be of the form

$$u = \frac{f(y)}{y} e^{i\alpha (x - ct)}$$

$$v = \frac{\alpha \phi (y)}{y} e^{i\alpha (x - ct)}$$

where the system of co-ordinates is selected with its x-axis in the axis of the flow, the radial distance being denoted by y. The perturbations of temperature, density and pressure are assumed to be of the form $Fn(y)\, e^{i\alpha (x - ct)}$. Using the equations of motion, continuity, energy and state, the disturbance equation for ϕ is obtained, in the conventional way, as follows:

$$(U - c) \left\{ \frac{d}{dY} \left(\frac{\phi'}{T} \right) - \frac{\alpha^2}{4TY} \phi \right\} - \frac{d}{dY} \left(\frac{U'}{T} \right) \phi = 0$$

The variable Y stands for y^2; U and T are the mean velocity and mean temperature profiles respectively; and prime denotes the differentiation with respect to Y. In the case of the axially symmetrical disturbance, the boundary conditions are

$$\frac{\phi}{\sqrt{Y}} = 0 \qquad \text{at} \quad Y = 0$$

$$2\sqrt{Y}\, \phi' + \alpha \phi = 0 \qquad \text{at} \quad Y = \infty$$

In the disturbance equation, $Y = 0$ is an apparent singular point.

Similar considerations on the two-dimensional case hold for the above disturbance equation (the general theory of the Sturm-Liouville equation is also applicable in this case), and the following criteria for the instability are derived:

1. The condition that $\frac{d}{dY}\left(\frac{U'}{T}\right)$ must vanish for some U (Ys) is necessary and sufficient for the existence of a neutral disturbance, and its phase velocity C_s is equal U (Y_s).

2. The condition is also sufficient for the existence of the neighboring self-excited disturbances.

Mean velocity and temperature profiles in an oscillating flame

A detailed study based on the instability theory is conducted on the diffusion flame of a laminar fuel jet (city gas flow rate : 30 cc/sec, primary air flow rate : 20 cc/sec), stabilized on a circular port of 8 mm diameter. The oscillation of the flame is distinct (axially symmetrical oscillation with the frequency of 18 c/s), but the fuel jet without combustion seems to be stable till considerable height. (See the photograph).

A particle-track technique is used to measure the velocity field. Since the amplitude of oscillation is not large, it is possible to obtain the mean velocity profile in the flame with the required accuracy. The velocity profile in the fuel jet without combustion is also obtained. The temperature field in the flame is measured by a bare platinum/platinum-rhodium thermocouple. In this case, the correction for the heat loss by radiation is possible, since the velocity is already known.

Discussions on the instability of the flame

The normalized velocity profile in the fuel jet without combustion is seen to approach to $\frac{1}{(1 + 0.414y^2)^2}$, Schlichting's theoretical profile, with increasing x (the origin of x-axis is at the port). According to the above criteria, the velocity profile is unstable in the vicinity of the port, but it soon becomes stable with increasing x.

The velocity profile in the lower part of the flame is rather complicated, and it has three inflection points. In the upper part, however, it becomes simple, and the normalized velocity is seen to approach to $\frac{1}{(1 + 0.24y^2 + 0.174y^2)^2}$ with increasing x. The temperature profile in the flame has a maximum at the reaction zone. According to the above criteria, it is shown that the velocity-temperature profile in the flame is unstable over the length of the flame, and in the lower part there exist several groups of neutral and self-excited disturbances, whereas in the upper part, there is only one.

The characteristic-value problem of the disturbance equation is solved numerically for the velocity-temperature profile in the upper part of the flame, and in this case it is shown that the following neutral disturbance exists: Frequency: 29 c/s, wave length: 4.7 cm. The frequency of the neighboring self-excited disturbance is considered to be lower than that of the neutral disturbance, so the value of frequency obtained seems to be reasonable.

Finally, it was established that the aspect of the flow lines around the oscillating flame in the photograph agrees with that expected from the instability theory. From the above, it will be seen that the hypothesis, that flame oscillation of this type is caused by instability of the jet flow, is reasonable.

References

1. Kimura, I., and Ukawa, H.: Ninth Symposium Abstracts, 76.

2. Tollmien, W.: Nachr. Ges. Wiss. Göttingen, Math.-Phys. Klasse. 1 (1935), 79.

3. Lees, L., and Lin, C. C.: NACA T.N. No. 1115 (1946).

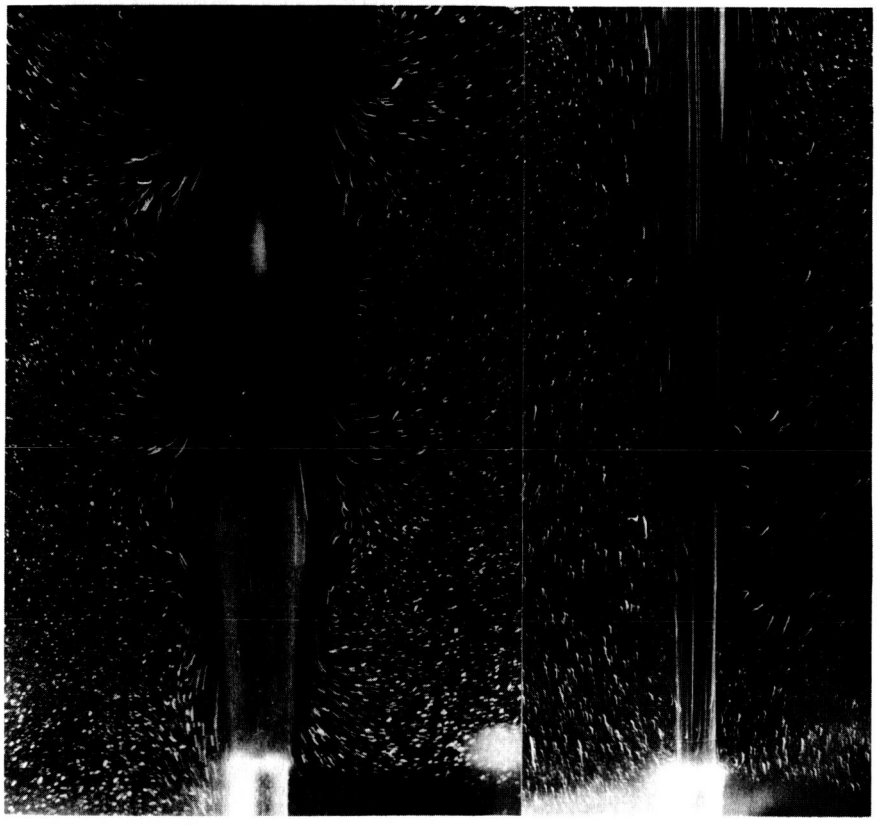

The aspect of stream lines around the oscillating flame and the fuel jet without combustion.

85. MECHANISMS OF COMBUSTION INSTABILITY

Tau-Yi Toong, Richard F. Salant, John M. Stopford
and Griffin Y. Anderson

Massachusetts Institute of Technology

This paper presents results of a study aimed at understanding mechanisms involved in triggering, amplification and suppression of acoustic waves due to presence of flames. Experiments performed demonstrate that strong interactions between acoustic and flame oscillations can exist through flow oscillations and that these interactions are due to energy transport between various oscillation modes through both linear and non-linear couplings.

The intensity of the interactions can be altered by varying flow velocity through an organ pipe. Under reduced-flow conditions, the linear coupling is eliminated and the flame exhibits periodic self-sustained oscillations. However, with imposed acoustic excitation of sufficiently large amplitude, the interactions become again important due to non-linear effects. Non-linear coupling between longitudinal acoustic oscillations and tangential or radial flow and flame oscillations is also observed.

Supporting evidences are presented which show that onset of the above-mentioned self-sustained oscillations of diffusion flames is due to instability of traveling Tollmien-Schlichting disturbance waves--the same mechanism which leads to onset of transition from laminar to turbulent flows. Effects of changes in flow field due to presence of interacting burning and non-burning simulated fuel droplets on the oscillation characteristics are reported and interpreted in terms of the postulated mechanism of boundary-layer instability. Under some conditions, oscillations can actually be stopped by placing non-burning cylinders near an (otherwise) oscillating flame.

86. PERIODIC SOLUTIONS TO A CONVECTIVE DROPLET BURNING PROBLEM: THE STAGNATION POINT

Warren C. Strahle*

Princeton University

An understanding of the convective droplet burning process when acoustic oscillations are taking place in the ambient gas stream may be extremely important in understanding unstable combustion processes. With this in mind, a theoretical study of an unsteady diffusion-controlled droplet burning configuration is performed. In this investigation the unsteadiness is imposed by introducing a small amplitude sound wave in the free stream.

The steady state analysis is carried out for a fuel droplet immersed in a flowing, uniform free stream which contains the oxidizer. Then, introducing a traveling isentropic sound wave into the free stream, small perturbations about the steady state are considered. The effects of this sound wave for arbitrary frequency are analyzed primarily with respect to burning and vaporization rate perturbations. High Reynolds

---

*Present address: Aerospace Corp., San Bernardino, Calif.

number, low Mach number flow are considered; a systematic, asymptotic expansion of the governing gasdynamic equations shows that boundary layer theory provides a reasonable first order approximation. With this type of flow the forward stagnation region is of extreme interest; for stagnation point flow an exact solution may be obtained in the unsteady state for arbitrary frequencies. For this reason this paper is only concerned with the stagnation point solution. However, there are indications that the entire leading edge of the droplet behaves qualitatively like the stagnation point.

In the model the primary assumptions are that reaction and evaporation kinetics are much faster than diffusion times, resulting in a diffusion-controlled system. As such, a proper limiting procedure also yields the theory of unsteady, compressible conventional boundary layer flow in the vicinity of the stagnation point. The theoretical results are easy to explain on a physical basis for very low frequencies of oscillation (quasi-steady) and for very high frequencies. The transition or intermediate frequency range defies a physical description or understanding and requires an exact theoretical treatment. This is the primary value of the stagnation region study since an exact solution may be found over the full frequency range and the transition from low to high frequency behavior becomes apparent. At very high frequencies the phenomenon of the "high frequency boundary layer" comes into being. It lends itself to simple asymptotic analysis which serves as a check on the exact numerical solution.

Because of the small perturbation analysis any wave shape can be synthesized by superposition. Therefore, the analysis is not restricted to a simple traveling wave. A wave shape of extreme practical importance is a standing wave composed of a superposition of two traveling waves. An important result in the case of such a standing wave is that in a narrow frequency range the burning rate undergoes a sort of resonance in phase with the pressure. This only occurs if the mass fraction of oxidizer in the free stream and the stoichiometric heat of reaction with respect to the free stream enthalpy are sufficiently large. For practical values of the parameters there is a frequency above which no response in phase with the pressure will result. Similar results are obtained for the vaporization rate perturbation.

The analytical treatment demonstrates that the results may be split into two parts. There is a contribution due to what is called a velocity effect and one due to a pressure effect. Regardless of the wave form considered in the ambient gas a velocity effect always takes the form of the velocity wave form and, simultaneously, a pressure effect takes the form of the pressure wave shape. The pressure effect vanishes for an incompressible fluid (zero steady state Mach number), whereas the velocity effect remains for an incompressible fluid. Unless the droplet is located very near a velocity node of the ambient gas osciallation the velocity effect is dominant. One further result is that frequency effects (unsteady effects) do not become important until quite high in frequency range; this is equivalent to the statement that quasi-steady behavior is followed quite far into the frequency range, contrary to expectation on a physical basis.

The analytical techniques employed are not restricted to the droplet burning problem, but may be extended to droplet wake burning, laminar jet burning, and coaxial jet rocket engine injector burning problems in the unsteady state.

87. AN EXPERIMENTAL INVESTIGATION ON HIGH-FREQUENCY COMBUSTION OSCILLATIONS

Hiroshi Tsuji and Tadao Takeno

University of Tokyo

A series of experimental investigations of high-frequency combustion oscillations has been conducted by J. R. Osborn, et al., using a cylindrical rocket motor burning premixed gases as propellants. By employing such a relatively simple combustion system of premixed gases, the effects of several variables which enter into the combustion process for a liquid propellant rocket motor, such as mixing, atomization, vaporization, etc., are eliminated, yet the observed high-frequency combustion oscillations have been found to have much the same character as when the propellants are initially in liquid form. Therefore, the essential features of the combustion oscillations can be studied under simplified conditions by using premixed gaseous propellants.

The present study was conducted using premixed gaseous propellants, with the object of investigating in detail the effects of several variables upon the high-frequency combustion oscillations in a rocket motor and making clear the driving mechanism of these oscillations. The effects of the combustion chamber length, the propellant equivalence ratio, the mean chamber pressure and the injector configuration upon the combustion oscillations were examined. In this paper, the experimental results obtained for the longitudinal-mode combustion pressure oscillations are presented and an explanation of some of the results is suggested, based on a possible mechanism for initiating and sustaining the pressure oscillations.

The research rocket motor had a rectangular combustion chamber of 5 cm x 8 cm cross section; it was composed of a mixing chamber, water-cooled combustion chamber sections, spacers and a nozzle. The length of the combustion chamber was varied from 15.0 cm to 75.3 cm by combining the chamber sections and spacers. The propellant used was city gas premixed with air. The premixed gas was introduced into the injection section of the mixing chamber through a choked orifice and then injected into the combustion chamber through an injector which had small holes drilled parallel to the motor axis. The pressure oscillations were measured with water-cooled strain-gage type pressure transducers mounted in the wall of the combustion chamber and their associated electrical equipment. The temperature of combustion gas in the combustion chamber was measured with Pt - Pt. Rh thermocouples.

Three modes of longitudinal-pressure oscillations were observed. They are the fundamental, the second harmonic- and the third harmonic-mode (Fig. 1). Each mode of pressure oscillation occurred only for certain conditions of the chamber length L_c, the propellant equivalence ratio ϕ and the chamber pressure P_c. When L_c was 15.0 cm, no organized oscillations appeared in the pressure range of the present experiment. If L_c was increased to 18.0 cm, the fundamental mode oscillation began to occur near the stoichiometric mixture ratio of propellant. With increasing chamber length, the instability region represented in P_c - ϕ diagram for the fundamental-mode oscillation progressed steadily toward lower chamber pressure, extending its boundary both to the rich and the lean side. However, this instability boundary almost coincided with the blowoff curve of the flame in the combustion chamber if L_c was increased to 47.0 cm, and steady combustion without oscillation was not observed in the combustion chamber beyond this length. On the other hand, if L_c was increased to 38.0 cm, the second harmonic mode oscillation appeared inside the instability region of the fundamental-mode oscillation, and if L_c was increased to 66.0 cm, the third harmonic-mode oscillation was observed inside the instability region of the second harmonic-mode oscillation. These instability regions also progressed steadily toward lower chamber

pressure with increasing chamber length, extending their boundaries both to the rich and the lean side (Fig. 2).

The frequency of oscillation for each mode varies with the chamber length and the combustion gas temperature T_c. If the pressure oscillation is of the acoustic type in the combustion chamber, the period τ of oscillation is given by $\tau = 2(L_c + \Delta L)/nC_e$, in which ΔL, C_e and n are, respectively, the end correction length of the nozzle, the effective sound velocity of combustion gas and the positive integer giving the number of modes of oscillation. Although the amplitude of the shock-type pressure oscillation was finite, the measured period of oscillation for each mode was closely associated with the relation given by the above equation. Namely, the measured periods increased linearly with L_c and were inversely proportional to the square root of T_c (Figs. 3 and 4). On the other hand, though the amplitude of pressure oscillation and the shock strength of the propagating pressure wave increased with chamber pressure, the effect of the chamber pressure upon the rate of shock propagation was very small and only a slight decrease in period was observed.

In order to examine how the higher harmonic-mode pressure oscillations occurred in the combustion chamber, the pressure oscillations were measured at the same time at three positions in the chamber. It was confirmed from these pressure records that two and three shock-type pressure waves were propagating at the same time for the second and third harmonic-mode oscillations, respectively, and that these propagating waves were reflected respectively at the velocity nodes of the higher harmonic standing waves in the combustion chamber. Therefore it may be concluded from these results and the measured periods of the oscillations that the pressure oscillations in the combustion chamber may be treated essentially as standing waves, though the shock-type pressure waves are propagating.

The lower critical chamber lengths were found to be approximately 18.0 cm, 38.0 cm and 66.0 cm in the case of $P_c = 3$ kg/cm^2 abs. for the fundamental, the second harmonic and the third harmonic mode oscillations, respectively. The periods of the oscillations of each mode corresponding to these critical lengths had about the same value of approximately 500 μsec. This suggests that the initiation of combustion oscillations is governed essentially by the period of the oscillation rather than by the chamber length. Moreover, it was confirmed that the instability boundaries in the ϕ - τ diagram for the fundamental, the second harmonic, and the third harmonic-mode oscillations were all expressed as one curve for a given injector and chamber pressure (Fig. 5). Therefore it may be considered that the combustion oscillations are initiated and sustained only when the periods of the oscillations are larger than some combustion time lag determined by chamber pressure, fuel composition, mixture ratio, injection velocity of propellant, etc., and that the higher harmonic mode oscillations will occur, rather than the fundamental mode oscillations, if the above conditions are satisfied by the higher harmonic mode oscillations.

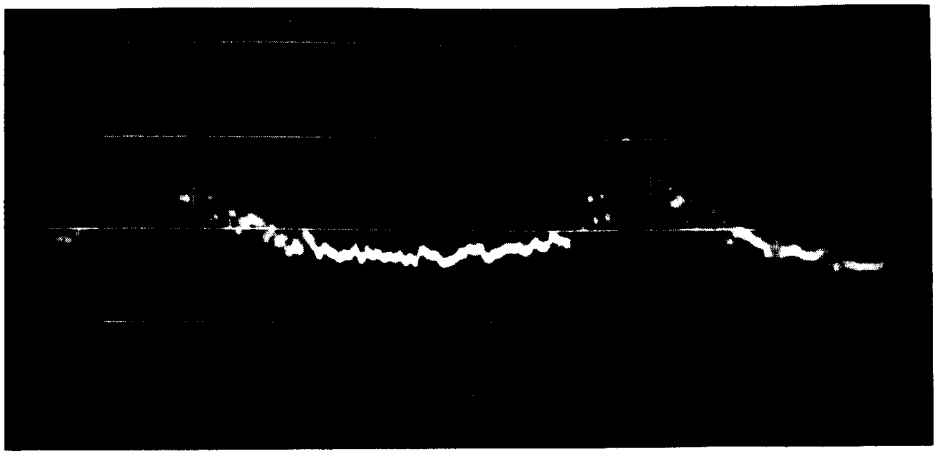

(a) Fundamental-mode. 500 sec/div.

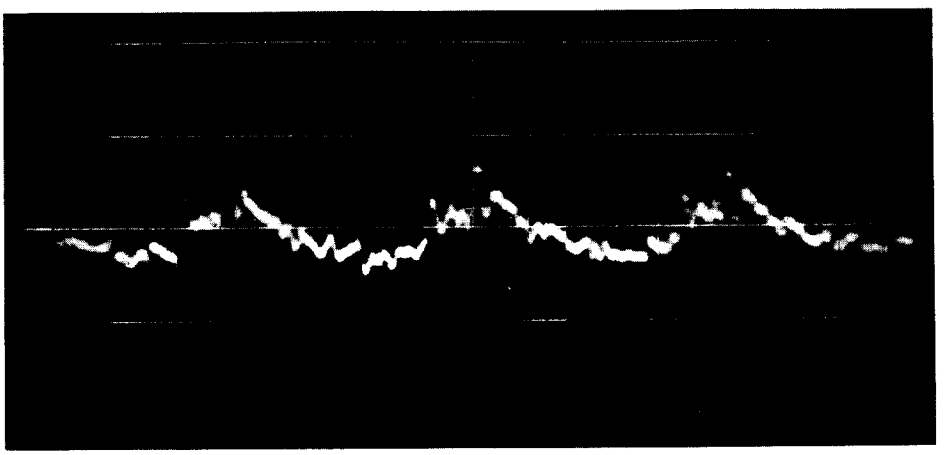

(b) Second harmonic-mode 500 sec/div.

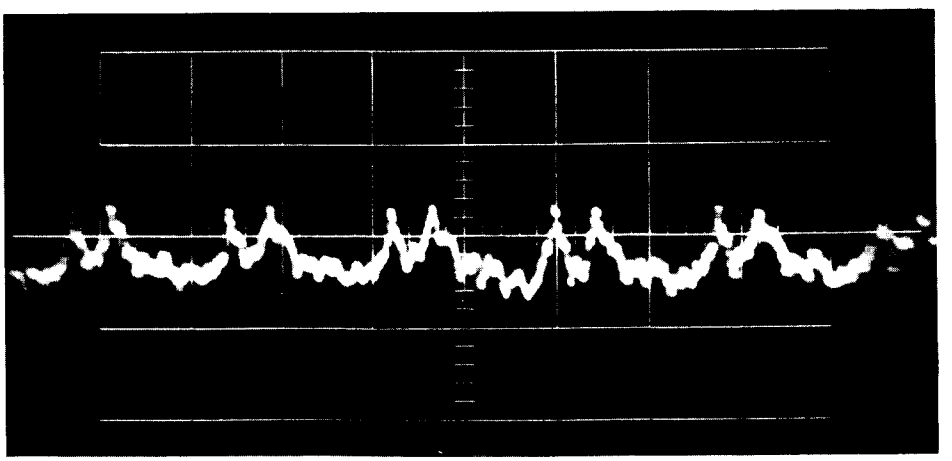

(c) Third harmonic-mode 500 sec/div.

Figure 1. Typical traces of shock-type pressure oscillations.

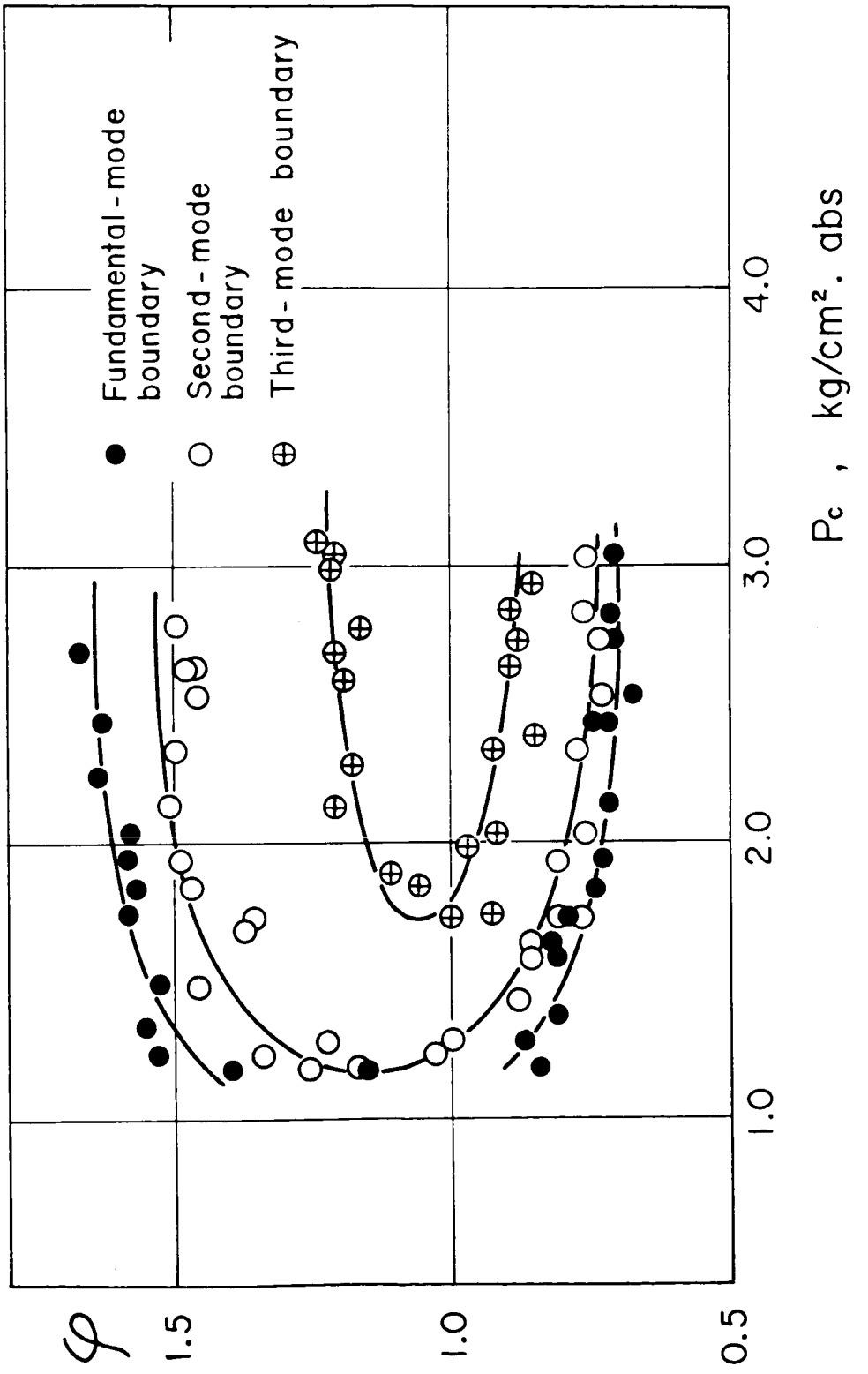

Figure 2. Instability regions: L_C = 75.3 cm

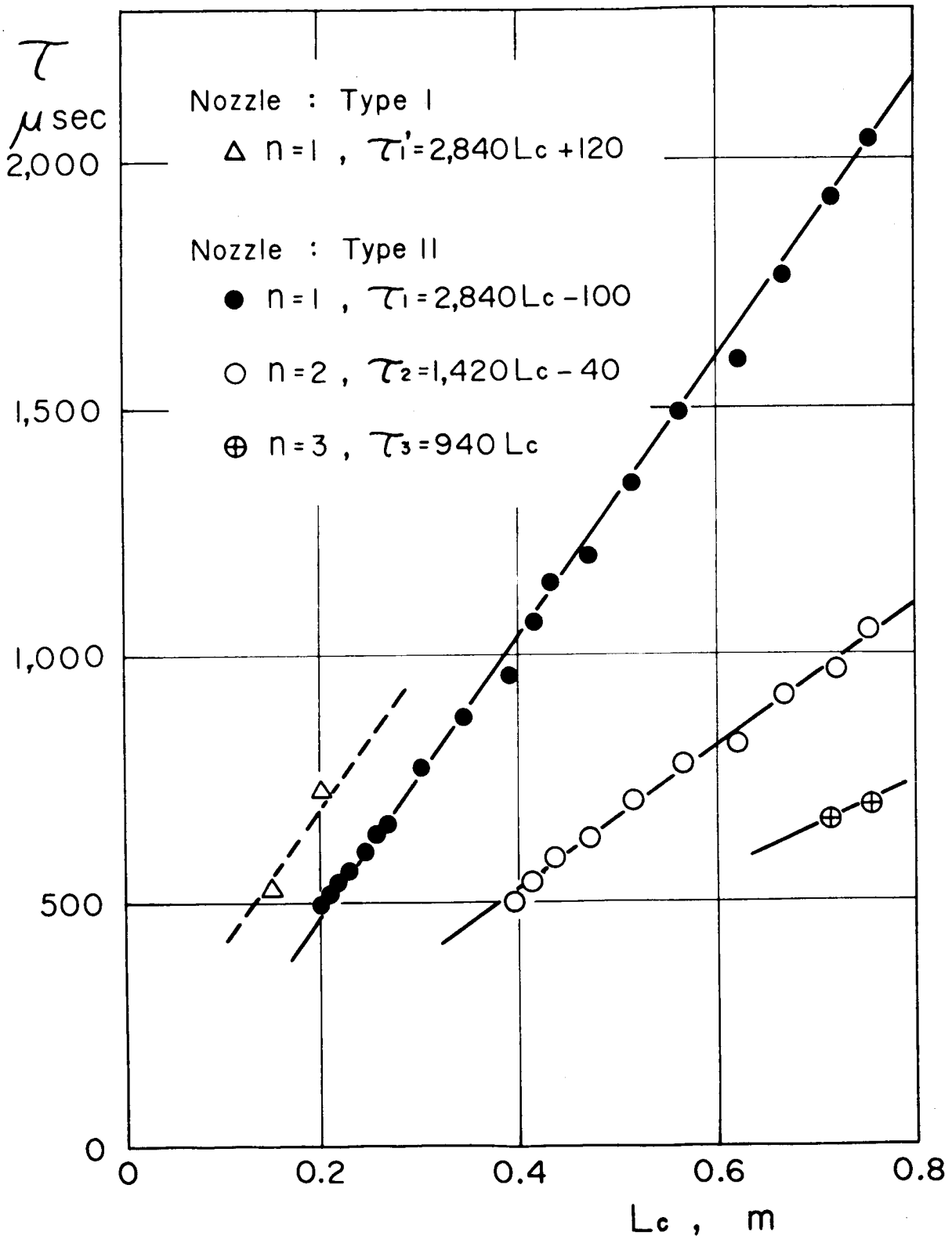

Figure 3. Period of pressure oscillations vs. combustion chamber length: T_c = 1.600°K.

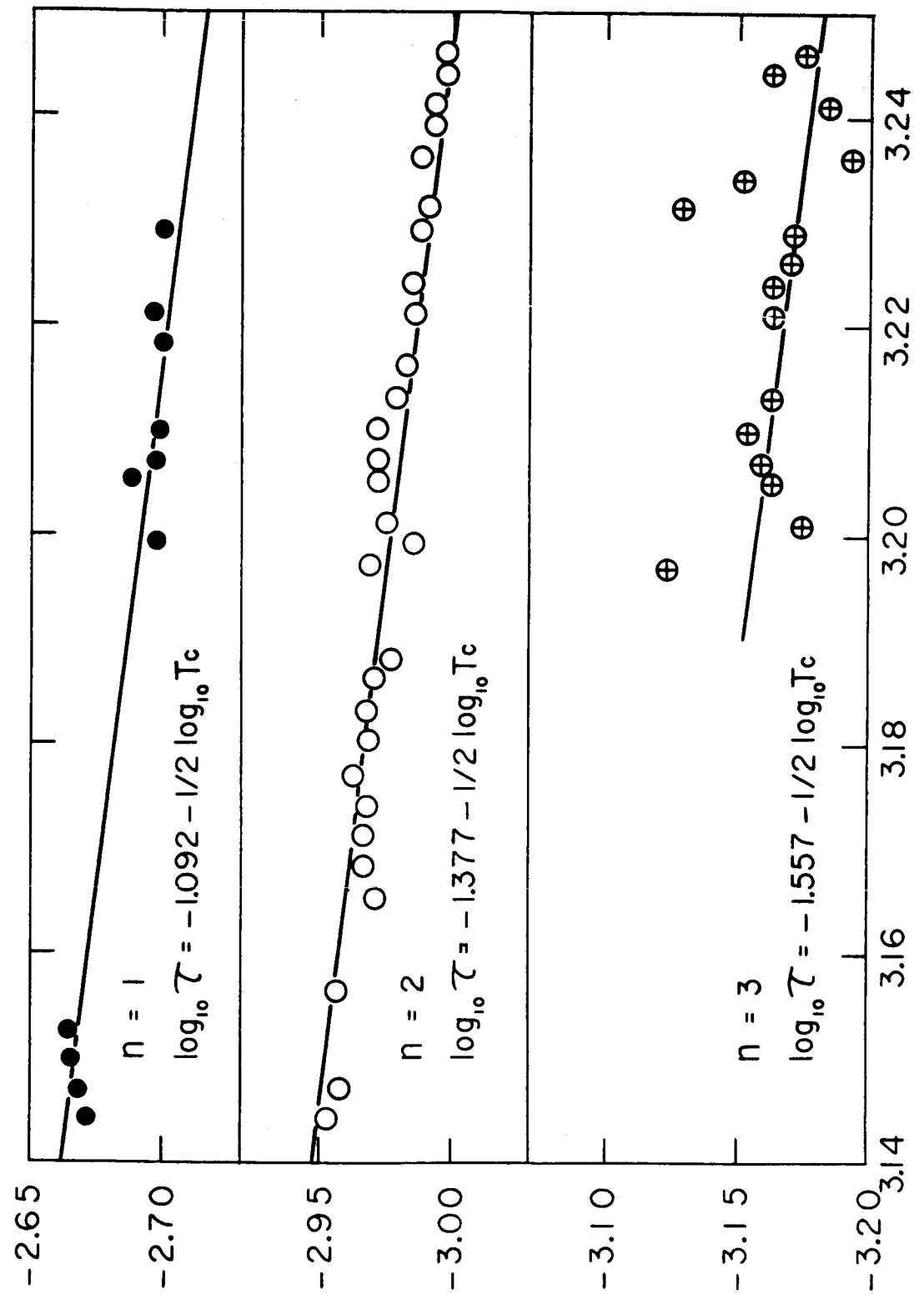

Figure 4. Period of pressure oscillations vs. combustion gas temperature: L_c = 75.3 cm.

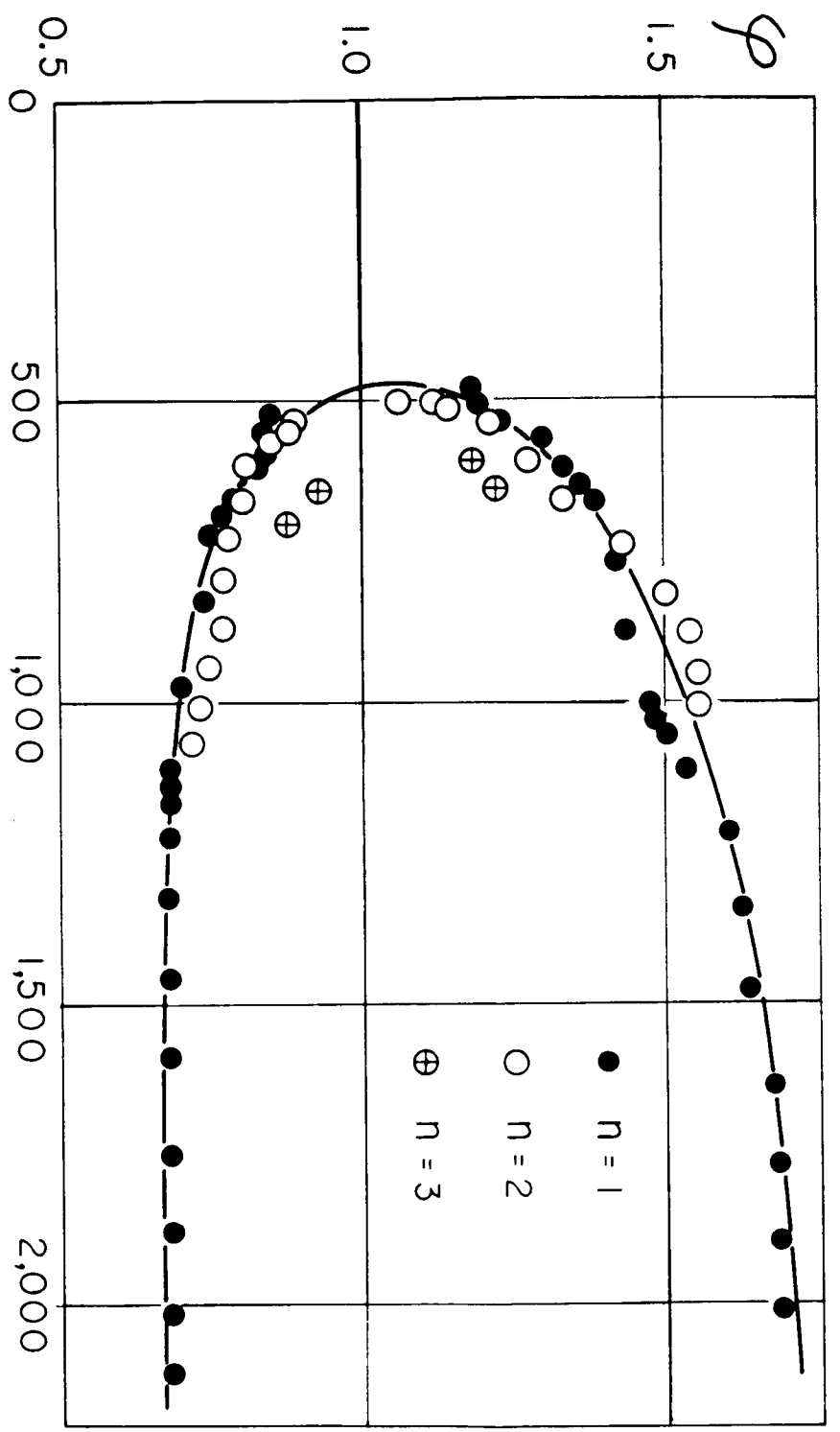

Figure 5. Instability regions: P_c = 3 kg/cm^2 abs.

88. COMBUSTION IN THE TURBULENT BOUNDARY LAYER ON A VAPORIZING SURFACE

Gerald A. Marxman

United Technology Center

The problems associated with ablative cooling, combustion of liquid fuel droplets, erosive burning of solid propellants, and hybrid rocket combustion have stimulated a number of investigations of heat and mass transfer in reacting gases, particularly during the past decade. The theoretical understanding of reacting laminar boundary layers has evolved rapidly, and some experimental data pertinent to the laminar case are now available in the literature. The reacting turbulent boundary layer has received far less attention, although it is clearly of great importance in many modern applications. Probably this is due primarily to limitations imposed by our poor understanding of turbulent processes, which preclude the purely analytical approach possible in laminar flow.

At the Ninth International Symposium on Combustion, M. Gilbert and the author presented some preliminary results of a study of the turbulent boundary layer with combustion. The present paper gives an account of subsequent developments in that continuing investigation of turbulent boundary layer combustion. Two topics are considered in this paper: (1) convective heat transfer in a reacting turbulent boundary layer with mass addition at the gas-solid interface, and (2) the influence of the boundary layer flow field on the stoichiometry of a diffusion flame within the boundary layer.

By extending the Schvab-Zeldovich formulation for low-speed, constant-pressure flames, Lees has shown that the assumption Le = 1 allows the prediction of heat transfer through a reacting boundary layer without reference to the position, width, or reaction kinetics of the combustion zone. This general approach is equally applicable to either the laminar or turbulent boundary layer and leads to many important conclusions concerning the qualitative nature of the heat transfer process. However, it is frequently less satisfactory for determining quantitatively the heat transfer: a simplified combustion model is generally required to permit convenient calculation of the "driving force" for heat transfer (or the mass transfer number B, in Spalding's terminology). For example, it may be assumed that all reactions occur within a thin flame sheet (infinite reaction rates). Then by using the Burke-Schumann procedure, which has previously been employed in laminar boundary layer studies, a relatively simple evaluation of B is possible.

An alternative approach to the turbulent combustion problem, also utilizing the thin flame approximation, was formulated in the author's Ninth Symposium paper. The present paper summarizes the heat transfer theory which has evolved from recent studies based upon that formulation. It is shown that B may be expressed in terms of a mixture-ratio parameter Ω which tends to remain practically constant over the Reynolds number range of interest, for a given system of reactants. This representation of B is particularly useful in "internal flow" applications, where the mass fractions and sensible enthalpy at the boundary layer edge may change substantially with Reynolds number.

The analysis leads to an equation relating the mass transfer to B; aside from the different method of determining B, this formulation differs from earlier ones primarily in the way of accounting for the heat transfer "blocking effect" associated with mass injection. At high values of B where the frequently-used "thin film" treatment is inaccurate, the present approach appears quite satisfactory. Also, the coordinate transformation method studied during the past decade by several investigators is employed to account for the effect of variable fluid properties, and it is shown that a relatively easy measure-

ment of the boundary layer thickness will fix the reference state with reasonable accuracy. The present analysis has found application in hybrid combustion studies, and previously-reported mass transfer data are cited in support of the theory.

Experimental studies of the turbulent boundary layer combustion in hybrid motors indicate that the flame does not necessarily occur at the stoichiometric (or ideal) mixture ratio. In these experiments the vaporizing surface is ordinarily the fuel, and the over-all combustion mixture ratio tends to be fuel-rich relative to the stoichiometric ratio. This is at variance with the assumption, often used in droplet-burning analyses and laminar boundary layer studies, that the thin diffusion-flame sheet occurs at the position above the vaporizing surface where the mixture ratio is stoichiometric. Furthermore, it seems intuitively reasonable that the mixture ratio may depend to a significant degree on the boundary layer flow field, wherein fuel is carried to the reaction primarily by a convection current normal to the flame, while the oxidizer flows almost parallel to the flame and must reach the combustion zone by diffusion. This situation lacks the symmetry of a bunsen burner flame, for example, in which both fuel and oxidizer reach the combustion zone by diffusion.

By using the standard boundary layer approximations it can be shown that part of the reactant leaving the vaporizing surface (typically 10 per cent or less) is carried along beneath the flame by convection and fails to reach the combustion zone. This "reactant loss" alters the over-all mixture ratio of the combustion process, but it is incapable of explaining the observed degree of deviation from the ideal ratio.

However, the present analysis indicates that the boundary layer flow field also influences the local stoichiometry of the flame, and as a result considerable departures from the stoichiometric mixture ratio are predicted in some cases. By applying the boundary layer integral technique to the appropriate conservation equations and adding an equation relating the heat of reaction to the fuel-oxidizer system, a set of equations is obtained which can be solved simultaneously to determine the local mixture ratio, position, and mass transfer number of the flame. Several examples are discussed. In general, the theory shows that the flow field of the turbulent boundary layer may substantially affect the reaction stoichiometry, with combustion usually occurring at a mixture ratio which is rich in the substance vaporizing at the wall. It also indicates that a gradual shift in the local mixture ratio may occur along the flame (i.e., with Reynolds number) under certain circumstances, and that in a given geometry with given flow conditions some substances may undergo boundary layer combustion more efficiently than others.

Experiments have been performed by other investigators in which plexiglas tubes were burned with oxygen flowing axially through the control port and combustion samples taken at various positions along the centerline. These experiments appear to confirm the theoretical prediction that as the Reynolds number rises the local mixture ratio approaches a value of about 1.4, while the stoichiometric value is 1.92 (oxidizer/fuel). The theoretically predicted qualitative behavior of the mixture ratio and flame position is in striking agreement with the currently available experimental results. Although this is encouraging, more precise experiments as well as additional data from other fuel-oxidizer systems will be required to fully establish the validity of the theoretical conclusions concerning boundary layer combustion stoichiometry.

89. MEASUREMENTS IN A COMBUSTING TURBULENT BOUNDARY LAYER WITH POROUS WALL INJECTION

C. E. Wooldridge and R. J. Muzzy

United Technology Center

Recently a great deal of interest has been generated in boundary layer combustion phenomena by the advent of the hybrid rocket engine as a propulsion device and by the application of combustible ablative materials to high-speed re-entry bodies. Several theoretical analyses of laminar boundary layer flows with sublimation and combustion based upon the numerical solution of Blasius-type equations have been presented in the literature. A few experimental measurements in laminar flows with very low mass injection rates corresponding to sublimation have also been reported. However, measurements in noncombusting flows have shown that the influence of any appreciable wall mass injection is to lower drastically the transition Reynolds number. The presence of combustion as well should be expected to enhance this effect so that in most situations of practical interest the combusting boundary layer will be turbulent unless some mitigating influence, such as a strong favorable pressure gradient, acts to prevent transition. Surprisingly, only a limited amount of work has been done on combustion in turbulent boundary layers with wall mass injection.

The general analytical attack upon the turbulent problem involves several basic assumptions concerning the nature of the combustion process and the general structure of the boundary layer. An almost universal assumption is that the Lewis number. Prandtl number, and Schmidt number are unity. This is equivalent to assuming that the generalized Reynolds analogy is valid; i.e., that the turbulent transport coefficients for mass, momentum, and energy are equal. It is usually assumed that the chemical reactions in the boundary layer are confined to a thin flame zone which is controlled by diffusion. Most authors have also assumed as a carry-over from burning droplet theory that the reaction at the flame zone is stoichiometric. However, this last assumption was not required by Marxman, et al., [1] in their theoretical development, and they have indicated that such an assumption is not necessarily valid. A series of basic experiments has been undertaken in order to check the validity of these assumptions and to gain some fundamental knowledge about the structure of a turbulent boundary layer with mass addition and combustion.

A wind tunnel with low free-stream turbulence has been designed according to standard tunnel practice. The test section is 7 in. by 7 in. in cross section and 8 ft. long with a porous plate section inserted in the top wall. The opposite wall of the tunnel is adjustable so that a wide range of axial pressure gradients can be imposed on the boundary layer. The leading edge of this porous section is located downstream of the inlet to the tunnel test section at a point where the wall boundary layer has a fully-developed turbulent velocity profile. This procedure of injection into an already turbulent boundary layer results in an adjustment to a new equilibrium profile after passage over a short length of porous plate. The distance required to achieve an equilibrium profile is less than would be required if the boundary layer with mass injection had its origin at the leading edge of the porous plate. Consequently, less total wall mass injection is required. The free-stream velocity was varied between 35 and 70 ft. per second for the experiments reported here and the pressure gradient was set at zero.

Before beginning the combustion experiments, the operation of the wind tunnel was examined by measuring the velocity profiles of the wall boundary layer with no mass injection and with cold-flow injection of nitrogen. In the absence of mass injection the measured profiles agreed well with the classical one-seventh profile and the univer-

sal logarithmic profile of Coles. [2] Velocity profiles were obtained with nitrogen injection for values of the mass transfer number, $B = \frac{(\rho v)_w}{\rho_e u_e C_{f/2}}$, ranging between 2 and 50. These profiles also agreed well with previous measurements by others and with the semiempirical analysis of Marxman and Gilbert. [3]

The combustion experiments were performed with a mixture of hydrogen and nitrogen which was injected through the porous surface and burned with the air in the boundary layer. Because of the flammability limits of the hydrogen-air flame it was possible to establish a flame zone with a very dilute mixture of hydrogen in the injected fuel. The flame temperatures were then low enough to obtain profile measurements in the boundary layer with metal probes. In addition, the combustion process of this system is simpler than that of most hydrocarbon flames and the combustion products are easier to analyze.

Simultaneous measurements of velocity, temperature, and species concentration are obtained by traversing the combusting boundary layer with a small probe containing an impact pressure tube for velocity measurements and a thermocouple for temperature measurements. Samples of material drawn off through the impact tube were analyzed for species concentration on a mass spectrometer. The velocity, temperature, and concentration profiles at various values of B are compared and similarity among the profiles is discussed. The velocity profile is also compared to its counterpart obtained during cold-flow mass injection with the same values of the mass transfer number B.

If Reynolds analogy is valid, the aerodynamic blowing parameter B used to reduce the velocity profiles to a nondimensional form can also be expressed as a thermodynamic parameter. Measurements of B by each of the two independent methods are presented and compared. The interaction between the flame height and the enthalpy difference between the flame and the surface which is discussed by Marxman, et al., [1] is examined in the present system.

Diffusion of fuel and oxidizer to the flame zone is markedly influenced by the presence of the boundary layer. In such a situation the diffusion of the injected fuel toward the flame is aided by convection normal to the wall while the diffusion of the main-stream oxidizer is hampered by this convection. The flame will become located at that position where a combustible mixture can be maintained by these boundary layer transport processes. The flame zone position is coupled to the surface mass addition through the mass transfer number B which determines the local shape of the velocity profile. The experiments show that as the rate of wall mass injection increases the flame position moves away from the wall relative to the total boundary layer thickness.

References

1. Marxman, G. A., Wooldridge, C. E., and Muzzy, R. J.: "Fundamentals of Hybrid Boundary Layer Combustion", paper presented at AIAA Heterogeneous Combustion Conference, Palm Beach, Florida, December 1963.

2. Coles, D.: "Measurements in the Boundary Layer on a Smooth Flat Plate in Supersonic Flow. I. The Problem of the Turbulent Boundary Layer", Jet Prop. Lab. Rep. 20-69, 1953, or Z.A.M.P., V, 1954, p. 181.

3. Marxman, G. A., and Gilbert, M.: Ninth Symposium (International) on Combustion, p. 371, Academic Press, 1963.

90. A NEW EXPERIMENTAL TECHNIQUE FOR THE STUDY OF ENERGY RELEASE IN EXPANDING COMBUSTION PRODUCTS

N. H. Pratt* and J. E. C. Topps

National Gas Turbine Establishment, England

On account of the many chemical reactions involved in the recombination of dissociated combustion products in expanding nozzle flows, [1] and the present uncertainty surrounding some of the rate constants, information concerning the rates of energy release to be obtained in ramjet propelling nozzles can be determined only by the simulation of the pressures, temperatures and rates of expansion which actually occur. Exact simulation is possible only in a nozzle, but experimentally a simpler system is desirable. For this reason laboratory scale experiments using one-dimensional unsteady centered expansions were considered. Such expansions must have cooling rates of up to $\sim 3 \times 10^6$ °K per second, and be produced in gases at temperatures up to 3000°K and pressures up to 10 atm.

These rates cannot conveniently be obtained by Glick's [2] original shock-tube method, nor by Bauer's [3] modification of it. Jacobs' [4] method, involving the rupture of a cylindrical diaphragm by a reflected shock can give the required rates, but our method is simpler and more appropriate to a study of combustion products since constant volume combustion can give the requisite pre-expansion conditions. A rarefaction wave is therefore passed into freshly burned combustion products and observation made of the virtually stagnant gas in the reflecting rarefaction at the end of the combustion chamber. The rate of expansion (and the rate of change of the variables p, T, ρ and concentration) at the observation station is controlled by the speed of sound in the combustion products and by the distance from the diaphragm. It may be evaluated analytically when there is no chemical reaction and the specific heat ratio is constant and this permits the more complex actual system to be approximated for design purposes. Because of non-idealities, such as finite diaphragm rupture time, and the need for a one-dimensional wave system, the length of the combustion chamber required must be a compromise and has to be proved experimentally. The facility developed is similar to a combustion driven shock-tube, but is better described as a rarefaction tube. The experimental explosion chamber is of internal dimensions 21.6 x 7.6 x 7.6 cm, and is separated from an evacuated dump chamber by a thin diaphragm. C_2H_4 - O_2 - N_2 mixtures burned at constant volume simulate the pre-expansion compositions, temperatures and pressures likely to be obtained in hydrocarbon-fueled ramjets; replacement of N_2 by He permits some variation in the expansion rate at given conditions of temperature and pressure. Ignition is by means of five spark gaps mounted flush with the surface along the length of the chamber. Pressure is measured on the end wall of the combustion chamber by piezo-electric transducers, and sapphire windows mounted in the side walls with axes 1.0 cm from the end, so as to avoid interference from the cool thermal layer, permit spectroscopic measurements in the range 0.3 to 5.0 μ.

Pressure-time traces obtained from early experiments using a 7.6 x 7.6 cm constant area dump chamber indicated effectively one-dimensional but irregular expansions, whether with natural or artificially induced bursting of the diaphragm, both with pressurized nitrogen and combustion gases. Photographic investigation using blackened diaphragms with the dump chamber disconnected showed a "clean" expansion required a diaphragm which shattered on bursting. This was most readily obtained using cellulose acetate sheet mounted in a sharply diverging section, for which the

---

*Present address: Southampton University, England

bursting time was about 200μ second. The original dump chamber was replaced, therefore, by one of 23 cm diameter and 120 cm long mounted on a 7.6 cm divergent section.

With good diaphragm bursts expansions in room temperature nitrogen compared favorably with expansions calculated from the analytical expression for gases of specific heat ratio $\gamma = 1.40$,

$$\frac{t}{t_o} = \frac{3}{8}\left(\frac{p}{p_4}\right)^{-\frac{5}{7}} + \frac{1}{4}\left(\frac{p}{p_4}\right)^{-\frac{3}{7}} + \frac{3}{8}\left(\frac{p}{p_4}\right)^{-\frac{1}{7}}$$

where t_o is the time for the head of the expansion to reach the end of the explosion chamber; and p_4 is the pre-expansion pressure.

With chamber length effectively 23.6 cm (to allow for the curvature of the diaphragm) $a_4\ (N_2) = 3.5 \times 10^4$ cm sec^{-1} at 293°K, the time needed for p/p_4 to equal 0.20 is theoretically 740μ sec whereas experimental results indicated 665μ sec.

Combustion typically required 3 ms for the attainment of peak pressure, and by choice of diaphragm thickness rupture could be made to occur 1 to 2 ms after this for various starting pressures, so that the expansion passed into relatively well equilibrated and stagnant mixtures. The measured time for various expansion ratios, using C_2H_4-$3O_2$-$6N_2$ mixtures compares with those calculated for stoichiometric $C_nH_{2_n}$-air combustion products at 2780°K expanded in a nozzle of 30 cm throat diameter, of throat radius of curvature 30 cm and of cone angle 25°, as follows.

p/p_4	Expansion time μsec	
	Rarefaction tube	Nozzle
0.50	260	425
0.25	500	530
0.10	800	700

In the above instance a maximum expansion rate in the rarefaction tube was found at $p/p_4 \simeq 0.80$. By comparison, an ideal rarefraction would give a highest rate at $p/p_4 = 1.0$, and in the nozzle considered it would be a maximum at $p/p_4 \simeq 0.60$.

In the preliminary work described here the carbon dioxide absorption for a part of the ν_3 vibration-rotation band at 4.4μ and the temperature are simultaneously determined by interrupting radiation from a high temperature grey-body source at about 50 kc/sec. Using the reversal technique in its simplest form each experiment permits a measurement of temperature for a single condition in the expansion, but absorption is measured throughout. Given knowledge of the pressure and of the absorption characteristics of CO_2 at the measured temperature, its concentration may be determined for this condition.

In order to prove the temperature measuring technique and to obtain the absorption characteristics of carbon dioxide (and of any other species which may subsequently be of interest) at relevant temperatures and pressures, a subsidiary shock-tube was constructed, of diameter 7.6 cm, so that the spectroscopic instrumentation was calibrated directly.

Results obtained so far indicate that the techniques described will yield useful results, and that the spectroscopic methods may be extended to include other species.

References

1. Westenberg, A. A., and Favin, S.: Ninth Symposium (International) on Combustion, p. 785, Academic Press, 1963.

2. Glick, H. S., Squire, W., and Hertzberg, A.: Fifth Symposium (International) on Combustion, p. 393, Reinhold Publishing Corp., 1955.

3. Lifshitz, A., Bauer, S. H., and Resler, E. L.: J. Chem. Phys. 38, 2056 (1963).

4. Jacobs, T. A., Hartunian, R. A., Giedt, R. R., and Wilkins, R.: Phys. Fluids, 6, 972 (1963).

91. CONCENTRATION INTERMITTENCY IN JETS

H. A. Becker*, H. C. Hottel and G. C. Williams

Massachusetts Institute of Technology

A paper by the authors [1] presented at the Ninth Symposium reported a study of furnace mixing patterns as represented in the cold by a round jet of oilfog-marked air issuing axially into a cylindrical duct fed by a uniform stream of clear air. Emphasis was on the regime in which appreciable recirculation occurs. The fields of mean velocity, mean concentration, and static pressure were mapped. A single similarity parameter, named the Craya-Curtet number after its discoverers and denoted by Ct, was shown to govern the flow and mixing patterns at high jet Reynolds number and low ratio of nozzle to duct diameters. It was, unfortunately, beyond the scope of the paper to report the results of parallel investigations of the fields of velocity fluctuations (deduced from data on static pressure defect in the jet) and of concentration fluctuations. Some of these results have since been presented at the A. I. Ch. E. National Meeting at Houston, Texas, in December, 1963, and will duly be published.

In the interim since the last symposium, a study has been made of concentration intermittency in the ducted jet, with emphasis again on the regime in which recirculation occurs. The intermittency factor χ is defined as Prob ($r > 0$), the probability that at a given point the instantaneous concentration is greater than zero. In the present investigation of isothermal air/air mixing, r signified the concentration of nozzle air. The nozzle air was marked with an oilfog of which the point concentration was detected by the scattered-light technique previously described. [1] An electronic "modifier" system transformed the concentration signal into an intermittency signal. In conjunction with suitable transducers, this modifier has many other possible applications in combustion research, a simple example being the mapping of flame boundaries in terms of the probability that there is burning gas at a point in question.

For a turbulent jet in a non-turbulent surrounding "free" stream, χ is identifiable with the probability that there is turbulent fluid at a point in question. It is well known that in this case the instantaneous boundary of a jet is sharp; there exists at

*Queen's University, Kingston, Canada.

every instant a very thin contorted envelope or laminar superlayer on the inner (jet) side of which the fluid is turbulent, and on the outer (free stream) side of which the fluid is in potential flow. The turbulent fluid has the following features: (i) the vorticity is non-zero, and there exist vorticity fluctuations; (ii) the concentration of nozzle fluid is non-zero, and there exist concentration fluctuations; and (iii) the turbulent fluid is in mean motion relative to the free stream. Ordinary experimental measurements of the mean and fluctuating values of variables in jets (velocity, concentration, eddy diffusivity, etc.) give values time-averaged over the turbulent and non-turbulent periods of flow. When the intermittency factor χ is known, these values can be transformed to yield the statistical properties of the turbulent fluid itself. Since chemical processes involving the nozzle fluid obviously require the presence of this fluid, it is clear that such processes occur only within the turbulent fluid of the jet. Hence the proper description, analysis, and understanding of such processes require knowledge of the statistical properties and boundaries of the turbulent fluid.

The fundamental significance of knowledge of concentration intermittency for the understanding of turbulent diffusion flames, with or without recirculation, is therefore readily appreciated. For a turbulent diffusion flame, χ represents the probability that there is present fuel, burned or unburned, at a point in question, and $1 - \chi$ is the probability there is present fresh combustion air, unmixed with fuel or combustion products.

The present work with a cold ducted-jet furnace model has shown that in isothermal, chemically neutral jet mixing, the flow in the jet core, within a distance of one mean-concentration half-radius of the jet axis is non-intermittent; $\chi = 1$ at $r < r_{\Gamma, 1/2}$, where $r = r_{\Gamma, 1/2}$ at $\bar{\Gamma} - \bar{\Gamma}_a = \frac{1}{2}(\bar{\Gamma}_c - \bar{\Gamma}_a)$. Here $\bar{\Gamma}$ is the mean concentration and $\bar{\Gamma}_a$ and $\bar{\Gamma}_c$ are the ambient (free-stream) and centerline (also radial maximum) values of $\bar{\Gamma}$. $\bar{\Gamma}_a > 0$ when recirculation is present. Surrounding this fully turbulent core there is an "intermittent annulus" extending outwards to about 1.5 concentration half-radii when there is no recirculation, and up to the duct wall when there is. One-half or more of the total flow of nozzle fluid proceeds through the intermittent annulus.

At sections where there is no recirculation, the radial profiles of the intermittency factor define the statistical boundaries of the jet. These profiles are well described by the relation

$$\chi = \tfrac{1}{2}\left\{1 + \operatorname{erf}\left(4.4(1 - \eta_\chi)\right)\right\},$$

where $\eta_\chi \equiv r/r_{\chi, 1/2}$, and $r = r_{\chi,1/2}$ at $\chi = 1/2$. A crude description, accurate only over $0.87 < \eta_\chi < 1.13$, is given by

$$\chi = 1, \quad \eta_\chi < 0.775$$

$$\chi = 1 - 2.22(\eta_\chi - 0.775), \quad 0.775 < \eta_\chi < 1.225.$$

This formula gives as a characteristic breadth of the intermittent annulus the value $0.45\, r_{\chi, 1/2}$. The limiting ratio (in self-preservation) between the intermittency half-radius of the jet and the concentration half-radius is $r_{\chi,1/2} / r_{\Gamma, 1/2} = 1.55$.

In recirculatory regimes of operation, insufficient fresh "ambient" or "free-stream" air is supplied to the duct to satisfy the entrainment needs of the jet. The deficiency is made up with fluid recirculated from regions farther downstream. The recirculated fluid originates in the jet itself, largely in the region where the jet strikes the duct wall and ceases to be. The region in which the feed and recirculatory streams meet is broad and diffuse, owing to the massively turbulent, eddying nature of the latter. In terms of the intermittency factor, this region extends over a downstream distance of about 1-1/2 duct radii. The point at which $\chi = 1/2$ in the free stream recedes toward the nozzle section with decreasing Craya-Curtet number;

at Ct = 0.51 it is located 2.8 duct radii downstream of the nozzle, but at Ct = 0.13, 0.4 duct radii.

The foregoing constitutes a small sample of the results obtained in this investigation. In all, the field of the intermittency factor in the ducted jet was mapped at six different Craya-Curtet numbers, ranging from 0.13 to 1.22, and also in a free jet. With such complete data on the intermittency factor, the properties of the turbulent fluid have been calculated from data previously obtained; the mean concentration, the concentration fluctuation intensity and the eddy diffusivity. As should be expected, the eddy diffusivity in the turbulent fluid is nearly independent of radial position. These results will be presented and interpreted in this paper, and should contribute to a better understanding of furnace aerodynamics and mixing patterns.

Methods have now been developed by which the scattered light technique can be used to measure all the salient statistical features of point concentrations in turbulent mixing fields: mean value, fluctuation intensity, spectrum, correlation, and intermittency factor. Work is now underway in which measurements are being made on turbulent flames.

Reference

1. Becker, H. A., Hottel, H. C., and Williams, G. C.: Ninth Symposium (International) on Combustion, p. 7, Academic Press, 1963.

92. ON PROCESSES OF TURBULENT EXCHANGE BEHIND FLAMEHOLDERS

Gert Winterfeld

DVL Institut fur Luftstrahlantriebe

In combustion chambers and afterburners of jet engines, flames are mostly stabilized by means of turbulent recirculation zones, which are filled with hot gases and serve as a heat source. Between these recirculation zones and the surrounding flow there exists a turbulent exchange by which the unburned gases are supplied continuously with the energy necessary for ignition. This holds both for the initial flame in the immediate neighborhood of the flameholder and for the main flame spreading from the recirculation zone. Marble and Zukoski (Gas Dyn. Symp. Northwestern Univ., Evanston, 1956, p. 205) found the length of the recirculation zone playing an important part in flame stabilization. As was shown by Löblich (9th Symp. on Comb., 1963, p. 949) the spreading of the main flame is determined by the heat flux from the initial flame to the unignited gas flowing along the recirculation zone. This heat flux is, like the transport of mass and momentum, a consequence of the turbulent velocity fluctuations in this part of the flow field. It depends not only on the temperature gradient but on the coefficient of turbulent exchange, too.

The present paper deals with processes of turbulent exchange in recirculation zones created by axisymmetric flameholders located in cylindrical ducts. The study was carried out experimentally. To obtain information about the magnitude of the exchange and its dependence on the different influences, one first has to define the boundary of the recirculation zone. This will be done suitably by choosing that stream surface which starts from the line of flow separation from the flameholder and which

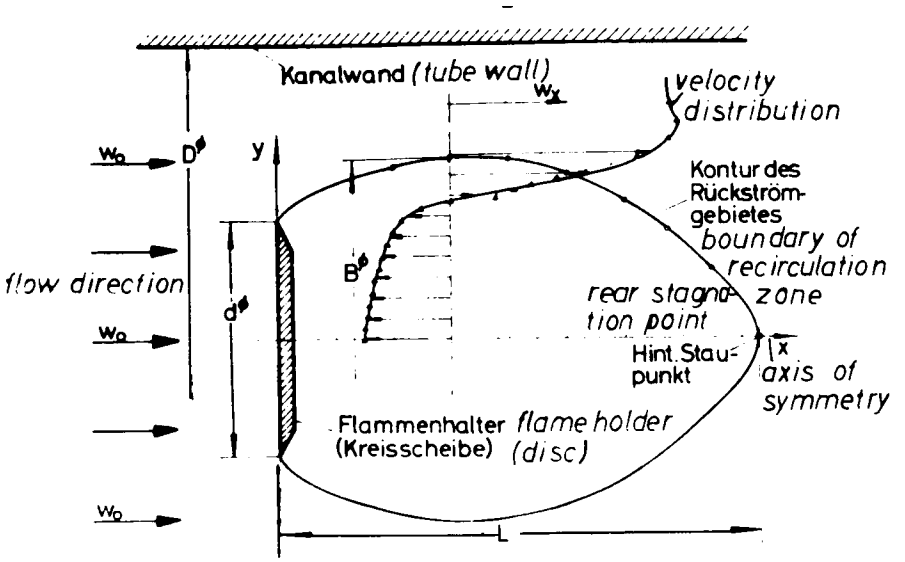

Illustration of some notions used in the present abstract.

is given by the time mean value of the local stream velocity. Close to the flameholder the state of flow in the free boundary layer will be laminar, at first; however, along the greatest part of the boundary surface the flow will be turbulent, at least in that range of Reynolds numbers which is of technical interest. The turbulent velocity fluctuations normal to the boundary carry mass into the recirculation zone and out of it. The magnitude of the mass flow is equal in both directions. Each mass element entering will stay in the recirculating flow for a different time. A. W. Quick (DVL-Bericht Nr. 12, 1956) has defined a mean residence time $\bar{t}_v$ for all mass elements, which is connected to the mass flow $\dot{m}_e$ entering the recirculation zone as follows:

$$\bar{t}_v = \frac{\rho \cdot V_R}{\dot{m}_e} \qquad (1)$$

(ρ = density, V_R Volume of recirculation zone). All quantities on the right-hand side of this equation can be measured. The volume can be calculated if the boundary is determined from velocity measurements. For the measurement of the mean residence time $\bar{t}_v$, A. W. Quick has given a procedure which uses a test substance fed to the recirculation zone (i.e., gas, smoke, excited atoms in flames). After a sudden cut-off of this feeding the concentration of the test substance decreases with time under the influence of the exchange. With some simplifying assumptions this decrease obeys an exponential function, the time constant of which is equal to the mean residence time. The concentration measurement is carried out optically by absorption or scattering of light.

Numerous measurements have been carried out for determining the mean residence time and the geometry of recirculation zones (length, maximum diameter, surface, volume). Discs, cones with 45° and 90° apex angle and cylinders with axis parallel to the flow were used as flameholders; all bodies were inserted in a tube of 100 mm i.d. The blockage ratio and the basic turbulence in the flow have been varied. Experiments have been done with and without flame; propane was used as the fuel. For the measurment of the residence time in flames, sodium atoms emitting yellow light have been used; in the experiments without flame, boron trifluoride was used which, with humid air, produces a dense white smoke.

For discussion of the results the well-known equation for the turbulent transport of mass shall be used:

$$\dot{m}_f = A \cdot F_R \cdot \frac{\partial c}{\partial y} \qquad (2)$$

where $\dot{m}_f$ denotes the mass flow of the test substance out of the recirculation zones, A represents the coefficient of turbulent exchange, F_R is the free boundary surface of recirculation zone, and $\frac{\partial c}{\partial y}$ is a concentration gradient of the test substance. As this concentration is much greater inside the recirculation zone than outside, its gradient can be set proportional to the inside density ρ_F of the test substance, divided by a suitable reference length, i.e., the flameholder diameter d. If the Reynolds number is high enough molecular diffusion of the test substance is negligible compared with the turbulent transport. Then, Eq. (1) holds for the transport of test substance, too, and the residence times for the test substance and for the elements of the basic flow are equal. From Eqs. (1) and (2):

$$\frac{\rho_F \cdot V_R}{\bar{t}_v} = \dot{m}_f = A_R \cdot F_R \cdot \frac{\rho_f}{d} \qquad (3)$$

where A_R now denotes a mean coefficient of exchange valid for the total free surface of recirculation zone:

$$A_R = \frac{V_R \cdot d}{F_R \cdot \bar{t}_v} . \qquad (4)$$

Eq. (4) shows that the coefficient of turbulent exchange will be dependent both on geometry and on the turbulent properties of the flow field.

The results of the measurements, represented graphically in a number of diagrams, will be discussed in terms of mean residence time resp. exchange coefficient. Main quantities of influence are: stream velocity, size and shape of flameholder, blockage ratio, basic turbulence of the flow, the presence of the flame and the mixture ratio of the combustible gas. The residence time is inversely proportional to the stream velocity, hence, the coefficient of turbulent exchange increases linearly with flow velocity. This result departs from the relations for the exchange coefficients in turbulent pipe flow, (J. Nikuradse, Forsch. Arb. Ing. Wes. Heft 356, 1932). The residence time increases with flameholder diameter and decreases with blockage ratio. Likewise, the residence time will be reduced by increasing the basic turbulence of flow. The presence of flame causes the largest variation; it reduces the exchange coefficient to about half its value without flame. This can probably be attributed to the damping of the turbulence, generated in the separated boundary layer, due to the increase in density and viscosity caused by the flame. On the other hand, the exchange shows a flat maximum for stoichiometric mixtures which indicates a contemporary generation of turbulence by the flame. All other influences exhibit the same tendency as without flame. The measurements have been compared with those of Bovina (7th. Sym. on Comb., 1958), carried out with two-dimensional recirculation zones behind 30°-wedges, which show quantitative differences. A discussion of the present results with regard to the flame stabilizing properties of flameholders completes the paper.

93. FLAME IN A BUOYANT METHANE LAYER

H. Phillips

Safety in Mines Research Establishment, England

The occurrence of buoyant layers of methane in the air of roadways in coal mines and their participation in explosions has led to a study of combustion in such layers, particularly by means of models.

Two types of model were used for the experiments. In one, a uniform layer of methane was introduced beneath the ceiling of a 6 ft long gallery, and flame propagated along the layer. The base of the gallery was open to atmosphere so that flame speed was not influenced by gross movements of the layer ahead of the flame front. As the characteristics of the layer were continually changing due to the methane input, and to molecular diffusion, all measurements had to be taken immediately before the flame propagated along the gallery; optical techniques were used to record methane concentration, flame speed, and flame volume.

The other model permitted a more detailed analysis of the propagating head of the flame. The flame was stabilized in a slightly diverging observation chamber by supplying a stratified flow of methane and air. With this technique it was possible to introduce probes into the flame to withdraw gas samples, and to take other measurements which require a longer time than was available with the propagating flame.

The speed of the propagating flame, in the first model mentioned, was constant at 6 ft/sec over a wide range of methane inputs and concentration gradients. As the base of the gallery was open to atmosphere this speed will correspond to the theoretical case of a thin methane roof layer in a gallery of infinite height.

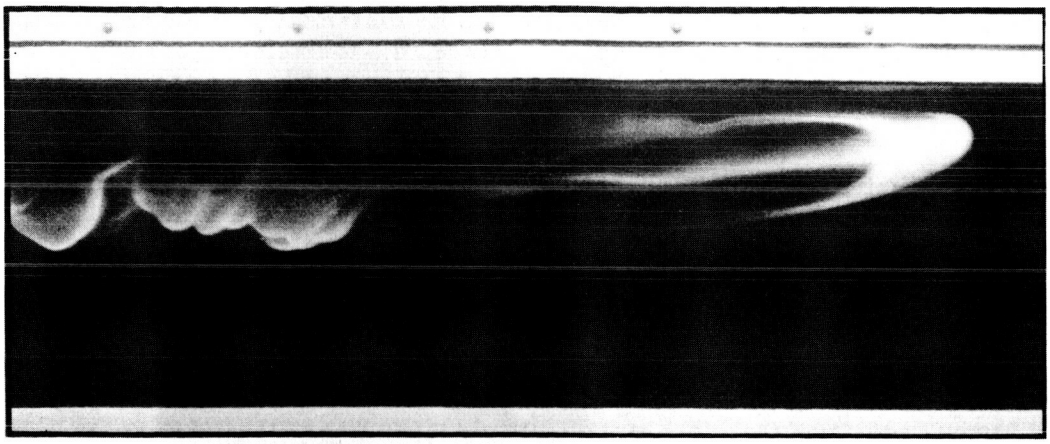

Fig. 1 - Flame in a model gallery

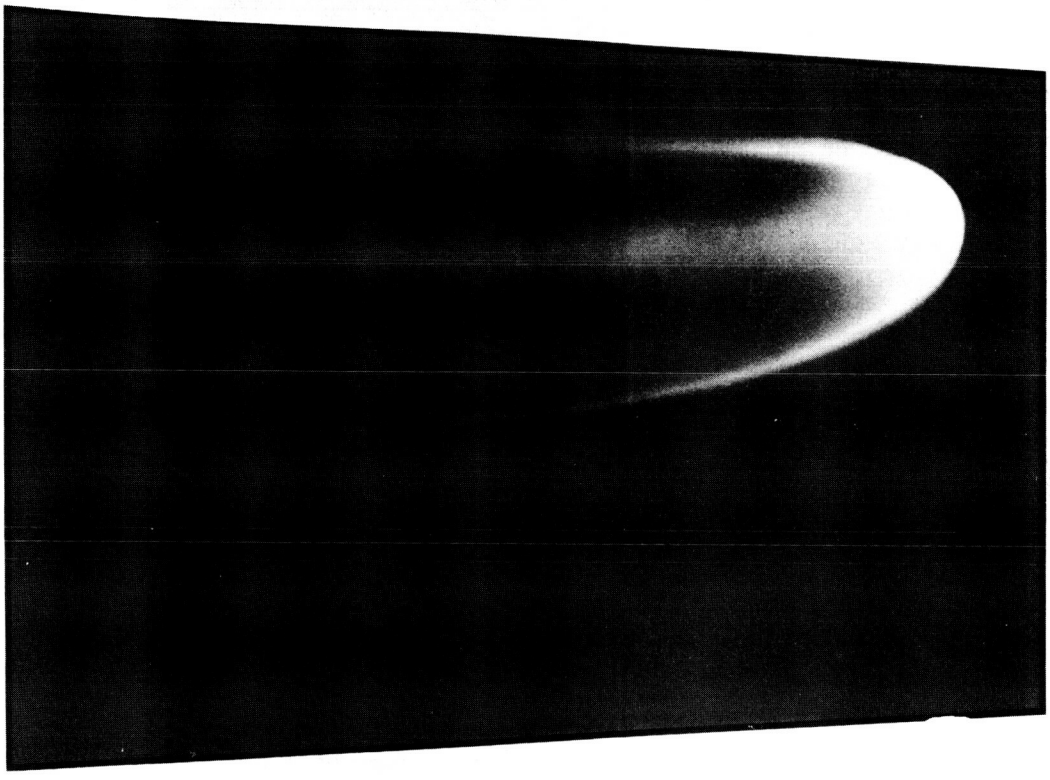

Fig. 2 - Stabilized layer flame

A dimensional analysis suggested that the depth of flame produced by combustion of a layer, (f), might be a function of the total quantity of methane present (characterized by the equivalent depth of a 100% methane layer, q) its distribution in the layer (characterized by the depth of the layer to the 5% mixture, d), the velocity of the flame, (V), viscosity (η) and density (ρ) in the manner:

$$\frac{f}{q} = \phi\left(\frac{qV\rho}{\eta}\right)\left(\frac{d}{q}\right)$$

The term involving velocity takes the form of a Reynolds number. Experimentally, the Reynolds number could be varied only by changing the quantity of methane, and to a lesser extent, by roughening the gallery roof to reduce the velocity. Reynolds number was shown to have a negligible effect on the flame spread over the range tested, and so the depth of flame depended only on the quantity of methane present and its distribution. Variations in density or viscosity were not attempted.

The characteristic shape of the propagating flame is shown in the photograph. A flame front advances through that part of the methane layer where the mixture is within the flammability range. In its wake the products are divided into two zones: the upper containing excess fuel, the lower, excess air. The zones are separated by a diffusion flame. Eventually, buoyancy forces disturb the equilibrium of the system and fresh methane is displaced downwards by the rising layer of hot combustion products, giving a ragged flame controlled by convection.

The same shape of flame has been observed in the second model when a stratified fuel/air mixture approaches a stationary flame (except that the final convection flame was quenched by the nitrogen introduced at each side to cool the observation chamber).

Analyses of oxygen concentration across the flame confirm the description of the flame shape. In the zone above the diffusion flame no oxygen was present, yet in the lower zone the oxygen concentration rose from zero at the diffusion flame, to 20% at the lower part of the advancing flame front.

Once again the relative speed of the flame along the layer is constant. With very steep concentration gradients, giving flame fronts with a small radius of curvature, flame speed is reduced, presumably due to the increased heat losses from the curved flame front. Particle-track photographs show that the speed of the gas entering the stoichiometric zone of the flame is about 1.5 ft/sec which is the burning velocity of a stoichiometric methane/air flame as measured by bunsen burner experiments.

Two important results are suggested by this work:

1. The depth of flame produced by a burning layer depends only on the quantity of methane and its distribution. Therefore, where flame speed is low, as in the experiments described, extrapolation of the results suggests that a scale model of the movement of flame through a layer can be made in which the distribution of both gas and flame obey geometrical scaling laws. At higher flame speeds the transition to turbulent burning and violence probably depends on a Reynolds number and roughness, and cannot, therefore, be modeled unless the model is operated at an increased pressure, or unless some other form of compensation is used.

2. Flame speed is independent of fuel distribution, except where the radius of curvature of the flame is small. This defines a lower limit to the size of model in which the scaling relation may be expected to hold true.

94. CHARACTERISTICS OF LAMINAR AND TURBULENT FLASHBACK

L. N. Khitrin, Ph. B. Moin, B. B. Smirnow and V. U. Shewchuk

The Krzhizhanovsky Institute of Energetics, Moscow

The laminar flame flashback mechanism seems to be clear if one considers a combustible gas mixture issuing from the port of a cylindrical tube. The Lewis and von Elbe "gradient flame flashback theory" has now received conclusive proof based on numerous experimental data for the burning of many gaseous but unheated mixtures.

Fewer investigations, however, have been dedicated to flashback under other conditions: at high laminar burning velocities, particularly in preheated mixtures, or when the gas velocity profile differs from the classical type for laminar steady flow in tubes (parabolic profile). The fundamentals of the flashback in turbulent flow also need further clarification. In this field, experimental data are limited and no attempts have been made to establish criteria for their evaluation.

This paper describes and discusses the influence of some factors which are essential from the standpoint of the flame flashback, such as the wide variation of the laminar burning velocity, the type of gas velocity profile of the stream issuing from the burner port (tubes, nozzles), the burner diameter variation, the state of flow (laminar or turbulent), and the type of mixture.

Experimental results

Laminar flashback in tubes. The influence of pre-heating methane-oxygen mixtures on the flashback velocities was investigated at temperatures ranging from 20° to 400°C., for a wide range of mixture compositions. Such investigations were made also with regard to the laminar (normal) burning velocity. It was noted that the velocity gradient, g , increased considerably with increasing temperature but somewhat more slowly than the laminar burning velocity, U_b , and not as would have been expected from the results for unheated mixtures, where it was proportional to U_b^2 . This is explained by the nature of the heat conductivity coefficient, a , which is practically independent of the mixture composition but rises markedly with the temperature.

Taking into account the temperature dependence of a and using the experimental data for the flashback velocity w and for U_b , one can obtain good agreement with the well-known Putnam and Jensen relation,

$$Pe = kS^2 \qquad (1)$$

where $Pe = \frac{wd}{a}$ and $S = \frac{U_b d}{a}$

The coefficient k was found to be 0.01 which is close to the corresponding value of Putnam and Jensen, $k = 0.0125$.

It should be noted here that the maximum value of U_b reached in the experiments under discussion was $U_b \sim 1500$ cm/sec., which is 30 times higher than that obtained hitherto when investigating flashback phenomena.

Laminar flashback in nozzles. Here, methane-air mixtures and nozzles of different shapes and sizes were used. It was found that the flashback depended upon the ratio of the inlet nozzle diameter to the outlet nozzle (D:d) : if this ratio increases, the flashback velocity increases too, even when the outlet diameter is smaller. Correspondingly, the greater difference between these diameters, the higher the flash-

back velocity, so that the latter may sometimes reach the blowout velocity. This is due to the great uniformity of the velocity profile at the nozzle port, which is characterized by a sharp drop in velocity at the center of the stream. Special washers of different thickness were used to vary the velocity distribution at the nozzle orifice. Thus, different flashback velocities could be achieved. Two typical regimes were observed: with a short nozzle the flame had a meniscus shape and flashed back along the nozzle axis; when on the contrary the nozzle was long, the flame had the usual Bunsen cone form and flashed back near the tube wall.

Correspondingly, in these two regimes one may observe different relations between the flashback velocity and the length of the nozzle orifice, h; for a short nozzle w diminished with increasing h ; for a long nozzle the result was quite the reverse. When the velocity profile was plane, the flashback velocity reached minimum and equaled U_b . Thus, quite different results may be obtained depending upon the actual radial velocity profile of a nozzle orifice.

Turbulent flashback. Turbulent flame flashback in methane-oxygen, methane-air and hydrogen-air mixtures was investigated using cylindrical tubes of different diameters. It was found that contrary to laminar flashback, the burner diameter effect upon the flashback velocity was rather negligible.

Evaluation of the laminar boundary layer thickness δ , corresponding to the turbulent flashback velocity indicates that its value must be 1.5 - 2.5 times the possible value of the so-called "penetration distance," χ, in the mixtures under consideration.

From this deduction it follows that in turbulent flow the flashback process would have to develop in the vicinity of a tube wall, namely in the boundary layer: generally speaking, visual observations confirm this.

Hence, according to the gradient-flashback theory the following equation may be obtained:

$$Re = k\, Pr^{0.55}\, S^{1.11} \qquad (2)$$

where $Re = \frac{wd}{\nu}$, $Pr = \frac{\nu}{a}$, and ν is the kinematic viscosity coefficient.

This relation proved to be in good agreement with the experimental data mentioned above. Thus, the flashback mechanism in turbulent flow from the port is the same as the laminar flashback mechanism.

95. FLUID DYNAMIC EFFECTS IN THE LIFT OF DIFFUSION FLAMES

H. Edmondson and J. E. Garside

University of Leeds

The paper reports work directed towards an elucidation of the mechanism of lift of diffusion flames with particular reference to the flat flame burners or Bray jets commonly used in Europe. The lift of flames from these burners seriously limits their use with hydrocarbon rich gases.

It is shown that a region of premixing of gas and air prior to combustion is essential for creation of a stable flame. The stabilization of a diffusion flame may be regarded, therefore, as essentially similar to the stabilization of a premixed flame -- involving a balance between mixture flow velocity and burning velocity, but complicated by the need for creation of a flammable mixture by intermixing of gas and air.

A well-designed Bray jet causes air to be entrained downwards, counter current to the emergent gas stream, resulting in rapid mixing of air and gas in a region of low flow velocities. Such conditions are obviously ideal for flame stabilization and the resulting flame is very resistant to lift. When a flame does lift from such a jet it is probably as a result of turbulent mixing producing over aeration of the stabilization zone.

The theory of flame stabilization by reverse air flow is developed with particular reference to Bray jets but it is applicable to all other types of burner.

DISCUSSION

ON

ELECTRICAL PROPERTIES OF FLAMES

96. ON THE APPLICATION OF THE H. F. RESONANCE METHOD IN THE ANALYSIS OF FLAME IONIZATION

A. J. Borgers

State University, Utrecht

The advantages and disadvantages of the h. f. resonance method in comparison with the microwave absorption methods are discussed. In particular the capability of the h. f. resonance method to detect heavier ions may be noted. Besides, this method is, in general, more sensitive in the detection of electrons than the microwave method.

A detailed theoretical analysis is given in order to understand the behavior of the resonant circuit, containing a parallel-plate condenser with a flame as dielectric. In this analysis two dimensionless parameters are introduced, both being functions (a) of the real and the imaginary part of the complex conductivity in the flame, and (b) of the ratio between the flame thickness and the interplate distance of the parallel-plate condenser. Under certain conditions these parameters enable us to calibrate the resonant circuit in terms of electric flame properties, without knowing exactly the values of the circuit elements. If the content of heavier ions is in excess in comparison with the electron density it seems to be possible to determine the mean collision frequency of the ions by varying the field frequency.

In the experimental work to be described the electron concentration, as a function of the concentration of alkali metal introduced into the flame, was derived from the shift in resonant frequency as well as from the damping of the circuit. The results with both methods proved to agree with each other. The lower limit for the detection of electrons by measurements of the frequency band-width was found to be 3×10^{14} electrons/m^3.

From combined h.f. and additional optical measurements an electron collision frequency of about 8×10^{10} sec^{-1} was found.

A discrepancy was noted between the degree of ionization found experimentally with several alkali elements and that predicted by the Saha formula at the measured flame temperature.

97. ION SAMPLING FROM CHEMICAL PLASMAS*

G. N. Spokes and B. E. Evans

Stanford Research Institute

Studies of ion sampling from nitrogen afterglows at a pressure of a few Torr indicate that the ion sampling process involves competition between hydrodynamic flow and the local electric fields at the sampling apertures.

---

*Investigation sponsored in part by Air Force Cambridge Research Laboratories (Contract AF 19(628)-1651), and in part by the Air Force Space Systems Command (Los Angeles) (Contract AF 04(694)-128). The work was begun under the sponsorship of the Physical Sciences Divisions Research Committee of Stanford Research Institute.

Semiquantitative estimates are made of plasma sheath thickness. At gas pressures of the order of 5 Torr and with plasma densities of the order 10^{13} to 10^{15} m^{-3} and for applied potentials of the order of ten volts, sheath thicknesses are respectively 4 and 1.3×10^{-3} m. With small negative applied potentials the corresponding sheath thicknesses may be of the order of 0.3 and 0.1×10^{-3} m. Sheath thicknesses of this order are required to explain the features of the experimental results.

Ions sampled from a nitrogen afterglow were primarily N_2^+, N_3^+, and N_4^+. At constant pressure the balance between N_2^+, N_3^+, and N_4^+ is almost independent of the nature of the material from which the sampling electrode is constructed and of the potentials used for ion extraction.

Dielectric coatings on electrode surfaces lead to very long duration ($\sim$30 sec) time effects in the ion sampling process. These effects are explained in terms of a semiquantitative theory of surface charging.

Similar long term time dependencies of ion currents have been found in a system with gold electrodes. These effects can be explained in terms of a changing surface condition (e.g., work function) associated with the applied potential changes.

Ions were sampled from a low pressure atomic oxygen-acetylene diffusion flame. Ion currents were higher when a "pusher" electrode was given a negative potential than when given a positive potential. Again, this is explained in terms of competition between hydrodynamic flow and the electrical draw-out field.

98. ION CONCENTRATION MEASUREMENTS IN A FLAT FLAME AT ATMOSPHERIC PRESSURE

G. Wortberg

Institute of Applied Mechanics, Aachen

Positive ion concentration measurements have been performed in a lean methane air flat flame at atmospheric pressure by means of a Langmuir probe consisting of a thin wire extended parallel to the flame plane. Simultaneously to the ion concentration measurement the temperature profile was obtained from an interferometric density measurement. The interferometer was so adjusted that the probe, the interference pattern and a perpendicular cross-section through the middle of the flame were focused on the same plane of film in the camera. Ion concentrations were measured at various distances from the burner mouth and simultaneously an interferogram was photographed. The distance between burner mouth and probe was measured with a traveling microscope, which was also used to check the interference pattern, and determine whether irregularities in the flow system had moved the flame by a distance of more than 0.1 mm perpendicular to its plane. If this occurred the measurement had been rejected. The error in the displacement between the temperature and ion concentration profile is therefore not larger than 0.1 mm. The heat release rate was calculated from the temperature profile. The resulting curves are presented in the diagram. It is seen that the maximum of ion concentration almost coincides with the maximum of heat release rate. This together with the fact that the ion concentration starts to rise farther downstream than the heat release rate shows that ionization is not produced by the initial reaction steps. From the decay of ion concentration downstream of the reaction zone the ion recombination coefficient is evaluated as 1.1×10^{-7} cm^3/sec.

99. THE USE OF ELECTRICAL PROBES IN FLAME PLASMAS

B. E. L. Travers and H. Williams

Rocket Propulsion Establishment, England

A technique is established for the determination of positive ion densities in hydrocarbon flame gases by considering the positive ion saturation region of electrical probe characteristics in high-pressure plasma conditions, i.e., at pressures above 1 mm Hg; in particular a new theoretical treatment for the collection of positive ions by a spherical probe is given. For spherical probes, agreement between theory and practice is found when leakage currents are experimentally eliminated. For cylindrical probes, similar agreement is found when end effects are also eliminated. It is shown that the use of symmetrical double floating spherical probes is preferable to the use of a single probe for the determination of free electron temperature.

100. ELECTRODE INTERACTIONS IN SEEDED COMBUSTION PRODUCTS*

Donald L. Turcotte and William Friedman

Cornell University

The interaction of a lightly ionized plasma with a cold electrode is considered. The voltage-current characteristics of a stagnation point probe have been measured in a subsonic flow of combustion products. Propane and air are burned in a channel to produce a lightly ionized gas. The combustible mixture was seeded with various concentrations of potassium-hydroxide to enhance the degree of ionization of the products and therefore the electrical conductivity. A pair of copper electrodes are embedded on the stagnation line of a cylindrical ceramic tube inserted into the combustion products. The copper electrodes are cooled to approximately room temperature.

Voltage-current characteristics have been measured when a battery voltage was applied between the electrodes and also when a single electrode was biased positive and negative with respect to ground. A range of voltages from +50v to -50v has been considered. The current drawn was of the order of milliamps. With steady state operation seed material was deposited on the electrode which served as the cathode and affected the reproducibility of the data. Also, at the higher voltages arcing adjacent to the cathode was observed. To eliminate the contamination, measurements were carried out using an AC voltage applied between the two electrodes. The frequency was sufficiently low so that unsteady effects could be neglected. Over the entire range of applied voltages the current-voltage characteristic was linear. Therefore a resistance could be defined. This resistance was found to be linearly dependent on the rate of seeding.

Measurements of the interaction of a lightly ionized gas with a cold electrode have also been carried out in a shock tube. The degree of ionization for the shock tube measurements was approximately equal to the degree of ionization in the combustion products. Other conditions were sufficiently similar so that one might expect

*This study was partially supported by the Air Force Office of Scientific Research.

the results of the two experiments to be comparable. In the shock tube experiments a saturation ion current was observed as predicted by the simple Langmuir probe theory. The voltage-current characteristic was linear except when the probe acted as a cathode at voltages greater than about 5v in which case the current drawn was independent of voltage.

A theory is presented for the structure of a boundary layer in which current flows to an electrode in a lightly ionized gas. It is found that ambipolar diffusion governs the motion of charged particles in the boundary layer except in a plasma sheath adjacent to the wall, which is thin compared to the boundary layer thickness. The flux of ions to the wall is restricted to the number that can diffuse through the boundary layer. Since the mobility of electrons is much greater than ions, there is essentially no limit on the number of electrons that can reach the wall. As long as no electrons are emitted by the wall the theory predicts a saturation ion flux.

The shock tube experiments are in complete agreement with theory. Since the theory requires a saturation ion current for the combustion experiments, these measurements can only be explained on the basis of electron emission from the surface. Since cooled copper electrodes are not expected to emit electrons in the electric fields of these experiments and in fact do not emit electrons in the shock tube experiment, the conclusion must be that electron emission is related to the presence of either the combustion products or the seed material. The fact that a coating of seed material was observed on the cathode after some period of operation indicates that this is the source of electrons through an emission mechanism.

The results of these experiments indicate that magnetohydrodynamic power generation in seeded combustion products will not require heated electrodes in order to obtain sufficient electron emission. This is in agreement with measured performance of generators with cooled electrodes.

101. IONIZATION IN ROCKET EXHAUSTS

W. W. Balwanz

U. S. Naval Research Laboratory

Experimental studies, measuring the absorption of a focused beam of electromagnetic energy, are utilized to determine the electron distribution in the exhaust of rocket motors. Identified sources include thermal, shock and afterburning ionization. Thermal ionization is frozen at or near the rocket throat area. The nonequilibrium shock and afterburning ionization decrease rapidly with reduction in ambient pressure over the range of simulated altitudes studied. Attachment at the exhaust boundaries, and attachment to micron-sized particles when present in the exhaust stream are the principal mechanism for reduction in the total number of free electrons in the exhausts. Dilution by entrained air reduces the concentration of electrons in the stream until the dilution provides sufficient cooling for attachment processes to control. Electron recombination is insignificant in reducing the electron concentration.

102. INTERACTION OF SOLID PARTICLES WITH AN IONIZED GAS*

S. L. Soo and R. C. Dimick

University of Illinois

Consideration of equilibrium of ionization of a gas-solid suspension shows that the solid particles will always become positively charged if the ionization of the gaseous atoms is negligible. However, the combination of high value of thermionic potential and low value of ionization potential of the gas may leave the solid particles negatively charged. Experiments with an arc flame of argon show that addition of metals tends to increase the recombination rate while oxides tend to decrease the recombination rate of argon.

---

*This work was supported by Project SQUID under Contract Nonr 3623(00), NR-198-038.

103. THE RESPONSE OF DROPLETS AND PARTICLES TO ELECTRIC FIELDS, IN THE PRESENCE OF IONS

K. Gugan, J. Lawton and F. J. Weinberg

Imperial College

A theoretical study of the motion of charged molecular clusters, droplets and particles is presented as an essential part of an investigation into electrical control of certain combustion processes. The information required is the charge and mobility of each such charge-carrier, in the presence of flame-ions, under the influence of large fields. The study is subdivided by particle size and by whether the particles are charged to a constant level, or are free to continue acquiring charge along their trajectories in a field. Subdivision by size follows the response to molecular collisions. For the smallest, the target area for impact is greater than geometrical, because of dipoles induced in neighboring molecules. In the next size range, such forces of attraction are negligible, while interaction with neutral gas can still be treated as individual collisions. Larger particles experience such collisions only as a viscosity -- leading into the Stokes regime. Lastly, particles of sufficiently large Re are treated in terms of Newton's law and it is shown that this regime includes the largest sizes likely to be encountered in practice. Particles carrying constant charge occur when, after a region of relatively plentiful space charge (corona discharge, flame) their trajectories lie where no smaller charge carriers exist, or where the theoretical equilibrium charge is no greater than initial. The mechanisms and rates of charging due to ion bombardment, diffusion and thermionic emission are next examined and it is shown that in the most relevant case -- the drifting of particles toward electrodes in the company of ions -- the particles' charge, together with field intensity, tends to increase continuously.

The conclusions are analytical expressions for charge, mobility and range of applicability for each combination of regimes. One noteworthy result is that the largest particles, when free to acquire charge, attain a constant mobility greater than 1/20 of that of H_3O^+.

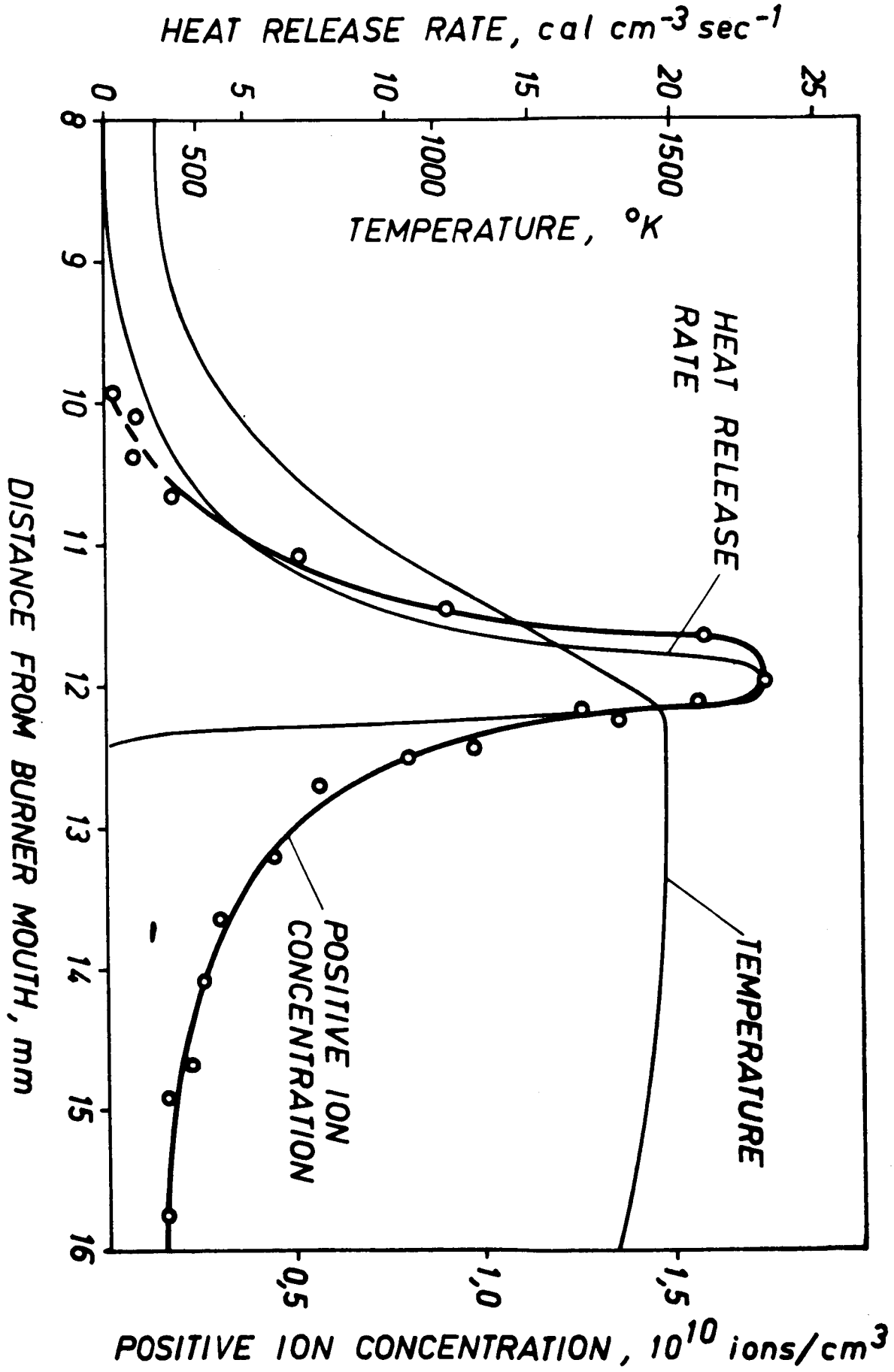
HEAT RELEASE RATE, cal cm⁻³ sec⁻¹
0
5
10
15
20
25
500
1000
1500
TEMPERATURE, °K
HEAT RELEASE RATE
TEMPERATURE
POSITIVE ION CONCENTRATION
DISTANCE FROM BURNER MOUTH, mm
8
9
10
11
12
13
14
15
16
0,5
1,0
1,5
POSITIVE ION CONCENTRATION, 10¹⁰ ions/cm³

104. ON THE EFFECT OF KINETICS OF ELEMENTARY REACTIONS ON IONIZATION IN STATIONARY AND NONSTATIONARY SUPERSONIC EXPANSION AND COMPRESSION OF GASES

N. I. Yushchenkova and S. I. Kosterin

USSR Academy of Sciences

The present investigation was designed to determine the ionization ratio of the air flow, as well as the ionization ratio in the presence of an alkali metal in the air for different laws of supersonic expansion, at the initial temperatures in the adiabatic slowdown flow of T_0 = 6000-2000°K and initial pressures of P_0 = 100-0.1 atm. and for $\alpha_{Na} = 10^{-4} + 10^{-2}$. The results of the calculations indicated significant deviation of the ionization ratio from equilibrium during supersonic expansion (in the range $1.2 \leqslant \delta \leqslant 10$ at 1 cm $\leqslant l_0 \leqslant$ 100 cm) and made it possible to determine the dependence of the limit ionization ratio upon the initial expansion parameters, the law of aerodynamic expansion and a specific size of flow l_0. It is shown that there is a flow region for some range of δ with a gradual transition of the equilibrium ionization ratio toward the freezing one, while the size of the region depends significantly on the law of aerodynamic expansion. For example, the region of transition of δ for an axisymmetrical source is two or three times smaller than for a conical nozzle with a small aperture angle. The latter condition results in the fact that for flow from a supersonic source and during expansion of a supersonic stream in the vacuum, the limit ionization ratio is maximum and produces flow regions with negative dielectric constant. For the laws of expansion with slower variation of $\delta = f(\ell)$ during flow from nozzles and flow around a blunt body, the existence of a wide range of δ with negligible deviation from the equilibrium value is typical. At the same time the limit ionization ratio is significantly less than for flow from a supersonic source. For example, for initial values of the adiabatic slowdown flow of T_0 = 6000°K and P_0 = 1 atm, the limit ionization ratio of air for a supersonic source is $2\frac{1}{2}$ or 3 times greater than for expansion with a supersonic conical nozzle $\xi = 10°$. Similar relations apply in the presence of an alkali metal in the air but the limit ionization ratio in this case corresponds to higher values of δ.

105. A NOVEL CHEMICAL SYSTEM FOR GENERATION OF ELECTRON-RICH GASES

Raymond Friedman and Andrej Maček

Atlantic Research Corporation

A unique self-oxidized combustion system, consisting initially of a solid mixture, is described which burns to yield an all-gas plasma containing over 10^{15} (measured) or 10^{16} (calculated) electrons/cc at atmospheric pressure. The ingredients are tetracyanoethylene, hexanitroethane, and cesium azide, formulated to be stoichiometric to CO, N_2 and Cs. The mixture is compacted to 1.6 gm/cc by pressing at 20,000 psi. The strand burning rate at one atmosphere is 1.3 mm/sec and the pressure exponent is about 0.6. The flame temperature, calculated as 3660°K, was measured as 3520°K by the spectral line intensity method and 3000-3100°K by the line reversal method. In view of the radial non-uniformity of the plasma, the former value is considered more likely to be correct. Electron densities were determined both from measurements of individual

spectral line shapes (Stark-broadening) and by the Inglis-Teller series limit method. The two methods agreed with one another. Strands of 1.27 cm diameter gave three or four times higher electron concentrations than strands of 0.79 cm diameter; however electron concentrations, while extremely high, were still below calculated values, even after the lowering of flame temperature below theoretical because of heat loss was considered. We believe that adequate time was available for cesium ionization, under our experimental conditions, but time was not adequate for complete oxidation of CN and CN^- to CO and N_2, so electrons were largely attached as CN^- rather than free. Hence longer residence times allowing a closer approach toward equilibrium should give even higher yields.

106. AUGMENTING FLAMES WITH ELECTRIC DISCHARGES

D. C. C. Chen, J. Lawton and F. J. Weinberg

Imperial College

A few individual methods for augmenting flame enthalpies and ionization levels electrically have been considered previously. This communication summarizes a more general study of the problems involved and of the experimental approaches to their solution. It is shown that the maximum rates of electrical energy input required are only a few times greater than those due to chemical energy and that the main obstacle lies in the requirement to spread the discharge energy throughout the flame, in spite of its tendency to be released along a thin arc channel. One of the chief attractions of distributing the discharge and associating it with the combustion zone is that the combination is very difficult to blowoff and large throughputs thus become feasible for quite small burners. This attribute is lost once mixing becomes rate-controlling.

The following approaches to this problem are considered theoretically and/or experimentally.

1. The use of (a) "plasma jets", (b) devices developed on allied principles.
2. Inducing turbulence.
3. Seeding with readily ionizable materials.
4. The use of high-frequency alternating discharges.
5. Inducing rapid oscillation or rotation of arcs by magnetic fields.

The following are among the conclusions. Methods based on gas movement -- either random or organized -- convey the impression, to the eye or camera, that they succeed, without in fact doing so. The rapid movement of the gas-borne discharge occurs only with respect to the stationary observer, not with respect to the pockets of gas which carry it. Methods which can be applied only in hot product gas -- such as (3) above -- succeed in spreading the discharge but depend on the presence of the flame and blowoff with it. They do not appreciably augment combustion intensity. Other quite feasible methods -- notably (4) -- are very expensive in bulk, weight and cost of equipment as well as in incidental power losses. The most promising group of methods appears to be that based on feeding reactants through discharges, either held stationary or spinning at such high rates (order 10^5 rpm.) that every part of a fast gas stream experiences the passage of the discharge through it at least once. Power fluxes of 5.7 kw/cm^2 of burner area are attained, of which 40% can be chemical.

107. HEAT TRANSFER MEASUREMENTS ON ELECTRICALLY BOOSTED FLAMES

R. M. Davies

Gas Council, Midlands Research Station, England

Electrically boosted burners of the type described by Karlovitz have been developed to run on town gas/air mixtures to assess their potentialities as industrial burners. This paper describes the heat transfer aspects of the investigation in which comparisons have been made with unboosted and gas/oxygen flames.

Modified air blast tunnel burners were used with maximum fuel gas inputs of 50 cu ft/hr (7.1 kw) or 200 cu ft/hr (28.4 kw). A maximum AC input of 6 kw gave a range of energy addition from 50 to 125% for the smaller burner. Calculations to predict heat transfer coefficients and heat flux have been made using a simplified technique to allow for changes in transport properties due to the dissociation-recombination reactions occurring at high temperatures.

It was found that the average experimental heat flux from a boosted gas/air flame having equal proportions of chemical and added electrical energy was 3.6 times greater than an unboosted flame of equal energy. A gas/oxygen flame gave a 2.7-fold increase when compared with gas/air on an equal energy basis. Peak heat transfer from the core of a boosted flame was found to be twice the average value. In general, experimental heat flux from boosted flames was 20% greater than values calculated, whereas experimental gas/oxygen figures were 5% less than predicted.

It is concluded that the difference in the boosted case can be accounted for by nonuniform distribution of added energy. The increases in heat transfer are primarily caused by change in transport properties of the combustion products. Increased flame temperature differentials, although significant, are of secondary importance. For greater precision in predicting heat transfer from boosted flames, information is needed on the effect of the electrical discharge on the temperature and mass velocity profiles of turbulent flames.

FIRE RESEARCH

(Co-sponsored by the Committee on Fire Research,

U. S. National Academy of Sciences-National Research Council)

108. DIFFUSION-CONTROLLED IGNITION OF CELLULOSIC MATERIALS BY INTENSE RADIANT ENERGY

Stanley Martin

U. S. Naval Radiological Defense Laboratory

Superficially the radiant ignition of cellulosic materials (as well as many other organic solids) is controlled over a wide range of conditions by diffusion of heat into the solid. Numerous ignition criteria and ignition theories have been advanced in an attempt to provide a more fundamental, mechanistic picture of the process. Objective evaluation of such proposals has been hindered by a lack of basic information about such things as the details of the transient-temperature profiles and the evolution rates and chemical composition of pyrolysis products. The objective of the work described in this paper is to provide such information and to consider its implications in ignition processes.

As expected, the pre-ignition, non-steady-state temperature profile is a function of parameters derivable from conduction theory for the case of a simple, hypothetical heat-flow model. In detail, however, the actual profile is quite different from the theoretical and shows significant perturbation by heat of reaction and phase change. Extrapolation of the profile to the irradiated surface indicates that the temperature of the surface at the instant of ignition is independent of irradiance level and is probably in excess of 600°C. Direct optical measurement of the "ignition temperature" confirms both its magnitude and constancy.

Measurements (in an inert atmosphere) of the volatile pyrolysis products show a maximum in the rate of evolution at a time close to the instant of ignition (in air). Levoglucosan, the main volatile-fuel component, increases in yield from about 25 per cent of the theoretical upper limit early in the exposure to about 75 per cent at the ignition time (the actual values depending to some extent upon irradiance). However, no evidence was found, of an ignition criterion based on a threshold rate (or amount) of volatile-fuel evolution.

Calculations of the rate of surface decomposition, based on assumed first-order kinetics, indicate that, over a wide range of irradiance levels, the surface is well charred prior to ignition. On this basis it seems likely that the role of the exposed surface in spontaneous ignition is as a site for secondary reactions. Hydrogen, methane, ethylene and ethane first appear and increase rapidly in amount at about the time when spontaneous-flaming ignition would occur in air. They are almost certainly products of secondary reactions in the incandescent char layer of the exposed surface. While their quantities are always relatively small, their sudden appearance suggests the distinct possibility of ignition being "triggered" by reactive intermediates.

Product analyses of nearly identical exposures of thick and thin specimens indicate that the persistence of flaming depends only upon achieving a temperature profile during exposure whose relaxed value is sufficient to maintain the flow of flammable volatiles and not on any unique composition of them.

109. BASIC STUDIES OF THE MECHANISM OF IGNITION OF CELLULOSIC MATERIALS

W. D. Weatherford, Jr. and D. M. Sheppard

Southwest Research Institute

Mathematical and experimental studies are being conducted on the thermal processes involved in the ignition of slabs of wood-like substances. The results of extensive finite-difference machine computations suggest that the specified fuel-generation-rate criterion for sustained ignition proposed by Bamford, Crank, and Malan is incorrect. These results, however, also suggest that the experimental data of Bamford, Crank, and Malan reflect a thermal criterion of sustained ignition which has not been recognized previously.

In order to adequately describe this critical thermal condition for symmetrical, two-sided heating of plane infinite-width slabs, a concept of a "thermal feed-back wave" being propagated from the surface of symmetry to the heated surface is introduced, and the time required for this wave to reach the heated surface has been derived. Expressed in terms of dimensionless time (Fourier No.) this critical heating time appears to be constant for inert slabs of constant thermal properties. Also, it is approximately constant for noninert slabs of variable thermal properties, and it may decrease somewhat with increasing slab thickness when heat generation effects are present.

Experimental measurements of piloted-ignition thresholds have been conducted in an apparatus designed to simulate convective-source symmetrical heating of plane slabs. These experimental results and published data of prior investigators have been analyzed in terms of various ignition criteria. For such purposes, a generalized correlating concept is described which relegates each of the various ignition criteria to its proper position of relative importance for a particular set of conditions. As an aid for this generalized correlation technique, improved transient heat conduction data have been machine computed with the analytical solution for inert slabs, and the results are presented in graphical form.

110. HEAT AND MASS TRANSFER TO, FROM, AND WITHIN CELLULOSIC SOLIDS BURNING IN AIR*

Perry L. Blackshear, Jr. and Kanury A. Murty

University of Minnesota

In this paper the problem of cellulosic material burning in air is explored in the following three ways:

1. The bouyant boundary adjacent to a fuel surface was examined to obtain heat and mass transfer coefficients for fuel elements of a variety of sizes and orientations.

---

*This work is sponsored in part by the National Bureau of Standards, U. S. Department of Commerce, under contract CST-677.

The measurements were conducted on alcohol soaked ceramic wicks presenting cylindrical and plane fuel surfaces. A flame sheet hovered near the surface where the vaporizing fuel reacted with the room air. The character of this flame sheet (laminar or turbulent, attached or separated) was observed and mass transfer rates were measured directly. The results show (a) that although flame appearance is markedly different in the two cases the vertical and horizontal (with burning surface up) square flat plates have nearly the same ranges of laminar-turbulent transition and nearly the same burning rates per unit of surface area. For turbulent flow this rate is independent of the dimensions of the plate. Transition Grashof numbers and Nusselt numbers are reported for the several geometries and orientations studied and a recommended procedure for predicting mass (and heat) transfer coefficients is outlined.

2. The gross behavior of burning cellulose cylinders, pressed from pure α cellulose filter clippings, is studied. With the above mass transfer coefficients we are able to compute the "driving force" for mass transfer, B, as having a value of 1.5 (for specimens 1" in diameter), about the value one would expect of a heavy fuel oil burning in air. It was found that these apparent values of B varied only slowly with time and varied as (initial diameter of the specimen)$^{-0.6}$. Thus the initial (maximum) mass loss rate divided by the initial mass was found to vary with diameter as $\dot{m}/m_o \propto d_o^{-1.6}$ in agreement with the work of Gross at the National Bureau of Standards. In no existing theories on wood burning are these two characteristics predicted, i.e., no theory predicts that (I) the initial burning rate varies only slowly with time, and (II) burning rate depends on specimen diameter according to $\dot{m}/m_o \propto d^{-1.6}$. These departures from the behavior predicted by currently held models prompted the following exploration into the internal behavior of burning cellulose.

3. Cellulose cylinders were pressed, cured, and dried. Thermocouples were installed on the surface and at varying depths. Tests were run at temperatures which precluded pyrolysis but permitted the determination of the thermal diffusivity and the uniformity of the material. Then the specimens were ignited and the temperature-time history on the surface and within the specimen was recorded. Calculations were then made comparing measured successive temperature distributions with successive temperature distributions predicted from pure heat conduction. From these calculations apparent source and sink strengths of the local processes were determined. Finally, calculations of gasification rates as a function of local temperature and temperature history were employed to obtain a comparison between local heat sources and local mass loss rates. These data are employed to obtain a fairly detailed account of happenings on and beneath the surface. The following results are of particular interest:

a. The surface temperature is not uniform, but has cellular shaped isotherms not directly related to the solid structure.

b. Shortly after ignition water vapor and other condensible vapors diffuse into the solid and condense. As the solid is heated these vapors are regasified and leave by way of the surface. Immigration, condensation and regasification have a pronounced effect on the temperature-time histories near the center of the specimen.

c. The initial thermal decomposition in which the cellulose is gasified does not appear to be strongly exo- (or endo-) thermic. There does appear, however, a high temperature regime in the char near the surface where secondary pyrolysis occurs, this time with a substantial quantity of heat released.

d. The energy carried by the gaseous pyrolysis products approaches in magnitude the energy flux by conduction.

The influence of this last result is felt to hold the key to the two anomalies mentioned earlier, i.e., $\dot{m} \approx$ const, $\dot{m}/m_o \propto \frac{1}{d^{-1.6}}$.

111. THE COMBUSTION OF WOODEN DOWELS IN HEATED AIR

E. Roy Tinney

Washington State University

The investigation in a laboratory of forest fire spread presents a host of interrelated problems not the least of which are the selection of suitable homologous fuel elements, the adoption of a particular array or configuration of elements, the choice of atmosphere, and the determination of the effects of other ambient conditions such as wind, slope and humidity. Nevertheless, some significant features of forest fires can be studied in a laboratory as shown by Fons, et al.[1] who found, by burning cribs of dowels of square cross section, that the rate of fire spread varied as the 3/2 power of the fuel element size. Barrows [2] continued this free burning technique using beds of ponderosa pine needles in a wind tunnel and piles of logging slash in the field to find the effects of moisture content, fuel loading, and wind.

These experiments lead naturally to the question of how the front of a free fire advances from one element to another, which first requires an answer to the question of how one single element is burned. This paper considers the latter phenomenon. Theoretical and experimental results are presented for the combustion of single, small, circular, wooden cylinders or dowels inserted horizontally into a pre-heated air furnace.

Following Bamford, Crank, and Malan,[3] the dowels were considered to be heated both from the exterior and by exothermic reactions accompanying the thermal degradation of the wood. The Fourier conduction equation with a source term was solved in cylindrical coordinates with boundary layer heat transfer coefficients. A first-order Arrhenius equation was used to determine the rate of thermal degradation. Bamford, Crank, and Malan assumed that only a certain fraction (which had to be assumed a priori) of the total fuel was consumed. Roberts and Clough[4] showed later that this fraction depended upon the heating conditions. In this paper, the full weight of the wood was subject to degradation, but the thermal properties of the fuel, particularly the exothermic heat, the energy of activation and the velocity constant, were allowed to vary as the degradation proceeded inwardly from the surface. Computations based on this procedure showed that the rate of weight loss would approach zero prior to complete consumption of the dowel in fair agreement with the experimental results for several values of the ambient temperature and dowel diameter.

The numerical computations were carried out on an IBM 709 by dividing the cross section into 10 and sometimes 20 shells of equal thickness. First the weight losses and remaining densities were computed at all interior points based on the last known rates and temperature profiles. Then the exothermic heat was calculated based on this weight loss. Finally, the exothermic heat effects were added and the Fourier equation was solved using an iterative procedure to determine a new temperature profile.

The changes in thermal properties mentioned above were inserted only once for each shell at a so-called "breakpoint" (several such breakpoints would be more realistic but the computational time would be considerably extended). This breakpoint was chosen when the remaining fuel density was approximately half the original value (assuming the dimensions of the dowel remained unchanged). At the breakpoint, the energy of activation was increased from 30 to 32-34 kilocalories per mole, the exothermic heat raised from 30 to 300 calories per gram and the velocity constant from 6×10^7 to 4×10^8 sec^{-1}. These changes in thermal properties produced a significant change in

both the calculated rate of weight loss and the temperature profile that matched the experimental data quite well.

The experimental program was divided into three minor series and two major series of tests. One minor series was devoted to finding the surface temperature of dowels of different wood species subjected to radiant heating and another series of tests to the comparison of thermal conductivity and diffusivity of charred and uncharred white fir. The latter series showed that both the conductivity and the diffusivity of wood, which had been thermally degraded at temperatures of about 315°C, varied linearly with the remaining density in the vicinity of 80°C.

Two major series of tests were conducted to determine weight loss and internal temperatures of 1/4, 3/8 and 1/2-inch diameter white fir dowels 5-inches long after insertion into a furnace whose internal temperature was held constant at temperatures in the range of 300°C to 650°C. Approximately 160 such tests were made for comparison with the theoretical work described above.

In general, at the lower furnace temperatures, the temperature at the center of the dowel reached a temperature slightly above the furnace temperatures in a few minutes and then remained unchanged for several minutes until the exothermic reaction began. At this time the center temperature rose rapidly to about 900°C. This behavior which was also reported by Kinbara and Akita[5] for a spherical model, produced an S-shaped weight-versus-time curve which approached a steady but low rate of weight loss which terminated when 70-80% of the dowel weight was consumed. At high furnace temperatures, the center temperature rose almost linearly to about 1000°C in one minute followed by a sharp decrease in rate of temperature rise. Similarly, the weight decreased in a nearly linear fashion until about 90% of the weight (larger values for smaller diameters) was gone, at which time the rate of weight loss rapidly approached zero. All of these effects were reproduced by the computational procedures outlined above with fair agreement with the experimental data.

Finally, a short series of tests was made to determine the significance of gas diffusion by measuring pressures attained in the center of the dowel. The maximum internal pressure recorded was 8.25 pounds per square inch above the ambient pressures. This internal pressure dropped rapidly at a time which appeared to coincide with the end of the rapid loss of volatiles and the apparent onset of charcoal combustion. This same point, which agreed roughly with the breakpoint assumed in the theory, also coincided with the development of deep cracks and fissures in the wood. This last feature was readily observed by photographing the dowel during combustion. Photographs were also taken of polished cross sections of dowels, which had been cast in resin to preserve the cracks, after having been extinguished at various stages of thermal degradation.

References

1. Fons, W. L., Clements, H. B., and George, P. M.: Ninth Symposium (International) on Combustion, p. 860, Academic Press, 1963.
2. Barrows, J. S.: "1962 Status and Activities of Forest Fire Research Laboratories," Northern Forest Fire Laboratory, Missoula, Montana, 1962.
3. Bamford, C. H., Crank, J., and Malan, D. H.: "The Combustion of Wood, Part I," Proceedings of Cambridge Philosophical Society, 42, pp 166-182, 1945.
4. Roberts, A. F., and Clough, G.: Ninth Symposium (International) on Combustion, p. 158, Academic Press, 1963.
5. Kinbara, T., and Akita, K.: "On the Self-Ignition of Wood Materials," First International Symposium on the Use of Models in Fire Research, National Academy of Sciences Publication 786, 1961.

112. EXPERIMENTAL FIRES IN ENCLOSURES

D. Gross and A. F. Robertson

National Bureau of Standards

Results are presented of experimental measurements of the mass rates of burning, temperatures and gas compositions in model enclosures of three sizes. Interest was confined to the fully-developed stages of fires in which a single (or multiple) ventilation opening limited the burning rate of a reproducible crib-type cellulose-base combustible load.

The burning rate, as has been reported previously,[1, 2] was found to be generally proportional to $A\sqrt{h}$ (A = area, h = height of window opening), but a characteristic transition region was found for each enclosure which resulted in a discontinuity in the plot of the data. The transition region is associated with a characteristic change in the position of flaming from predominantly within the crib to regions of more ready access of oxygen accompanied by a change in the fraction of the window opening used as inlet and exhaust ports. Burning rate data from the three sizes of enclosures were correlated in terms of the ventilation parameter $A\sqrt{h}$ and the exposed surface area of the crib, A_s. Despite a definite pattern of differences between the scales, a general concordance was found to exist. The maximum burning rate was found to be 0.0007 g/sec per cm^2 of crib surface area for all scale sizes, and the location of the transition region corresponded to a value for $A\sqrt{h}/A_s$ of approximately 0.1 $cm^{1/2}$.

For each enclosure, the average temperature measured by the thermocouples increased with $A\sqrt{h}/A_s$, but tended to level out for window openings greater than those at the transition region. There was a slight upward shift in temperature from the smallest to the largest size enclosure.

Continuous exhaust gas composition measurements were made by means of a sampling tube placed at the top front of the burning crib, using infrared absorption analyzers for CO and CO_2 and a magnetic susceptibility analyzer for O_2. At this sampling position, the CO percentage increased with $A\sqrt{h}$ for the two largest enclosures. The O_2 concentration decreased with $A\sqrt{h}$ and remained at or below 1 per cent for window openings for which active flaming was observed, while the CO_2 concentration increased and remained above 16 to 18 per cent.

Analysis of the combustion reaction in terms of the exhaust products was made. The measured CO/CO_2 ratios were found to increase slightly with the measured temperature at the probe inlet, and comparisons were made with temperature-equilibrium compositions of simple carbon combustion reactions.

The over-all process involved in enclosure fires appears to be a combined gravity-controlled fluid dynamic regime and a radiation-controlled thermal regime. Although the similarity conditions are generally incompatible, partial modeling appears to be feasible if heat conduction through the boundary walls is the same in model and prototype. For a gravity-(buoyancy)-controlled regime, the dimensionless Froude group is the criterion for similarity, and, from the limited agreement found among the data for two enclosures, this group appears to include the essential parameters in the scaling of burning rates of fires in geometrically similar enclosures.

The heat content of the sampled product gases was calculated and its fraction of the total lower heat of combustion of cellulose was found to vary with $A\sqrt{h}$. It may

be concluded that for a ventilation-limited enclosure, the major portion of the generated heat is transferred by radiation from the flames and glowing fuel.

References

1. Kawagoe, K.: Japanese Ministry of Construction Building Research Institute, Report No. 27, Tokyo, (Sept. 1958).

2. Thomas, P. H.: Research, 13, pp. 69-77, (Feb. 1960).

113. HEAT TRANSFER AND BURNING RATES OF POOLS OF LIQUID METHANOL

K. Akita and T. Yumoto

Fire Research Institute of Japan

In the present study, the burning rates of liquid methanol were measured carefully in specially designed concentric vessels having three compartments of the same area (outside diameter 10-30 cm) as well as in the usual circular vessels (diameter 1-60 cm). Methanol was chosen as a fuel which produces a nonluminous flame. In these experiments, the liquid surface was kept at a constant level near the vessel rim by means of a refueling device of the overflow type, and the amount of fuel consumed was calculated from the difference between the fuel supplied and the fuel which overflowed. The flow lines in flame were visualized by the particle-track method using a cloud of fine magnesium oxide.

According to these experiments, the relation of burning rate (mm/min) and the diameter of the single vessels is in good agreement with Hottel's hypothesis[1] and the result of Burgess and Grumer[2] for the region of large diameter. In addition, the results obtained for concentric vessels show that the burning rate decreases quickly with the radial distance from the vessel rim which supports the flame base, but this tendency decreases in the turbulent flows generated with large vessels. As this result indicates radial flow at liquid surface, it helps to explain the discrepancy reported by Hirst and Sutton[3] between calculations based on a simple conduction theory and the actual temperature profiles at the surface layer of liquid. Moreover, in our experiments, the total sum of fuel consumed in each compartment of the concentric vessel was equal to that consumed in the single vessel. In addition, the rates in the outer compartments were not in the least affected by replacing the fuel in the inner compartments with water. These results are very important for the development of new theory as they show that the inside rims in concentric vessels have little effect upon heat transfer from flame to liquid.

Theories for the burning of pools of liquid fuels are presented by Hottel[1] and by Spalding[4] The former theory divides heat transfer into three types, corresponding to conduction, convection, and radiation; it considers the burning rate as controlled by the total heat absorbed by the liquid. The latter theory is well known as a form of free-convection theory obtained by modifying the author's theory of droplet burning. Spalding's theory has the support of Rasbash[5] and Fons,[6] but it is not quite satisfactory for the present data because the index n calculated from the slope of the Nusselt number-Grashof number curve is fairly small in comparison with the theoretical value ($n = 0.19$ to $n = 0.25$). This lack of agreement is attributed to the fact that the theory does not consider the vortexes found in our particle-track photographs.

Accordingly, in the present study, an attempt was made to extend Hottel's theory by applying the local heat transfer coefficients:

$$K = K_f \quad \text{at} \quad r = r_f, \quad K = 0 \quad \text{at} \quad r \neq r_f, \tag{1}$$

$$U = U_f \exp\left[-\alpha (1 - r/r_f)\right], \quad r_f > r > 0. \tag{2}$$

where K_f and U_f are conduction and convection coefficients at the radius r_f related to the flame base, and α is an attenuation coefficient. The empirical equation (2) assumes that the convection heat transfer decreases exponentially toward the center of the vessel. The radiation term was neglected on account of the nonluminous nature of the methanol flame.

Thus, for an arbitrary compartment which consists of radii r_1 and r_2, the following equation is obtained:

$$v = \frac{2(T_f - T_b)\, U_f}{\rho \Delta H_v (r_2^2 - r_1^2)} \left[r_f \left(\frac{K_f}{U_f}\right) + \frac{r_f}{\alpha} \left\{ \left(r_2 - \frac{r_f}{\alpha}\right) e^{-\alpha\left(1 - \frac{r_2}{r_f}\right)} - \left(r_1 - \frac{r_f}{\alpha}\right) e^{-\alpha\left(1 - \frac{r_1}{r_f}\right)} \right\} \right] \tag{3}$$

where T_f is the flame temperature, T_b is the surface temperature of the liquid, ρ is the liquid density, ΔH_v is the heat of evaporation of the liquid, and v is the burning rate. Since T_f, K_f, U_f and α are unknown, the absolute rates are not obtained from this equation, but if K_f/U_f and α are given, the relative rates can be calculated. Then, through the use of the above two parameters determined so as to satisfy the rate-diameter data for single vessels, the ratios of burning rates of fuel in the various concentric vessels can be calculated. The results obtained agree very well with the experimental data within the limits of our study.

In conclusion, it appears that Hottel's theory is applicable not only to turbulent luminous flames as pointed out by Burgess, Strasser, and Grumer, [7] but also to nonluminous flames in laminar flow. As K_f/U_f estimated by the preceding procedure is 0.7, it is possible that heat transfer by conduction via the vessel rim will not exceed 70 per cent of heat transfer by conduction at the flame base.

References

1. Hottel, H. C.: Fire Research Abstracts and Reviews, 1 41 (1959).

2. Burgess, D. S., and Grumer, J.: Fire Res. Abst. and Rev., 4 236 (1962).

3. Hirst, R., and Sutton, .D.: Comb. and Flame, 5 319 (1961).

4. Spalding, D. B.: Fire Res. Abst. and Rev., 4 3 (1962); "Some Fundamentals of Combustion," p. 126, Butterworth, 1955.

5. Rasbash, D. J., Rogowski, Z. W., and Stark, G. W.: Fuel 35 94 (1956).

6. Fons, W. L.: Comb. and Flame, 5 283 (1961).

7. Burgess, D. S., Strasser, A., and Grumer, J.: Fire Res. Abst. and Rev., 3 177 (1961).

SOLID PROPELLANT COMBUSTION FUNDAMENTALS

114. PERCHLORIC ACID FLAMES: I. PREMIXED FLAMES WITH METHANE AND OTHER FUELS

G. A. McD. Cummings and A. R. Hall

Rocket Propulsion Establishment, England

The study of the ammonium perchlorate flame is made difficult by the fact that the flame remains very close to the solid surface even at low pressures. Moreover only under very restricted conditions can ammonia and perchloric acid vapor be mixed without rapid formation of ammonium perchlorate. However, the study of premixed flames of other simple fuels with vaporized perchloric acid allows some general conclusions to be drawn about the mechanism of reaction of this acid in flames.

Premixed flames of methane, ethane and methyl alcohol with perchloric acid (72% by weight) have been stabilized on burners using conventional apparatus and techniques, suitably modified to allow for the need to produce a steady flow of vapor from the liquid acid, and to prevent subsequent condensation of the vapor. Burning velocities have been measured at atmospheric pressure for the three fuels and also at approximately 4 cm Hg. with methane, being deduced from the total volume flow and the total area of the inner surface of the luminous flame cone. The spectra of the flames have been recorded, and some temperatures have been measured by OH line reversal in flames at atmospheric pressure.

The results obtained are best discussed by comparison with the corresponding properties of the better known fuel/oxygen flames.

Burning Velocity

A stoichiometric methane/perchloric acid flame has a burning velocity of approximately 400 cm sec^{-1}, i.e., about three times that of a stoichiometric methane/oxygen mixture with the same flame temperature. The burning velocities of the other fuel/perchloric acid flames had similarly high values.

The two systems are alike in that the burning velocity does not vary significantly with change in pressure but differ in that the burning velocity of the perchloric acid mixtures reaches a maximum with a composition well on the fuel-rich side rather than at stoichiometric. In the latter respect a similar result has been found with flames of methyl alcohol and ethane with perchloric acid.

Spectra

In addition to the C_2, CH and OH bands customarily obtained with hydrocarbon flames all the spectra with fuel/perchloric acid mixtures exhibit "cool" flame bands. With the spatial resolution obtained at low pressure it can be seen that these bands are confined to the early part of the flame, at least with the faster burning mixtures, and seem to appear before the C_2 and CH bands.

On addition of molecular oxygen to the methane flame at low pressure, a second flame zone is formed downstream of the original zone which continues to show the features of the perchloric acid flame, and this second zone shows the spectrum associated with the methane/oxygen flame. The OH and CH bands reveal two maxima corresponding to the two luminous zones.

Temperature

Temperature measurements have been made of the burned gas immediately downstream of the reaction zone of methane/perchloric acid flames stabilized, at atm. pressure, on silica burners with a rectangular slit; about three moles of nitrogen as diluent were required to reduce the flame temperature and burning velocity to more convenient values. The technique used was that of line reversal using the OH bands at 3064A. For a stoichiometric flame the temperature measured was 2360°K. The temperature calculated assuming equilibrium is 2460°K, and that calculated assuming oxidation did not proceed beyond the formation of carbon monoxide is 2110°K.

Discussion

It is clear from the above comparison that the perchloric acid is not simply decomposing to liberate molecular oxygen as the chief oxidizer but that the acid or its decomposition products are more reactive oxidizers than oxygen. Furthermore the results suggest that the oxidation of the fuel proceeds through the formation of formaldehyde as intermediate in a similar manner to that suggested for a lean methane/oxygen flame by Fristrom and Westenberg (8th Symposium on Combustion, p. 438) and the initial reaction of oxidizer and fuel is faster than in the methane/oxygen flame. The fact that the observed flame temperature is close to the value calculated assuming equilibrium indicates that the conversion of carbon monoxide to dioxide in the perchloric acid flame does not lag significantly behind the main oxidation reactions.

It seems reasonable also to conclude that the burning velocity of a premixed ammonia/perchloric acid flame would be significantly greater than that of an ammonia/oxygen flame of the same flame temperature.

115. THE SURFACE TEMPERATURE OF AMMONIUM PERCHLORATE BURNING AT ELEVATED PRESSURES

J. Powling and W. A. W. Smith

Explosives Research and Development Establishment, England

A method of measuring the surface temperature of burning propellant ingredients by an infrared emission technique [1] and its application to the problem of ammonium perchlorate deflagration at pressures within the range 760 to 20 mm Hg have been reported. [2, 3]

It would be of some interest to know how the surface temperature of ammonium perchlorate changed as the pressure increased beyond atmospheric towards rocket operating pressures. In particular, it would be useful to see if any departure from the low-pressure relationship between surface temperature and pressure could be detected. At sub-atmospheric pressures the burning surface condition could be represented by the equilibrium

$$NH_4ClO_{4(s)} \rightleftharpoons NH_{3(g)} + HClO_{4(g)} \quad ; \quad \Delta H = 56 \text{ kcal/mole} \qquad (1)$$

and the following relationship was valid:

$$\ln (K_{p_1}/K_{p_2}) = \ln (P_1^2/P_2^2) = \Delta H_s \, (1/T_2 - 1/T_1)/R \qquad (2)$$

where K_p = equilibrium constant for reaction (1) = $p_{NH_3} \times p_{HClO_4}$

P = ambient pressure,

ΔH_s = heat of dissociation, reaction (1)

T = surface temperature.

Such a condition may not continue to apply at elevated pressures, when the surface temperature would be required to approach the flame temperature of the reaction between NH_3 and $HClO_4$ and the partial pressures of these products at the surface would approach zero. The present paper describes the development of the infrared optical method for measurement of the surface temperatures of ammonium perchlorate burning at elevated pressures and some results are given for very weak fuel/perchlorate mixtures. The natural limitations of the technique are indicated.

The change of surface temperature with pressure, from 15 psia to 60 psia, was in accord with the predictions from results at sub-atmospheric pressure, [3] from which it was possible to deduce that the process taking place at the ammonium perchlorate surface during burning was most probably the reaction:

$$NH_4ClO_{4(s)} \rightleftharpoons NH_{3(g)} + HClO_{4(g)}$$

with near-equilibrium conditions existing between the solid and gaseous phases. Up to 60 psia, the surface temperature and the ambient pressure can still be related through equation (2), but above this pressure the scatter of temperature values is too great for positive conclusion, although the latter continue to follow the trend of the lower pressure results. Extrapolation to rocket operating pressures, although a procedure of questionable value, would give ammonium perchlorate surface temperatures of $\sim$650°C at 300 psi, $\sim$680°C at 500 psi and $\sim$720°C at 1000 psi.

The difficulties experienced in extending the measurements of surface temperature successfully to high pressures led the authors to examine, as far as possible in practical examples, the limitation on the method imposed by the increase of gas emission, which masks the emission from the surface, and the decrease of the effective emissivity of the surface when the temperature gradient within the surface becomes large (at high rates of burning).

References

1. Powling, J., and Smith, W. A. W.: Combustion & Flame 6, 173, (1962).

2. Arden, E. A., Powling, J., and Smith, W. A. W.: Combustion & Flame, 6, 21, (1962).

3. Powling, J., and Smith, W. A. W.: Combustion and Flame, 7, 269, (1963)

116. COMBUSTION OF SPHERES OF AMMONIUM PERCHLORATE IN A STREAM OF COMBUSTIBLE GAS

M. Barrère and L. Nadaud

ONERA, France

The burning velocity of solid composite propergols depends largely on the rate of regression of the combustible. For this reason, numerous investigations have been devoted to measuring the rate of pyrolysis of certain solid combustibles, such as ammonium perchlorate. However, these experiments have been conducted under conditions rather different from the practical ones.

The purpose of the present investigation was to study the combustion of ammonium perchlorate under conditions which approximate those that exist at the propergol surface. In this connection the best procedure is to determine the rate of regression of spheres of ammonium perchlorate located in a flow of combustible gas.

In considering the propergol, one can assimilate the perchlorate crystals to spheres which become progressively exposed through pyrolysis of the plastic binder, the combustion of the perchlorate being ultimately determined by a decomposition flame at the surface and a diffusion flame above the surface which results from the presence of combustible gases formed by pyrolysis of the binder.

The first part of the present paper deals with the theoretical analysis of the combustion of a perchlorate sphere located in a combustible gas.

We assume a decomposition flame near the surface and a diffusion flame surrounding the decomposition flame. Thus we have a first temperature for the completion of the decomposition of the order of 1200°K, and at some distance from the sphere we have a temperature for completion of the combustion of the perchlorate with the combustible which is much higher, of the order of 2600°K.

The rate of regression of the sphere in continuous flow depends largely on the temperature of the completion of the combustion of the diffusion flame. Thus ultimately it is the diffusion flame which controls the burning velocity of the sphere in the decomposition flame. Perchlorate burns according to the equation $D^2 = D_o^2 - Kt$, which can be used in plotting the combustion of composite powders. This velocity also depends on the nature of the combustibles surrounding the perchlorate sphere and for this reason pyrolysis rates measured in an inert gas are less interesting as they are different from those observed in a combustible gas.

The second part of the paper describes an experimental study of the combustion velocity of spheres of compressed perchlorates. These spheres vary in diameter from 2 to 15 mm. They are placed in a flow of gas and maintained in a certain position by a metal screen. Parameters which can be studied with this arrangement are the nature of the combustible gas; the velocity of the combustible gases; the pressure; the temperature of the perchlorate sphere and of the gases.

Ignition was insured by a wire heated to fusion by the passage of an electric current. The gases used were propane, ammonia, hydrogen and mixtures of hydrogen and nitrogen. These gases were chosen in such a way as to determine the effect of the elements which enter into the composition of the binder (hydrogen, carbon, nitrogen). Experiments were first carried out at atmospheric pressure. Whereas decomposition of the perchlorate alone cannot be obtained at this pressure, it burns readily in a

combustible gas. With the ignition source placed downstream of the sphere, the flame is observed to propagate against the flow. This can, to some extent, represent the regression rate of the plastic binder.

The propagation velocity of the flame depends principally on the nature of the combustible. It is of the order of 0.77 mm s^{-1} with propane and 0.35 mm s^{-1} with ammonia, for an average flow velocity of the gases of 0.25 cm s^{-1}. Moreover the propagation velocity is maximum for a certain velocity of the gases.

The structure of the combustion zone also depends on the nature of the combustible. With propane, a decomposition flame is observed very close to the surface surrounded at some distance from the sphere by a dim diffusion flame, with a second very bright diffusion flame downstream. With ammonia and hydrogen, we observe only the decomposition flame and a diffusion flame which is more or less luminous depending upon the concentration of hydrogen. The equations for the combustion velocity for propane and ammonia are similar and have the form of $D^2 = D_o^2 - Kt$, where $K = 2.9$ mm^2 s^{-1} for propane and 2.8 mm^2 s^{-1} for ammonia. The diameter D is measured perpendicular to the flow. With pure hydrogen or hydrogen more or less diluted with nitrogen, the equations are of the form $D^3 = D_o^3 - Kt$, where $K = 25$ mm^3 s^{-1} for pure hydrogen and $K = 18$ mm^3 s^{-1} for the composition $(1.5\ N_2, H_2)$.

Thus the linear velocities are not constant and depend on the diameter of the perchlorate particle. For a sphere of 1 mm diameter, the linear velocities are six times as high with pure hydrogen as with propane.

The values of K were determined as a function of the velocity of the gases, maintaining a constant Reynolds number. The effect of pressure was also studied for the above three combustible gases. To conclude, these experiments stress the effect of the following on the rate of regression of the solid propergol: (a) particle size of the perchlorate; (b) nature of the gases surrounding the perchlorate crystals; (c) velocity of the combustible gases near the perchlorate, for low Reynolds numbers; (d) pressure.

117. REGRESSION RATES AND THE KINETICS OF POLYMER DEGRADATION

B. Rabinovitch

United Technology Center

Hitherto, all attempts to predict regression rates of solid rocket fuels have been almost exclusively based upon considerations of energetics, thermodynamics, mass and heat transfer rates. The only prior attempt to calculate the regression rate of a burning surface of a relatively simple polymer on the basis of chemical kinetics was made by Houser and Peck (AIAA Heterogeneous Combustion Conference, December, 1963) but their results were too low by a factor of 10 to 100.

We have succeeded in applying the principles of chemical kinetics and polymer degradation to this problem and have been able to predict regression rates that do not differ by more than a factor of 2 from those measured. The method is open to refine-

ment. The basic hypothesis involved is that, in the polymer degradation process, the fragments produced will not volatilize unless the energy binding them to the other polymer molecules (cohesive energy density) is less than the energy required to break a C-C bond in the polymer chain. If this is not so, then it is energetically more economical to continue to reduce the size of the fragments by further degradation, until, in fact, it is so. When it is so, for a given plane within the solid fuel, then all polymer at his plane, but none beyond it, will be volatile. and thus we must identify this plane as the regressing surface.

In the simplest picture, we can work with the number average size (degree of polymerization) of the critical fragment, and assume a degradation mechanism of random scission. The only parameter in the calculation is the temperature of the burning surface T_s. The heat of reaction of the degradation process may or may not be included in calculating the temperature profile from

$$(T - T_o) = (T_s - T_o - \Delta)\ e^{-\dot{r}x/\chi} + \ldots e^{-(p\dot{r}x/\chi)} \qquad (1)$$

where $\Delta = \dfrac{\Delta H \cdot n_x}{\rho \cdot c \cdot (1-p)}$ for a first order degradation process.

$$p = E/R\ T_s\ (1 - T_o/T_s) \qquad (2)$$

and n_x = number of chain bonds per cc distance x from the surface.

We have been able to demonstrate that all simple mechanisms for the depolymerization (degradation) process except for one, (chain-end initiation with a kinetic chain length $\xi < P_o$, the initial degree of polymerization of the homogeneous polymer) will conform to the experimentally observed first order rate-of-loss-in-weight relationship for isothermally degrading polymers.

$$\frac{m_l}{m_o} = 1 - e^{-k^1 t}$$

where m_l = the total monomer found in the volatilized fragments at time t, irrespective of size

and m_o = total monomer of initial polymer

by using a first order law governing the rate of bond rupture

$$-\frac{dn}{dt} = k.\ n.$$

Putting equations (1) and (2) together, we obtain

$$\ln \frac{n_o}{n_{t_c}} = -B \int_{t_c - t = t_c}^{t_c - t = o} \exp\left\{ - \frac{E_a\ d(t_c - t)}{R(T_s - T_o)e^{-(\dot{r}^2/\chi)(t_c - t)} + RT_o} \right\}$$

where t_c = the time taken for the regressing surface to reach an arbitrary plane parallel to this surface, from an arbitrary zero time during steady state burning,

and n_{t_c} = number of chain bonds per cc of polymer at this plane after time t_c, i.e., at the regressing surface,

and taking $\Delta = 0$.

In order to calculate the regression rate, $\dot{r}$, for a given T_s, we need only determine the rate constant $k = Be^{-E_a/RT}$ for the over-all isothermal degradation process, and E_a, the activation energy. The quotient n_o/n_{t_c} is readily obtained from a knowledge of the heat of vaporization of the basic monomeric unit as it appears in the polymer, and the C-C bond strength binding these units together.

The same considerations apply to a chain-initiation reverse polymerization mechanism, or a weak link mechanism of degradation. Several refinements beyond those already indicated can be introduced, such as the use of the following equation to describe the rate at which volatile fragments (critical fragment size = i) are produced in random scission:

$$\frac{d\sum_1^i pN_p}{dt} = \frac{dm_1}{dt} = 2kN_oP_oe^{-ikt}(1-e^{-kt})\sum_1^i p.$$

This general technique has also been applied to composite solid fuels, such as polystyrene plus potassium perchlorate, where the only products of oxidizer decomposition are potassium chloride and oxygen. In this case we find, allowing $T_s = 1100^oK$, that the extent of decomposition of the potassium perchlorate in the solid fuel is minimal, being about 3 per cent. The suggestion is that oxidative degradation of the polymer is not important and this is borne out by the calculation that the regression rate calculated on the basis of a thermal degradation alone is 1.65 ips whereas oxidative degradation gives either 0.36 or 3.58 ips (100 π chamber pressure) depending upon whether one assumes a first order or a second order dependence upon oxygen pressure. In the former case there would be a square root dependence of $\dot{r}$ upon pressure, while in the latter a direct dependence upon pressure.

In our considerations we have been able to show that both a first order and a second order dependence on oxygen pressure is possible depending upon whether or not a stationary state concentration of activated chains is reached. Extension to other solid oxidizers has been made, but the complexity of the calculations increases as the number of oxidizing products of oxidizer decomposition increases, e.g., ammonium perchlorate.

118. CHEMICAL KINETICS OF THE CORDITE EXPLOSION ZONE

G. Sotter

Sheffield University, England

Theoretical investigations of combustion instability in solid propellant rocket motors have always been plagued by lack of knowledge of the physical and chemical details of steady-state combustion. Early theories suggested that it was pressure-dependent chemical time lags which enabled the combustion process to feed energy into acoustic pressure oscillations. The durations of these lags could only be guessed; thorough investigation of the kinetics of solid propellant combustion would be an enormous task. We can hope to make a start, however, by beginning consideration in a region where the composition of the reactants is relatively simple: the gas-phase

induction zone of cordite. The gases as they emerge from the complex reactions of the fizz zone (just above the solid surface) consist mainly of inorganic molecules. These travel through what is usually called the gas-phase induction zone, finally entering a tertiary combustion stage in the explosion zone. Various experimenters have analyzed the constituents of the induction zone at low pressures, and have found that the principal species present are CO, NO, H_2O, CO_2 and H_2. The temperature of the induction zone is estimated to be 1200-1400°C. With these initial conditions, a set of chemical reactions was chosen which might represent the processes leading to, and comprising, the explosion zone. These reactions are shown in Table 1, and include the twelve species

N	O	H
N_2	O_2	H_2
NO	CO	OH
N_2O	CO_2	H_2O

Reactions $4b_c$, $5b_c$ and $6b_c$ are merely the back reactions of 4, 5 and 6, with NO acting as a "catalytic" third body. This is to account for the effects of reactions which involve formation of HNO, but for which rates are not known. As an approximation, the backward rate constants for reactions 4, 5 and 6 were multiplied by 100 to provide constants for the "catalytic" reactions. Using the net rates of the various reactions, a differential equation was written for the concentration of each reactant. By ignoring diffusion of species, heat radiation, and conduction, and using the equations for conservation of mass, energy, and momentum, one may derive equations for the derivatives (with respect to distance) of temperature, enthalpy, velocity, pressure, and density, of an ideal gas. The set of reactants chosen thus requires seventeen simultaneous differential equations (twelve for species concentrations, five for fluid dynamic variables). These equations have been integrated numerically, using a digital computer, for the case of combustion at 1000 psi. Temperature, velocity and concentration profiles are given. The results presented required some one hundred hours on the high-speed digital computer. The important reactions in the induction zone were found to be 1, 7 and 17:

1) $H + H_2O \rightleftharpoons H_2 + OH$

7) $CO + OH \rightleftharpoons CO_2 + H$

17) $2NO + H \longrightarrow 2HNO \; (+H_2 \xrightarrow{\text{fast}} 2H_2O + N_2)$

It has long been thought that reactions 11 and 12 were the important ones in the decomposition of NO in nitric ester flames, but the calculations show that these are much too slow to initiate the flame. Apparently it is the termolecular reaction 17 which supplies the heat leading to explosion.

The results agree with published experimental work within the accuracy of the experimental data used.

TABLE 1

Reactions used in the theoretical kinetic study of the cordite "explosion zone":

1) $H + H_2O \rightleftharpoons H_2 + OH$

2) $H + O_2 \rightleftharpoons O + OH$

3) $H_2 + O \rightleftharpoons H + OH$

4) $H_2O + M \rightleftharpoons H + OH + M$

$4b_c$) $H + OH + NO \longrightarrow H_2O + NO$

5) $H_2 + M \rightleftharpoons H + H + M$

$5b_c$) $H + H + NO \longrightarrow H_2 + NO$

6) $O_2 + M \rightleftharpoons O + O + M$

$6b_c$) $O + O + NO \longrightarrow O_2 + NO$

7) $CO + OH \rightleftharpoons CO_2 + H$

8) $NO + M \rightleftharpoons N + O + M$

9) $N_2 + O \rightleftharpoons N + NO$

10) $NO + O \rightleftharpoons N + O_2$

11) $N_2 + O_2 \rightleftharpoons NO + NO$

12) $NO + NO \rightleftharpoons N_2O + O$

13) $N_2O + M \rightleftharpoons N_2 + O + M$

14) $N_2 + O_2 \rightleftharpoons N_2O + O$

15) $H_2O + O \rightleftharpoons OH + OH$

16) $OH + M \rightleftharpoons H + O + M$

17) $2NO + H_2 \longrightarrow 2HNO \ (+H_2 \xrightarrow{fast} 2H_2O + N_2)$

119. EMITTANCE OF CONDENSED OXIDES IN SOLID PROPELLANT COMBUSTION PRODUCTS*

Donald J. Carlson

Philco Research Laboratories

The combustion products of metallized solid propellant compositions contain an appreciable mass fraction of condensed phase matter which forms a finely divided particle cloud. The presence of such matter modifies the radiative behavior of the flame both within and external to the engine. Thus, nozzle heat transfer, base heat transfer, and nozzle performance may all be affected by the particle cloud. The investigation described here consists of the experimental determination of the emittance of alumina and magnesia particles present in the exhaust flow of slurry-fueled solid propellant simulator engines. Comparison of the results with appropriate emissivities based upon Mie theory and available oxide optical properties obtained from slabs of the pure crystalline substance is made, and the exhaust particle emittance is found to be considerably in excess of the predicted emissivities.

The magnesia emittance measurements were obtained in the nozzle of a slurry-fueled solid propellant simulator rocket engine. Such engines produce a controlled gas-particle flow by burning a liquid fuel (RP-1 in this case) into which has been suspended a known quantity of known size distribution metal oxide particles. The oxide is used in preference to the unburned metal because the combusted metals form a cloud of oxide particles of unknown size distribution, and experimental determination of the size distribution would then be necessary by means of difficult exhaust sampling techniques. The oxides, on the other hand, are more likely to pass through the engine unchanged in size distribution if their boiling point is not exceeded. The emittance of the individual magnesia particles was obtained by measuring the spectral steradiance of the particle cloud (at $\lambda = 0.59\ \mu$) and comparing this with the blackbody steradiancy based upon the true temperature of the particles as predicted by thermal lag theory. The calculation of the blackbody radiancy was made by computing the radiative flux per unit cross sectional area of the particle cloud. In order to keep the analysis of the experiments simple, the particle cloud was kept optically thin (scattering mean free path greater than flame dimension) so that multiple scattering effects were negligible and radiant flux in a given direction could be obtained merely by summing over the distribution. The flux originated from particles of different sizes and hence different true temperature, and thus the measured emittance represents an average over a range of temperatures and particle sizes. The emittance found for magnesia particles of about one to ten microns in diameter was 0.32. No consistent temperature dependence appeared for the range of gas temperatures (about 2000° to 3000°K) studied. The emissivity predicted from Mie theory for particles of these sizes using the best available optical properties of pure magnesia was found to be about three orders of magnitude smaller than this.

Similar measurements were obtained for alumina using a smaller rocket engine with the nozzle removed so the flow could be observed at near-stagnation conditions. This smaller engine burned gaseous hydrogen and oxygen and a water/alumina slurry mixture. Temperatures ranging from about 3400°K to below the alumina melting point

---

*This work was sponsored by the Advanced Research Projects Agency under Contracts NOw 61-0905-c and NOnr 3907(00).

(2320°K) could readily be obtained. The particle size distribution was measured both before and after the firing to test for possible changes in size distribution. Also, infrared transmission measurements were made, providing experimental verification of computed particle concentration and pre-run size distribution. The particle cloud steradiance was obtained by scanning the infrared spectrum from 1 to 5 microns; it was possible to obtain the emittance of the alumina particles at wavelengths corresponding to spectral windows in the H_2O molecule infrared spectrum. Again, the results for one to ten micron diameter particles show the rocket exhaust environment emittance of the oxide to be several orders of magnitude greater than the emissivity based upon Mie theory and available sub-melting point optical properties of pure single crystal alumina.

FLAME SPECTROSCOPY

120. A BAND RATIO TECHNIQUE FOR DETERMINING TEMPERATURES AND CONCENTRATIONS OF HOT COMBUSTION GASES FROM INFRARED EMISSION SPECTRA

C. C. Ferriso, C. B. Ludwig and F. P. Boynton

General Dynamics/Astronautics

An infrared band ratio technique (BRT) has been developed, which uses integrated emission ratios from various bands of H_2O and CO_2 in the 1 to 3.5μ spectral region to determine the temperature and concentration ratio (CO_2/H_2O) of hot gas combustion products. The present infrared BRT is based on the fact that the integrated intensities of various H_2O and CO_2 bands or portions of these bands are highly temperature dependent and that the emission in the 2.7μ region is due to both H_2O and CO_2. The present BRT unlike the traditional two-color technique for temperature determinations does not depend on variations of the blackbody function.

The traditional two-color technique for determining temperatures has been used quite extensively with great success in the visible portion of the spectrum; however, it has not been applied in the infrared because of low sensitivity. The traditional technique has low sensitivity because the slope of the blackbody function does not vary very much in limited regions in the infrared. The two-color method can be used only if the emissivity of the hot gas is assumed to be equal or is known in the two spectral regions. On the other hand, if the emissivities are not known an emission-absorption technique can be used at one wavelength to determine the emissivity and hence the temperature. If the emissivities cannot be assumed to be equal in two spectral regions nor can the emissivity be measured in one spectral region, the radiant emission spectrum between 1 to 3.5μ can still be used to determine temperature using the present BRT. The various bands of H_2O and CO_2 which were used to develop the present BRT are given in Table I.

Table I

Various CO_2 and H_2O band region defined for BRT

Region Symbol	Spectral Interval	Radiating Specie	Type of vibrational mode
		H_2O	Portion of the fundamental ν_3
A	2.63 - 3.3 μ	CO_2	Combinations ($\nu_1 + \nu_3$) and ($2\nu_2 + \nu_3$
a	2.94 - 3.3 μ	H_2O	Portion of the fundamental ν_3
B	2.3 - 2.63 μ	H_2O	Portion of the fundamental ν_3
C	1.7 - 2.1 μ	H_2O	Combination ($\nu_3 + \nu_2$)
D	1.3 - 1.6 μ	H_2O	Combination ($\nu_3 + \nu_1$)

Based on extensive studies of various bands in Table I made by the present authors, the best set of ratios has been evaluated for both the temperature and concentration ratio, $\xi = (CO_2/H_2O)$, determinations.

Spectral emissivities of the 2.7μ, 1.87μ and 1.38μ bands of H_2O, and the 2.7μ band of CO_2, which have been measured between 1000° and 2500°K will be given. Emissivity spectra in the 2.7μ band for mixtures of H_2O and CO_2 have also been measured between 1000° and 2500°K for $\xi = (CO_2/H_2O) = 1$ through 0. A small tri-propellant rocket burner produced the pure H_2O, CO_2 and variable (CO_2/H_2O) mix-

tures by burning hydrogen, oxygen and carbon monoxide. The spectral emission measurements were made at the nozzle exit of the burner where the composition, total pressure and temperature could be defined. The spectral emissivities were determined from a calibrated emission spectrum and a spectroscopic determination of the temperature of the hot exhaust gas of the rocket burner. The composition of the exhaust gas was evaluated from a semi-empirical fit to a thermochemical flow calculation. The hot H_2O, CO_2 and H_2O - CO_2 mixtures were observed at a total pressure of 1 atm in the optically thin absorption region with a constant geometric path length and CO_2, H_2O, and H_2O-CO_2 density.

All the experimental measurements were made with a double pass prism (CaF_2) monochromator, a thermocouple detector, and a standard blackbody calibration source. The water-cooled rocket burner which was used to produce the hot gas samples was specially designed to provide an exhaust jet which was uniform in temperature, pressure and composition, and free of shock disturbances. This was achieved by using (1) a symmetrical injector for admission of propellant into the combustion chamber; (2) a sufficiently long chamber to insure complete combustion, and (3) an expansion nozzle with Foelsch contour to provide an axially parallel exhaust jet. All the details of the experimental apparatus including the design and performance of the burner will be given.

All the experimental results are used to develop the formalism of the BRT which will be given, The radiance ratios θ(B, C) and θ(B, D) are obtained and are present as a function of the temperature, (B, C, D refer to the bands given in Table I). These ratios can be used to determine the temperature of a hot gas sample. The technique has been applied to systems where there is an independent check on the temperature. Small laboratory flames, rocket burner exhausts and other published results have been used to test the temperature BRT. Very good agreement has been observed in the comparison and the results will be given.

The radiance ratio ϕ (A, B) was determined and will be presented as a function of the temperatures of the gas and $\xi = (CO_2/H_2O)$ in the hot gas sample. Since the temperature can be evaluated from θ(B, C) or θ(B, D), the ϕ(A, B) can be used to determine the concentration ratio ξ in the sample. The concentration BRT has also been tested with systems where there is an independent check on the concentrations. The comparisons showed good agreement and these results will also be given.

The application of the BRT to systems which also include continuum emission from soot particles will also be given. The presence of continuum emission from carbon and molecular emission form H_2O and CO_2 does require reformulation of the BRT; however, the changes are small since we are taking ratios of areas in various spectral regions. The BRT procedure is also applicable to radiometer type measurements where three detectors together with filters in regions A, B, and C are used. Since in most cases the detector-filter response as a function of wavelength is not rectangular, it will be necessary, in general, to formulate new area ratios, θ and Φ as a function of temperature and concentration ratio, ξ . The detail procedure for generating new area ratios from the reported emissivity results will be given for a typical case.

The limitations, accuracy, and restrictions of the BRT will be given and discussed in detail.

121. AN ANALYTICAL AND EXPERIMENTAL STUDY OF MOLECULAR RADIATIVE TRANSFER IN NONISOTHERMAL GASES

Frederick S. Simmons

University of Michigan

There are a number of engineering problems involving radiative transfer from nonisothermal hot gases for which neither the thin gas approximation (negligible probability of an emitted photon being absorbed before escaping the system) nor the gas approximation (near-unity probability of absorption in a distance small compared with the dimensions of the system) is justified. One such problem of current interest is the determination of the thermal emission from the exhaust plume of a rocket booster during its powered flight. In an intermediate temperature range from ambient to a few thousand degrees, the radiant emission from many hot gases, e.g., combustion products, is concentrated in the molecular vibration-rotation bands in the near infrared. Although empirical relations for total band emission and absorption in isothermal systems have long been available, [1] and more recently have been correlated with theory and extended to simple nonisothermal systems, [2] it would be more generally useful to be able to handle the radiative transfer on a spectral basis. This is particularly the case for applications involving a further calculation of atmospheric transmission between the radiating source and the detecting instrument. Some analytical and experimental efforts have been and are being made in this direction. [3-6] The present work is an attempt to obtain approximate relations for calculating the spectral distribution of the net radiance at the boundary of a nonisothermal region given the distributions of temperature, pressure, and emitter concentration within the region, and the appropriate experimentally measured values of isothermal absorptance over a sufficient range of optical depths and temperature for the species involved. For the purpose of obtaining these limiting approximations, molecular bands are characterized as either "overlapping" or "nonoverlapping" in reference to the extent to which absorption in a particular small spectral interval is due to contributions from a number of lines as opposed to absorption by a particular well isolated line.

Equations for the transfer of molecular radiation in a nonisothermal gas which is neither thick nor thin were derived for two limiting cases. For overlapping lines the standard integral expression of the general equation of transfer [7] is shown to be appropriate by virtue of the slow variation of the absorption coefficient with wavelength. In this case, the absorption coefficient is equal to the ratio of the mean line strength to the mean line spacing, and is determined by isothermal experiment in which Beér's law growth is observed. This result is well known.

The more significant result of the present analysis is a relation which provides the means of calculating the spectral radiance in a nonisothermal gaseous system for the case of strong nonoverlapping lines. For use in this relation, a strong line parameter, distinct from the absoprtion coefficient, must be determined by isothermal experiment in which "square-root" growth is observed. Furthermore, the variation of the mean line strength with temperature must also be determined.

An experimental study of nonisothermal growth in molecular bands is described. A combustion tube furnace having seven individually controlled sections was built into a double-beam ratio-recording spectrophotometer constructed for this purpose. Gradients in temperature from ambient to 1000°C can be created as desired in a gas sample cell extending through the furnance. Both emission and absorption can be measured; for the former a built-in blackbody provides an absolute calibration.

A study was made of the water vapor bands in the 2.7 micron region using a double-pass monochromator with a cooled PbS detector which provided sufficient resolution that the growth of individual lines could be observed. Concentrations and total pressures were selected and temperature gradients imposed such that strong-line nonisothermal growth could be experimentally observed and compared with the previously described theoretical relation. The resultant data, obtained at moderate resolution from 2.4 to 3.4 microns, are presented and discussed in some detail.

References

1. Hottel, H. C.: Radiant Heat Transmission. Ch. III in Heat Transmission by W. H. McAdams, McGraw-Hill Book Co., 2nd ed. 1942.

2. Penner, S. S.: Quantitative Molecular Spectroscopy and Gas Emissivities. Addison-Wesley, Reading, Mass. 1959.

3. Olfe, D.: Radiant Energy Transfer from Nonisothermal Molecular Emitters with Nonoverlapping Dispersion Lines. Tech. Rept. No. 31, Contract Number Nonr-220(03) NR 015 401, Cal. Inst. Tech. (1959).

4. Burch, D. E., and Gryvnak, D. A.: Infrared Radiation Emitted by Hot Gases and Its Transmission through Synthetic Atmospheres. Aeronutronic Rept. No. U-1929 (1962).

5. Edwards, D. K.: Studies of Infrared Radiation in Gases. Rept. No. 62-65, Dept. of Eng'g., U.C.L.A., (1963).

6. Tourin, R. H.: Warner and Swasey Co., Flushing, N. Y. (Private communication).

7. Chandrasekhar, S.: Radiative Transfer, Dover Publications, Inc., New York.

122. SPECTRAL EMISSIVITY OF WATER VAPOR AT 1200°K

U. P. Oppenheim and A. Goldman

Israel Institute of Technology

The study of the spectrum of heated water vapor is of great interest in many combustion problems, such as the measurement of radiant infrared power emitted by rocket motors. The spectrum of H_2O has also been of continuing theoretical interest and it has been the subject of a large number of quantuum theoretical studies on its structure and intensity. The complicated structure of the spectrum of this molecule is due to the fact that it is a strongly asymmetric top. At higher temperatures this causes a very large number of additional lines to appear. For a number of technical reasons the spectrum of H_2O is difficult to study quantitatively at elevated temperatures, although a number of studies has been made on its near infrared bands. [1, 2]

Spectral band models can be used for the prediction of the emissivity of hot H_2O vapor as a function of path length and pressure. In atmospheric studies of H_2O

at room temperature it has been established that the random or statistical model gives a good representation of the total absorption of a number of H_2O bands. [3] Good results were obtained also by applying the statistical model to the spectral emissivity in 6 cm^{-1} intervals of the 6.3μ band at room temperature. [4] It is to be expected that at higher temperatures the increase in the number of spectral lines will cause an even better fit to the statistical model. It is interesting to note that only a relatively small number of vibration bands is excited at elevated temperatures, whereas for a linear molecule, such as CO_2, many new bands become active and cause a transition from the Elsasser model (at room temperature) to the statistical model at temperatures higher than 1000°K.

In order to find the basic parameters of this model it is necessary to study the emission or absorption of the gas as a function of pressure and optical path length. It is the purpose of the present study to show how the spectral emissivities of the 1.9 and 2.7μ bands of H_2O were determined under varying conditions of temperature, pressure and optical path length. Correlations were obtained between these quantities using the statistical band model and an analysis of the type described by Oppenheim. [5]

Samples of pure H_2O were introduced in a quartz absorption cell with fused-on quartz windows. The cell was heated in an electric furnace to 1200°K and absorption spectra were observed by the use of a Perkin-Elmer 12G grating spectrometer, using a thermocouple detector. The entire optical system, including the spectrometer, was placed inside hermetically sealed enclosures and flushed with dry N_2. Absorption cells of varying length were used in order to find the regions in which the gas was "optically thin" or had a "square root" behavior. By varying the pressure for a given path length (at 1200°K) the appropriate band model was selected. It was found that the relation

$$\frac{\ln \bar{T}_\nu}{p} = \text{const.}$$

held throughout the band for any value of the spectral transmittance $\bar{T}_\nu$ averaged over the spectral slit width and measured at a pressure p between 0 and 4 atm. Therefore the statistical model was assumed to be valid. [4, 5, 6]

The cell length was varied between 10 mm and 500 mm and the curve of growth was established for a large number of frequency intervals in both bands. The basic parameters of the statistical bands representing the transmittance in these frequency intervals are given by S/d and γ/d, where S is the intergrated intensity of these statistical bands, d is the average distance between lines and γ is the half-width of the lines. The curves of growth permitted the calculation of S/d and γ/d in many instances. With the help of these parameters it was possible to predict the spectral emissivity for any desired value of pressure and optical path length.

From measurements in the "linear region" the integrated intensity of the band was estimated and compared with results of other authors. [2]

It should be pointed out that the spectral slit width of the spectrometer was purposely increased from 1 cm^{-1} or less to about 10 cm^{-1} for the present measurements. It has been shown [4, 6] that in this case the spectrometer slit averages over a large number of spectral lines at a time, and the resulting transmittance is therefore independent of slit-width.

References

1. Tourin, R. H.: J. Opt. Soc. Am., 51, 799 (1961).

2. Ferriso, C. C., and Ludwig, C. B.: Technical Report, Contract Nonr - 3902(00), April 1963, General Dynamics-Astronautics.

3. Goody, R. M.: The physics of the stratosphere, pp. 161 - 163, Cambridge University Press, Cambridge, 1954.

4. Oppenheim, U. P. and Ben-Aryeh, Y.: J. Quant. Spectr. Rad. Trans. (to be published).

5. Oppenheim, U. P.: Ninth Symposium (International) on Combustion, p. 96, Academic Press, 1963.

6. Oppenheim, U. P. and Ben-Aryeh, Y.: J. Opt. Soc. Am., 53, 344 (1963).

123. SPECTROSCOPIC DETERMINATION OF CO_2 CONCENTRATION IN SITU

Gunter J. Penzias

The Warner & Swasey Company

In order to develop techniques of combustion gas analysis in situ, we have studied quantitative relations between infrared spectral transmittances of combustion gases and concentrations of the respective infrared-absorbing species. We found that for CO_2 at 4.40-μ the statistical band model can be used to establish quantitative relationships for use in gas analysis. We determined the necessary statistical model parameters from 600° to 2400°K, and developed a procedure for using the statistical model to measure concentrations. The method was tested by determining CO_2 concentrations in situ in shock-heated gases, with good results.

124. COLLISION BROADENING OF OH EMISSION LINES, MEASURED IN THE INFRARED*

S. H. Bauer, Cornell University

and

J. H. Jaffe, The Weizmann Institute, Israel

Kaskan's reanalysis of Oldenberg's classical work on absorption by OH at the 3063 Å band had indicated that collisional broadening was practically negligible. Carrington recently reinvestigated this question, using the "curve of growth" technique. He found, that the collisional line width for this radical was small indeed, being of the order 0.02 cm^{-1}. These are perplexing results, since OH has a dipole moment of 1.65 D and, when generated in a flame, is surrounded by polar combustion products at temperatures around 2500°K, at one atmosphere pressure. Since line shape parameters are measures of the interaction potential between the emitter and collider species, if these results are corroborated, the OH radical would be a most unique diatom.

---

* Experimental work was performed at the Weizmann Institute where S. H. B. spent a sabbatic leave as an NSF Senior Post Doctorate Fellow.

We recorded the OH emission spectrum in the infrared for the $(1 \rightarrow 0)$ vibrational transition, the P(10) through the P(20) lines, covering the spectral range 3.15μ to 3.81μ. Line widths were measured directly. For comparison, the significant experimental parameters for Carrington's measurements and for those performed by the authors are tabulated below.

	Carrington	Bauer and Jaffe
Transition	(0, 0) of $^2\Sigma^+ \rightarrow {}^2\Pi_{3/2,1/2}$	$(1, 0)^2\Pi_{3/2,1/2} \rightarrow (0, 0)$
λ location	3063Å and longer	3.1μ and longer
slit function (w at half max)	0.24 cm^{-1}	0.055 cm^{-1} (at 3000 cm^{-1})
doppler width (at half max)	0.25 cm^{-1}	0.024 cm^{-1}
collision width reported	0.02 ± .02 cm^{-1} via "curve of growth"	

It is worth noting that in a beautiful experiment Carrington had demonstrated that for the OH in the $^2\Sigma^+$ state the probability for a quenching collision is considerably greater than the probability for a collision leading to rotational relaxation. The fact that rotational energy and hence the electronic energy are easily transferred in collisions means that even distant encounters terminate coherence of the radiation. At a temperature of about 2500°K collisions between OH and H_2O should induce appreciable phase shifts. It is evident that the infrared possess a significant advantage, for two reasons. First, the slit function for the spectrometer at Rehovoth is 1/5 of that used by Carrington; second, the doppler width is 1/10 in the infarred than in the ultraviolet region of the spectrum.

Experimental

For the source of OH radicals we used a H_2/O_2 flame from an acetylene torch, No. 5; the burner opening was 2.3 mm in diameter. The flow rate of hydrogen was 9.50 liters per minute, and that of the oxygen 4.00 liters per minute. The portion of the flame selected for projection onto the spectrograph slit was 5 cm above the burner tip. To amplify the light which entered the spectrograph, a 3-mirror system was set up, such as described by Plyler; it provided a factor 3.7 - 3.8 in the light-gathering power. These flames are optically thin in the infrared. To estimate the rotational temperature for the OH radicals the peak height of each line was compared with the radiation intensity from a glow-bar viewed under the same geometric conditions. The optical arrangement is shown in Fig. 1. The glow-bar was run at a temperature estimated to be approximately 1000°K. The only essential assumption is that the glow-bar radiates as a gray body (i.e., follows a λ^{-4} law). The conditions for operating the burner were similar to those used by Carrington for his measurements of the UV band. The highly favorable conditions for measuring line widths in the infrared are not without a price. In this region of the spectrum many of the OH lines are overlapped by H_2O lines of which there is an enormous number. Hence, only selected OH lines may be used for line width measurements. That ratio of hydrogen to oxygen and the flow rates were chosen which maximized the ratio of OH/ H_2O line intensity at 3094 cm^{-1}. The current heating the glow-bar was maintained relatively constant (to ± 0.01 amp. out of a total of 3.0 amp) by the aid of a ballast lamp and by manually monitoring the current throughout the experiment. The flame composition and temperature were maintained constant by monitoring the pressures developed across venturi constrictions inserted in the hydrogen and the oxygen lines. The back pressures were followed manomerically and maintained constant to ± 0.1 cm out of 41 for O_2 and 12 for H_2. As was indicated in the table, when in a double pass position, the width at half-maximum for the slit function was effectively 0.055 cm^{-1} or less over the region where

these measurements were taken. The actual slit width used was 250 microns; its spectroscopic width was measured by recording the width at half-maximum of a mercury (198) line in second order (at a wavelength 1.3673μ).

Results

Data were recorded for the P branch K = 10 through K = 18. Lines for K < 10 and lines for the R branch could not be studied, in spite of several attempts because of overlapping by the numerous water lines. For each of the transitions there are four lines corresponding to the two states of total angular momentum 3/2 and 1/2, in turn each of which is split by the "Λ doubling." All the lines were recorded using the "Scanner" in a way which provided an internal dispersion calibration. The wavelengths for these lines have already been measured on an absolute basis by Plyler. There were several instances in which our measured line separations came closer to those experimentally recorded by Plyler than to the values predicted from the molecular parameters as deduced from the ultraviolet spectrum. Before and after each of these scans the glow-bar was swung into position and its emission intensity recorded. In this manner, the ratio of the line intensity to the glow-bar intensity provided a check on the amplification factor of the amplifier, the transmission of the lenses, mirrors and spectrograph, and the sensitivity of the detector at each wavelength. After reading the width at half-maximum, it was reduced to reciprocal centimeters and a slit correction was applied, as proposed by Izat. This proved to be of the order of 20%. Typical values for several lines are given below.

	$\Delta\nu_{1/2}$(measured)	$\Delta\nu_{1/2}$(corrected)
$P_1^a(10)$; $P_1^b(10)$	0.121 cm^{-1}	0.099 cm^{-1}
$P_1^b(11)$	0.117	0.096
$P_2^b(12)$; $P_2^a(12)$	0.115	0.096
$P_1^a(12)$; $P_1^b(12)$	0.112	0.093

Estimated flame temperature: $\approx$ 2600°K

The corrections refer to the slit function; the doppler contribution has been neglected since its half-width is less than half of the slit width.

Conclusion

Collisional broadened half-widths equal to or greater than 0.10 cm^{-1}, as observed in the infrared are just what one would have expected for a molecule such as OH. In this respect, excited OH in a flame behaves like a stable polar gas. One should therefore question the value reported by Carrington based on his curve of growth measurements. The simplest explanation appears to be that the curve of growth method is not reliable when the slit function and the doppler width are comparable, and each is twice as large as the collision width which is to be measured.

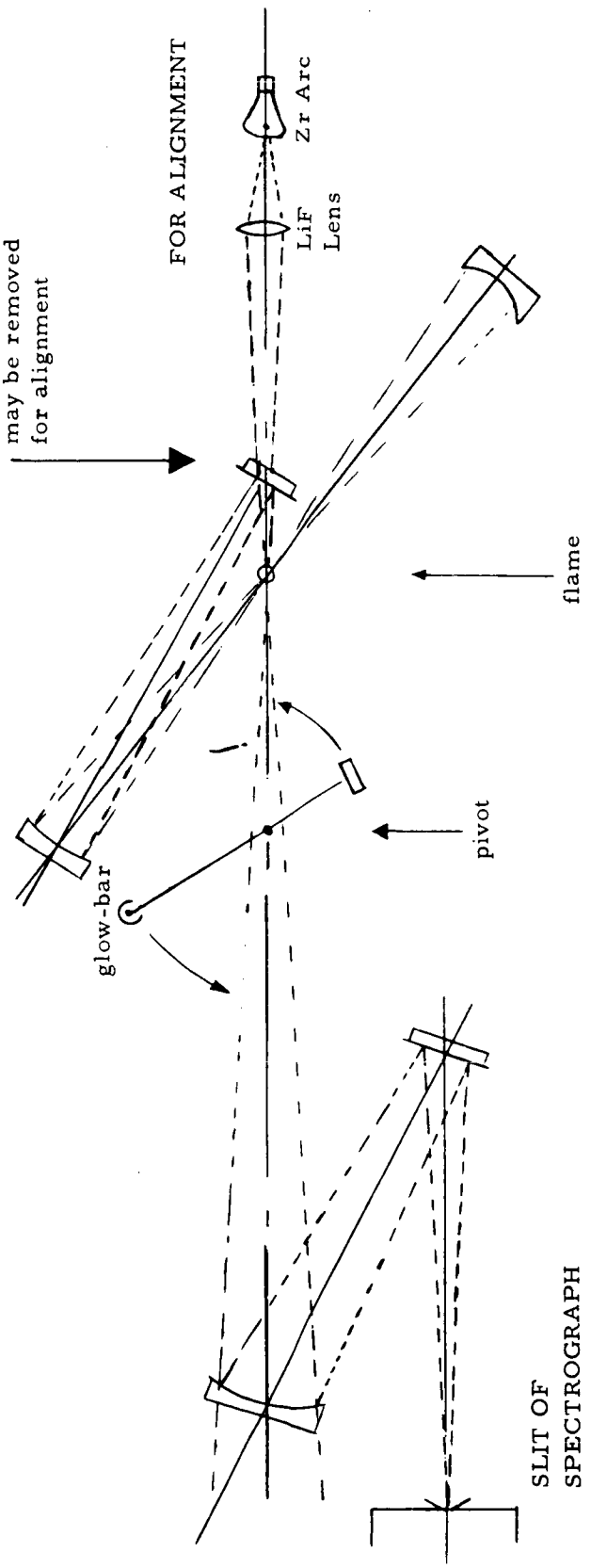
may be removed
for alignment
FOR ALIGNMENT
Zr Arc
LiF
Lens
flame
pivot
glow-bar
SLIT OF
SPECTROGRAPH

FIGURE 1

125. EXCITATION AND QUENCHING OF SODIUM ATOMS BEHIND SHOCK WAVES

Soji Tsuchiya and Kenji Kuratani

University of Tokyo

Gaydon and Hurle have concluded that the temperature observed by the sodium D-line reversal method agrees with the vibrational temperature of the shock-heated diatomic gas.[1] They also found that the reversal temperature of argon gas behind the shock wave was lower than the calculated value owing to the lack of radiative equilibrium. However, they have given no satisfactory explanation for the radiative nonequilibrium state. The present report offers a more quantitative elucidation of the problems proposed by Gaydon and Hurle, and aims at verifying the exciting or quenching mechanism of sodium atoms behind the shock wave.

The shock tube is composed of driver and low-pressure sections whose lengths are 160 and 480 cm, respectively. The shock velocity was determined by use of two platinum resistance gauges, 60 cm apart from each other. The gaseous temperature was obtained by the simultaneous measurement of emission and emission plus absorption of sodium D_2-line (5890 Å).[2] A very small quantity of sodium vapor was introduced into the gas occupying the low pressure section by feeding the gas into the tube through the glass pipe in which a piece of sodium metal was heated to 250-350°C. The present shock condition was around 2000-3500°K and 250-1000 mm Hg.

The explanation of the temperature obtained by the present method is based on the assumption that the emission of sodium D-line is a thermal radiation. This assumption provides the physical meaning of the temperature, that is, it determines the populations in ^2P and ^2S states of sodium atom according to the Boltzmann distribution.

In the shock-heated argon containing traces of sodium vapor, the intensity of sodium D-line emission rises very fast in less than 10 μsec (lab. time), and is almost constant in the high temperature region behind the shock wave. However, the temperature obtained from emission and absorption measurements is 600-1000°K lower than the temperature calculated from the shock velocity. On the other hand, the experimental results in the case of the 1% N_2 - 99% Ar mixture show that the emission rises gradually after the passage of the shock front and reaches a steady value of intensity as if there were a relaxational process. The temperatures obtained in the steady regions far from the shock front agree with the calculated temperature. In this case, the observed temperature drops as the content of nitrogen in argon decreases. Very similar results were obtained in the case of CO-Ar mixture, and the only difference is that the emission of sodium D-line behind the shock front rises a little faster than in the case of N_2-Ar mixtures.

The populations of sodium atoms in ^2P and ^2S states are considered to be determined by the following reaction scheme:

$$Na(^2S) + M^* \underset{Z_Q}{\overset{Z_E}{\rightleftharpoons}} Na(^2P) + M \qquad (1)$$

$$Na(^2P) \xrightarrow{\gamma_{eff}} Na(^2S) + hc\,\omega_d, \qquad (2)$$

where M may be an atom, a molecule or an electron, and M* is an M which possesses enough energy to excite a sodium atom to ^2P state. Two processes concerned with collisions between sodium atom and electron, i.e., $Na^+ + e \longrightarrow Na(^2P) + hc\,\omega_d$ and $Na(^2P) + e \longrightarrow Na^+ + 2e$, are neglected, because the concentration of electrons is assumed to be too small to make effective collisions with $Na(^2P)$ or Na^+, especially just behind the shock front.[3] The rate of the process (1) is expressed by exciting and quenching collision frequencies, Z_E and Z_Q. γ_{eff} is the reciprocal of the effective radiative life-time which is defined on the basis of radiation imprisonment, which states that a light quantum emitted spontaneously by $Na(^2P)$ is re-absorbed by a neighboring atom and re-emitted and so on.[4] The reaction schemes (1) and (2) give the relation between the observed temperature T_g and the calculated temperature T_2,

$$\exp\left[-\frac{hc\,\omega_d}{k}\left(\frac{1}{T_g}-\frac{1}{T_2}\right)\right] = 1/\left(1+\frac{\gamma_{eff}}{Z_Q}\right). \qquad (3)$$

Thus, the quenching collision frequency Z_Q for $Na(^2P)$ can be derived from the temperature observed by the present method. In order to explain the value obtained for Z_Q, the effective cross section σ^2_{eff} is calculated on the assumption that the collisional excitation of quenching is due to the nitrogen molecules in the N_2-Ar mixture. The values of σ^2_{eff} agree well with the values reported by Norrish and Smith.[5] This leads to the conclusion that the molecular collisions with sodium atoms are dominant to quench $Na(^2P)$, that is, to excite $Na(^2S)$ in the shock-heated N_2-Ar mixture, even if the concentration of nitrogen is 0.05% or less. The experimental results in shock-heated argon lead to the conclusion that impurities such as nitrogen and oxygen play a dominant role in exciting or quenching collisions with sodium atoms rather than argon atoms or electrons do, and that the quenching cross section of the argon atom in collisions with $Na(^2P)$ is less than $10^{-20}cm^2$ at 2500-3500°K.

As for emission rise in N_2-Ar mixtures just behind the shock front, the observed temperature follows the vibrational temperature defined by Montroll and Shuler.[6] The vibrational relaxation time in N_2-Ar collisions is about three times as long as in N_2-N_2 collisions.

To conclude, there is no translational-electronic energy exchange and only vibrational-electronic energy transfer is possible in the shock wave under the present shock condition.

References

1. Gaydon, A. G., and Hurle, I. R., Eighth Symposium (International) on Combustion, p. 309, Williams & Wilkins, 1962.

2. Tsuchiya, S.: J. Chem. Soc. Japan, Pure Chem. Sec. 84, 300 (1963).

3. Haught, A. F.: Phys. Fluid 5, 1337 (1962).

4. Holstein, T.: Phys. Rev. 72, 1212 (1947); 83, 1159 (1951).

5. Norrish, R. G. W., and Smith, W. MacF.: Proc. Roy. Soc. (London) 176A, 295, (1945).

6. Montroll, E. W., and Shuler, K. E.: J. Chem. Phys. 26, 454 (1957).

126. MASS SPECTROMETRIC SAMPLING OF ONE ATMOSPHERE FLAMES

Thomas A. Milne and Frank T. Greene

Midwest Research Institute

The burned gas region of flames at one atmosphere is being examined by means of a molecular beam sampling system and a Bendix Time-of-Flight mass spectrometer. The ultimate goal is the use of suitable flames to create a highly oxidizing atmosphere at high temperatures without the materials limitations present in Knudsen cell and transpiration experiments. The emphasis is on equilbrium studies of light-metal containing species in high partial pressures of oxygen and water at temperatures from 2000-3000°K.

There is evidence that a good approximation to chemical and thermal equilibrium exists in the region well removed from the reaction zone of the flame and that flame-probe interactions can be minimized. Thus, our work to date has been mainly concerned with the crucial problem of sampling reactive and condensable species from one atmosphere systems. The direct conversion of gas at one atmosphere into a molecular beam for introduction into the mass spectrometer involves a continuum expansion in the earliest stage for any practical sized sampling orifice. A simplified model describing this process was first given by Kantrowitz and Grey[1] in connection with their so-called aerodynamic molecular beam system. The initial expansion is nearly adiabatic, resulting in extreme cooling of the sampled gas and conversion to a supersonic jet which quickly passes over into molecular flow.

A differentially pumped sampling system, using rather modest pumps, is described. With it molecular beams of intensities of the order of 1×10^{17} molecules/cm^2/sec, 10 cm. from the sampling orifice, are obtained. These beams behave similarly to those reported by Scott[2], Fenn[2] and Bier[2] and have been studied under the conditions required for sampling flames with condensable species.

Several features of the performance of the sampling system are presented. The first is the molecular weight dependence observed in sampling mixtures. It has been found that for a number of species in various concentrations at room and flame temperatures, the beam formed from one atmosphere is depleted in the lighter component by the first power of the molecular weight. Thus, the observed beam intensity is related to the partial pressure and molecular weight of species X by $I_x = kP_x (M.W.)_x$. Secondly, we have confirmed the observations by Bentley[3] and by Becker's[4] group that a series of polymeric species is created during formation of molecular beams from high pressure sources. Argon polymers as large as $(Ar)_{30}$ have been seen from a 5-atmosphere source of argon at room temperature. Studies on the nature and conditions of formation of these species are briefly discussed together with the implications for sampling studies.

Finally, the results of actual sampling experiments with flames are presented. Analyses of stable flame products, additives taking part in known equilibria, free radicals and condensable metal containing species are presented. Flames ranging from relatively cool, lean CO-O_2 mixtures to stoichiometric H_2-O_2, CH_4-O_2 and C_2N_2-O_2-N_2 are being used. The dissociation of Cl_2 and HCl has been studied in flames as have the species in the B-H-O system at high temperatures. A very approximate analysis of the expected shift in composition of systems of known kinetics, during the very rapid initial expansion during sampling is also made.

References

1. Kantrowitz, A. and Grey, J.: Rev. Sci. Instr. 22, 328 (1951).

2. Third International Rarefied Gas Dynamics Symposium, Vol. I, Academic Press (1963)

3. Bentley, P. G.: Nature 190, 432 (1961).

4. Becker, E. W., Bier, K. and Henkes, W.: Z. f. Physik 146 333 (1956).

GENERAL

127. A TEST OF THERMAL IGNITION THEORY IN AUTOCATALYTIC REACTIONS*

P. G. Ashmore and T. A. B. Wesley

The Manchester College of Science and Technology, England

The Semenov-Frank-Kamenetskii treatment of thermal ignition has been applied to a complex reaction scheme for the formation of hydrogen chloride in mixtures of hydrogen, chlorine, nitric oxide and nitrosyl chloride. When conditions are chosen to lead to non-autocatalytic reactions, for example when nitric oxide is added but [NOCl] is low, the simple Frank-Kamenetskii treatment predicts pressure limits of ignition accurately. When nitrosyl chloride is added initially and the reaction is autocatalytic in nature, the basic equations for the rate of heat production and the rates of removal of reactants and additives, with values of the rate constants and other parameters measured in quite independent experiments, can be solved on a computer to derive the pressure limits of ignition accurately for a wide variety of conditions of temperature or additive concentration. The induction periods for the autocatalytic reaction are of the correct order of magnitude, although differences between two sets of experimental values cannot be accounted for.

A complete correlation of the limits and of the slow reaction in different vessels requires changes in the values of the rate constants of the surface reactions of chlorine atoms and molecules, or changes in the reaction scheme. It is not possible without further experimental work to decide which are the best changes.

---

*This work was carried out in the Department of Physical Chemistry, University of Cambridge, England.

128. THE EXPLOSIVE DECOMPOSITION OF AZOMETHANE

Norman J. Gerri and Frederick Kaufman

Ballistic Research Laboratories

The theoretical description of thermal gas explosions is based on a simple model which treats the balance of heat generation and of heat conduction to the wall in either of two limiting cases: (1) The non-stationary model (Semenov, Rice, Gray) which describes the temporal behavior of an exothermic reaction, but neglects the space variation of gas temperature, i.e., assumes thermal gas conduction to be so fast that heat transfer to the surface becomes rate determining; or (2) The stationary model (Frank-Kamenetskii) which describes that critical, spatial temperature distribution in the reaction vessel which separates the regime of slow reaction from that of explosion, but assumes the temperature of the wall to remain constant at its initial value, T_o.

These two complementary aspects of the theory permit the calculation of explosion limits, induction periods τ, and maximum temperature rises without explo-

sion, ΔT_M, as functions of initial temperature and concentration, vessel size, heat capacity and conductivity, heat of the reaction, and rate constants. A critical comparison of theory and experiment has not been possible so far, because τ, ΔT_M, and T vs. t could not be measured unequivocally, or because the mechanism of the explosion was in doubt.

In earlier work at this laboratory,[1] detailed pressure-time records of the explosive decomposition of gaseous hydrazine were obtained by means of fast, sensitive electrical pressure transducers. Because that work resulted in poor agreement with thermal theory, the measurements were extended to include temperature-time records at the center of the spherical vessel and at a point near the wall. Moreover, the explosive and slow decomposition of azomethane was reinvestigated, because it was reported to be a good example of a thermal explosion and much information is available on its isothermal kinetics.

In the present experiments pure gaseous azomethane or a known gas mixture was rapidly admitted to the heated vessel and isolated from a reservoir. The pressure was continuously measured by a transducer (Pace Engineering Co., Model 7) and the temperatures by Pt - Pt, 10% Rh thermocouples (0.001 inch diameter). All three signals were amplified, simultaneously displayed on a multichannel oscilloscope and photographed by a Polaroid Land Camera. For each experiment, the time-resolved pressure and temperature records permit the accurate measurement of initial pressure, rate of pressure rise, final pressure, induction period and rate of temperature rise at the center and near the wall. From a series of experiments at constant temperature, the explosion limit pressure, p_o, and the maximum temperature rise, T_M, could also be measured with good accuracy.

Such experimental results were gathered for pure azomethane and for mixtures with He, H_2, and N_2 from 606° to 714°K. p_o decreased from 160 to 2.2 mm Hg over this temperature range, but the plot of $\ln (P_o/T_o^3)$ vs. $1/T_o$ which should be linear and of slope E/R for a thermal explosion brought on by a first-order, exothermic reaction, (where E is its activation energy) was linear only between about 636° and 690°K and there gave an E of 33 kcal/mole, substantially lower than the reported E=51 kcal/mole of earlier work. Over this limited temperature range, all measured data were in good agreement with thermal theory. The maximum temperature rise at the center, ΔT_M, equaled $1.6\, RT_o^2/E$; the rate of temperature change at any pressure below the explosion limit was in good agreement with calculations in which the heat transfer coefficient of the non-stationary theory was replaced by $3\lambda/r$ (where λ is the coefficient of thermal conductivity and r the radius); the measured induction period was in agreement with the modified theory where account was taken of the lowering of the temperature rise before explosion at initial pressures which are substantially above P_o; and the observed effect of added diluents was at least qualitatively in accord with the estimated change in the thermal conductivity. Moreover, the temperature-time records of explosions showed the expected sharp initial rise, followed by a slower rise depending on how far the initial pressure exceeded P_o, then an inflection point, and finally an increasing slope leading to explosion.

The utility of the experimental method was strikingly shown by the change of the p vs. t and T vs. t records of azomethane below T_o= 635°K. The nature of the explosion became increasingly non-thermal at lower T_o as shown by ΔT_M too low by a factor 2.4; by p and T records which showed an initial rise, then a long flat portion, and finally an abrupt onset of explosion; and by induction periods which were twice as long as calculated from thermal theory. These results indicate the increasing importance of branched-chain processes at the lower temperatures. The fact that in this temperature range there is an increase in the slope of $\ln(P_o/T^3)$ vs. $1/T_o$ suggests that the heat evolution is not controlled by a single reaction step even at the higher temperatures where the process is thermal, because the chain-type explosion occurs at

higher pressures than those extrapolated from the thermal region, i.e., the thermal reaction scheme appears to be inhibited at low temperatures.

Further evidence for the complex nature of the reaction under these conditions was obtained from gas chromatographic analysis of the reaction products below the explosion limit. From 40 to 50% of the carbon and from 20 to 30% of the hydrogen were missing in the gaseous products (mostly N_2 and CH_4) and the formation of polymeric liquid materials was indicated. A discussion of the present results and of recent work by Rice and co-workers thus gives new insight into the mechanism of the slow and explosive decomposition of azomethane and provides a detailed comparison of theory and experiment.

Reference

1. Kaufman, F. and Gerri, N. J.: Eighth Symposium (International) on Combustion, p. 619, Williams & Wilkins, 1962.

129. EXPERIMENTAL INVESTIGATION OF THE IGNITION OF COMBUSTIBLE GASES AT HOT SURFACES UNDER CONDITIONS OF NONSTEADY STATE

G. Adomeit

Technische Hochschule, Aachen

The ignition of gases at suddenly heated circular rods has been investigated by measuring the temperature field and its development with time with a Mach-Zehnder interferometer. Except near the ignition limits, the ignition was found to set in abruptly, with a considerable delay (up to 60 msec) after the rod had been heated. During this period the temperature distribution in the gas was found to be determined essentially by heat conduction. Applying the concept of heat balance, an approximate relation was derived for the ignition delay, which is in accordance with the measured data and which agrees closely with expressions given for the condition of ignition at a hot body in steady-state cross flow. This relation explains the ignition delay as determined mainly by the initial heat conduction process in the gas. The experiments were performed in mixtures of pentane, propane, and hydrogen with air at various equivalence ratios, the gas pressure was varied between 0.5 and 6 atmospheres, the rod temperature between 700° and 1200°C, the rod diameter was 3.5 mm.

130. STUDIES OF HYPERVELOCITY FIRINGS INTO MIXTURES OF HYDROGEN WITH AIR OR OXYGEN

H. Behrens, W. Struth, F. Wecken

Institut Franco-Allemand de Recherches de Saint-Louis

Plastic spheres of 9 mm diameter were fired with velocities of 1500-3000 m/s into mixtures of hydrogen with air or oxygen. High-speed shadow and schlieren pictures gave good results before and after the missile. Most experiments were made with a stoichiometric H_2/air mixture at 0.55 atm. Whereas with shots at velocities higher than the detonation velocity a steady combustion front is established, instabilities in the form of oscillation appear at lower velocities. A quantitative study of the frequencies, shock pressures and stagnation temperatures associated with the missile velocities showed that the reciprocal frequency, or period of oscillation, is equal to the induction time for self ignition. Similar results were obtained with H_2/air mixtures with a twofold partial pressure of H_2 at a total pressure of 0.72 atm. However, frequencies did not vary with stagnation temperatures for the H_2O_2 mixture at 0.24atm. Probably these are acoustic oscillations with no relation to induction. Photographs were also taken some distance behind the missile when it had already passed the observation field. These pictures show a horizontal combustion gas column with a shock wave formed by propellant gases emitted by the gun muzzle. By taking two pictures, one over the other, with a definite delay, the shock wave velocity in the column is determined as v = 950-1200 m/s. By considering the intensity of secondary shock waves in the ambient gas, the sound velocity in the combustion gas column is estimated from the shock velocity. This value allows us to calculate approximately the temperature of the combustion gas to T = 1100-1200^{o}K for H_2 -air and H_2O_2 mixtures. However, experiments with stoichiometric H_2O_2 mixtures showed the development of a detonation wave along the combustion gas column with a detonation velocity D = 2000 m/s. These findings demonstrate that the combustion reaction before and around the missile is rather incomplete. A calculation with an intermediate temperature, T_1=1200^{o}V, gave a value of D = 2270 m/s for a Chapman-Jouguet detonation.

131. RADIATION PROCESSES RELATED TO OXYGEN-HYDROGEN COMBUSTION AT HIGH PRESSURES

Marshall C. Burrows

Lewis Research Center, NASA

Radiation related to the combustion of liquid-oxygen jets in a gaseous hydrogen atmosphere was studied by measuring the intensities of OH, O_2, and H_2O radiation in a combustion chamber equipped with windows. Over-all oxidant-fuel weight ratio was varied from 1 to 10 at a chamber pressure of 24 atmospheres. Maximum intensities from the radiating species were obtained near stoichiometric mixture ratios. Gas temperatures derived from the measured color temperature of a tungsten plate in the gas stream agreed with theoretical temperatures of the products. Gas radiation appeared to be thermally excited and in local equilibrium at all locations within the combustor.

Radiation measurements made in the upstream region of a stable combustor showed that intensities varied little with oxidant-fuel weight ratio. Measured intensities initially increased in the direction of gas flow due to the increased extent of reaction and then decreased when diluted with excess reactant or cooled by heat transfer to the walls. Ultraviolet and total radiation data showed that the reaction proceeded at approximately a constant rate until the limiting reactant was consumed. The distance required to complete the reaction varied from 1.5 to 12 inches for a variation in oxidant-fuel weight ratio of 1 to 9.

During combustion with pressure and velocity oscillations along the axis of the combustion chamber, average intensities of the radiating gases showed that the axial distance required to react the liquid oxygen and hydrogen was reduced. The distance required to complete the reaction in this case varied from 1 to 6 inches for an oxidant-fuel weight-ratio variation of 1 to 9.

The extent of reaction as determined by radiation measurements in the two combustors was compared to the predicted trends where turbulent mixing or vaporization was considered to control the reaction.

132. THE RATE OF GROWTH OF SOOT IN TURBULENT FLOW WITH COMBUSTION PRODUCTS AND METHANE

K. S. Narasimhan and P. J. Foster

University of Sheffield, England

This brief paper presents the results of an investigation into the formation of soot when methane is rapidly mixed with hot gaseous combustion products. This situation is relevant to the formation of soot in the turbulent jet diffusion flame. A knowledge of soot spatial mass concentration, particle size, and complex refractive index allows the calculation of its radiant properties. Specific knowledge of the soot forming processes would provide one of the bases for the design of flames.

Apparatus

The experimental furnace used was a plug flow reactor designed to simulate the instantaneous conditions in the soot forming region of a practical flame. Hot combustion products from a towns-gas/air surface combustion burner were passed along a vertical four inch diameter circular duct in foamed refractory concrete. Methane could be mixed continuously into this stream through four water-cooled nozzles on a ring main. Injection velocities up to sonic were used to attain fast macromixing of the two gas streams in the region of the nozzles. The reacting mixture of gases and soot passed up the duct and could be sampled by probes directed axially against the flow. Runs were conducted both with and without free oxygen in the initial hot gas stream. A nominal Reynolds number of 5,000 was maintained in the reacting stream and the Reynolds number of the methane jets was varied from 250,000 to 25,000 using interchangeable nozzles of different sizes. Under these conditions passage through the reaction chamber 30 inches in length represented a time interval of 40 milliseconds.

Measurements

Properties of the reacting stream measured against time included a) temperature by suction pyrometer, b) gas analysis for CO_2, O_2, C_hH_m, CO, H_2, CH_4 by absorption and gas chromatography, c) soot mass concentration, d) particle size of soot by electron microscope, e) velocity fluctuations by pitot tube.

Data were collected under the following conditions:

a) Initial methane concentration 5 to 25 mole per cent.
b) Initial oxygen concentration 0 to 8 mole per cent.
c) Initial mixture temperature 1400° to 1800°K.

Results

Under these conditions hydrogen and carbon monoxide appeared on injection and soot mass flow increased linearly with time. Any oxygen present initially was completely consumed within 8 milliseconds. This was too rapid to accurately assess the oxygen consumption rate.

Electron micrographs gave no evidence of increase of soot particle size with time outside the experimental error, on the other hand no evidence was found for the formation of new particles with time. A significant variation of average particle size with initial mixture temperature was found from 33Å at 1413°K to 230Å at 1763°K.

Soot Formation

Tesner has proposed that soot formation proceeds by decomposition of the hydrocarbon molecules on nuclei and that no new nuclei are formed after the initial precipitation. The electron microscope data support this model as no new particles were observed during passage through the reactor. Convincing evidence of particle growth could not be expected in the above experiments as the particle size would vary with the cube root of the soot mass flow and lie within the experimental error of particle size measurement, up to 50 per cent. While the above soot formation model leads to separate questions about nucleation and growth we propose only to consider the growth of particles already formed as nucleation appears to be a complicated process requiring further analysis.

Mechanism of Soot Growth

All possible over-all reactions between the hot combustion gases themselves and the soot were considered. Their relative significance has been estimated by comparing the theoretical equilibrium conditions with the measured gas concentrations. Thus the only reaction proceeding to completion in 40 milliseconds was

$$CO_2 + H_2 \longrightarrow CO + H_2O$$

and the only other reaction proceeding towards equilibrium at a significant rate was

$$CH_4 \longrightarrow C + 2\,H_2$$

Accordingly only methane decomposition was considered in the development of a rate equation.

Rate Equation

The kinetic theory bimolecular collision equation has been employed considering the carbon particle to act as a large molecule. The resultant expression was

found to correlate the experimental data:

$$\frac{dC}{dt} = \text{constant.} \; (Ns)^{1/3} \; (C)^{2/3} \; \frac{\chi}{T^{0.5}} \; \exp.\left(-\frac{E}{RT}\right) \qquad (1)$$

where C = soot mass concentration mg./ml. reduced to N. T. P.
E = apparent activation energy Kcal/g. mole.
N = number of particles per ml. of wet gas at N. T. P.
T = stream temperature, ^{o}K.
χ = mole fraction of methane.

Experimentally the constant was found to be 3.87×10^{8} and E to be 57.6 Kcal/g. mole.

Conclusions

The process of formation of a disperse phase of soot particles appears to conform to the model proposed by Tesner whereby two regimes may be distinguished, initial precipitation of nuclei and their growth. Under the conditions specified the growth of soot particles is related to their mass and number concentrations, and methane mole fraction and temperature by Eq. 1.

133. THE ROLE OF INERTS IN HYDROCARBON FLAMES

R. H. Atalla and the late Kurt Wohl

University of Delaware

The investigation to be reported was conceived in an effort to explore the role of inerts in combustion processes. The particular case chosen is that of nitrogen in flames of hydrocarbons with air. A study was made of the spatial variation of the intensity of emission by excited radicals in the visible and ultraviolet regions of the spectrum. The spatial variation of absorption and emission by CO_2 at 4.5 μ (in the infrared region) was also determined. This enabled the computation of the temperature at various points within the flame.

The flames studied were flat. They were held above a cooled porous metal plate burner. They were viewed edgewise by a spectrophotometer of low aperture, capable of examining very thin horizontal segments of the flame. At selected wavelengths representative of the various emitters, spatial traverses were made by moving the burner vertically past the axis of the optical system.

The flames chosen for investigation were: (a) a stoichiometric butane-oxygen flame at a pressure of 38 mm Hg (1/20 atm.) to be used as a standard for comparison purposes; (b) a stoichiometric flame of butane with a 40% N_2-60% O_2 mixture at 60 mm Hg; and (c) a stoichiometric butane air flame at 162 mm Hg. The velocity of the unburned mixture for all three flames was 25 cm/sec. The total pressures were chosen such that the partial pressures (and hence the mass flow rates) of butane and oxygen were the same in all three flames.

The spatial variation of the absolute intensity of emission by CO_2 at 4.5 μ was determined by comparison with a standard lamp. The absorption at the same wave-

length was measured by placing a spherical mirror behind the flame and using the reflected radiation as an outside source of approximately the same intensity as the flame itself. Values of the absolute intensity and the absorptivity were then used to calculate the temperature of the flame gases at the particular point.

The observed temperature profiles indicate that the influence of nitrogen in decreasing conductive heat losses to the burner more than compensates for the increased heat capacity of the mixture. Although the final temperatures of all three flames were rather close, those of the two flames including nitrogen were higher than that of the flame with oxygen alone. These unanticipated results are in good "order of magnitude" agreement with theoretical estimates. It was also found that the heat release downstream of the visible intensity maxima is primarily because of the formation of CO_2, the H_2O being formed earlier in the reaction.

In the visible and ultraviolet region, sprectral traverses were made at a number of points both in the main reaction zone and in the post combustion zone. At the wavelengths characteristic of the radicals CH, CC, and OH, and the background continuum ascribed to CO_2^*, spatial traverses were made. The absolute intensities of emission were measured at the points of maximum intensity. The information from all three sources was then combined to determine the spatial variation of the absolute intensity for each emitter.

From these it was found that both the rate of rise of radical (CH, CC, and OH) emission, and its rate of decay increased with added nitrogen. Thus the separation of the points of maximum intensity from the porous plate decreased regularly with increasing nitrogen content. The increase in the rate of rise with added nitrogen, although qualitatively similar to the theoretically calculated temperature profiles, can also be attributed to the increased resistance to diffusion caused by the presence of nitrogen. In the decay region the concentration gradients and diffusion rates are much reduced. Thus the increased decay rate can be attributed to the increased frequency of termolecular collisions, leading to the removal of radicals, relative to bimolecular collisions leading to their formation. The increase in collision deactivation of excited radicals also contributes to the increased decay rate. The maximum intensity of CC emission was the same for the three flames, while that of CH emission decreased regularly with added nitrogen. The OH maximum varied irregularly.

The maximum intensity of the background (CO_2^*) radiation decreased with added nitrogen, while the rate of decay increased. This suggests that the collision product CO_2^* which emits the background continuum can be stabilized without emission if a third body participates in the collision.